DETECTION AND EVALUATION OF DECAY IN PULP AND PAPER FIBRE SUPPLIES

by

RODERICK ANTHONY STIRLING

B.Sc., University of Victoria, 2000

A THESIS SUBMITTED IN PARTIAL FULFILMENT OF
THE REQUIREMENTS FOR THE DEGREE OF

DOCTOR OF PHILOSOPHY

in

THE FACULTY OF GRADUATE STUDIES

(Forestry)

THE UNIVERSITY OF BRITISH COLUMBIA

March 2005

ABSTRACT

Decay of wood chips is a significant economic threat to the pulp and paper industry. It results in reduced wood chip quality, which in turn causes decreased pulp yields and poorer pulp properties. The currently accepted methods to measure decay content in wood, such as buffering capacity and 1% caustic solubility, are too laborious to be of practical use in mill environments. The present research developed and investigated methods for rapidly quantifying decay in wood chips. Partial Least Squares (PLS) models were developed, based on FTIR and NIR spectra, to predict the extent of decay in wood chips, using caustic solubility, buffering capacity and basic wood density as indicators of decay. Data from these models were found to be highly correlated with existing methods ($r^2 > 0.80$). In order to provide further validation for the PLS models, changes in wood chemistry underlying the decay were also examined. Extent of decay, as shown by the PLS models, was found to correlate with changes in the concentration of acetyl groups and lignin in the wood samples.

Following the development and validation of the PLS models, the impacts of inoculum size and storage time on chip and thermo-mechanical pulp properties were determined. Results showed that both sound chips and chips incubated with varying quantities of a brown rot decay fungus for up to four months showed little decay and few changes in thermo-mechanical pulp properties. The most significant change was a drop in pulp brightness that was accounted for by the storage time, rather than fungal inoculation, of the wood chips.

In order to understand the effects of pulping samples with high levels of brown-rot decay, softwood chips were heavily decayed by a brown rot fungus under ideal growth conditions in the laboratory. Both kraft and refiner mechanical pulps produced from these heavily decayed chips showed significant differences from pulps produced from equivalent sound chips. Mechanical pulps were prepared to a given freeness with less energy, but had significantly poorer strength and optical properties. Kraft pulps were produced in lower yields and consumed more alkali. The length of kraft fibres decreased with increasing decay and resulted in poorer strength properties. Existing research has shown that kraft pulping of chips heavily decayed by brown rot fungi is not economical (Hunt, 1978b). These results confirm this existing research and extend it to mechanical pulping, showing that heavily decayed chips exhibit similar detrimental effects on both kraft and mechanical pulping. The PLS models developed to estimate extent of decay were able to identify wood chips with poor pulping properties.

TABLE OF CONTENTS

Abstract ii

Table of Contents iii

List of Tables vii

List of Figures x

List of Equations xiv

List of Abbreviations xv

Acknowledgments xviii

CHAPTER 1 General Introduction 1

1.1 Industrial Relevance of Wood Decay 1

1.2 Introduction to Wood 2

1.3 Decay Fungi 7

1.4 Sources of Decay 12

1.4.1 Decay in the Forest 13

1.4.2 Decay in Storage 14

1.5 Wood Chip Quality 18

1.6 The Effects of Decay 20

1.7 Chip Utilization Procedures 22

1.8 Measuring Decay 23

1.8.1 Fungal Indicators 23

1.8.2 Physical Methods of Measuring Decay 26

1.8.3 Spectroscopy and the Measurement of Decay 28

1.8.3.1 Mid-IR 28

1.8.3.2 Near-IR 31

1.8.3.3 Raman Spectroscopy 33

	1.8.4	Measuring Decay in the Pulp and Paper Industry	36
1.9	Managing Decay		39
1.10	Research Objectives		42
CHAPTER 2	**General Methodology**		**44**
2.1	Wood and Fungal Samples		44
2.2	Analysis of Wood Samples		46
2.3	Spectroscopy		48
2.4	Statistical Analyses		49
CHAPTER 3	**Partial Least Squares Models of Decay and Wood Density**		**51**
3.1	Introduction		51
	3.1.1	Modeling Caustic Solubility and Buffering Capacity	52
	3.1.2	Modeling Basic Wood Density	53
3.2	Methods		54
	3.2.1	FTIR Method Optimization	54
	3.2.2	PLS Model Development and Validation – Caustic Solubility and Buffering Capacity	55
	3.2.3	Basic Wood Density	57
3.3	Results		58
	3.3.1	FTIR Modeling	65
	3.3.2	Model Validation	69
	3.3.3	NIR Modeling	76
	3.3.4	Raman Modeling	79
	3.3.5	Basic Wood Density	82
		3.3.5.1 FTIR Modeling of Wood Density	82

3.3.5.2 NIR Modeling of Wood Density 83
3.3.5.3 Field Samples 85
3.3.5.4 Leachate COD 86

3.4 Discussion 87

CHAPTER 4 Analysis of Decay Indicators 95

4.1 Introduction 95

4.1.1 One Percent Caustic Extracts 95

4.1.2 FTIR Spectra of Decay 96

4.1.3 Fungal Damage to Fibres 97

4.2 Methods 98

4.2.1 One Percent Caustic Solubility Fractionation 99

4.2.2 Chemical Analyses 99

4.2.3 FTIR Analyses 100

4.2.4 Microscopic and Fibre Quality Analyses 100

4.3 Results 102

4.3.1 Chemical Analyses 102
4.3.1.1 Caustic Extraction 105
4.3.1.2 Buffering Capacity Fractionation 110

4.3.2 FTIR Spectroscopy 110

4.3.3 Microscopy and Fibre Quality Analysis 114

4.4 Discussion 116

CHAPTER 5 Chemical and Mechanical Pulping of Decayed Wood 121

5.1 Introduction 121

5.2 Methods 123

5.2.1 Wood Chip Preparation 123

5.2.2 Mechanical Pulping 123

5.2.3 Kraft Pulping 126

5.2.4 Pulp Testing 127

5.3 Results 127

5.3.1 The Effects of Inoculum Size and Wood Chip Storage 127

5.3.2 Refiner Mechanical Pulping 135

5.3.3 Kraft Pulping 139

5.4 Discussion 146

CHAPTER 6 Conclusions and Future Work 151

6.1 Conclusions 151

6.2 Future Directions 155

References 158

Appendix I Concentration Datasets 176

Appendix II Partial Least Squares Modeling 186

Appendix III Factor Loadings for PLS Models 191

Appendix IV Correlograms for PLS Models 194

Appendix V PRESS Diagrams for PLS Models 196

Appendix VI Chromatograms of Alditol Acetates 198

Appendix VII Mass Spectra and GC Data 199

Appendix VIII FTIR Spectra 206

Appendix IX Thermomechanical Pulping Data 208

Appendix X Refiner Mechanical Pulping Data 215

Appendix XI Kraft Pulping Data 219

LIST OF TABLES

Table 1.1	Organic Constituents of Wood	3
Table 1.2	Fungi Commonly Found in Wood Chip Piles	16
Table 2.1	Wood Species Used in Model Development	45
Table 2.2	Fungi Used to Decay Wood Samples	46
Table 3.1	TAPPI Standard Methods of Wood Density Determination	53
Table 3.2	Hand-sorting Douglas fir and Black spruce into Sound and Decayed Fractions Based on Visual Assessment	59
Table 3.3	Analysis of variance in caustic solubility ($\alpha = 0.05$) attributable to wood species, fungal type, wood/fungal interactions and time	61
Table 3.4	Analysis of variance in buffering capacity ($\alpha = 0.05$) attributable to wood species, fungal type, wood/fungal interactions and time	61
Table 3.5	Mean and Standard Deviation for Decay Detection Methods on Six Replicates of Sound Wood Samples (Standard Deviations Shown in Parentheses)	62
Table 3.6	PLS Modeling Statistics for the Calibration and Validation of Caustic Solubility and Buffering Capacity Models	66
Table 3.7	PLS-Prediction Statistics for Mixtures of Sound and Decayed Spruce, Pine and Fir	71
Table 3.8	Modeling Statistics for Independent Wood Species and Fungal Type Models	72
Table 3.9	PLS Predictions of Freeze-Dried and Oven-Dried Samples ($n = 3$, Standard Deviations in Parentheses)	74
Table 3.10	Comparison of Autoclaved and Untreated Sample Predictions by FTIR-Based Caustic Solubility and Buffering Capacity Models	75
Table 3.11	PLS Modeling of Caustic Solubility and Buffering Capacity for NIR Dataset	77
Table 3.12	PLS Modeling Statistics for Raman Spectra	80
Table 3.13	PLS Models of Basic Wood Density	83
Table 3.14	PLS Models of Leachate COD from the Basic Wood Density Test	86

Table 4.1	One Percent Caustic Solubility and Buffering Capacity of Sound, White-rot, and Brown-rot Decayed Spruce Samples (Standard Deviation in Parentheses)	102
Table 4.2	Summative Analysis of Spruce Samples	104
Table 4.3	Fractionation of Lignin in Sound, White-rot, and Brown-rot Decayed Spruce Samples and Their 1% Caustic Soluble and Insoluble Fractions. Determined in Duplicate. Standard Deviations in Parentheses.	107
Table 4.4	Percent Composition of Caustic Extracts from Sound, White-rot and Brown-rot Decayed Spruce Samples	110
Table 4.5	Absorbance Maxima and Relative Intensities in FTIR Spectra of Sound, White-rot and Brown-rot Decayed Spruce Samples and Wood Fractions	113
Table 4.6	PLS-Predicted Caustic Solubility and Buffering Capacity of a Single Wood Chip, Half Covered with either White- or Brown-rot Fungi	114
Table 4.7	Fibre Quality Analysis of Sound, White-rot and Brown-rot Decayed Spruce Samples, Std. Dev. in Parentheses (n = 8)	116
Table 5.1	TMP Conditions	125
Table 5.2	Kraft Pulping Conditions (Constant H-factor)	126
Table 5.3	Colony diameter of *G. trabeum* on Malt Extract Agar after 7 days of incubation at varying temperatures	128
Table 5.4	Caustic Solubility Bench Scale Analysis of Variance ($N = 80$, $\alpha = 0.05$) for Lodgepole Pine Chips Inoculated with *G. trabeum*. Time was specified as a covariate.	130
Table 5.5	Caustic Solubility and Buffering Capacity in Lodgepole Pine Chips before and after 115 Days Storage. Standard Deviation in Parentheses	131
Table 5.6	Lodgepole Pine TMP Pulp Properties Interpolated or Extrapolated to 100 mL CSF	132
Table 5.7	Properties of Lodgepole Pine Chips Used for RMP and Kraft Pulping. Standard Deviations in Parentheses.	136
Table 5.8	RMP Properties of Lodgepole Pine Interpolated to 100 mL CSF	138

Table 5.9	Lodgepole Pine Kraft Pulp and Black Liquor Properties (EA = 16%, H-factor = 1290)	142
Table 5.10	Kraft Pulping of Lodgepole Pine Samples (Target Kappa = 30)	144
Table 5.11	Kraft Pulp Properties of Lodgepole Pine Interpolated to 300 mL CSF	145

LIST OF FIGURES

Figure 1.1	Canadian Forestry Exports, 2000 (Source: NRC, 2003)	2
Figure 1.2	Two β-D-Glucopyranose subunits in a cellulose molecule	4
Figure 1.3	Structure of Some Softwood Lignin Subunits	5
Figure 1.4	A Typical DRIFT Spectrum of Milled Spruce Wood	31
Figure 1.5	A Typical NIR Spectrum of Milled Spruce Wood	33
Figure 1.6	A Typical Raman (SERDS) Spectrum of Milled Spruce Wood	35
Figure 3.1	A Three Factor, Four Level Lattice Design for Mixtures of Sound Spruce, Pine and Fir. Points of intersection indicate where mixture samples were obtained. The corners of the largest triangle represent pure wood species.	56
Figure 3.2	Correlation between the 1% Caustic Solubility and Buffering Capacity of All Wood Samples Measured	60
Figure 3.3	Typical FTIR spectra of sound, white-rot and brown-rot decayed spruce samples	62
Figure 3.4	FTIR Spectral Variance of Four Milled Wood Samples with 64 scans and 4 cm^{-1} resolution	63
Figure 3.5	The Difference of FTIR Spectra from Sound and Brown-rot Decayed Wood	64
Figure 3.6	FTIR-Based Model: PLS-Predicted vs. Measured Caustic Solubility	66
Figure 3.7	FTIR-Based Model: PLS-Predicted vs. Measured Buffering Capacity	67
Figure 3.8	Calibration models: studentized residuals as a function of sample leverage. A studentized residual greater than an absolute value of 2.5 is considered high (Beebe *et al.*, 1998).	69
Figure 3.9	PLS-Predicted vs. measured caustic solubility in milled wood mixtures. The dotted line represents where predicted data equal measured data. The thin solid lines bounding the dotted line represent the 95% confidence interval based on the RMSEP of the caustic solubility model. The thick solid line is a best-fit line.	70

Figure 3.10	PLS-Predicted vs. measured buffering capacity in milled wood mixtures. The dotted line represents where predicted data equal measured data. The thin solid lines bounding the dotted line represent the 95% confidence interval based on the RMSEP of the buffering capacity model. The thick solid line is a best-fit line.	71
Figure 3.11	PLS-Predicted caustic solubility of milled lodgepole pine stored at 105°C and 130°C. Error bars represent the standard deviation of three replicates.	73
Figure 3.12	Visible/NIR spectra of lodgepole pine with varying caustic solubility	78
Figure 3.13	NIR-based Model: PLS-Predicted vs. Measured Caustic Solubility	78
Figure 3.14	NIR-based Model: PLS-Predicted vs. Measured Buffering Capacity	79
Figure 3.15	SERDS spectra of sound, white-rot, and brown-rot decayed spruce samples.	80
Figure 3.16	Raman-based Model: PLS-Predicted vs. Measured Caustic Solubility	81
Figure 3.17	Raman-based Model: PLS-Predicted vs. Measured Buffering Capacity	81
Figure 3.18	FTIR-based Model PLS-Predicted vs. Measured Basic Wood Density in Lodgepole Pine	83
Figure 3.19	First Derivative (23 point Savitzky-Golay) NIR Spectra of Lodgepole Pine Samples with Varying Density	84
Figure 3.20	NIR-based Model PLS-Predicted vs. Measured Basic Wood Density in Lodgepole Pine	85
Figure 4.1	Constituents of Spruce Samples and 1% Caustic Fractions (S = Sound, WR = White rot, BR = Brown rot, Ins = Insoluble, and Sol = Soluble)	103
Figure 4.2	Gas Chromatograms of Acetone Extractives from Sound, White-rot, and Brown-rot Decayed Spruce Samples	105
Figure 4.3	Gas Chromatograms of Benzylated Acetic Acid and Crotonic Acid (Internal Standard) from the 1% Caustic Extracts of Sound, White-rot, and Brown-rot Decayed Spruce	106

Figure 4.4	Fractionation of Carbohydrates by 1% Caustic Extraction of Sound and White and Brown Rot Decayed Wood (S = Sound, WR = White rot, BR = Brown rot, Ins = Insoluble, and Sol = Soluble)	108
Figure 4.5	Gas Chromatograms of the Caustic Degradation Products of Sound, White-rot and Brown-rot Decayed Spruce Samples	109
Figure 4.6	Normalized FTIR Spectra (31 point Savitzky-Golay Smoothed) of Sound, White-rot, Brown-rot Decayed Spruce Samples from 1850 to 1550 cm^{-1}. Spectral Assignments (Faix, 1991).	111
Figure 4.7	FTIR Spectra (31 point Savitzky-Golay Smoothed) of Sound Spruce, Delignified, Acetylated and Delignified and Acetylated from 1850 to 1450 cm^{-1}	112
Figure 4.8	Micrographs of Decayed Wood Taken Through a 20X Lens (A) Incipient Decay by *P. igniarius* in Lodgepole Pine, (B) Incipient Decay by *G. trabeum* in Lodgepole Pine, (C) Advanced Decay by *P. igniarius* in White Spruce, (D) Advanced Decay by *G. trabeum* in White Spruce.	115
Figure 5.1	PLS-Predicted Caustic Solubility as a Function of Inoculum Size and Time (Bench Scale)	129
Figure 5.2	Specific Refining Energy vs. Canadian Standard Freeness for Thermomechanical Pulps	133
Figure 5.3	Photographs of Lodgepole Pine chips Used for RMP and Kraft Pulping (A) Sound, (B) Discoloured (Stored at room temperature for 8 months), (C) Intermediate Decay (*G. trabeum*), (D) Advanced Decay (*G. trabeum*)	137
Figure 5.4	Specific Refining Energy of Lodgepole Pine Chips vs. Canadian Standard Freeness for Refiner Mechanical Pulps.	137
Figure 5.5	Screened Yield vs. the Kappa Number of Pulps Produced at 16% EA and 1290 H-factor. Error bars represent the standard deviation of the kappa number determination (n = 4).	140
Figure 5.6	Screened Yield and Kappa Number as a Function of H-Factor for Kraft Pulps Produced from Sound Lodgepole Pine Chips (EA = 16%)	141
Figure 5.7	Effective Alkali Consumed vs. Kappa Number for Sound, Discoloured, Intermediate and Advanced Decay Samples Pulped to a Constant H-factor (1290) and EA (16%). Error bars represent the standard deviation of EA consumed and kappa number (n = 4).	142

Figure 5.8 Effective Alkali Consumed during the Kraft Pulping of Lodgepole Pine to an H-factor of 1290 vs. Buffering Capacity of the Wood Chips 143

LIST OF EQUATIONS

Equation 2.1	Predicted Residual Error Sum of Squares	50
Equation 2.2	r^2 Determination	50
Equation 2.3	Root Mean Standard Error of Cross Validation	50
Equation 3.1	The Beer-Lambert Law	51
Equation 4.1	Length-Weighted Fibre Length	101

LIST OF ABBREVIATIONS

AD	Air-dried
ANOVA	Analysis of Variance
BC	British Columbia
BR	Brown-rot
BSTFA	N,O-*bis*(trimethylsilyl)-trifluoroacetamide
CCD	Charge Coupled Device
CP MAS NMR	Cross polarization Magic Angle Spin Nuclear Magnetic Resonance
CSF	Canadian Standard Freeness
CTMP	Chemithermomechanical Pulp
DBH	Diameter at Breast Height
df	Degrees of Freedom
DNA	deoxyribonucleic acid
D.P.	Degree of polymerization
DRIFTS	Diffuse Reflectance Infrared Fourier Transform Spectroscopy
DSC	Differential Scanning Calorimetry
ELISA	Enzyme-linked Immunosorbent Assay
FD	Freeze-dried
FIFO	First-in First-out
FQA	Fibre Quality Analyzer
FTIR	Fourier Transform Infrared
GC/MS	Gas Chromatography/Mass Spectrometry
HCl	Hydrochloric acid
InGaAs	Indium Gallium Arsenide

IR	Infrared
ITS	Internal Transcribed Spacer
KCl	Potassium Chloride
LIF	Laser-Induced Fluorescence
LIFO	Last-in First-out
LWFL	Length Weighted Fibre Length
M	Molar
MEA	Malt Extract Agar
MLR	Multiple Linear Regression
mol	Moles
MRI	Magnetic Resonance Imaging
m/z	mass-to-charge ratio
NADH	Nicotinamide adenine dinucleotide
NADPH	Nicotinamide adenine dinucleotide phosphate
NaOH	Sodium hydroxide
Nd:YAG	Neodymium: Yttrium Aluminum Garnet
NIR	Near Infrared Spectroscopy
NMR	Nuclear Magnetic Resonance Spectroscopy
OCS	Outside Chip Storage
OD	Oven-dried
OSC	Orthogonal Signal Correction
Paprican	Pulp and Paper Research Institute of Canada
PAPTAC	Pulp and Paper Technical Association of Canada
PCA	Principal Component Analysis
PCR	Polymerase chain reaction

PCR	Principal Component Regression
PLS	Partial Least Squares
PRESS	Predicted Residual Sum of Squares
REA	Residual Effective Alkali
RFLP	Restriction Fragment Length Polymorphism
RH	Round hole
RMP	Refiner Mechanical Pulp
RMSECV	Root Mean Standard Error of Cross Validation
RMSEP	Root Mean Standard Error of Prediction
Rpm	Revolutions per minute
S_2	Secondary Wall, second layer
SERDS	Shifted Excitation Raman Difference Spectroscopy
SPF	Spruce, Pine and Fir
SS	Sum of Squares
Std. Dev.	Standard Deviation
SU	Sheffield Units
TAPPI	Technical Association of the Pulp and Paper Industry
TGA	Thermogravimetric Analysis
TMP	Thermomechanical pulp
TMS	Trimethylsilyl
UBC	University of British Columbia
U.S.	United States
UV	Ultraviolet
Vis	Visible
WR	White-rot

ACKNOWLEDGEMENTS

I would like to thank Paprican for their generous support of this research as well as for their personal support. I had the good fortune to work with many skilled Paprican employees and was aided by the strong intellectual, research-focused environment found at Paprican. Most importantly, I would like to thank my supervisor at Paprican, Paul Bicho, for his continual support and insight. Also, the assistance of Thanh Trung, Wai Gee, Surjit Johal, Bernard Yuen, Ashif Hussein, Maxwell McRae, Shannon Huntley, Val Lawrence, James Drummond and Kathy Woo is greatly appreciated.

I would like to thank my supervisor from UBC, Colette Breuil, and my committee members Shawn Mansfield and Mike Blades for their support.

Financial support from the Science Council of British Columbia's GREAT scholarship program, NSERC's industrial post-graduate scholarship program and Paprican is gratefully acknowledged.

Finally, on a personal note I would like to thank my wife, Rosalind Catchpole. She has been a consistent source of inspiration and strength. Without her love and support, and extensive proofreading and statistical consulting, this dissertation would not have been possible.

CHAPTER 1

General Introduction

This thesis describes the development and application of new methods for determining wood chip decay. This work is part of Paprican's fibre supply and quality program, and is focussed on providing solutions to help pulp mills store and utilize their fibre more effectively. Chapter 1 provides a context for this research by reviewing the nature of wood decay and exploring the ways in which it impacts Canada's pulp and paper industry. The merits of different methods of measuring decay and management options are discussed. Finally, the objectives of this research are outlined.

1.1 Industrial Relevance of Wood Decay

With over 4.1 million km^2 of forested land, Canada has approximately 10% of the world's forests (NRC, 2003, Rodden *et al.*, 2003). This vast resource contributes significantly to the Canadian economy, providing $28.5 billion of exports and directly employing 352 800 people in 2001 (Figure 1.1, NRC, 2003). The pulp and paper industry is one of the principal users of Canada's wood fibre and from it produces 16% of the world's wood pulp and 23% of the world's newsprint (NRC, 2003). Fibre supply is the most important component for producing pulp. Its cost typically represents 30 to 40% of the cost of pulp production (Rudder, 2002). As demand for wood and fibre products is projected to increase steadily, so too will the pressures on our fibre supplies (Simula, 2002). Effective wood procurement and utilization strategies are needed to protect fibre supplies. Moreover, procedures are needed to ensure that optimum value is extracted from the resource.

Decay can reduce the value of wood for pulping. To combat this threat we must first understand the differences between sound and decayed wood and how decay occurs.

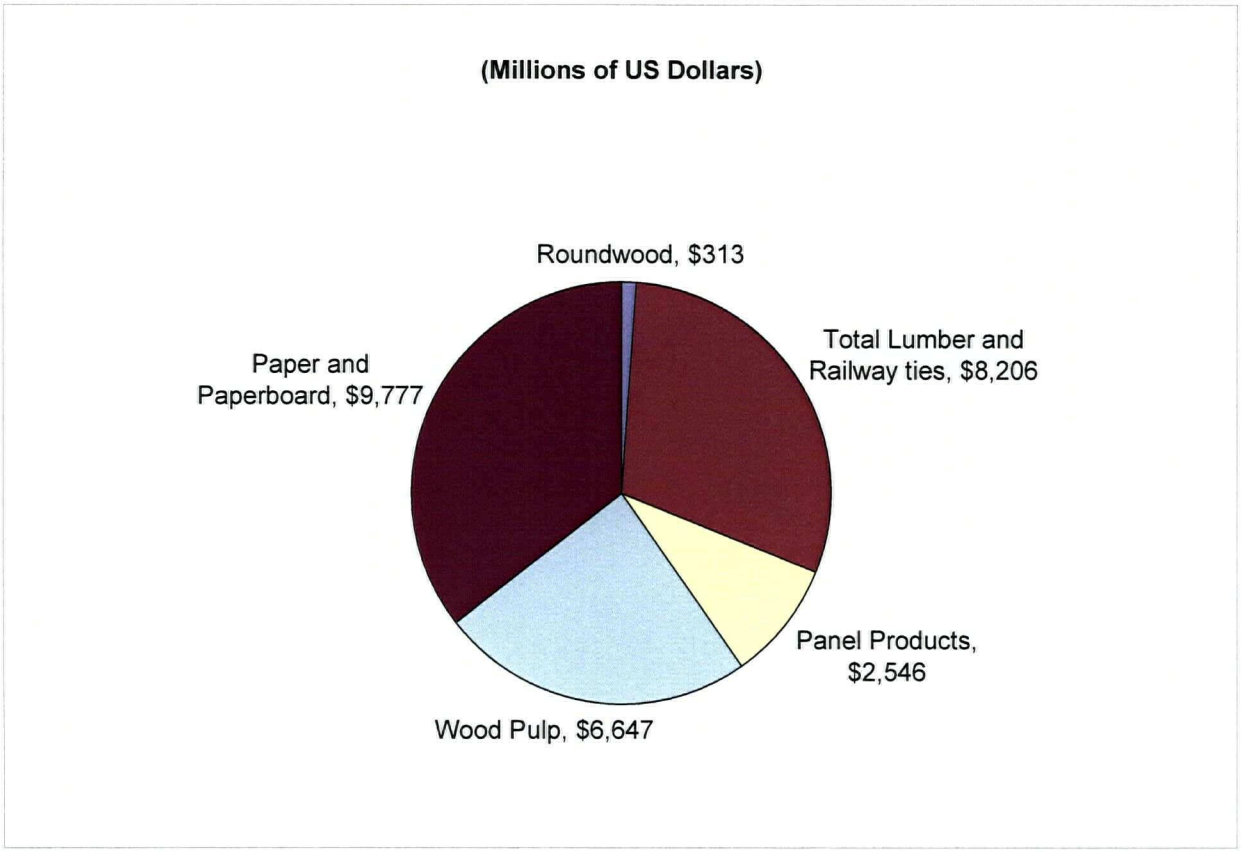

Figure 1.1 Canadian Forestry Exports, 2000 (Source: NRC, 2003)

1.2 Introduction to Wood

Forests cover approximately 30% of the world's landmass, and provide many social and economic benefits to humanity (FAO, 2001). Among these benefits is the production of wood, which is used for fuel, construction, pulp and a variety of consumer products. I shall give a brief introduction to wood chemistry and anatomy as a context for the work described in this thesis.

Taxonomically, trees are categorized by their Sub-Division as either Angiosperm or Gymnosperm. Angiosperms (hardwoods) produce seeds within ovaries, whereas gymnosperms (softwoods) produce a naked seed (Sjöström, 1993). Angiosperms and gymnosperms can also be differentiated by the chemistry and anatomy of the wood produced by the trees.

Wood is defined as the vascular support system of a tree; it is the tissue responsible for both support and conduction (Hoadley, 1990). In a tree, the wood (xylem) is surrounded by a

thin layer of cells called the cambium which produces new xylem and phloem cells. Bark (phloem) surrounds the cambium and serves to protect the tree. Economically, the xylem is the most important component of a tree.

The most significant anatomical differences are in the structure and function of the cells in the xylem. Hardwood xylem consists of vessel elements, which form vessels for conduction of water, and fibres, which provide structural support. Hardwoods also contain libriform and ray parenchyma cells (Sjöström, 1993). Softwood xylem consists primarily of longitudinal tracheids, which provide both conduction and structural support. Softwoods also contain parenchyma cells for storage and ray cells for lateral transport (Sjöström, 1993).

The principal chemical components of wood are cellulose, hemicellulose, and lignin. A diverse range of compounds known as extractives, as well as small amounts of protein and inorganic compounds, are also found in wood. The components of wood vary both qualitatively and quantitatively between hardwoods and softwoods (Table 1.1).

Table 1.1 Organic Constituents of Wood

Type	Cellulose (%)[1]	Hemicellulose (%)[1]	Lignin (%)[1]
Hardwoods	42-48	15-35	18-25
Softwoods	40-44	20-32	25-35

[1]As dry weight of extractive-free wood.
Source: Bowyer *et al.*, 2003, p. 48.

The most abundant and economically significant wood component is cellulose, a linear polymer of D-glucopyranose joined by β-1,4-glycosidic bonds with a degree of polymerization up to 10 000 (Sjöström, 1993). Figure 1.2 shows a cellobiose subunit, as it would be found in a chain of cellulose. Cellulose gives wood and wood pulps much of their tensile strength.

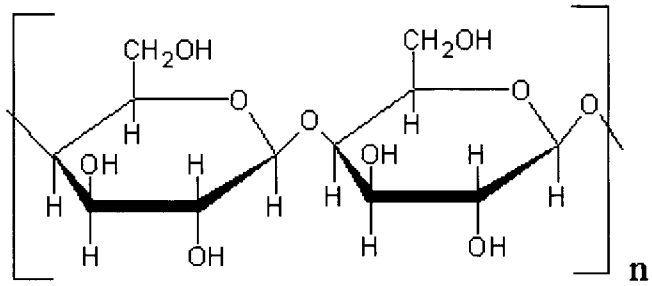

Figure 1.2 Two β-D-Glucopyranose subunits in a cellulose molecule

Hemicelluloses consist of a number of heteropolymers comprised of various carbohydrates such as glucose, xylose, mannose, galactose, arabinose and uronic acids. Hemicelluloses typically have a degree of polymerization between 150 and 200 for hardwoods and 50 to 300 for softwoods (Baeza and Freer, 2001). Typical hardwood hemicelluloses include O-acetyl-4-O-methylglucuronoxylans and glucomannans, while softwoods typically contain partially acetylated galactoglucomannan and arabino-4-O-methylglucuronoxylan (Baeza and Freer, 2001).

Lignin is a 3-dimensional polymer formed by the enzymatic dehydrogenation of phenolpropanes followed by radical coupling (Sakakibara and Sano, 2001). In softwoods it is primarily comprised of coniferyl alcohol monomers, while in hardwoods it is made up of both coniferyl and sinapyl alcohol monomers. These monomers are linked by a variety of different linkages. The most common inter-unit linkage in both hardwoods and softwoods is the arylglycerol-β-aryl ether (β-O-4) linkage (Sjöström, 1993). Other linkages between lignin monomers found in hardwoods and softwoods include: α-O-4, β-5, 5-5, 4-O-5, β-1, and β-β (Sjöström, 1993). In combination with polysaccharides, lignin gives wood its compressive strength and rigidity (Hocking, 1998). Figure 1.3 shows a portion of the structure of spruce lignin (Hocking, 1998).

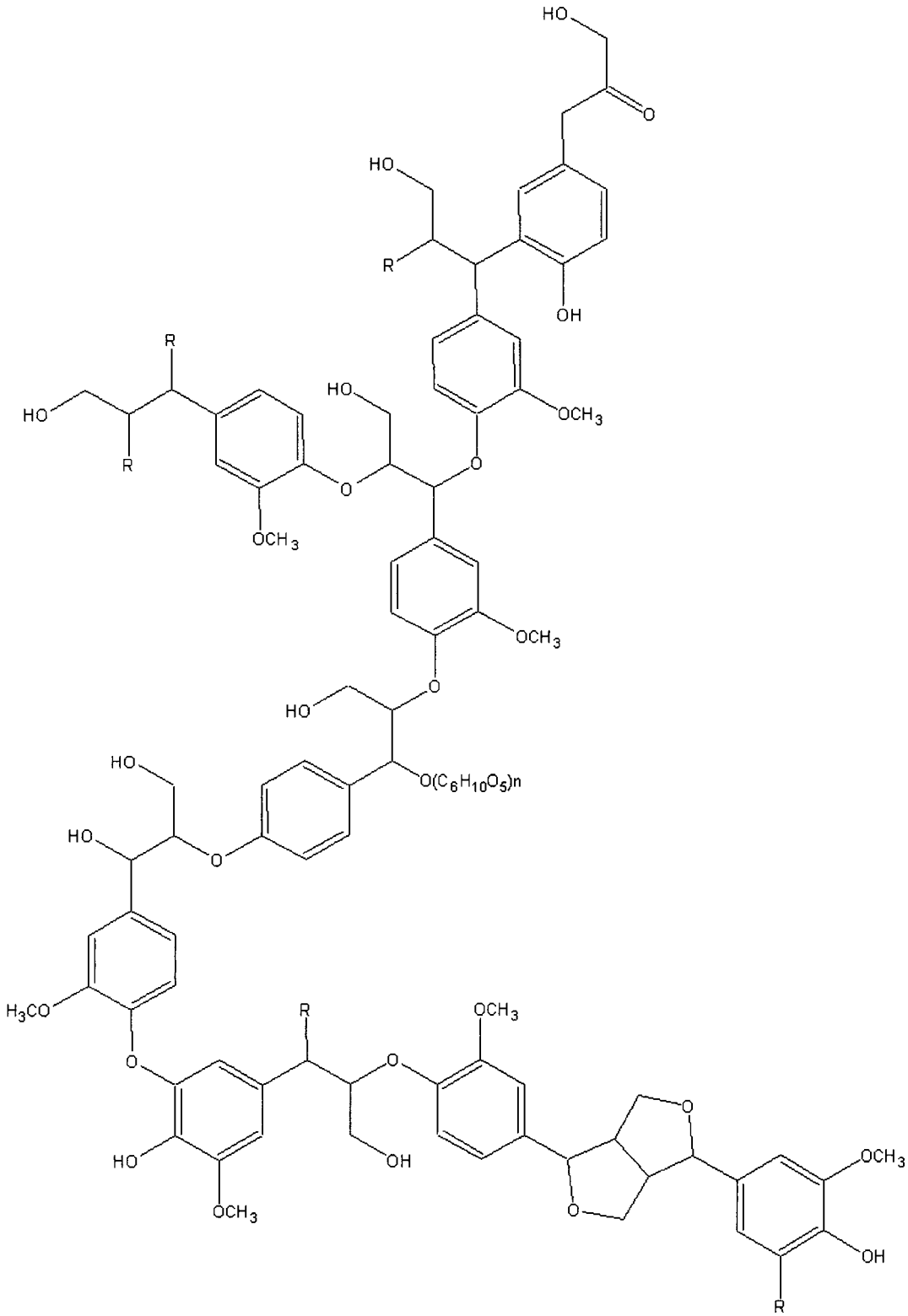

Figure 1.3 Structure of Some Softwood Lignin Subunits

Extractives are an eclectic group of chemicals that give wood its colour, smell and contribute to its durability (Umezawa, 2001). Extractives typically make up between 0 to 10% of wood and include lignans, flavonoids, stilbenes, terpenoids, steroids, tropolones, quinones, tannins, sugars, glycerides, waxes, phenolics, starches, fats and fatty acids (Umezawa, 2001).

A typical wood cell is a straw-like structure consisting of several layers. Beginning at the outermost point and progressing inward, there is the middle lamella, a primary wall, and a secondary wall, which consists of three layers: S_1, S_2 and S_3 (Côté, 1976). The middle lamella and primary wall, collectively termed the compound middle lamella, are thin and highly lignified. The secondary wall is much thicker and contains the highest concentrations of cellulose and hemicellulose. The S_2 layer is the thickest layer in the secondary wall, typically varies between 1 and 5 μm in thickness (Sjöström, 1993). The cellulose is arranged into microfibrils, which provide the cell with its strength. The angle between the microfibrils and the longitudinal axis of a fibre is called the microfibril angle. This angle has a significant impact on the tensile strength and elastic modulus of the fibre (Mark and Gillis, 1973, Page *et al.*, 1972, Yang and Evans, 2003).

Wood chemistry, morphology and ultrastructure vary significantly between species, sites and within a single tree. The different types of fibres/tracheids found in trees will be briefly discussed.[1] Alternating earlywood and latewood fibres give rise to the ringed structure of wood in cross-section. Earlywood is formed in the spring and has thinner cell walls and wider lumina for efficient water transport, while latewood is formed in the summer and has thick cells walls for increased strength (Fujita and Harada, 2001). Heartwood, which is found in the interior of the tree, is often darker due to the deposition of extractives and provides structural support for the tree (Fujita and Harada, 2001). The outer portion of the xylem, sapwood, provides structural

[1] The word "fibre" is often used loosely to include both softwood and hardwood cells. I will use this definition throughout this thesis.

support, stores nutrients, and conducts water (Fujita and Harada, 2001). Fibres can also be classified as juvenile or mature wood. Juvenile wood fibres are formed by the vascular cambium in the crown (the top of the tree) and where it is under the influence of the apical meristem. As a tree grows, the vascular cambium, no longer under the influence of the apical meristem, forms mature wood (Bowyer *et al.*, 2003). Juvenile wood has more lignin, thinner cell walls and shorter fibres than mature wood (Bowyer *et al.*, 2003).

When a tree is growing at an angle, gravitational forces induce the formation of reaction wood to provide structural support for branches (Sjöström, 1993). Hardwoods produce a type of reaction wood called tension wood on the upper side of leaning stems and branches. Tension wood contains thick-walled fibres with a gelatinous layer of highly crystalline cellulose in the secondary fibre wall (Sjöström, 1993). Softwood reaction wood is called compression wood, and is produced on the lower side of leaning stems and branches. Compression wood is characterized by short, thick-walled tracheids with rounded ends, a thicker S_1 layer, helical striations in the S_2 layer and the absence of the S_3 layer (Sjöström, 1993).

The value derived from wood depends to a large extent on the chemical and morphological properties of the wood. Optimizing these properties and the processes that derive value from them is critical to effectively manage fibre supply.

1.3 Decay Fungi

Wood decay is the biochemical and enzymatic degradation of wood, and is caused primarily by fungi. Fungi are eukaryotic heterotrophs that utilize carbon compounds for energy (Zabel and Morrell, 1992). They can take either a unicellular form (yeasts) or a filamentous form. Filamentous fungi are made up of long tube-like cells called hyphae, collectively referred to as a mycelium.

Fungi are grouped into four phyla based on sexual spore production: Ascomycota, Basidiomycota, Chytridiomycota and Zygomycota. A fifth group, the Deuteromycota (Fungi Imperfecti), either lack a sexual stage or it has not been identified in their life cycle, and thus do not fit into this system. Deuteromycota are a "catch all" group with few relationships to one another; however, many bear resemblance to the asexual stages found in Ascomycota (Eriksson and Winka, 1998). Fungal taxonomy is frequently revised, as sexual stages in some Deuteromycota are discovered or as new information becomes available. Most wood decay fungi belong to the Ascomycota, Basidiomycota or Deuteromycota.

Ascomycota and Basidiomycota can reproduce either sexually or asexually. In the Ascomycota, sexual spores are produced inside a sac-like structure called an ascus. Asci are often found in specialized structures called fruiting bodies (Zabel and Morrell, 1992). In the Basidiomycota, sexual spores are formed on top of a club-shaped structure called a basidium (Zabel and Morrell, 1992). Basidia are often found in large sexual structures such as mushrooms or bracket fungi. Asexual reproduction can take place through budding, as in yeasts, or through the formation of asexual spores called conidia (Zabel and Morrell, 1992).

Wood decay fungi are commonly classified into three categories based on their effect on wood: white-rot, brown-rot, and soft-rot. White-rots and brown-rots primarily belong to the Basidiomycota, whereas soft-rot fungi belong to either the Ascomycota or Deuteromycota. Each group of wood decay fungi has a unique way of metabolizing wood. Within these groups there is also considerable variation between taxa.

White-rot fungi are a diverse group capable of degrading cellulose, hemicellulose and lignin (Blanchette, 1995). They can colonize cell lumen and erode the entire cell wall, or preferentially remove lignin leaving white pockets of delignified wood (Blanchette, 1995). A single fungus can exhibit both types of degradation in wood (Blanchette, 1995). Fungal species

and environmental conditions control the rate of lignin and polysaccharide degradation (Blanchette, 1980).

Cellulose degradation in white-rot fungi can occur both enzymatically and non-enzymatically. The enzymatic process is controlled by three major groups of enzymes: endo-β-1,4-glucanases, exo-β-1,4-glucanases and β-1,4-glucosidases (Hegarty *et al.*, 1987). Endo-β-1,4-glucanases leave non-reducing ends of cellulose chains on the outer microfibrils. These are then hydrolyzed by exo-β-1,4-glucanases to yield cellobiose which is cleaved by a β-glucosidase to yield glucose, which can be metabolized by the fungus (Highley and Dashek, 1998). This process is repressed by glucose and induced by cellulose (Highley, 1973).

Non-enzymatic cellulose degradation in white-rot fungi occurs when oxidative enzymes produce chemical species such as hydroxyl radicals, superoxide anions and singlet oxygen (Highley and Dashek, 1998). These very small, reactive molecules are able to permeate into microfibrils and react with cellulose chains facilitating enzymatic attack on the outer walls (Hammel *et al.*, 2002).

Generally, hemicellulose degradation in all decay fungi occurs via endo-acting glycosidases specific for different hemicellulose classes. It is, however, complicated by the presence of different sugars and sugar linkages (Highley and Dashek, 1998). Mannanases and xylanases attack their respective hemicelluloses, breaking them into increasingly smaller chains. Glycosidases then hydrolyze these short chain polymers to their simple sugars (Highley and Dashek, 1988). Acetyl esterases are also produced to cleave acetyl groups found attached to many of the sugars (Zabel and Morrell, 1992).

Lignin degradation by white-rot fungi is a process begun in secondary metabolism and initiated by nitrogen, carbon or sulphur limitation (Dass *et al.*, 1995). Oxidases, peroxidases, laccases and aryl alcohol oxidases can be involved in lignin degradation by white-rot fungi (Highley and Dashek, 1998). In the model species *Phanerochaete chrysosporium*, two types of

peroxidases dominate: manganese peroxidase and lignin peroxidase (Bonnarme and Jeffries, 1990, Wariishi *et al.*, 1992). Manganese peroxidase generates Mn (III) is highly reactive and can diffuse to attack the lignin (Bonnarme and Jeffries, 1990). Lignin peroxidase abstracts a single electron from aromatic structures in the lignin which leads to radical cation formation and subsequent cleavage (Bonnarme and Jeffries, 1990). Lignin peroxidase does not diffuse into non-decayed areas (Srebotnik *et al.*, 1988). A source of hydrogen peroxide is necessary for these peroxidase systems to function (Highley and Dashek, 1998, Wariishi *et al.*, 1992), can be synthesized by one of two mechanisms: (1) Manganese peroxidase with O_2 in the presence of NADH, NADPH or glutathione, or (2) glyoxal oxidase, an enzyme produced during secondary metabolism (Highley and Dashek, 1998). These enzymes can cause, either directly or through induced radical reactions, demethylation, oxidation of α-carbon atoms, side chain cleave, β-aryl ether cleavages and hydroxylation of aromatic rings (Zabel and Morrell, 1992). The exact mechanism of lignin degradation by the model species *Phanerochaete chrysosporium* is still not fully understood. The endeavour to understand the mechanism is complicated by the large diversity in the enzymes produced by different white-rot species (Highley and Dashek, 1998).

Brown-rot fungi consume only the carbohydrates, leaving a modified lignin behind (Blanchette, 1995, Smith, 1974). Although the utilization of wood is not as complete as with white-rot fungi, brown-rot fungal attack can be more devastating because the polysaccharides degraded are responsible for much of the strength properties associated with the wood fibres (Blanchette, 1995, Zabel and Morrell, 1992). The S_2 layer of the secondary cell wall is often attacked first because of its accessibility and relatively high polysaccharide concentration (Curling *et al.*, 2002).

The degradation of polysaccharides by brown-rot fungi is also both an enzymatic and a non-enzymatic process. The initial stages of brown-rot decay are thought to be non-enzymatic, since enzymes are too large to penetrate the sound wood (Blanchette, 1995, Green *et al.*, 1991,

Jensen *et al.*, 2001). Incipient brown-rot decayed cellulose, which contains increased carbonyl and carboxyl groups, is similar to cellulose treated with acid hydrolysis or Fenton's reagent (Blanchette, 1995, Espejo and Agosin, 1991). Small diffusible acids, such as oxalic acid, penetrate the wood and degrade the polysaccharides by Fenton-type chemistry, which produces hydroxyl radical from Fe^{2+} and hydrogen peroxide that can indiscriminately attack the polysaccharides degrading hemicelluloses and depolymerising cellulose in amorphous regions (Blanchette, 1995, Green *et al.*, 1991, Jensen *et al.*, 2001, Jordan *et al.*, 1996, Shimada *et al.*, 1997). Following the initial attack, the wood fibre is left vulnerable to degradation by cellulases and hemicellulases (Green *et al.*, 1991). Unlike white-rot fungi, brown-rot fungi lack an exo-1,4-β-glucanase (Zabel and Morrell, 1992). However, with the non-enzymatic methods of degradation, only endo-1,4-β-glucanases and glucosidases are required for cellulose degradation. These enzymes, as well as the enzymes involved in hemicellulose degradation, are analogous to those produced by white-rot fungi (Zabel and Morrell, 1992).

Although brown-rot fungi do not degrade lignin to the same extent as white-rot fungi, they do modify it in several important ways. Hydroxyl radicals produced by brown-rot fungi to enable enzymatic attack on polysaccharides also react rapidly with lignin (Hammel *et al.*, 2002). Lignin from brown-rot decayed wood has increased caustic solubility, decreased methoxy content, increased carboxylic acid groups generated from the oxidation of alcohol and aldehyde groups, increased phenolic hydroxyl groups and cleaved aromatic rings (Highley and Dashek, 1998, Zabel and Morrell, 1992).

Soft-rot fungi can be divided into two types: type I, which attack carbohydrates in the S_2 layer of the cell wall forming longitudinal cavities, and type II, which degrade the wood cell wall from the lumen outward (Daniel and Nilsson, 1998, Zabel and Morrell, 1992). Soft-rot fungi preferentially remove the polysaccharide fraction (Daniel and Nilsson, 1998). They can also

remove lignin, although they exhibit a preference for syringyl lignin and are not as aggressive as white-rot fungi (Daniel and Nilsson, 1998).

There are few studies on enzymes produced by soft-rot fungi (Daniel and Nilsson, 1998, Zabel and Morrell, 1992). Like brown-rot decay, soft-rot decay is focussed on utilizing polysaccharides; however, the hydrolytic enzymes produced by soft-rot fungi are analogous to those produced by white-rot fungi (Zabel and Morrell, 1992). The enzymes involved in lignin degradation by soft-rot fungi are not well understood (Daniel and Nilsson, 1998, Zabel and Morrell, 1992). Similarly, degradation by non-enzymatic means is poorly understood, although reactive oxygen species have been implicated (Hammel *et al.*, 2002).

Non-decay fungi, which include moulds, yeasts and staining fungi, do not normally cause significant damage in comparison to decay fungi. They utilize extractives and water-soluble starches but do not cause significant fibre damage. Wood decaying, anaerobic bacteria can cause significant degradation, particularly in water-saturated wood with high extractives and phenolic content (Blanchette, 1995). They operate by one of three mechanisms: tunnelling, erosion or cavitation (Blanchette, 1995). Decay is typically slow even under favourable conditions. However, bacteria can act indirectly to promote wood decay by increasing permeability, which consequently aids fungal colonization (Zabel and Morrell, 1992). Since decay caused by bacteria is rare under typical wood chip storage conditions, it will not be considered in this thesis. In this thesis, the term decay will be limited to the degradation of wood caused by white-, brown- or soft-rot fungi.

1.4 Sources of Decay

Decay may enter the fibre supply either from harvesting decayed stands or from prolonged or improper wood storage.

1.4.1 Decay in the Forest

Decay fungi can attack living trees through roots or wounds caused by fire, lightning, animals, insects, branch stubs or machinery. Although decay is a natural part of forest ecology and is essential for nutrient recycling of dead wood, it is undesirable in living trees intended for commercial use. Decay of living trees can be limited by reducing damage to trees and by removing decayed trees, which can serve as a source of inoculum. Restricting pruning to branches that are less than 30 mm in diameter and to times when occlusion will be most rapid can help to limit the spread of decay (Montagu *et al.*, 2003). Paints and sealants can also be effective ways to prevent infection from pruning, but are often prohibitively expensive (Montagu *et al.*, 2003). Ensuring careful logging operations is also necessary to protect remaining trees (MacLeod, 1967). Stand age should be considered by forest managers when they choose to harvest a site, especially when dealing with species or sites prone to decay, because decay increases with stand age (MacLeod, 1967).

In Canada, the exact amount of decay in trees is unknown; however, stem rots and decay are estimated to result in the loss of approximately 25 million cubic metres of wood per year (MacLeod, 1967, Singh, 1993). Hunt (1978a) estimated that 17.5% of the total wood volume in trees with a diameter-at-breast-height (DBH) greater than 10 cm had some decay. In aspen, a species very susceptible to decay, the incidence of stem decay is estimated to be 25% across the country, and up to 75% in Western Canada (Knoll *et al.*, 1993). Often, decayed wood is harvested in greater proportions than it exists naturally to facilitate returning the forest to a productive state. In areas of insect epidemic, such as the Spruce Bud Worm in Eastern Canada or the Mountain Pine Beetle in British Columbia, infested and subsequently decayed stands may be harvested more rapidly to salvage fibres that can be recovered prior to a major outbreak of decay (Basham, 1984). Since decayed wood is often removed during logging operations and since it

cannot be used in the solid wood products industry, a disproportionate amount of this decayed wood enters pulp and paper fibre supplies.

1.4.2 Decay in Storage

Outside stored wood chip piles are the most common means of fibre storage for the pulp and paper industry. Outside chip storage (OCS) is used to ensure a continuous supply of fibre (Fuller, 1985, Hajny, 1966). It has many advantages over storing logs, including lower costs of handling, transportation, labour and storage (Hajny, 1966, Nilsson, 1973). Moreover, with wood products residuals being a major source of fibre, whole log storage is no longer an option (Fuller, 1985).

OCS has several drawbacks, including yield and extractive losses, poorer pulp quality and increased consumption of pulping and/or bleaching chemicals (Hajny, 1966, Hatton, 1970, Smith and Hatton, 1971). Yield losses, based on the amount of wood entering a chip pile, occur primarily from losses of wood material prior to pulping. Wood losses of approximately 0.75% per month for pine and 0.65% per month for spruce are typical for OCS (Hatton, 1970). Much of the wood substance loss can be attributed to loss of extractives (Hatton *et al.*, 1969). This can be detrimental to kraft mills that sell tall oil and turpentine; however, it is beneficial where extractives lead to pitch deposition on machines, felts and screens, excessive foaming in washers, discoloured pulps and increased bleaching costs (Levitin, 1967, Schmidt, 1990). Pulp yield losses, based on the amount of wood entering the digester, can occur at high temperatures when acid hydrolysis reduces cellulose degree of polymerization or when brown-rot fungi predominate (Hatton and Hunt, 1972, Procter, 1973). Pulp quality can also be diminished during OCS. Although there is considerable variance between mills, a loss of tear index appears to be the most prevalent problem followed by burst index, folding endurance and brightness (Eslyn and Lindgren, 1961, Hajny 1966, Hatton and Hunt, 1972).

Over the past 40 years chip inventories have been reduced, which, since the drawbacks of OCS are exacerbated with time, limits many of the losses (Hajny, 1966, McDonald and Twaddle, 2000). Sixty percent of U.S. mills now have a maximum inventory of less than 15 days with similar inventories likely in Canada (McDonald and Twaddle, 2000). Despite these short storage times, mills are still concerned with losses due to fungal decay, and losses of by-products and brightness (McDonald and Twaddle, 2000).

Wood chip pile conditions are diverse and dynamic. Above ambient temperatures, increased surface area and increased availability of nutrients allow many species of fungi to grow (Table 1.2). As a result of this unique environment, the fungi that grow in chip piles are often different from those commonly found in the forest (Lindgren and Eslyn, 1961). Decay fungi may enter chip piles from spores that are transported on the wood, or by wind, rain, insects and contact with soil. The fungi that grow in chip piles depend on the environmental conditions of the pile such as wood species, moisture content, temperature, and pH, as well as geographical location, season, and ecological factors, such as interactions with bacteria and other fungi.

Moisture in chip piles varies significantly (Hajny, 1966, Hatton, 1970). Wood moisture content in the pile's interior decreases as the pile heats up. In large piles, where the interior remains hot, water evaporates in the interior and condenses in the cooler, upper regions of the pile (Hajny, 1966, Hatton, 1970). This "chimney effect" results in the lower interior region of the pile becoming dry, while the upper region of the pile becomes wet (Hajny, 1966). In smaller piles, where the interior of the pile cools off after the initial temperature rise, the moisture content re-equilibrates so that moisture content is fairly uniform throughout the pile (Hajny, 1966). The optimal moisture content for most basidiomycetes is between 40 and 80 % (Nicholas and Crawford, 2003). The amount of moisture tolerable by many basidiomycetes is limited by their access to oxygen (Nicholas and Crawford, 2003). Since soft-rot fungi have a greater tolerance for low oxygen concentration, they are able to grow in environments that are too wet

for basidiomycetes (Nicholas and Crawford, 2003). Chip pile interiors may inhibit fungal decay not only by high temperature, but also from low moisture content. Conversely, the region of high moisture content at the top of a pile may be too wet for fungal growth.

Table 1.2 Fungi Commonly Found in Wood Chip Piles

Acrotheca sp.[9]	*Gliomastix subiculosa*[6]	*Phialophora* spp.[1,4,5,9]
Allescheria terrestris[1,3,5,8]	*Gloecystidium tenue*[8]	*Phomopsis* sp.[6]
Alternaria sp.[1,4]	*Gloeophyllum separium*[4]	*Pinocladiella masonii*[5]
Arthobotrys sp.[9]	*Graphiopsis* sp.[9]	*Polyporus* sp.[1,2,4,5,7,8]
Ascocoryne sarcoides[1]	*Graphium* spp.[1,4,6]	*Poria ambigua*[2,8]
Aspergillus sp.[1,5,6,9,10]	*Harpographium* sp.[1]	*Ptychogaster* sp.[1]
Aureobasidium sp.[1,4,5]	*Helicosporium* sp.[9]	*Pyrenochaeta* sp.[1]
Bactrodesmium sp.[9]	*Hormodendrum* sp.[1]	*Rhinocladiella* sp.[1]
Bispora sp.[1,9]	*Humicola* sp.[1,4,5,6,8,10]	*Rhizopus arrhizus*[5]
Bisporomyces sp.[9]	*Hyphodontia* sp.[1]	*Rhodotorula* sp.[1]
Brachysporiella sp.[1]	*Hypoxylon rubiginosum*[1]	*Saccharomyces* spp.[1]
Byssochlamys spp.[1]	*Lenzites saepiaria*[1]	*Scopulariopsis* sp.[8,10]
Calcarisporium sp.[1]	*Leptographium* sp.[4,9]	*Scytalidium* sp.[1,5]
Candida sp.[6]	*Libertella betulina*[7]	*Sistotrema* sp.[1,5,8]
Cephaloascus fragrans[1]	*Malbranchea pulchella*[6]	*Sistotremastrum suecium*[8]
Cephalosporium sp.[1,6]	*Melanographium* sp.[9]	*Sphaeropsis* sp.[6]
Ceratocystis sp.[1,4,5,9]	*Merulius tremellosus*[2,5,8]	*Spicaria* sp.[9]
Chaetomium sp.[4,5,6,8,9]	*Mucor* sp.[8]	*Spondylocladium* sp.[9]
Chrysosporium sp.[1,2]	*Myrothecium* sp.[10]	*Sporobolomyces* sp.[1]
Cladosporium sp.[1,5,10]	*Odontia bicolor*[2,5]	*Sporotrichum* sp.[1,5,8,9]
Cladotrichum sp.[9]	*Oedemium didymum*[1]	*Stereum* sp.[2,5,7,8]
Cochliobolus lunatus[6]	*Ophiostoma* sp.[4]	*Streptomyces* sp.[6]
Coniothyrium fuckelii[1]	*Papulospora* sp.[6]	*Talaromyces emersonii*[3,5]
Cordana pauciseptata[1]	*Paradiplodia* sp.[9]	*Thermoascus aurantiacus*[3,8]
Corticium sp.[1,7,8]	*Parodiella* sp.[6]	*Trametes versicolor*[4]
Curvularia sp.[6]	*Paecilomyces* sp.[1,5,6]	*Trechispora raduloides*[8]
Cylindrocephalum sp.[1]	*Penicillium* spp.[1,5,6,8,10]	*Trichocladium canadense*[1]
Epicoccum nigrum[6]	*Peniophora* sp.[1,2,5,7,8]	*Trichoderma* sp.[1,5,6,9]
Fomitopsis rosea[4]	*Pestalotia* sp.[6,9]	*Verticicladiella brachiata*[1]
Fusarium sp.[1,6,9]	*Phanerochaete chrysosporium*[5]	*Verticillium terrestre*[1]
Geotrichum sp.[6]	*Phanerochaete gigantea*[4]	*Xeromphalina campanella*[1]
Gliocladium sp.[1,5,9]	*Phialocephala bactrospora*[1]	

[1] Shields, 1969. [2] Nilsson, 1973. [3] Smith, 1973. [4] Zabel and Morrell, 1992.
[5] Hulme, 1979. [6] Greaves, 1973. [7] Henningsson, 1967. [8] Nilsson, 1965.
[9] Lindgren and Eslyn, 1961. [10] Eklund *et al.*, 1973.
[*] Fungal taxonomy is constantly changing. Names listed are from the primary sources.

White-rot fungi are more commonly found in hardwoods and brown-rot fungi are more commonly found in softwoods (Hajny, 1966, Schwarze *et al.*, 2000). Only Type I soft-rot fungi can fully utilize guaiacyl-lignin; as a result type II soft-rot fungi are rare in softwoods (Nilsson *et al.*, 1989). Many species of fungi can be present in a single chip pile, and although their interactions have been investigated, in general they are poorly understood due to the multitude of factors that affect fungal ecology in wood chip piles (Zielinski, 1988).

Chip pH decreases with increasing pile height and time (Hatton, 1970). The hot interior of the pile facilitates the hydrolysis reactions necessary to release acetic acid and drop chip pH (Springer and Hajny, 1970). Most decay fungi grow best in an environment with pH between 3 and 6 (Nicholas and Crawford, 2003). Only in the most severely affected piles would pH be too low for fungal growth, and in these situations pulp yield and quality will already be compromised by the acidic environment.

The degradation processes that occur in OCS vary with pile temperature. Frozen chips in OCS are not degraded (Hatton *et al.*, 1969). Ambient temperatures below 5°C inhibit the respiration of parenchyma cells and, as a result, piles do not heat up (Hulme, 1979). Between 5°C and 45°C, parenchyma cells respire and release heat, enabling the growth of bacteria, moulds and decay fungi (Fuller, 1985, Hulme, 1979, Springer and Hajny, 1970). Temperatures between 20°C and 50°C are optimal for the growth of most species of decay fungi (Zabel and Morrell, 1992). Chips stored in this temperature range are susceptible to wood substance and quality losses from fungal decay. If air circulation is limited by high fines content, compaction from tractors or excessive chip pile height, temperatures will continue to rise from fungal growth (Fuller, 1985). Mesophilic fungal decay is minimal above 50°C (Hulme, 1979). However, despite inhibiting decay by most fungi and running a low risk of fire, the temperature range between 50°C and 60°C does allow hydrolysis and autoxidation reactions to occur (Saunders and Singh, 1988, Springer and Hajny, 1970). Hydrolysis cleaves acetyl groups from hemicelluloses,

resulting in lower pH (Feist *et al.*, 1973, Fuller, 1985, Kubler, 1982). Autoxidation is a process in which fatty acids, resin acids and terpenes found in the wood chips react with atmospheric oxygen to produce organic acids and heat (Saunders and Singh, 1988). The increased heat perpetuates the process while the resulting acids further the deacetylation of the hemicelluloses. This in turn liberates more acids that can degrade hemicellulose and eventually depolymerise the cellulose and modify the lignin (Fuller, 1985). At 80°C and above, chip piles are likely to combust if exposed to air, resulting in substantial losses of fibre and posing safety and environmental hazards (Fuller, 1985). High fines or bark content and metal contamination dramatically increase the risk of fire (Hulme, 1979).

1.5 Wood Chip Quality

Chip quality is a measure of how suitable a chip is for a given use. It describes a number of factors including wood species, fibre type (sapwood/heartwood, juvenile wood/mature wood, normal wood/compression or tension wood, earlywood/latewood), chip dimensions, chip size distribution, bark content, presence of contaminants, bulk density and decay content (McGovern, 1979). A number of these properties are influenced by biogeoclimatic factors and genetics (Bennett, 1997). Biogeoclimatic factors are controlled by the location of the growing site. Genetic factors cannot be controlled in first-growth stands, however, in plantations, tree genetics can be controlled by selected planting.

Chip dimensions, size distribution and uniformity are the most significant factors affecting chip quality. For chemical pulping, chip size, especially thickness, is critical as it affects the rate of liquor penetration, whereas for mechanical pulping chip size is secondary to chip size uniformity, which affects refining energy and the degree of fibrillation (Barnes, 1979). Softwood chips are typically classified as oversize (> 45 mm round hole (RH)), overthick (> 10 mm slot), accepts (> 7 mm RH), pins (> 3 mm RH) and fines (< 3 mm RH). Hardwood chips are

often classified using a narrower slot because chip thickness has a greater impact on the amount of screened rejects than in softwoods (Hartler, 1996, Hatton, 1977).

Pulp mills typically either screen out or re-chip oversized chips (Hartler, 1996). However, if present at low levels oversized chips are often ignored, which can result in slightly lower kraft pulp quality and higher screen rejects (Hartler, 1996). Overthick chips are often screened out, and are either split along the grain into thinner chips or compressed to induce cracks (Hartler, 1996). When untreated, overthick chips result in minor increases in wood consumption and screen rejects (Hartler, 1996, Svedman *et al.*, 1998). Pins are most often tolerated, but may be separated and used for fuel or added at low levels to improve uniformity while fines are usually removed by screening prior to pulping and used as fuel (Hartler, 1996). Excessive pins and fines can result in the liquor extraction screens in continuous digesters becoming plugged, as well as decreased kraft pulp yield and quality, and poorer pulp uniformity (Hatton, 1975).

Chip size is largely determined by the type of chipper and how it is used, although wood species, wood moisture, season and decay contents will also have an impact (Hatton, 1977, Hunt, 1978). In general, chipping edgers produce fewer pins than chipper canters, which in turn, produce fewer pins than chipping head rigs (Hatton, 1975). Temperature, disc speed and knife angle all impact the quality of the chips produced from a disc chipper (Stuart and Leary, 1992). Regular maintenance and precision control are required to consistently produce high quality chips (Bennett, 1997, Shaw, 2000). Chipper setting should be optimized for the type of wood entering the chipper (whole logs vs. slabs) and for the wood species being chipped (Hatton, 1975, Stuart and Leary, 1992).

Seasonal variations have a significant impact on chip quality (Fuhr *et al.*, 1998, Hatton, 1977). Chipping frozen wood results in an increase in pins and fines production (Hatton, 1977). Debarking frozen wood is also more difficult, resulting in increased bark content in the winter

(Fuhr *et al.* 1998, Hatton, 1977, Hatton, 1987). Bark contamination results in increased equipment wear, decreased kraft pulp yield and quality, increased chemical consumption, poorer pulp machine drainage, decreased brightness in mechanical pulps, increased dirt counts and decreased runnability of newsprint (Fuhr *et al.*, 1998, Hartler, 1996, Hatton, 1987). Bark is most easily removed in the spring when the cambium is active and immature cells are being produced (Hatton, 1987).

1.6 The Effects of Decay

Decayed wood impacts many steps along the supply chain, from harvesting to the properties of the final products. Initial losses due to decay are incurred during the harvesting and transportation of rotten logs due to increased breakage (Hatton, 1978, Hunt and Hatton, 1979). Further wood losses are incurred during chipping due to increased fines formation (Hunt, 1978, Procter, 1973). When decayed wood is kraft pulped, yield losses based on the mass of chips entering the digester occur because of the chemical degradation of the wood carbohydrates by fungal decay and the corresponding increase in caustic solubility. There is also an increase in demand for effective alkali to reach a target kappa number (Hunt and Hatton, 1979). Economically, the loss of yield is the most significant consequence of chip decay.

Kraft pulp produced from decayed wood has poorer properties than pulp produced from equivalent sound wood, including, lower tear, tensile and burst indices, folding endurance, stretch, and brightness (Hunt, 1978a, Hunt, 1978b, Mischki *et al.*, 2005, Procter, 1973). Variability in these pulp properties arises when the decay content of the chip furnish is not controlled. Maintaining a constant level of decay helps to minimize the variation of pulp properties; however, this is typically not technically feasible, due to limited chip handling capabilities, and so it is not a common practice. Non-uniformity of decay content in the furnish leads to variable alkali consumption, pulp yield and pulp quality (Hunt, 1978b).

The type of decay has a significant impact on subsequent kraft pulp quality. Pulping white-rot decayed wood results primarily in lower yields; however, losses in brightness, and burst, tear and tensile strength may also be observed (Messner, 1998, Procter, 1973). Brown-rot fungi degrade the cellulose, thus, brown-rot decayed wood has a higher concentration of lignin, which when pulped results in increased alkali consumption and recovery boiler loading (Hunt, 1978). Brown-rot can have such a negative impact on kraft pulp yield and properties that Hunt (1978b) recommended avoiding kraft pulping of wood heavily decayed by brown-rot fungi. Some kraft pulps produced from advanced brown-rot decayed samples have been shown to be so weak that handsheets could not be couched and, thus, no strength values obtained (Hunt, 1978b). The negative effects from pulping soft-rot decayed wood chips are minor, but include yield loss, decreased tall oil yield, and consumption of active alkali (Chong and Jones, 1982, Logan *et al.*, 1987, Mroz and Surewicz, 1986, Olszewski, 1968). More significant is the synergistic interactions that soft-rot fungi may have with other decay fungi in chip piles (Zielinski, 1988). However, this synergy is poorly understood.

In mechanical pulping, brown-rot decay will typically have a negative effect on the quality of mechanical pulps, while some white-rot fungi may actually improve pulp quality and reduce energy consumption. Groundwood pulping of brown-rot decayed wood results in darker pulp, lower strength, and lower yield, as well as foaming and increased sticking (pitch deposition) (Christie, 1979). Christie (1979) reported that a one-point drop in ISO brightness is observed for every 4% increase in visible decay. Chemithermomechanical pulp produced from decayed aspen can have lower brightness, breaking length, burst and tear indices, and higher scattering coefficient than equivalent pulps made from sound wood (Becker and Briggs, 1983, Jackson *et al.*, 1985, Whitty *et al.*, 1991). However, TMP and CTMP pulps produced from chip furnishes with less than low levels of decay are likely to behave similarly to sound wood (Hatton and Johal, 1989).

Decay fungi do not always result in increased costs. Biopulping is a process that uses specific white-rot fungi, such as *Phanerochaete chrysosporium* and *Ceriporiopsis subvermispora*, to selectively delignify wood chips prior to pulping (Messner, 1998). Fungal pre-treatment of wood chips has most often been used to decrease refining energy and, improve pulp yield and mechanical pulp properties (Akhtar *et al.*, 2000, Kang *et al.*, 2003, Messner, 1998, Sachs *et al.*, 1989, Wolfaardt and Rabie, 2003), however it can also be used to lower the kappa number and improve the strength properties of kraft pulps (Wolfaardt *et al.*, 2004). Despite the appeal of this technology, losses in brightness and the cost of incubation have prevented it from being more widespread (Akhtar *et al.*, 2000, Messner, 1998).

1.7 Chip Utilization Procedures

A number of storage systems have been utilized by mills to optimize the value of their chip piles. From the perspective of minimizing the effects of decay, two factors need to be considered: chip age and uniformity of chip age. When older chips are utilized there is a greater risk of lower chip quality. Five chip storage and utilization systems, with various effects on chip age and variability, have been outlined by Schmidt (1990). First, the FIFO (first-in first-out) system stores incoming chips and utilizes the oldest chips first (older chips have a higher probability of being decayed). Second, the LIFO (last-in first-out) system utilizes the freshly cut chips first and discards very old chips. Third, the FIFO/Excess system uses chips as they arrive and stores extra chips using a FIFO procedure. Fourth, Blending adds chips from two piles to increase uniformity by mixing old and new chips. Finally, the Standby system uses fresh chips as they arrive. If chips are in excess they are added to a pile and withdrawn when needed.

The FIFO system minimizes variation in chip age, but often has a higher average chip age than other systems. The longer storage time results in a reduction of volatile extractives (this may be detrimental to mills producing tall oil or turpentine, but is important for sulfite mills),

and in an increased likelihood of decay. LIFO has the advantage of providing lower average chip ages, but has increased chip age variability. Schmidt (1990) studied chip utilization procedures and found Blending to be superior to Standby and FIFO. Blending was found to be superior to LIFO when the cost savings were greater than the losses accrued from the greater chip age. Similarly, Blending was superior to FIFO/Excess when the cost savings and lower age variability were of greater benefit than the lower chip age offered by FIFO/Excess. Mills are often limited as to which storage system they may use by the type of chip reclaim system they have. No system is best for all mills, although a FIFO-based system seems to be most prevalent (Hatton, 1985, Marcus, 1998, Shaw, 2000). Hatton (1985) found that five of twenty mills surveyed used a FIFO system and three used the LIFO system with the remaining mills withdrawing randomly from their piles.

1.8 Measuring Decay

Detection of fungi in wood and quantification of wood decay have been persistent problems for those who work with wood. A facile and reliable method of measuring decay is needed to address the problems presented by decayed wood. There are two groups of methods that can be used to measure decay content: those that measure parameters correlated with fungal biomass or metabolic activity, and those that measure the changes in the physical properties of wood or wood chemistry. I shall consider the former first.

1.8.1 Fungal Indicators

Methods based on measuring fungal biomass or metabolic activity are at a disadvantage compared to methods that directly characterize wood chemistry or physical properties because they do not directly show changes in the wood. Measurements that relate to fungal biomass can often be correlated to wood decay; however, this introduces an additional step, which increases

the error in estimating the extent of decay. Although such methods have a disadvantage for determining the properties of wood, they can be useful in studies primarily concerned with fungal growth in wood.

A number of methods based on dyes that selectively bind to fungal tissues or by-products of decay have been used to detect fungi. Some colorimetric dyes can bind to metabolic acids produced by decay fungi growing on wood (Eslyn, 1979). These dyes are very specific to both fungal species and wood species, and cannot be used as general indicators of decay. Fluorescent dyes that bind to various components in hyphae have also been used to quantify fungi (Krahmer *et al.*, 1982, Millard *et al.*, 1997, Moore, 1990). The intensity of the fluorescence observed, either with a fluorometer or fluorescent microscope, can be correlated with fungal biomass. With weight losses of only three percent, acridine orange was found to stain tracheids with incipient decay in pine (Krahmer *et al.*, 1982). Calcofluor and FUN-1 are fluorescent dyes that are effective for identifying live fungal cells in culture; however, they cannot be used on wood due to interference from wood components. Similarly, the fluorescein diacetate assay, a simple and inexpensive way to differentiate dead and metabolically active fungal cells and to determine living biomass, is not specific for decay fungi and is confounded by reactions in parenchyma cells that increase hydrolysis of the dye (Boyle and Kropp, 1992, Olsen and Schmidt, 1994).

Assays for chitin and ergosterol can be used to determine chemicals associated with fungi but not with wood. Chitin is a polymer composed of repeating units of N-acetylglucosamine found in fungal cell walls but not in wood and can thus be used as an indicator of fungi in wood (Boyle and Kropp, 1992). However, chitin content in the fungal cell wall varies with species, age, and growing conditions, and thus biomass determination based on chitin content is inherently inaccurate (Johnson and Chen, 1983). In addition, the assay is laborious and subject to interference from wood components (Boyle and Kropp, 1992, Johnson and McGill, 1990). Ergosterol is a sterol found in fungal membranes and absent in plants (Seitz *et al.*, 1979).

Incipient decay with one to two percent weight loss can be detected by the ergosterol assay (Bjurman, 1999). Although ergosterol, like chitin, does not correlate linearly with biomass throughout the entire life cycle of a fungus, it has been found to correlate linearly in the early stages of decay (Nilsson and Bjurman, 1990). However, ergosterol content in fungi is species-specific, so some knowledge of the fungal species involved in decay is necessary in order to accurately predict fungal biomass (Nilsson and Bjurman, 1990). Moreover, predictions of decay based on ergosterol content are subject to false positive results because all fungi, including non-decay fungi like yeasts and moulds, contain ergosterol (Gao *et al.*, 1993).

Protein content in wood are very low compared with those found in fungi, and can be used as an indirect measure of fungal content in wood (Boyle and Kropp, 1992). However, fungi produce proteins at different rates depending on their growing conditions, and therefore protein assays are poor predictors of fungal biomass in wood (Boyle and Kropp, 1992). Furthermore, the assay is laborious and subject to interference from wood extractives.

A number of immunological techniques have been developed to detect fungi in wood and have been reviewed by Clausen (1997). Both monoclonal and polyclonal antibodies have been developed to detect fungi and fungal metabolites (Clausen, 1997). The two most applicable assays are agglutination and the enzyme linked immunosorbent assay (ELISA). Both are based on the affinity of an antibody to a fungal antigen. Agglutination is a rapid test where antibodies designed to bind to specific fungal antigens are coated on latex beads. If the fungal antigens are present, then the beads stick together. Despite the simplicity of this test, the results are subjective and qualitative (Clausen, 1997). In ELISA, the fungal antigens bind to immobilized antibodies. Tagged antibodies, which can be quantified, are then added and bind to the immobilized antigens. ELISA can be used to quantify decay fungi growing in wood at very early stages (Jellison and Goodell, 1988, Kim *et al.*, 1991). However, the sensitivity of these immunological tests can be reduced by some wood extractives (Jasalavich *et al.*, 2000).

DNA-based assays are extremely sensitive and specific in determining the presence of fungi in wood. Taxon-specific primers have been designed to amplify regions of fungal DNA by the polymerase chain reaction (PCR). The DNA of the gene coding for ribosomal RNA contains a small and a large subunit separated by the Internal Transcribed Spacer (ITS) region. This region is a common target for taxonomic characterization because it has a high copy number and contains both variable and conserved regions (Jasalavich *et al.*, 2000). Assays have been shown to be sensitive enough to detect fungal DNA *in situ* (Kim *et al.*, 1999). Once the target DNA has been amplified by PCR, it can be sequenced or analyzed by restriction fragment length polymorphism (RFLP). RFLP involves cleaving the amplified DNA with restriction enzymes and results in fragments of DNA of different sizes that can be separated by gel electrophoresis (Schmidt, 2000). The resulting banding pattern can then be used to qualitatively identify various fungal taxa. Also, primers have been developed that are selective for basidiomycota (Adair *et al.*, 2000, Jellison and Jasalavich, 2000). This method has been used to differentiate basidiomycetes from ascomycetes in wood chips (Adair *et al.*, 2002). DNA-based techniques are limited when DNA from multiple species is found because the relative effects of each species on the extent of decay cannot be determined.

1.8.2 Physical Methods of Measuring Decay

There are a number of methods applied to solid wood to measure decay. These include compression tests, penetration resistance, the pick test, extensiometer tests, vibrational characteristics, electrical resistance, tomography, and acoustic emission (Zabel and Morrell, 1992). These tests are generally inadequate as they often lack specificity for decay and reliability, or rely on a subjective interpretation.

Weight loss is the standard method used to quantify the decay resistance of wood (ASTM, 1998). This method is based on incubating a piece of wood under standard conditions

for a given amount of time and measuring the loss of mass over time. It is useful for determining the decay resistance of wood and the ability of fungi to decay wood. However, weight loss is unsuitable for industrial use because chips are not stored discretely and initial weights are not known. Furthermore, this method is confounded by variable wood density and changes in the hygroscopicity of wood components during decay (Anagnost and Smith, 1997). As a result, losses due to brown-rot are often overestimated and losses due to soft-rot are often underestimated (Anagnost and Smith, 1997).

A thermogravimetric analysis (TGA) method for detecting decay in wood has been developed (Beall *et al.*, 1976). TGA measures mass loss under a controlled temperature and pressure. When heated, wood samples attacked by fungi were found to lose mass at faster rates than sound wood (Beall *et al.*, 1976). Differential scanning calorimetry (DSC) has also been used to detect decay based on thermal decomposition (Baldwin and Streisel, 1985). Decayed aspen has been differentiated from sound aspen based on different changes in thermal decomposition patterns (Knoll *et al.*, 1993). However, since some of these differences are dependent upon the extractives fraction (Knoll *et al.*, 1993), extractives should be removed or carefully monitored. Also, as some extractives are volatile, sample storage will affect the thermo-decomposition and resulting prediction of extent of decay. Although these methods may be effective on controlled samples, they cannot account for typical changes in wood chemistry between and within species.

Harris and Karnis (1988) estimated decay content by using a ball-milling technique. The mass of fines produced from grinding chips in a ball mill under standardized conditions correlates with extent of decay. Despite the method's simplicity and efficacy on well defined samples, it lacks the robustness necessary to become industrially applicable because it is affected by moisture content, wood species, chip dimensions and chipping technique.

^{13}C cross-polarization magic angle spin nuclear magnetic resonance (CP-MAS NMR) spectroscopy has been applied to the determination of decay content in wood (Irbe *et al.*, 2001, Preston *et al.*, 1998). This technique is effective for detecting heavily decayed samples, but has not been shown to possess the sensitivity to detect the early stages of decay. Magnetic resonance imaging (MRI), a technique based on NMR, has been used to detect decay and wood defects in wood samples (Muller *et al.*, 2002). MRI provides a way to measure spatial variations and was shown to be able to detect incipient decay in solid wood (Muller *et al.*, 2002). Unfortunately, the routine use of these techniques is limited by their expense.

None of the methods described above are suitable for the routine analysis of decay in wood samples. The variation found in field samples is too large for all of these methods, except perhaps NMR, which is too expensive to be used in the routine analysis of decay.

1.8.3 Spectroscopy and the Measurement of Decay

In recent years, a number of techniques that estimate wood characteristics based on spectroscopic modeling have emerged. FTIR, NIR and Raman spectroscopy can be used to measure various wood and pulp properties. As these techniques are used prominently in the work presented in this thesis, the advantages and disadvantages of each, their uses in wood and pulp property measurement, and a cursory overview of how they work, will be presented.

1.8.3.1 Mid-IR

Infrared (IR) radiation can be divided into three regions: near-IR (14000 – 4000 cm^{-1}), mid-IR (4000 – 400 cm^{-1}) and far-IR (400 – 20 cm^{-1}). The mid-IR region corresponds to the vibrational frequency of many common functional groups, such as alcohols, carboxylic acids and amines. These functional groups absorb IR radiation when the frequency of IR radiation is equal to the vibrational frequency of the functional group, the dipole of the molecule changes during

the vibration and the direction of the dipole change is the same as the electric field vector (ThermoElectron, 2003). An IR spectrum can be produced by plotting the intensity of transmitted (or reflected) radiation as a function of frequency. The frequency at which a peak occurs in the spectrum will be indicative of a specific functional group. The intensity of that peak can be correlated with the abundance of that functional group.

Traditional dispersive IR instruments have, for the most part, been replaced by FT (Fourier Transform) instruments due to affordable computing power. FT instruments have multiplexing advantages, including, the Jacquinot advantage of increased optical throughput and the Felgett advantage of simultaneous detection (Agarwal and Atalla, 1995). This contributes to a greatly reduced signal-to-noise ratio. FT techniques also result in the accurate determination of wavenumbers that allow for spectral subtraction and enable a more comprehensive statistical analysis of spectra (Agarwal and Atalla, 1995).

The FTIR instrument consists of a laser, a Michelson interferometer, an IR light source, a sample compartment, and a detector. IR radiation enters the interferometer and is split. Half of the radiation is directed towards a fixed mirror, the other half towards a moving mirror. The radiation then recombines, producing constructive and destructive interference. Laser radiation, at a much higher frequency, is added to the interferometer to measure the distance that the mirror moves. This radiation is then directed to the sample compartment, passes through the sample and is directed to the detector. The resulting interferograms are co-added and Fourier transformed from the time domain to the frequency domain, resulting in a FTIR spectrum (ThermoElectron, 2003).

Diffuse reflectance infrared Fourier transform spectroscopy (DRIFTS) measures a portion of the infrared radiation that reflected from a solid sample. When IR radiation hits a solid sample most of the radiation bounces off the sample at an angle complementary to the incident beam. This is termed specular reflectance. The portion of the radiation that passes through part

of the solid sample will emerge at any angle and carry information about the sample. This is termed diffuse reflectance (Baulsir and Tague, 2001). Since only a portion of the incident IR radiation passes through the sample, and only a portion of this is collected, signals are weaker in DRIFTS than in transmission FTIR. The principal advantage of DRIFTS is rapid, facile sample preparation. With small particle size and a sufficient number of scans, high quality DRIFTS spectra can be obtained. However, large particles will reduce the quality of DRIFT spectra (Anderson *et al.*, 1991). Neat or highly concentrated samples can also reduce spectral quality. The region between 1150 and 950 cm^{-1}, which corresponds to olefinic and aromatic C-H stretching, may be influenced by sample concentration and contain distorted data unless sample concentration is less than 2% (Pandey and Theagarajan, 1997). This distortion is due to specular reflectance, which can be removed by diluting the sample in an IR-transparent matrix such as KCl, reducing particle size below 10 μm diameter or mechanically removing specular reflectance (Anderson *et al.*, 1991). When analyzing neat samples by DRIFTS the region between 1150 and 950 cm^{-1} should not be used. Care must also be taken to ensure that the samples remain dry since water is a strong absorber in the IR region. A typical DRIFT spectrum of milled wood is shown in Figure 1.4.

Mid-IR spectroscopy has been used to detect incipient decay in Douglas-fir and Southern yellow pine, and to determine acetyl, lignin, glucose, xylose and holocellulose content in wood (Costa e Silva *et al.*, 1999, Gibson *et al.*, 1985, Schultz *et al.*, 1985, Supinski and Dziurzynski, 1988, Zanuttini *et al.*, 1998). Diffuse reflectance infrared Fourier transform spectroscopy (DRIFTS) and multivariate statistical analyses, such as PLS, have been used to estimate weight loss due to the fungal decay of wood (Backa *et al.*, 2001, Ferraz *et al.*, 2000). Ferraz *et al.* (2000) developed PLS models to predict weight loss, and change in chemical composition caused by several white- and brown-rot fungi in *Pinus radiata* and *Eucalyptus globulus*. Backa *et al.* (2001) correlated the FTIR spectra of *Betula pendula* samples, degraded by brown- and white-rot fungi,

to weight loss measurements. These models showed strong correlations between measured and PLS-predicted weight loss measurements over a wide range of decay (Backa *et al.*, 2001). FTIR spectroscopy has also been used to estimate basic wood density (Meder *et al.*, 1999). IR spectra have also been obtained on moving chips using transient infrared spectroscopy (Jones *et al.*, 2002). This technology is amenable to online analysis and has the potential to lead to real-time data and feed-forward process control (Jones *et al.*, 2002).

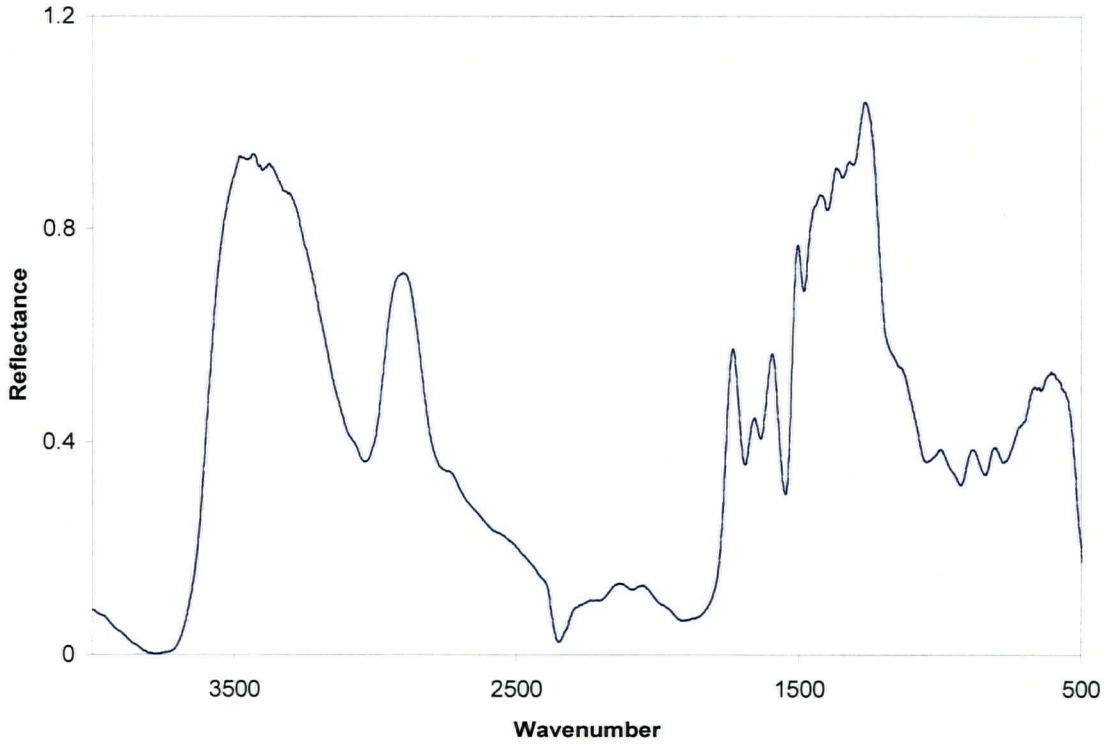

Figure 1.4 A Typical DRIFT Spectrum of Milled Spruce Wood

1.8.3.2 Near-IR

NIR is based on frequencies between visible light and mid-IR (700 to 2500 nm) (Hoffmeyer and Pedersen, 1995). Many of the peaks in NIR spectra correspond to combination bands of C-H, O-H, and N-H bonds and the overtone bands of functional groups that absorb in the mid-IR (So *et al.*, 2004). NIR bands are often broad and overlapping making interpretation

difficult. Multivariate statistical modeling has overcome this problem as it can look at the whole spectrum and not just a single wavelength. PLS with orthogonal signal correction (OSC) has been found to be a particularly effective modeling method for some datasets (Champagne *et al.*, 2001, Kelley *et al.*, 2004a).

NIR has several advantages over mid-IR including higher energy sources, very sensitive detectors, high throughput and transparence to silica and quartz (Michell, 1994). The transparence to silica and quartz allow for samples to be analyzed remotely through fibre optics or through glass sample containers. The main drawback of NIR is that it is often difficult to interpret directly and often requires the development of calibration datasets (So *et al.*, 2004). Furthermore, due to diminishing overtones, NIR spectra typically contain less data than mid-IR spectra.

A NIR spectrometer consists of a source, often Globars or Tungsten/Halogen lamps, a grating, and a detector. Reflected or transmitted radiation then enters another fibre optical cable and is sent to the detector. Detectors are comprised of either an indium-gallium-arsenide (InGaAs) photodiode array or a Charged Coupled Device (CCD).

NIR spectroscopy is the favoured method for developing models for industry because it is affordable, rugged and portable (So *et al.*, 2004). It has been used to develop multivariate models capable of predicting kappa number, and lignin and cellulose content in pulps and woods, as well as pulp yield, chip size distribution, and mechanical and basic wood properties from spectra of wood (Axrup *et al.*, 2000, Birkett and Gambino, 1989, Ferraz *et al.*, 2004, Hauksson *et al.*, 2001, Kelley *et al.*, 2004, Kelley *et al.*, 2004a, Michell, 1994, Olsson *et al.*, 1995, Schimleck *et al.*, 1999, Schimleck *et al.*, 2000, Schimleck *et al.*, 2004, Schimleck and Evans, 2003, Schultz and Burns, 1990, Yeh *et al.*, 2004). A typical NIR spectrum of milled wood is shown in Figure 1.5. NIR spectroscopy has been applied specifically to the problem of decay and used to predict extent of decay in solid wood by modeling changes in compression

strength due to decay (Hoffmeyer and Pedersen, 1995). It has also been used to model weight loss due to fungal decay by brown-rot fungi (Kelly *et al.*, 2002). Additionally, NIR imaging was employed to obtain spectra across a solid sample, which can then be used to show spatial variations in pulp properties (Bharati *et al.*, 2004). NIR spectra of wood chips in combination with TMP refiner data have been used to predict tear and tensile indices, brightness, scattering coefficient, and freeness of resulting pulps (Karlsson and Wancke Stahl, 2000). Moreover, these data have been used to control refiner energy to maximize pulp quality.

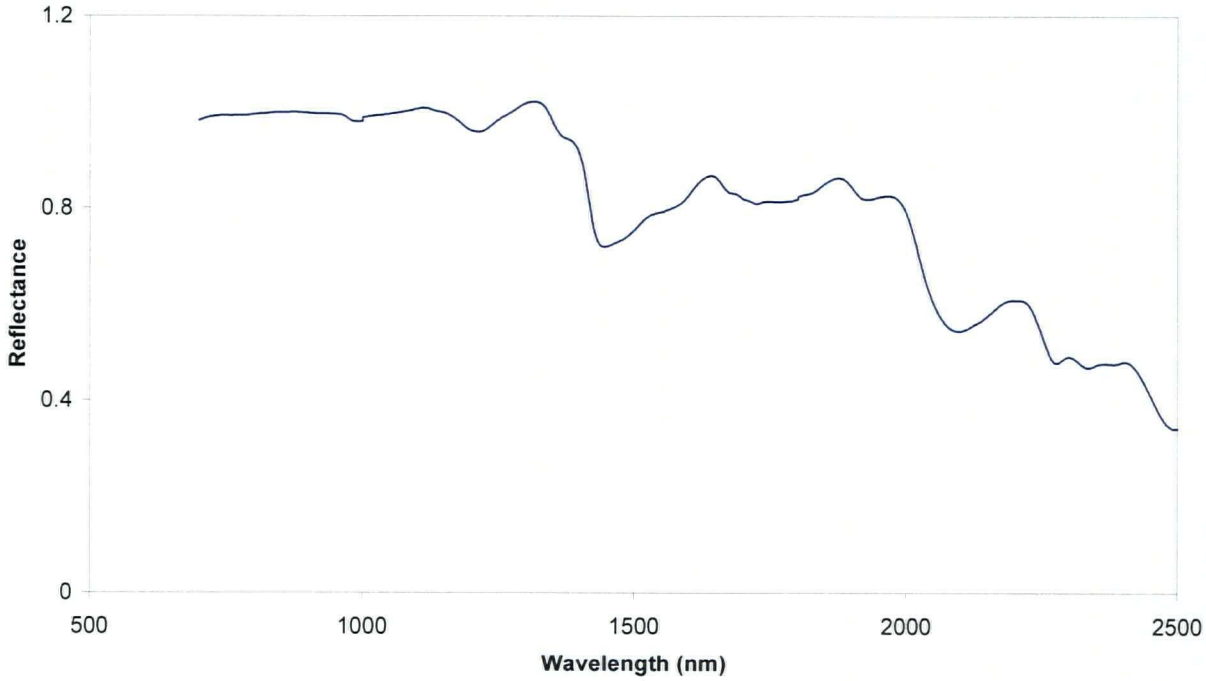

Figure 1.5 A Typical NIR Spectrum of Milled Spruce Wood

1.8.3.3 Raman Spectroscopy

Raman spectroscopy is based on the measurement of the radiation scattered by a sample that has been irradiated with an intense monochromatic light source (such as a laser). When this radiation hits the sample, electrons in the ground electronic state are excited to a virtual state equal to the energy of the incoming photon. The electrons in the virtual state then emit photons

to return to the ground state (Skoog and Leary, 1992). Three types of scattering take place when the photon is emitted: Rayleigh, Stokes, and anti-Stokes (Skoog and Leary, 1992). Rayleigh scattering occurs when an emitted photon from the sample has the same frequency as the laser. Stokes scattering occurs when the photon is emitted from the sample with a lower frequency than the laser, and anti-Stokes scattering occurs when the photon is emitted with a higher frequency than the laser (Skoog and Leary, 1992). Stokes and anti-Stokes scattering arise when a photon is incident on a molecule and interacts with the electric dipole of the molecule. The difference in frequency between the incident radiation and the Stokes radiation corresponds to the mid-IR region, and is influenced by the chemical structure of the sample (Skoog and Leary, 1992). Raman spectroscopy provides an indication of the polarizability of a bond, as opposed to IR spectroscopy, which is dependent upon changes in dipole moment. As a result, the two methods are often considered to be complementary. Strong IR absorbing samples often have weak Raman signals and vice versa. An important consequence is that Raman spectra are not significantly affected by water or glass, making sample preparation much easier than for IR (Atalla, 1987).

It is difficult to obtain high quality Raman spectra of wood using conventional instruments because of high levels of laser induced fluorescence (LIF) from the lignin present in the samples (Agarwal and Ralph, 1997). LIF has been minimized by the use of three techniques: FT-Raman, Automated Fluorescence Rejection by Shifted Excitation Raman Difference Spectroscopy (SERDS), and UV Resonance Raman Spectroscopy. FT-Raman typically uses an Nd:YAG laser with excitation at 1064 nm (most Raman lasers operate in the visible region). This lower frequency laser results in much weaker signals that are most easily detected with an FT method. However, the lower frequency also eliminates the electronic excitation of molecules, reducing fluorescence and allows the laser to be operated at higher power. FT-Raman has improved the signal-to-noise ratio of spectra obtained from wood, by minimizing the effects of

LIF from lignin (Agarwal and Atalla, 1995). SERDS can be used with time resolved instruments operating at higher frequencies. It removes fluorescence by obtaining two Raman spectra excited with two slightly different laser frequencies (Zhao *et al.*, 2002). Since the Raman scattering will be shifted, in absolute terms, by the changes in excitation frequency, and the fluorescence will not change, the fluorescence can be eliminated by comparing the two spectra (Zhao *et al.*, 2002). A typical SERDS spectrum of milled wood is shown in Figure 1.6. In UV Resonance Raman Spectroscopy the wavelength of the incident radiation is approximately the same as the electronic absorption frequency of the analyte (Saariaho *et al.*, 2003). This enhances Raman signals up to 10^6 times and enables detection of molecules found in trace amounts (Halttunen *et al.*, 2001).

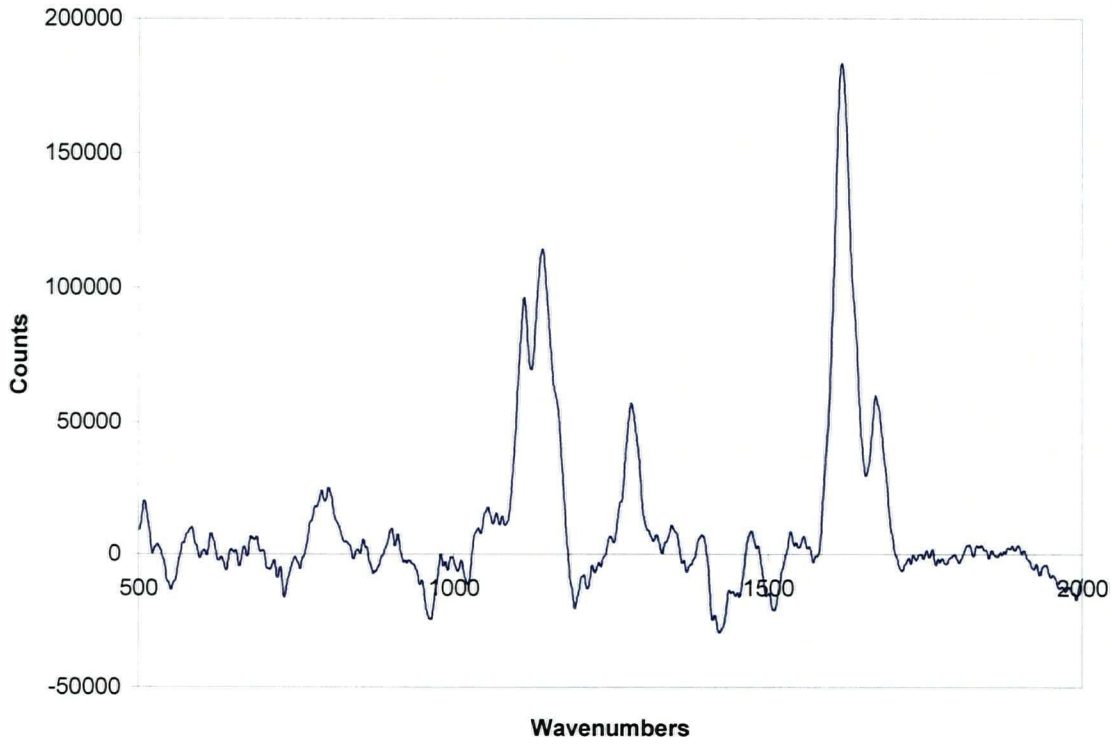

Figure 1.6 A Typical Raman (SERDS) Spectrum of Milled Spruce Wood

The Raman Spectrometer is made up of a laser, a system for sample illumination, and a spectrophotometer (Skoog and Leary, 1992). The laser is directed to the sample and then to a monochromator. The monochromatic light then is directed to a CCD for detection. FT-Raman applies the same principles as FTIR, the main difference being that the interferometer is located after the sample compartment in FT-Raman (Skoog and Leary, 1992). SERDS uses a tuneable laser so that the frequency of light can be altered by controlling the temperature of the laser.

Raman spectroscopy has been used to investigate a number of pulp properties, including differences in cellulose allomorphs, conformational changes in pulp from drying, photo-yellowing of pulps, kappa number, microfibril angle in bleached fibres, pulp yield, pulp strength properties, and unbleached brightness (Agarwal and Atalla, 1995, Atalla, 1987, Ona *et al.*, 2000, Pleasants *et al.*, 1998, Sun *et al.*, 1997). Despite these advancements, traditional Raman spectroscopy has been limited by the LIF from lignin and other chromophores (Agarwal *et al.*, 2003). FT-Raman spectroscopy of wood has reduced fluorescence, and has been used to investigate wood chemistry and quantify residual lignin in bleached kraft pulps (Agarwal *et al.*, 2003, Agarwal and Ralph, 1997). UV Resonance Raman Spectroscopy has also been used to quantify residual lignin and hexenuronic acids in kraft pulps (Halttunen *et al.*, 2001, Saariaho *et al.*, 2003).

1.8.4 Measuring Decay in the Pulp and Paper Industry

Since wood chips are so small, measuring the decay content requires different methods than those used on solid wood, such as strength testing. However, many of the methods used to measure decay in wood chips can also be used in solid wood. Chip piles are large and non-uniform which makes sampling extremely important. Proper sampling is essential if mills are to control or reduce decay in their chip piles.

Two indirect indicators of decay are chip size distribution and wood density. Chip size distribution is a critical parameter in both chemical and mechanical pulping and is routinely tested in 70% of U.S mills (McDonald and Twaddle, 2000). Decay content can result in fewer accept-quality chips and an increase in pins and fines (Hunt, 1978). However, chip size distribution is affected by many factors and is not specific for decay.

Wood density is probably the most critical wood quality parameter. Low density wood is less economical to transport either as chips or as solid logs. Chips with high wood density lead to increased shear stress and chipping energy (McGovern, 1979). Chemical pulps produced from high density wood require increased H-factor due to a slower rate of liquor penetration (Jones and Richardson, 2001). Variable wood density leads to variable liquor penetration, which can result in different pulping rates (Evans *et al.*, 1999, Jones and Richardson, 2001, Kibblewhite *et al.*, 1997).

Wood density can provide an indication of extent of decay, but only when the density of the equivalent sound wood is known (Hatton, 1970, McDonald and Twaddle, 2000). Environmental and genetic factors also affect wood density (Pitts *et al.*, 2004). Thus, like chip size distribution, wood density is not specific for decay.

Wood density can be measured in chips using a water displacement method (Tappi method T 258 om-02). In logs, mensuration density, based on a geometrically derived volume, resistance to outside pressure (penetrometry), and resistance along a drilling axis (resistography) are used to estimate wood density (Creed *et al.*, 2004, Rinn *et al.*, 1996). X-Ray densitometry has also been used to measure wood density (Gureyev and Evans, 1999). NIR spectroscopy has also been used to predict wood density from increment cores (Schimleck and Evans, 2003).

The ratio of sound and decayed wood can be determined by log scalers or by handsorting chips. Estimates of decay content from log scalers, although correlated with the decay content in

chips, lack the accuracy required for process control or economic analyses (Horng *et al.*, 1988). However, these estimates can serve as an early warning when decay increases significantly.

Visual detection of decay is the most basic test used to identify decayed wood in increment cores or in chips. However, this test is subjective and plagued by inaccuracy. Decay in increment cores can be tentatively identified by abnormal discolouration, shrinkage, wet zones, and the ease with which an increment corer penetrates a tree (Zabel and Morrell, 1992). Fernandez (2000) reports a 5-point scale to assess decay in increment cores based on discolouration and wood frailty. In chips, brown or white discolouration not associated with extractives, bluestain fungi, or moulds, or a soft, crumbly texture, can be indicative of decay. This type of classification provides a mass-based percentage of decay by hand-sorting chips into sound and decayed categories. Since the degree of decay is very difficult to identify by visual means, this method is again plagued by inaccuracy. Moreover, since decayed wood typically has a lower density than equivalent sound wood, mass-based determination will under-estimate decay content. This is critical since pulp mills use chips on a volumetric basis. In addition, placing chips into two categories, sound or decayed, does not account for variations in the extent or type of decay present. Hand-sorting chips also requires significant labour resources if done routinely.

The caustic solubility and buffering capacity tests are the best available, mill-applicable measures of extent of decay. One-percent caustic solubility (PAPTAC method G.6 and G.7), when referenced to sound wood, is indicative of chemical changes in wood due to fungal decay. A reference to sound wood is typically needed because of variations in 1% caustic solubility between wood species (Hunt and Hatton, 1979). However, when caustic solubility is high, a sample can be labelled as decayed without prior knowledge of wood species or species mix. Procter and Chow (1973) used this test as a basis for a rot-index. One-percent caustic solubility

has been correlated with both kraft pulp yield and effective alkali consumed (Hunt and Hatton, 1979).

Acidity and buffering capacity have also been used by a few mills as indicators of chip quality or extent of decay (McDonald and Twaddle, 2000). Buffering capacity is a more accurate, albeit more laborious, measure of acidic functional groups than a simple pH measurement. Like 1% caustic solubility, buffering capacity is indicative of fungal decay or chemical changes to the wood. The principal drawbacks of both methods are the time taken to perform the tests, the labour involved, and the cost of consumables. As a result, less than 10% of U.S. pulp mills regularly test for either caustic solubility or buffering capacity (McDonald and Twaddle, 2000); similar rates are expected in Canada.

1.9 Managing Decay

There are no easy ways to remove decayed material from a mill's fibre supply or mitigate its effect. However, there are a number of practices that can be employed to minimize decay content and preserve chip quality.

In plantations or managed forests there are management options that can reduce decay. These include only pruning branches less than 30 mm in diameter, using paints or sealants where risk of infection is high, removing decayed trees and ensuring that logging operations limit damage to remaining trees (MacLeod, 1967, Montagu *et al.*, 2003). Since best-practices vary with species and site, specific management plans to minimize the impact of decay also vary.

Debarking methods can influence the amount of decayed wood that enters a chipper. On sap-rotted woods, ring debarkers have been found to remove more of the decayed wood than drum debarkers (Basham, 1984). Although this results in greater wood loss, it does remove decayed wood from the fibre supply, which is beneficial for pulp quality. Conversely, for logs with heart-rot retaining the maximum amount of sapwood is beneficial.

For wood chips, a number of different techniques have been studied to reduce or eliminate decay in storage. Physical barriers, such as paving to eliminate contact with soil organisms, help preserve chip quality. High capital cost has prohibited employing enclosed storage units to protect wood chips. Irradiation of chips was investigated as a means of preventing fungal growth but, while effective, was not found to be economical (Saunders and Singh, 1988).

A number of chemical treatments designed to minimize decay while in storage have also been applied to chip piles, including chlorinated phenols, nickel sulphate, condensation products of aldehydes and ketones, green liquor, sodium hydroxide, borax, sodium pentachlorophenate, ammonium bisulphite, sulphur dioxide, propylene oxide, sodium carbonate, sodium N-methyldithiocarbamate and sulphur (Hulme and Hatton, 1978, Hulme and Shields, 1973, Smith and Hatton, 1971, Springer *et al.*, 1975). These compounds demonstrated varying efficacy, some posed an environmental threat, and none are cost effective with modern storage times (McDonald and Twaddle, 2000).

Biological treatments have the potential to prevent decay through antagonistic interactions with decay fungi. *Trichoderma viride* has been found to inhibit the growth of four fungi commonly isolated from wood in storage (Shields and Atwell, 1963). Such an approach has also been used with Cartapip, an albino strain of *Ophiostoma piliferum*, used to control pitch and resin problems (Farrell *et al.*, 1994). In short, the albino mutant is capable of out-competing blue staining fungi. However, biological control of decay cannot out-compete decay fungi without also utilizing structural components of the wood (Bruce, 1998). Such an approach could cause significant fibre losses and, as a result, biological control of decay fungi has only limited applications in specific areas (Bruce, 1998). Biological control of decay would also have to demonstrate that it did not detrimentally affect pulping and pulp properties.

Preventing decay in OCS can be difficult to perfect due to the wide diversity of fungal species and environmental conditions in a chip pile. Fuller (1985) outlines six techniques that mills can use to minimize decay and chip degradation in their chip piles. These include:

(1) Maintaining a pile height below 15 m

(2) Restricting tractor spreading of fresh chips to a minimum

(3) Avoid mixing species with different deterioration rates (hardwoods and softwoods)

(4) Store full tree chips in piles less than 8 m for less than 2 to 4 weeks

(5) Reducing fine particles, such as sawdust and fines mixed into the pile during its construction

(6) Monitoring pile temperature regularly and taking steps to reduce it when necessary

In addition to these guidelines, using a paved ground barrier to reduce dirt contamination and inhibit ground organism mobility, using a FIFO-based reclaim method, and avoiding the 20°C to 50°C temperature range should be attempted (Saunders and Singh, 1988). Regular monitoring of decay content would also be salutary. This would be facilitated by the development of new methods for the rapid detection of decay. Decayed piles or regions could then either be utilized more rapidly to prevent further degradation or utilized by mixing with sound chips. Quantification of decay extent would also alert mills to changes in their fibre supply and provide more information upon which to base operating conditions.

Where short storage times and FIFO-based reclaim systems are utilized, there is limited decay while in storage. The greatest opportunity to limit decay occurs in the forest where silvicultural and harvesting practices can significantly aid in reducing decay. Much of this wood will be used by the solid wood products sector. Since the value of solid wood is greater than

chips, the economic incentives to minimize decay will be greater for the solid wood products sector. However, the pulp sector is the recipient of sawmill residuals and will, therefore, benefit from any actions taken by the solid wood products sector to minimize the decay of wood in the forest.

1.10 Research Objectives

As discussed in the previous sections, decay can be a significant problem for the pulp and paper industry, and there is a lack of industrially suitable methods of estimating the extent of decay. A wide variety of methods have been investigated but none have been developed sufficiently to find use in mills. Quantification of decay has two main uses. First, it can assess the quality of chips that a mill purchases. Chip shipments could be assessed for decay and the value of these chips for pulp would be known. Second, chips in storage could be monitored for decay and, thus, allow the mill to optimize its chip handling procedures. Quantifying decay should allow for accurate mixing or segregation of decay to reduce variability in pulp properties and preserve fibre quality.

The purpose of the following research is to develop industrially applicable methods of estimating the extent of decay in wood chips. There are three main components to this research. First, I will investigate the ability of FTIR, NIR, and Raman spectroscopy to be used to model the extent of brown-rot decay in wood chips, as determined by caustic solubility and buffering capacity. The accuracy, precision, versatility and factors that affect these models will be determined. Second, the wood components responsible for the predictive ability of the spectroscopy-based models will be determined in order to understand how and why the models work and to fully exploit their potential. Finally, the models will be validated through the kraft and mechanical pulping of sound and decayed wood chip samples. The pulping experiments will also investigate the effects of chip storage with varying inoculum size and serve as a direct

comparison of brown-rot decayed wood pulped by kraft and refiner mechanical pulping. This research aims to provide mills with a well-tested technique for estimating extent of decay and with a better understanding of the effects of decay and the factors that lead to it.

CHAPTER 2

General Methodology

2.1 Wood and Fungal Samples

Wood chips used in the preparation of a decay dataset were obtained from various locations in Canada and the United States (Appendices 1 and 2). The species used to develop this dataset are shown in Table 2.1.

Fungal cultures were maintained on malt extract agar (MEA) which contained 1% malt extract (Difco, Sparks, MD), 1.2% agar (Oxoid, Hampshire, UK) and 0.1% tryptone (Fisher Scientific, Fairlawn, NJ). For long-term storage, slant cultures were prepared and stored at 4°C and sub-cultured annually. For day-to-day use, fungi were grown on MEA plates and stored at room temperature. Fungi were transferred approximately every 6 weeks to maintain healthy cultures. For some experiments fungi grown in liquid culture were prepared in 1% malt extract with 0.1% tryptone at 30°C with continuous shaking at 100 rpm. Fresh liquid cultures were also prepared approximately every six weeks.

Fungi were selected based on their ability to decay the wood species selected, prevalence, and destructive ability. *Phanerochaete chrysosporium* is widely distributed, and is reported to be one of the most destructive fungi in hardwood chip piles (Allen *et al.*, 1996, Nilsson, 1973). *Phellinus* and *Phialophora* species are also widely distributed and cause significant damage to living trees (Allen *et al.*, 1996, Blanchette, 1980, Hulme, 1979, Lindgren and Eslyn, 1961, Shields, 1969, Zabel and Morrell, 1992). *Gloeophyllum trabeum* is usually found in dead or diseased softwood, while *Postia placenta* is widely distributed in softwoods (Allen *et al.*, 1996, Zabel and Morrell, 1992). Both of these brown-rot fungi are very destructive and well studied (Davis *et al.*, 1994, Highley *et al.*, 1985, Kim *et al.*, 1991, Kim and Newman, 1995, Zabel and Morrell, 1992). All fungi were provided courtesy of Dr. Colette Breuil, University of British Columbia.

Table 2.1 Wood Species Used in Model Development

Wood Species	Latin Name
Balsam fir	*Abies balsamea* (L.) Mill.
Sub-alpine fir	*Abies lasiocarpa* (Hook.) Nutt.
Sugar maple	*Acer saccharum* Marsh.
White birch	*Betula papyrifera* Marsh.
Yellow cedar	*Chamaecyparis nootkatensis* (D. Don) Spach
Tamarack	*Larix laricina* (Du Roi) K. Koch
White spruce	*Picea glauca* (Moench) Voss
Alaskan spruce	*Picea glauca* (Moench) Voss x *P. sitchensis* (Bong.) Carrière
Black spruce	*Picea mariana* (Mill.) BSP
Jack pine	*Pinus banksiana* Lamb.
Lodgepole pine	*Pinus contorta* Dougl. var. *latifolia* Engelm.
Loblolly pine	*Pinus taeda* L.
Trembling aspen	*Populus tremulae* Michx.
Balsam poplar	*Populus balsamifera* L.
Douglas-fir	*Pseudotsuga menziesii* (Mirb.) Franco
Red oak	*Quercus rubra* L.
Western redcedar	*Thuja plicata* Donn
Western hemlock	*Tsuga heterophylla* (Raf.) Sarg.

Table 2.2 Fungi Used to Decay Wood Samples

Decay Type	Fungus
White-rot	*Phanerochaete chrysosporium* VKMK-1767
White-rot	*Phellinus pini* UAMH 8176
White-rot	*Phellinus igniarius* CBS 512.63
Soft-rot	*Phialophora bubakii* IMI 24000
Brown-rot	*Gloeophyllum trabeum* 61750M
Brown-rot	*Postia placenta* MAD 698
Bluestain (non-decay)	*Ophiostoma piliferum* NRRL 18690

Six decay fungi and one staining fungus (used as a control) were used to prepared decayed or stained wood (Table 2.2). Wood chips were inoculated with these fungi and grown on 1% MEA in 1L Erlenmeyer flasks according to the method of Ferraz *et al.* (2000). Autoclaved wood chips were added to the culture of growing fungi and incubated at room temperature for periods ranging up to 90 days.

2.2 Analysis of Wood Samples

Wood chip samples were oven-dried (OD) overnight and milled to pass through a 0.5 mm screen using a Thomas-Wiley mill (Arthur H. Thomas Co., Philadelphia, PA). This was done to maximize sample homogeneity and ensure that particle size would not contribute significantly as a source of variability in calibration model development.

Moisture determinations were made according to PAPTAC method G.3 (PAPTAC, 2000). For 1% caustic solubility, screened samples were analyzed in triplicate according to PAPTAC methods G.6 and G.7 (PAPTAC, 2000). Two grams of milled wood was added to a

250 mL Erlenmeyer flask with 100 mL of 1% NaOH and heated in a bath of boiling water for 1 hour. Samples were filtered through a coarse sintered glass filter and washed with 50 mL of hot water, 50 mL of 10% acetic acid, and an additional 50 mL of hot water. Filters were oven dried and weighed. The difference between the mass retained on the filter and the original mass of wood was used to determine the solubility of the sample.

Samples were measured for buffering capacity by potentiometric titration, using a modification of the method outlined by Subramanian *et al.* (1983). Two-and-a-half grams of OD equivalent milled wood was steeped in 50mL of 10% potassium acetate buffer for 24 hours. Samples were filtered, washed with potassium acetate buffer and deionized water, and made up to 100mL. A 25mL aliquot was titrated against standardized 0.5N sodium hydroxide. Buffering capacity was determined from the equivalence point in the resulting titration curves.

Acetone extractives were isolated by a six hour Soxhlet extraction at 70°C. The acetone was then removed by rotary evaporation and heating to 40°C under a stream of nitrogen. The extractives were freeze dried and determined gravimetrically. Some extractives samples were further analyzed by gas chromatography/mass spectrometry (GC/MS) according to the method of Fernandez *et al.* (2001). Heptadecanoic acid was used as an internal standard. A Saturn 2000 Series gas chromatograph/mass spectrometer (GC/MS) by Varian (Walnut Creek, CA) was used for all GC analyses. A 10m XLB column (Chromatographic Specialties, Brockville, ON) was used to determine extractives. One microlitre samples were added to the column by a splitless injection with injector temperature maintained at 320°C. The column was held at 50°C for 3 minutes, ramped to 340°C at 10°C/minute, held for 36 minutes, ramped to 360°C at 10°C/minute and finally held at 360°C for 5 minutes. Column flow was maintained at 2.5 mL/min.

Carbohydrate and lignin analysis was based on Tappi methods T249 cm-00 for carbohydrates, T222 om-98 for Klason lignin and TAPPI UM 250 for acid-soluble lignin (TAPPI, 2000). Calculations of acid-soluble lignin were based on an extinction coefficient of

110 L g^{-1} cm^{-1} (Favis and Goring, 1983). UV absorbance measurements were made on an Ultrospec 1000 UV/Vis Spectrophotometer (Pharmacia Biotech, Cambridge, UK). The sugars were converted to their alditol acetates as described by Cao *et al.*, (1997), and quantified by GC/MS with a 30 m RTX 2330 column (Restek, Bellefonte, PA). One microlitre samples were added to the column by a splitless injection with injector temperature maintained at 275°C. The column was held at 175°C for 4 minutes, ramped to 240°C at 5°C/minute, held for a minute, and ramped to 260°C at 15°C/minute. Column flow was maintained at 2.5 mL/minute. Automated quantitation was based on the peak area ratios between sugars and internal standards of solutions with known sugar concentrations. For pentoses, fucose was used as an internal standard, while for hexoses; inositol was used as an internal standard.

2.3 Spectroscopy

Screened, OD samples were analyzed in duplicate by a Perkin Elmer 1600 series FTIR spectrometer (Norwalk, CT) using a DRIFTS apparatus. Approximately 0.2 grams of wood were used to obtain each spectrum. All spectra were collected with 256 scans at a resolution of 4 cm^{-1} over a range of 4400 cm^{-1} to 450 cm^{-1}. The single-beam spectra were normalized against a potassium chloride background to yield the absorbance spectra. Background spectra were typically obtained once per day. Prior to PLS modeling or prediction, spectra were "zeroed" at 4282 cm^{-1} and in some models a 31-point Savitzky-Golay smoothing function was applied to minimize the effects of noise (Savitzky and Golay, 1964).

Reflectance spectra were obtained in the visible and near infrared region (350 to 2500 nm) using a QualitySpec Pro spectrometer (Analytical Spectral Devices, Boulder, CO). Two spectra were obtained from each sample with 10 scans obtained in each of 5 subfiles. Spectra were obtained on dry, milled wood stored in borosilicate glass vials. Reflectance spectra were normalized against a white Teflon background through glass to yield absorbance spectra.

Raman spectra were obtained from 250 to 2250 cm^{-1} with 60 seconds integration time and 5 co-adds with binning set to 10, using a Chromex Sentinel Raman Spectrometer (Albuquerque, NM) with a diode laser emitting at 785 nm. The cosmic ray removal was enabled and spectra were dark field subtracted. The laser was focussed on the milled wood samples in borosilicate glass vials.

2.4 Statistical Analyses

PLS models were developed using Thermo-Galactic's Grams/AI 7.01 software (ThermoGalactic Corp., Salem NH). All PLS models were developed using the following method. Spectral and concentration datasets were entered to create a training data file. From this, a correlogram that showed the correlation between spectral regions and the concentration dataset was examined to determine the effect of various manipulations on this relationship. The effects of using 1st or 2nd Savitzky-Golay derivatives, the Multiplicative Scatter Correction (MSC), the Standard Normal Variate (SNV) transformation, baseline correction and the exclusion of outliers were determined based on the correlogram. The most predictive regions of the spectra were then selected and modeled. The PLS-1 algorithm and full cross-validation were used to prepare all models. The developed models were first examined by looking at the Predicted Residual Error Sum of Squares (PRESS) diagrams to determine the optimal number of factors to use (Equation 2.1). With this information, the r^2 (Equation 2.2) and root mean standard error of cross validation (RMSECV, Equation 2.3) was examined. External validation datasets were used to provide the root mean standard error of prediction (RMSEP), an unbiased measure of the model's accuracy. Models were further inspected by looking at concentration residuals, spectroscopic residuals, factor loadings, and studentized concentration residuals as a function of sample leverage. Finally, calibration files were prepared to use the model to predict the concentrations of external

samples. All PLS modeling statistics were determined by PLS-IQ. All other statistical analyses (ANOVAs, t-tests) were performed by Systat 7.0 (SPSS Inc., Chicago, IL).

Equation 2.1 Predicted Residual Error Sum of Squares (ThermoGalactic, 2002)

$$PRESS = \sum_{i=1}^{n} (Xm_i - Xp_i)^2$$

Equation 2.2 r^2 Determination (ThermoGalactic, 2002)

$$r^2 = \frac{\sum_{i=1}^{n} (Xp_i - \bar{X}m)^2}{\sum_{i=1}^{n} (Xm_i - \bar{X}m)^2}$$

Equation 2.3 Root Mean Standard Error of Cross Validation (ThermoGalactic, 2002)

$$RMSECV = \sqrt{\frac{\sum_{i=1}^{n} (Xm_i - \bar{X}p_i)^2}{n-1}}$$

where, n = the number of factors in either the calibration or validation dataset, Xm = the measured concentration, Xp = the predicted concentration

RMSEP is calculated by the same formula for RMSECV when an external validation dataset is considered.

CHAPTER 3

Partial Least Squares Models of Decay and Wood Density

3.1 Introduction

The first objective of this research was to develop new methods of estimating the extent of fungal decay. To achieve this, spectral data obtained from FTIR, NIR and Raman spectroscopy were used to model caustic solubility, buffering capacity and basic wood density (see section 1.8.3). In order to relate spectral data to the traditional methods, chemometric techniques were employed.

Chemometrics is the statistical processing of analytical chemistry data, for example data obtained from IR spectra, with various numerical techniques in order to extract information. A simple example of this is the Beer-Lambert Law, which relates the absorbance at a single frequency with sample concentration (Harris, 1995; Equation 3.1). Linear regression can be used to develop a calibration that predicts concentration from absorbance.

Equation 3.1 The Beer-Lambert Law

$$\mathbf{A = \varepsilon_\lambda bC}$$

A = absorbance, ε_λ = molar absorptivity at wavelength λ, b = path length, and C = concentration

One significant drawback of classical linear regression is that the concentration of all constituents in the sample must be known in order to determine the molar absorptivity. Multiple Linear Regression (MLR) rearranges the Beer-Lambert Law by combining molar absorptivity and path length into a single term, and adding a matrix of concentration prediction error. This allows for the analyte concentration to be determined without knowing the concentrations of all sample constituents (Kramer, 1998). However, MLR requires the inversion of a matrix and often includes excess noise in the calibration (Beebe and Kowalski, 1987).

Principal Component Analysis (PCA) seeks to group spectral data into principal components (also known as factors) that represent the variance in a calibration dataset. The concentration data are then regressed against these principal components using Principal Component Regression (PCR). PCR requires no wavelength selection; models are less susceptible to noise and can be used on complex mixtures (Kramer, 1998). However, PCR requires a large number of calibration samples, takes longer to perform, and is not as easy to interpret as MLR (Kramer, 1998).

Partial Least Squares (also called Projection to Latent Structures) modeling is similar to PCR but instead of selecting factors based only on the spectral dataset, factors are selected that represent the major components of variance in both the spectral and concentration datasets (Beebe and Kowalski, 1987). These factors are used to define a subspace that can model concentration data in a more accurate manner (Beebe and Kowalski, 1987). Partial Least Squares (PLS) is similar to PCR, but has the advantage of increased robustness due to the incorporation of concentration data in the factor selection stage.

3.1.1 Modeling Caustic Solubility and Buffering Capacity

Currently, the best methods for measuring decay in chip furnishes are the 1% caustic solubility test (PAPTAC Standard G.6 and G.7), potentiometric titration to determine buffering capacity, and visual determination of decay by hand-sorting. Both caustic solubility and buffering capacity provide an indication of the extent of decay by brown-rot fungi and can be correlated with resulting pulp yield and properties (Hunt and Hatton, 1979) and, thus, were selected to be used as reference methods to develop spectroscopic models. In the present study, PLS models based on FTIR, NIR and Raman (SERDS) spectra were developed to predict the 1% caustic solubility and buffering capacity of milled wood samples. The caustic solubility and buffering capacity tests are discussed further in Chapter 4.

The hand-sorting method is the most commonly used method of decay detection because it is easy to perform, and the results are easy to interpret. However, this method cannot measure the degree of decay in a sample and, therefore, cannot be used to estimate potential changes in pulp yield or properties. The validity of the hand-sorting method will be examined by comparing the caustic solubility and buffering capacity of the fractions determined to be sound and decayed.

3.1.2 Modeling Basic Wood Density

Density is an important parameter because wood is commonly purchased and handled on a volumetric basis (TAPPI, 2002). In order to control a property such as density it must first be measured. Since wood swells when wet, wood density must be expressed at a specified moisture content. TAPPI standard methods for measuring wood density are listed in Table 3.1. All of these methods have high levels of precision, but are laborious and time-consuming. For wood chips, basic wood density is most commonly reported because oven-dry volume is difficult to obtain, since wood readily absorbs water, and wet weight is not as reliable a measure as oven-dry weight (TAPPI, 2002).

Table 3.1 TAPPI Standard Methods of Wood Density Determination (Tappi method T258 om-02, TAPPI, 2002)

Method	Mass	Volume
Green density	Water-saturated	Water-saturated
Oven-dry density	Oven-dry	Oven-dry
Basic density	Oven-dry	Water-saturated

Based on samples of sound and decayed Lodgepole pine, basic wood density will be modeled from the FTIR and NIR spectra of milled wood. Since wood density varies between tree

species and within a single tree, models were developed using a well-mixed, single-species dataset. Decay fungi were used to manipulate the density of these wood chips (Bucur *et al.*, 1997). The effect of field samples on the model will also be considered.

3.2 Methods

The hand-sorting method of decay determination was applied to a sample of Douglas-fir (*Pseudotsuga menziesii* (Mirb.) Franco) from Cranbrook, BC and to a sample of black spruce (*Picea mariana* (Mill.) BSP) from Donnacona, QC. Chips were classified as decayed based on white or brown discolouration in regular patterns. Stained chips were not classified as decayed. The resulting sound and decayed fractions were analyzed for caustic solubility, buffering capacity and by FTIR spectroscopy. To better understand the subjectivity of the hand-sorting method of decay detection, four people were asked to hand-sort the same sample of chips.

Seventy-two samples of laboratory-produced decayed wood were prepared and analyzed as described in Chapter 2. An analysis of variance (ANOVA) was performed on the caustic solubility and buffering capacity datasets. The η^2 correlation ratio was used to determine the relative effects of the fungus type, wood species, wood-fungus interaction, and time (specified as a covariate). From each wood species, five white-rot and five brown-rot samples were randomly selected to ensure equal sample sizes in each category.

3.2.1 FTIR Method Optimization

Milled wood samples were Soxhlet extracted in acetone at 70°C for 6 hours and oven dried at 105°C overnight. Samples of extracted and unextracted wood were mixed with spectroscopic grade KCl to make a 10% mixture (a 1% mixture was too dilute). Four 64-scan spectra were obtained on each of the four samples: neat, extracted neat, 10% wood in KCl and

10% extracted wood in KCl. The variance between the spectra in each category was determined to examine the repeatability of each method.

Spectroscopic parameters were optimized by obtaining three spectra with 4 or 8 cm^{-1} resolution and 16, 64 or 256 scans. The caustic solubility of these spectra were predicted by the PLS models to show the effect of changes in number of scans and resolution.

3.2.2 PLS Model Development and Validation – Caustic Solubility and Buffering Capacity

FTIR-based PLS models for caustic solubility and buffering capacity were developed from a calibration dataset of 117 smoothed FTIR spectra. MSC was applied to remove the effect of scatter inherent in diffuse reflectance methods from the spectra.

The 44 samples not used in the initial calibration data set were used as an external validation set. In addition, pine chips stained by the non-decay, bluestain fungus *Ophiostoma piliferum* were analyzed to determine the models' ability to differentiate between stained and decayed wood.

Mixtures of sound and decayed samples of the same wood species were prepared following a 2 factor (sound and decayed), 4 level (sound, one third decayed, two thirds decayed, all decayed) lattice design and analyzed by FTIR. Mixtures of sound spruce, pine and fir were prepared following a 3 factor, 4 level lattice design and analyzed by FTIR (Figure 3.1). Finally, a sound sample of spruce, pine and fir in equal proportions was mixed with a decayed sample of spruce, pine and fir in equal proportions, following a 2 factor (sound and decayed), 4 level (sound, one third decayed, two thirds decayed, all decayed) lattice design. The decayed spruce, pine and fir samples were decayed to approximately the same extent (as estimated by 1% caustic solubility) by *G. trabeum* for 22, 55 and 30 days, respectively. Sample mixtures were prepared by weighing previously characterized milled wood samples and mixing them in given proportions. These samples were thoroughly randomized by shaking prior to analysis by FTIR.

Caustic solubility and buffering capacity data for the mixtures were calculated from the pure samples.

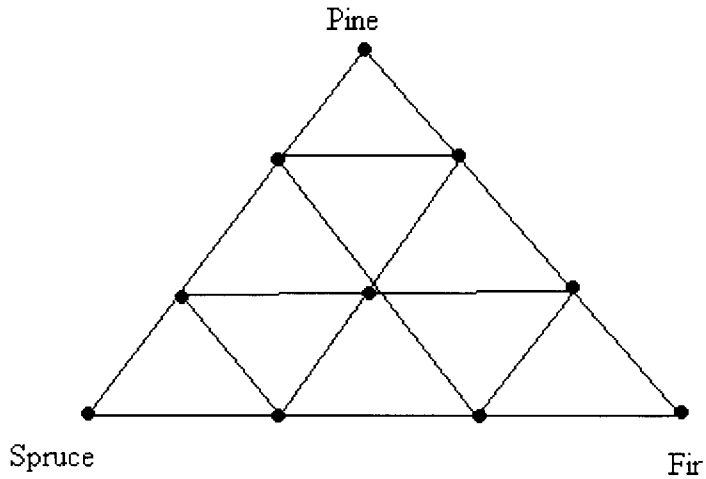

Figure 3.1 A three factor, four level lattice design for mixtures of sound spruce, pine and fir. Points of intersection indicate where mixture samples were obtained. The corners of the largest triangle represent pure wood species.

Within the 161 total samples, 79 field samples were characterized and used in PLS modeling (Appendix I). These field samples consisted of sound and decayed single-species samples, as well as mixtures of softwood chips obtained from wood chip piles.

Milled wood samples that were oven-dried at 105°C for extended periods of time became darker. To investigate this effect, an array of samples prepared from never-dried chips was air-dried, freeze-dried or oven-dried for various length of time at either 105°C or 130°C. FTIR spectra were obtained on these samples and used to predict caustic solubility.

Samples were autoclaved to prevent other fungi from growing on the chips. To examine the effect of autoclaving on the wood chips, duplicate samples of either autoclaved or untreated pine decayed by either *P. pini* or *G. trabeum* were incubated for either 20 or 40 days. Caustic

solubility and buffering capacity were measured and predicted for each sample. Residuals were determined by subtracting measured data from predicted data. The means of these residuals were compared using a two-sample t-test with a 95% confidence interval.

The NIR calibration dataset was based on 300 spectra obtained from 150 samples (72 laboratory-prepared samples and 78 field samples). Most of these samples were the same as those employed for FTIR model development, however, due to availability some of the field samples were of different origins. The Teflon-normalized spectra were regressed against the caustic solubility and buffering capacity datasets. Using Simca-P (Umetrics, Umeå, Sweden), the Orthogonal Signal Correction (OSC) was applied to the dataset in an attempt to improve the accuracy of predictions.

The Raman calibration dataset consisted of 62 laboratory-prepared samples of aspen, hemlock, spruce, pine and fir, used in the calibration with FTIR spectra. The 952 to 1044 cm^{-1} and 1627 to 1763 cm^{-1} region of the SERDS spectra were used to develop PLS models for caustic solubility and buffering capacity.

3.2.3 Basic Wood Density

Lodgepole pine obtained near Kamloops, BC was chipped using a 36 inch CM&E 10-knife disc chipper and mixed. A sample of these chips was screened through a Wennberg chip classifier and the portion retained on the 7 mm round-hole screen was used for further testing. This fraction was sterilized by autoclaving at 121°C for 40 minutes. Twenty-two 50g samples were decayed by fungi listed in Table 2.2 and incubated for up to 59 days at room temperature (Ferraz *et al.*, 2000). Thirteen Lodgepole pine field samples were obtained from clear and Mountain pine beetle-killed stands near Williams Lake, BC.

In order to determine the basic wood density on only 50g of chips, the standard method (Tappi T 258 om-02) was scaled down (TAPPI, 2002). Approximately 50g (OD equivalent) of

wood chips were soaked in water for 24 hours, and blotted dry with paper towel. The chips were weighed in a 1L Erlenmeyer flask, which served as a pycnometer. The flask was then filled with water to a line near the top of the flask, bubbles were dislodged from the chips with a glass stir rod and the weight recorded. The chips were oven-dried and weighed and the basic wood density determined by dividing the mass of the oven-dried chips by the volume of water displaced by the chips. The precision of this scaled-down method was determined by measuring the density of five wood chip samples, of different wood species, five times.

All models of basic wood density were developed using the PLS-1 algorithm and full cross validation from 23 point Savitzky-Golay 1st derivative spectra (Savitzky and Golay, 1964). Seventy spectra from 39 milled wood samples (22 laboratory-prepared, 17 field samples) were obtained. Twenty-three spectra were randomly selected and removed from the calibration dataset in order to serve as an independent validation dataset.

Leachate from steeping during the basic wood density test for the laboratory-prepared samples was collected and analyzed for COD using the accu-Test Standard Range Micro-COD Test Method (Bioscience, 2003).

3.3 Results

The reliability of the hand-sorting method was assessed by comparing the results obtained from four different people on the same sample. Estimates of the decay content ranged from 13.1% to 15.8%, with a mean of 14.6% and a standard deviation of 1.3%. This level of precision is extremely good for a subjective test.

To further validate the hand-sorting method, two samples of chips with visible signs of decay were hand-sorted into sound and decayed fractions (Table 3.2). The Douglas-fir sample had a high proportion of chips with visible signs of decay; however, the caustic solubility and buffering capacity were not higher in the chips visually identified as decayed. This is likely due

to the dominant type of decay being white-rot, which does not affect caustic solubility and buffering capacity to the same extent as brown-rot fungi. The black spruce sample had a relatively low proportion of decayed chips; however, these chips did have slightly higher caustic solubility and buffering capacity than the sound chips. Together, these two sets of data demonstrate the need for other methods of measuring decay besides hand-sorting based on visual detection.

Table 3.2 Hand-sorting Douglas-fir and Black spruce into Sound and Decayed Fractions Based on Visual Assessment

Sample	Douglas-fir		Black spruce	
% decay (w/w) determined by hand-sorting	17.0		2.4	
Hand-sorted fraction	Sound	Decayed	Sound	Decayed
Caustic Solubility (%)	20.8	17.5	17.8	19.6
Buffering Capacity (mol/g)	0.049	0.036	0.043	0.082

Caustic solubility and buffering capacity data cover a wide range, from 10.8 to 68.3% and 0 to 0.327 mol/g, respectively. Although both tests are independent, there was a strong correlation ($r^2 = 0.73$) between them (Figure 3.2). Within the dataset, there were more sound samples than decayed samples and more softwoods than hardwoods. This led to the low median caustic solubility (16.6%) and buffering capacity (0.059 mol/g) of the samples. These medians are typical of sound softwoods (Procter, 1973).

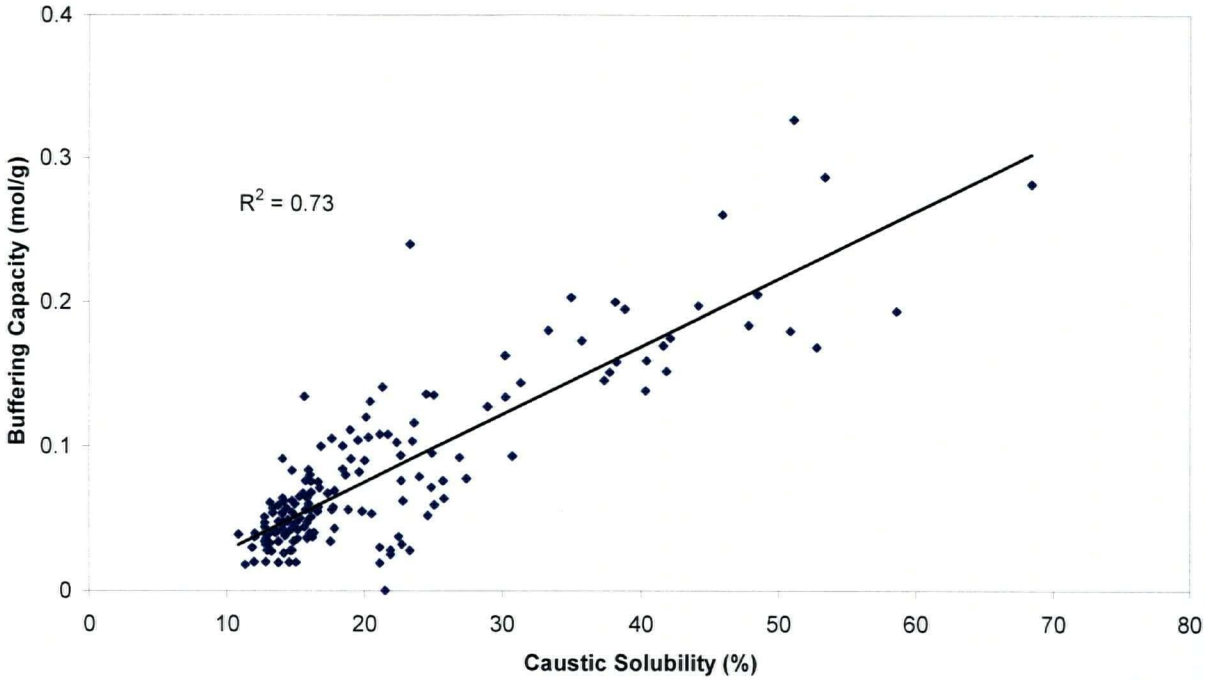

Figure 3.2 Correlation between the 1% Caustic Solubility and Buffering Capacity of Wood All Samples Measured

Analysis of Variance was performed on caustic solubility and buffering capacity datasets to determine η^2 correlation ratios, which show the proportion of the total variance attributable to wood, fungal type, wood/fungus interactions and time (specified as a covariate), respectively (Tables 3.3 and 3.4). Fungal type had the most significant effect on caustic solubility and buffering capacity. At the 95% confidence interval, only time and fungal type were significant contributors to both predictive models. Wood species was found to be a significant factor that affected buffering capacity but not caustic solubility. Wood/fungal interactions were not found to have a significant impact on caustic solubility or buffering capacity values. Error, which accounted for approximately 41% of the variance, suggests that additional factors affect the caustic solubility and buffering capacity of wood.

Table 3.3 Analysis of variance in caustic solubility ($\alpha = 0.05$) attributable to wood species, fungal type, wood/fungal interactions and time

Source	SS	df	MS	F ratio	P value	η^2
Wood	636	4	159	2.2	0.088	9.4
Fungal type	2821	1	2821	38.9	0.000	41.7
Wood x Fungus type	122	4	31	0.4	0.792	1.8
Time	354	1	354	4.9	0.033	5.2
Error	2932	39	73			41.9

Where SS = Sum of Squares, MS = Mean Square and df = Degrees of Freedom

Table 3.4 Analysis of variance in buffering capacity ($\alpha = 0.05$) attributable to wood species, fungal type, wood/fungal interactions and time

Source	SS	df	MS	F ratio	p	η^2
Wood	0.021	4	0.005	2.7	0.044	11.5
Fungal type	0.071	1	0.071	37.0	0.000	38.8
Wood x Fungus type	0.006	4	0.001	0.8	0.559	3.3
Time	0.010	1	0.010	5.4	0.025	5.5
Error	0.075	39	0.002			41.0

Where SS = Sum of Squares, MS = Mean Square and df = Degrees of Freedom

The means and standard deviations of caustic solubility and buffering capacity measurements for sound samples obtained with six replicates show the precision of these methods (Table 3.5). The coefficients of variance of the caustic solubility and buffering capacity measurements were between ± 2% and ± 7%, respectively. According to the 1% caustic solubility standard, PAPTAC (2000), the results of duplicate tests should vary by less than ± 5% and by less than ± 2% with "careful work." Although the caustic solubility tests comply with the precision outlined by the method (PAPTAC, 2000), the test has inherently low precision.

Table 3.5 Mean and Standard Deviation for Decay Detection Methods on Six Replicates of Sound Wood Samples (Standard Deviations Shown in Parentheses)

Wood Species	1% Caustic Solubility (%)	Buffering Capacity (mol/g)
Aspen	22.8 (0.6)	0.064 (0.004)
Pine	18.9 (0.7)	0.111 (0.004)
Hemlock	14.7 (1)	0.064 (0.004)

Figure 3.3 shows representative FTIR spectra of sound, white-rot and brown-rot decayed wood. There are few distinct variations between these spectra. This suggests that a multivariate statistical method may be required to gain useful chemical information from these spectra. Peak assignments for wood components are reported by Baeza and Freer (2001).

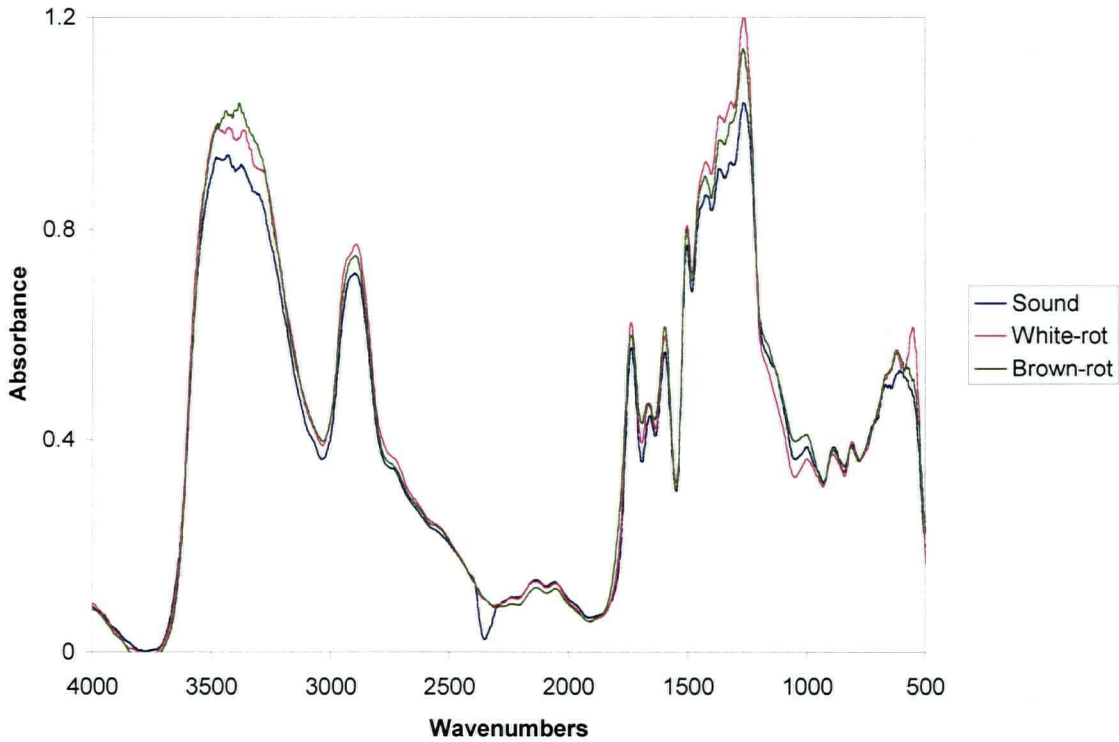

Figure 3.3 Typical FTIR spectra of sound, white-rot and brown-rot decayed spruce samples

The sample preparation methods examined showed little difference between acetone-extracted and unextracted samples. Spectra of neat samples were found to have better repeatability than samples in a KCl mixture. Figure 3.4 shows the variance as a function of wavenumber for these samples. Spectra obtained with 4 cm^{-1} resolution and 256 scans were found to have the lowest spectral variation and greatest sensitivity (in the region of interest). Spectra obtained with 8 cm^{-1} resolution had lower variation, which came at the expense of sensitivity. For these reasons, it was determined that all subsequent FTIR spectra should be obtained on unextracted, neat samples with 256 scans at 4 cm^{-1} resolution.

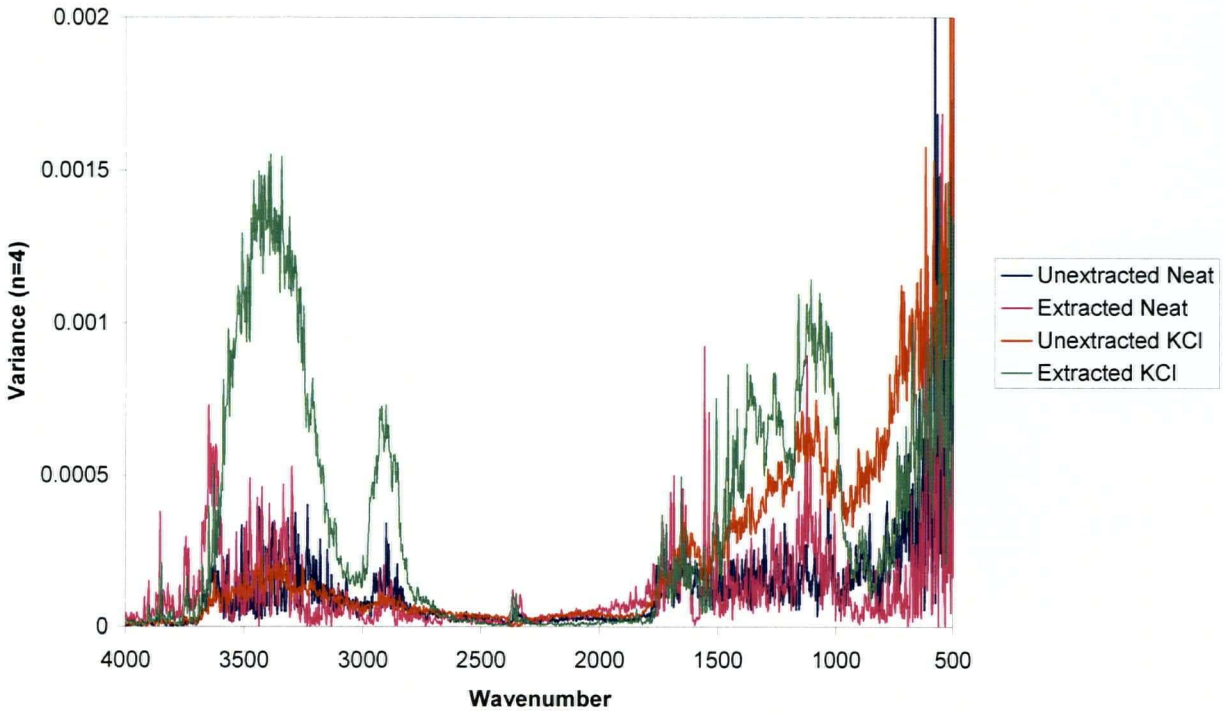

Figure 3.4 FTIR Spectral Variance of Four Milled Wood Samples with 64 scans and 4 cm^{-1} resolution.

Figure 3.5 shows the difference spectra obtained by subtracting the FTIR spectra of brown-rot-decayed and sound wood from five wood species to highlight the spectral changes due to decay. These differences are similar in each wood species. The region between 1872 and 1672

cm^{-1}, which corresponds to carbonyl and carboxyl stretching, shows the greatest variation in the difference spectra. The variance observed in these functional groups is consistent with the observation that acidity increases with extent of decay (Fuller, 1985).

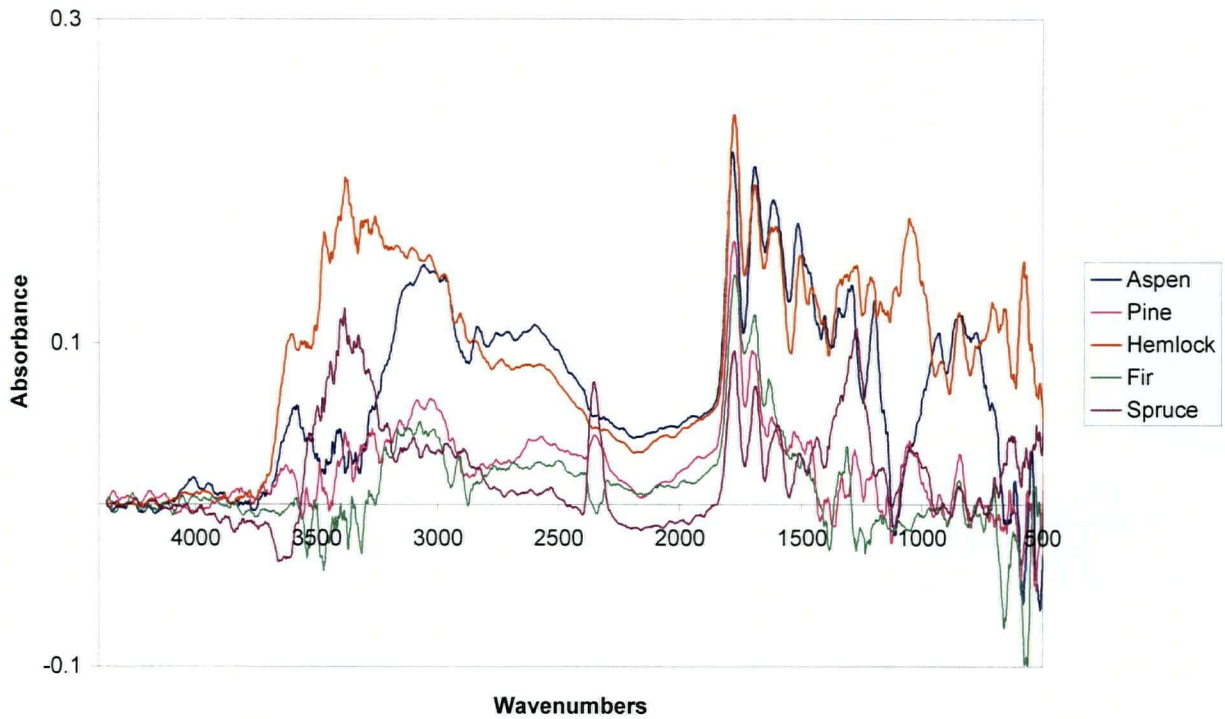

Figure 3.5 The Difference of FTIR Spectra from Sound and Brown-rot Decayed Wood

A correlogram plots the r^2 value between absorbance and concentration as a function of wavenumber. This provides a graph where the spectral regions with the highest correlation to caustic solubility have the highest peaks. Caustic solubility and buffering capacity correlograms are very similar, and as a result the models were based on the same spectral region. All correlograms are shown in Appendix IV. The correlograms indicated that the most highly correlated region was between 1872 and 1672 cm^{-1}. This is the same region that was highlighted by the difference spectra as being influenced by decay (Figure 3.5). Several models were prepared based on this region, the entire region, and combinations of other spectral regions,

however, models based on the region between 1872 and 1672 cm^{-1} were best able to predict caustic solubility and buffering capacity. Therefore, the region between 1872 and 1672 cm^{-1} was used to prepare the calibration models for caustic solubility and buffering capacity.

3.3.1 FTIR Modeling

The FTIR spectral data from the calibration dataset (Appendix I) were related to the 1% caustic solubility and buffering capacity using PLS modeling as described in Chapter 2. PLS model descriptions and factor loadings are presented in Appendices II and III. PRESS diagrams are used to determine the appropriate number of factors to use (Beebe *et al.*, 1998). All PRESS diagrams are shown in Appendix V. The PRESS diagrams for caustic solubility and buffering capacity show that as the factor number is increased to five the PRESS decreases, indicating that the model is accounting for a greater proportion of the variance in the calibration dataset. As the factor number is increased past five, PRESS increases slightly, indicating that noise is being modeled. Based on the PRESS diagram and modelling with different numbers of factors, five factors were determined to be optimum for both caustic solubility and buffering capacity. The optimum models, as determined by high r^2 and high RMSECV, were developed as described in Chapter 2.

The PLS models are shown by plotting predicted caustic solubility and buffering capacity data as a function of the measured data (Figures 3.6 and 3.7). The line shown in each of these graphs indicates a perfect prediction where the predicted and measured datasets are equal. RMSECV and RMSEP are the measures of deviation from this line for the calibration and validation datasets, respectively and are comparable to the standard deviations of the wet chemistry methods (Tables 3.5 and 3.6). Based on the RMSEP of the validation dataset, the uncertainty of the caustic solubility and buffering capacity models is ± 3.3% and 0.024 mol/g, respectively. Since error compounds, the PLS modeled data is slightly less precise than the wet

methods (Beebe *et al.*, 1998). The high r^2 values indicate a good correlation between measured and predicted data (Table 3.6).

Table 3.6 PLS Modeling Statistics for the Calibration and Validation of Caustic Solubility and Buffering Capacity Models

Method	r^2 - Calibration	RMSECV - Calibration	RMSEP - Validation	Standard Deviation of spectra obtained from sound pine
Number of samples		117	44	6
1% Caustic Solubility	0.85	4.1 %	3.3 %	1.5 %
Buffering Capacity	0.87	0.020 mol/g	0.024 mol/g	0.008 mol/g

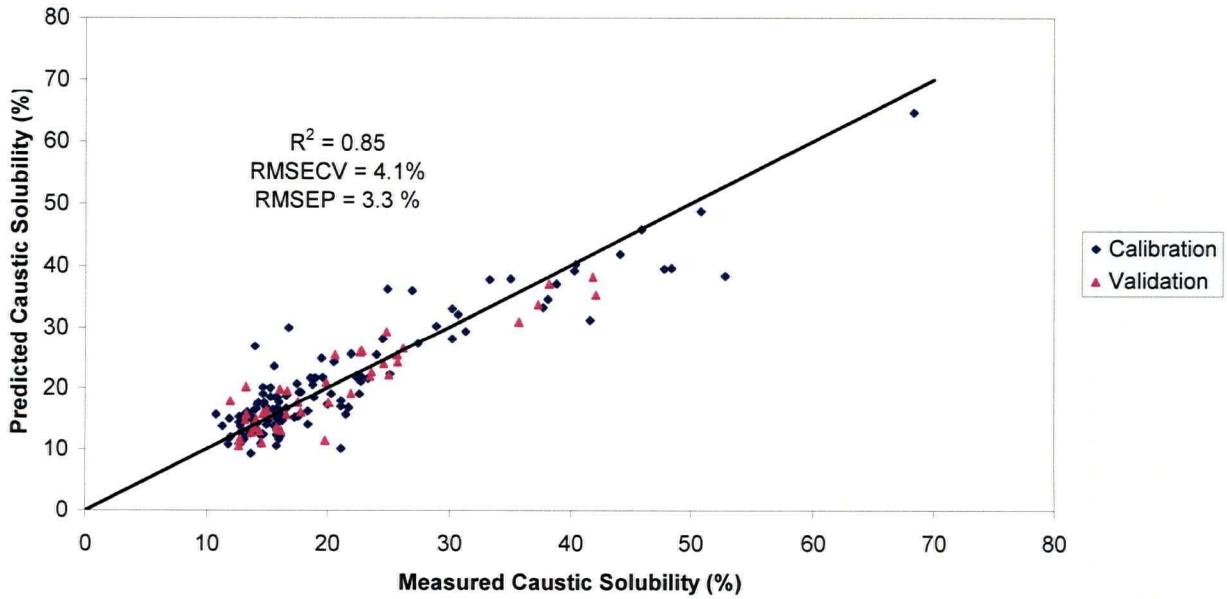

Figure 3.6 FTIR-Based Model: PLS-Predicted vs. Measured Caustic Solubility

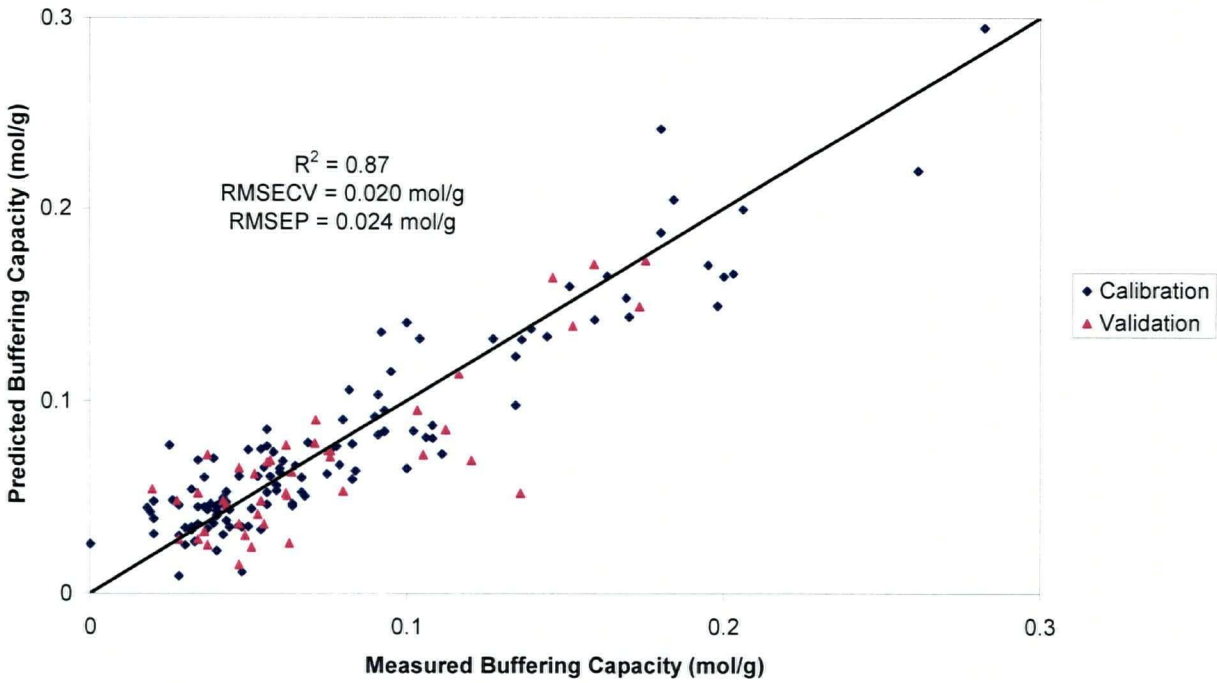

Figure 3.7 FTIR-Based Model: PLS-Predicted vs. Measured Buffering Capacity

The repeatability of the PLS model predictions was determined (Table 3.6). Six spectra were collected from a sample of sound pine, not used in the calibration dataset. The caustic solubility and buffering capacity of these samples were predicted by the calibration models. The low standard deviations indicate that spectroscopic repeatability was a minor source of error. However, spectroscopic repeatability was poorer than that of the wet methods (Table 3.5). The standard deviation of the PLS-predictions of sound pine was much lower than the RMSEP for the model, indicating that spectroscopic repeatability is a small factor affecting the overall predictive ability of the model.

Models were examined by plotting the Studentized concentration residuals as a function of sample leverage. This provides an indication of how well a sample's concentration is predicted, and its effect on the PLS model. Sample leverage is a measure of the degree of the effect that one sample has on the model. The Studentized residual measures how accurately the model predicts the concentration of a sample. Thus, samples with high leverage and Studentized

residuals greater than ± 2.5 are undesirable (Beebe *et al.*, 1998). Seven samples were excluded from the calibration model based on having very high leverage and being extremely poorly predicted. These included four extremely decayed brown-rot samples and two Western redcedar samples, which were significantly over-estimated by the models. The brown-rot samples had extremely high caustic solubility and buffering capacity. These wood chip samples were decayed and friable to the extent that they would likely not survive chip-handling procedures. The model's inability to accurately estimate extent of decay in these samples suggests that the models are unable to accurately estimate extent of decay in extremely decayed wood. The Western redcedar samples both had extremely high buffering capacity but normal caustic solubility. This is likely due to the presence of acidic extractives that increase buffering capacity. The Western redcedar samples contained very high amounts of acetone extractives (up to 11.1%). Removal of the extractives from the Western redcedar samples slightly improved the PLS predictions. Hunt (1979) found that for a 1% increase in caustic solubility the effective alkali consumed increased much more for Western redcedar than for other wood species. This suggests that decayed Western redcedar has more acidic groups than other decayed wood species and could explain its different spectral properties. Thus, in the case of Western redcedar, wood species appears to be an important factor. Overall, the removal of these outliers did not significantly impact the models.

Most of the modelled samples had low studentized residuals and/or low leverage. After removal of the outliers and remodelling, six additional samples were found to have caustic solubility studentized residuals greater than an absolute value of 2.5, however, none had high leverage and thus, although poorly predicted, these samples had little effect on the model (Figure 3.8). Three samples had buffering capacity studentized residuals greater than an absolute value of 2.5. Two of these had moderately high leverage. When these samples were removed from the

calibration dataset the model did not significantly change and so the previous calibration was retained.

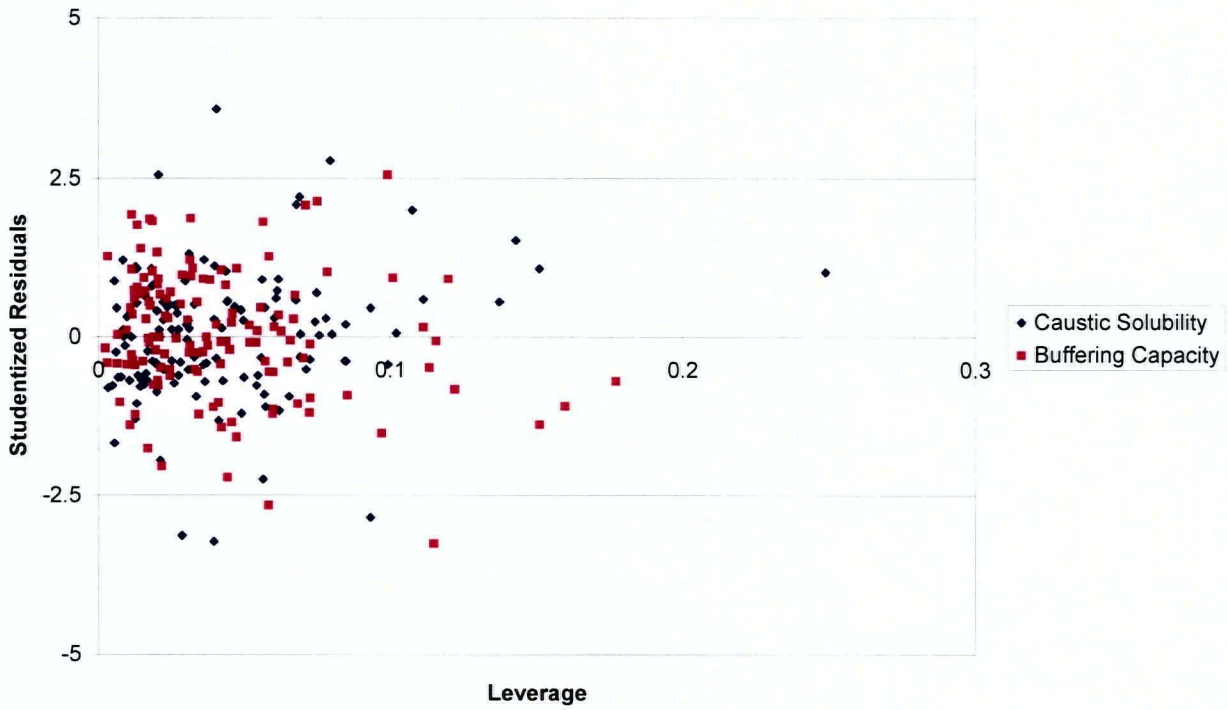

Figure 3.8 Calibration models: studentized residuals as a function of sample leverage. A studentized residual greater than an absolute value of 2.5 is considered high (Beebe *et al.*, 1998).

3.3.2 Model Validation

The caustic solubility and buffering capacity of the 44 randomly selected samples, not used in the calibration dataset, were predicted using the PLS models (Appendix I). Table 3.6 shows the Root Mean Standard Error of Prediction (RMSEP) for the validation datasets. A low RMSEP value is considered to be a better indicator of accurate predictions than low RMSECV because it is not based on samples used in the calibration stage. The RMSEP values in Table 3.6 were similar to the RMSECV values, confirming that the models accurately predict decay extent of samples not included in the calibration dataset. Figures 3.6 and 3.7 also show the validation dataset covers a range similar to that of the calibration dataset.

The PLS models were developed on single wood species samples. In order to assess the capability of the models to quantify the caustic solubility and buffering capacity of mixtures of wood species and decay extents, a situation more typical of mill furnishes, wood species mixtures with approximately the same decay extent (as measured by 1% caustic solubility) single species mixtures of samples with different extent of decay and combinations of mixed species and mixed decay extents were predicted by the PLS models. Caustic solubility data were all accurately predicted within a 95% confidence interval ($\alpha = 0.05$), defined by the RMSEP of the caustic solubility external validation (Figure 3.9). The predicted buffering capacities of four mixtures samples fell outside the 95% confidence interval defined by the RMSEP of the buffering capacity external validation (Figure 3.10). Nonetheless, more than 80% of the samples were accurately predicted.

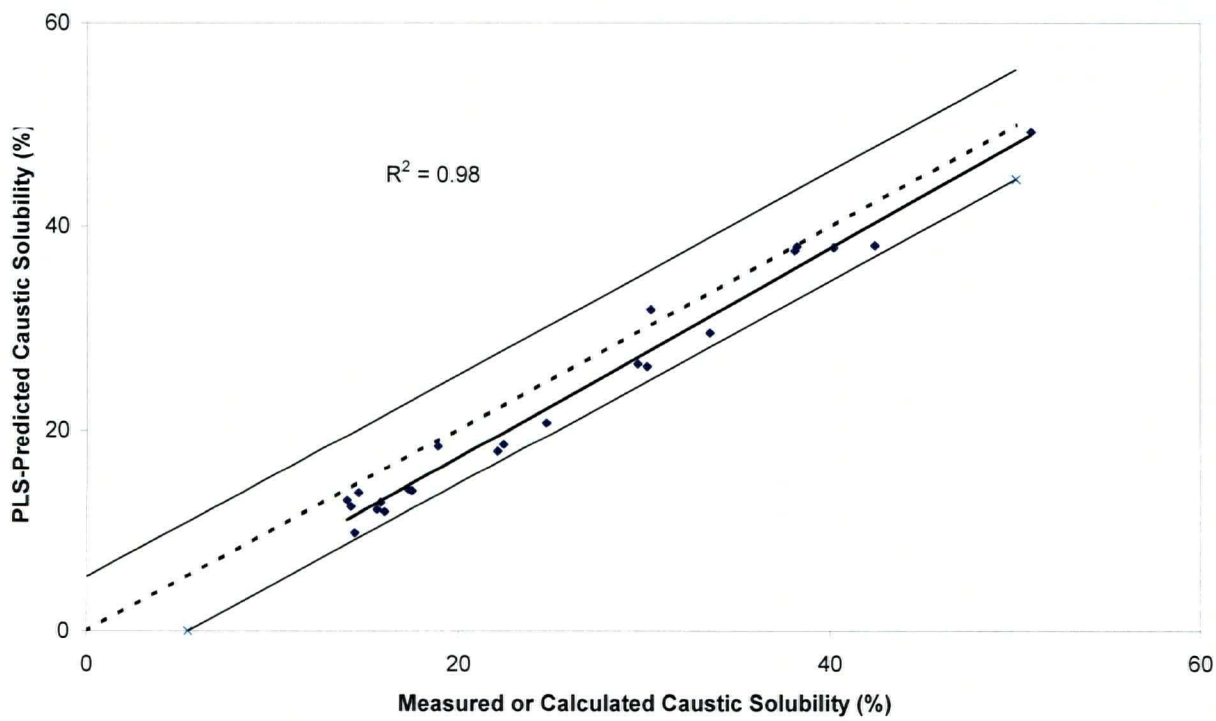

Figure 3.9 PLS-Predicted vs. measured caustic solubility in milled wood mixtures. The dotted line represents where predicted data equal measured data. The thin solid lines bounding the dotted line represent the 95% confidence interval based on the RMSEP of the caustic solubility model. The thick solid line is a best-fit line.

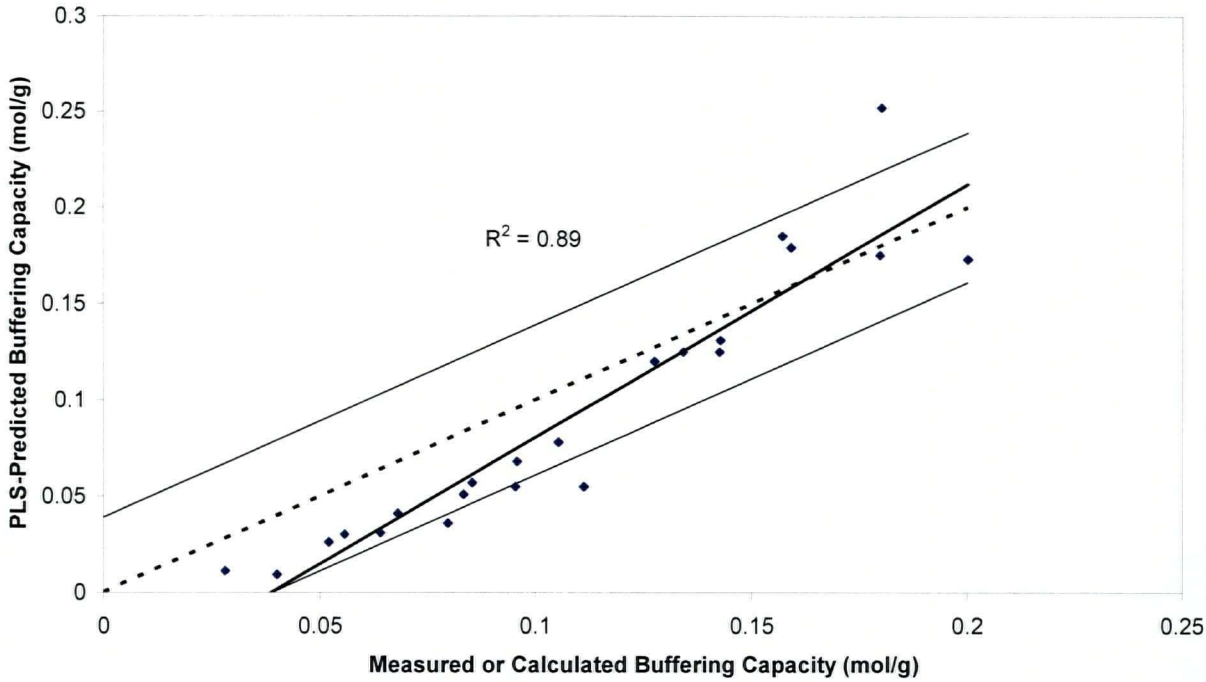

Figure 3.10 PLS-Predicted vs. measured buffering capacity in milled wood mixtures. The dotted line represents where predicted data equal measured data. The thin solid lines bounding the dotted line represent the 95% confidence interval based on the RMSEP of the buffering capacity model. The thick solid line is a best-fit line.

The r^2 and RMSEPs of the mixed samples are shown in Table 3.7. The strong correlations and low RMSEPs confirm that the models can accurately predict caustic solubility and buffering capacity in mixtures of wood species. The systematic deviation from perfect prediction shown in Figures 3.9 and 3.10 is attributed to the random error found in the prediction of the pure samples. The mixtures are exhibiting the same error found in the pure samples.

Table 3.7 PLS-Prediction Statistics for Mixtures of Sound and Decayed Spruce, Pine and Fir

Dataset	r^2	RMSEP
Caustic Solubility	0.98	3.1
Buffering Capacity	0.89	0.033

In order to better understand the effects of wood species on the predictive ability of the models, new PLS models were prepared from aspen and softwood samples (Table 3.8). The softwood model performed similarly to the overall model, with slight gains in RMSECV, attributable to the absence of the aspen samples. The aspen models were less robust than the overall model, which is primarily a result of the significantly smaller sample size. While some single wood species models may provide improved predictive ability, in most cases the versatility and robustness of the overall model would be of greater value.

Table 3.8 Modeling Statistics for Independent Wood Species and Fungal Type Models

Population	N	r^2	RMSECV
Overall Caustic Solubility	117	0.85	4.1
Overall Buffering Capacity	117	0.87	0.020
Aspen Caustic Solubility	20	0.68	8.3
Aspen Buffering Capacity	20	0.80	0.032
Softwood Caustic Solubility	65	0.91	3.2
Softwood Buffering Capacity	65	0.91	0.017
White-rot Caustic Solubility	29	0.26	2.4
White-rot Buffering Capacity	29	0.27	0.028
Brown-rot Caustic Solubility	32	0.90	3.7
Brown-rot Buffering Capacity	32	0.93	0.016

To better understand the effects of different types of decay, PLS models were developed separately on white- and brown-rot softwood samples (Table 3.8). The white-rot models were much poorer than the overall model, likely because of the reduced range in caustic solubility (11.9 to 20.1%) and buffering capacity (0.020 to 0.120 mol/g). The brown-rot models were

comparatively better than the overall model, however, the gains were small and this model would not be practical for field samples that may be decayed by different fungal types.

To determine the effect of oven-drying on the spectroscopic properties of the samples, the average PLS-predicted caustic solubility of three samples that were oven-dried for up to one week at either 105°C (the standard oven-drying temperature, PAPTAC method G.3) or 130°C was determined (Figure 3.11). The predictions of caustic solubility on the samples stored at 105°C increased, but at a much slower rate than those stored at 130°C. Thermal degradation of wood is reported to occur at temperatures as low as 100°C and can result in weight loss from the release of carbon dioxide and water vapour and loss of strength properties (Zabel and Morrell, 1992). However, there was no significant difference (95% confidence) in PLS-predicted caustic solubility between the sample stored for 24 hours and the sample stored for 72 hours at 105°C. It is thus safe to leave a sample in the oven at 105°C for a few days. PLS-predicted buffering capacity behaved in an analogous manner.

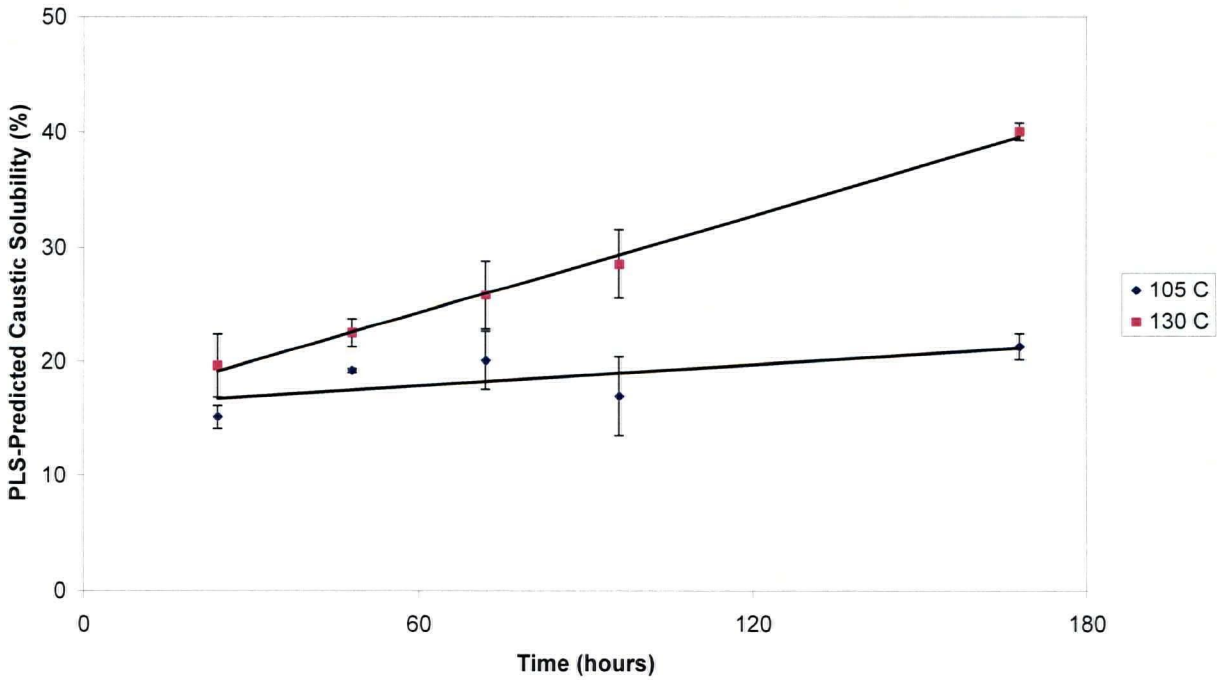

Figure 3.11 PLS-Predicted caustic solubility of milled Lodgepole pine stored at 105°C and 130°C. Error bars represent the standard deviation of three replicates.

Data from Table 3.9 indicate that the PLS-predicted caustic solubility of freeze-dried wood was much lower than for the oven-dried samples (likely due to the retention of more volatile extractives). The under-estimation of caustic solubility by the current model is attributable to the fact that the calibration dataset was all oven-dried. Either oven-drying or freeze-drying will yield reproducible spectra, however, there is a small difference in the spectra between samples dried by different methods. Thus, when obtaining spectra for PLS modeling, it is important to use the same drying method for all samples.

Table 3.9 PLS Predictions of Freeze-Dried and Oven-Dried Samples (n = 3, Standard Deviations in Parentheses)

Sample	PLS-Predicted Caustic Solubility (%)	PLS-Predicted Buffering Capacity (mol/g)
Freeze-dried (24 hours)	8.0 (2.6)	0.011 (0.005)
Oven-dried (24 hours)	15.1 (1.0)	0.045 (0.002)

Autoclaved wood chips inoculated with brown-rot fungi were found to decay more rapidly than non-autoclaved chips inoculated with the same fungus (Table 3.10). This was likely due to antagonistic interactions with moulds present on the untreated chips. Residuals (predicted minus measured data) were calculated to show the inaccuracies of the model. Paired t-tests (α = 0.05) were used to determine that there were no significant differences between the caustic solubility ($p = 0.578$) and buffering capacity ($p = 0.954$) residuals of the autoclaved and untreated samples. The caustic solubility and buffering capacity residuals indicated no systematic differences between the accuracy of predictions on autoclaved and untreated samples.

Table 3.10 Comparison of Autoclaved and Untreated Sample Predictions by FTIR-Based Caustic Solubility and Buffering Capacity Models.

Sample	Caustic Solubility (%) n = 3			Buffering Capacity (mol/g) n = 1		
	Measured (Std. Dev.)	Predicted	Residual	Measured	Predicted	Residual
A Gt 20	19.0 (2.4)	16.5	-2.5	0.092	0.061	-0.031
A Gt 40	35.7 (1.3)	26.7	-9.0	0.176	0.130	-0.046
A Pi 20	16.7 (0.7)	18.1	1.4	0.072	0.068	-0.004
A Pi 40	15.6 (0.5)	18.6	3.0	0.136	0.077	-0.059
U Gt 20	17.7 (0.2)	19.6	1.9	0.076	0.061	-0.015
U Gt 40	22.9 (1.3)	21.7	-1.2	0.136	0.074	-0.063
U Pi 20	17.4 (0.7)	18.8	1.4	0.080	0.065	-0.015
U Pi 40	15.0 (1.3)	12.9	-2.2	0.084	0.035	-0.049

A = autoclaved, U = untreated, Gt = *G. trabeum*, Pi = *P. pini*, 20 and 40 days of incubation

Many of the Lodgepole pine field samples came from trees attacked by the Mountain pine beetle (Appendix I). While there was heavy staining in all beetle-attacked samples, elevated caustic solubility and buffering capacity was only observed in samples three years after being attacked. The models were able to accurately predict the caustic solubility and buffering capacity of these samples. More significant was the model's ability to identify the sample from the tree three years post-beetle-attack as the only sample with significantly higher caustic solubility and buffering capacity (Appendix I). This further suggests that staining fungi do not influence the PLS models. In addition, laboratory-prepared stained pine was examined to confirm that the stain present in the wood did not affect the PLS model's ability to predict decay. The bluestain fungus, *Ophiostoma piliferum*, was selected because it is known to stain Lodgepole pine with little or no structural damage or decay (Smith, 1973). Pine infected with *O. piliferum* had lower caustic solubility and buffering capacity than sound pine, which is attributed to the fungus'

utilization of extractives (Brush *et al.*, 1994). The PLS models were able to accurately predict the caustic solubility and buffering capacity of this sample, which suggests that the presence of staining fungi does not confound the prediction of decay. This also suggests that the models are measuring changes in wood chemistry and not an increase in fungal biomass.

3.3.3 NIR Modeling

The dataset used to develop models from Visible/NIR spectra was developed based on a number of samples ranging in caustic solubility and buffering capacity from 10.8 to 68.3% and 0 to 0.326 mol/g, respectively. As in the FTIR dataset, sound and incipient decay samples predominated. The NIR dataset was PLS modelled with and without orthogonal signal correction. OSC was found not to significantly improve the models and was thus abandoned.

PLS models based on Visible/NIR spectra were developed iteratively as described in section 2.4 (Table 3.11). PLS model descriptions and factor loadings are presented in Appendices II and III. Correlograms indicated that the NIR region was more strongly correlated with caustic solubility and buffering capacity than the visible region, and thus the 1000 to 2400 nm region was used to develop all models (Appendix IV). This region included most of the NIR region. It contains regions that correspond to O-H stretching in cellulose, hemicellulose and lignin, O-H, C-H and C-C stretching and deformation in cellulose and C-H and C=C stretching in lignin (Ali *et al.*, 2001, Fourty *et al.*, 1996, Kelley *et al.*, 2004). Figure 3.12 shows the visible/NIR spectra of Lodgepole pine samples at various stages of decay. NIR spectra of brown-rot decayed wood showed increased reflectance from 1200 to 2500 nm. Kelley *et* al., (2002) observed similar trends in *G. trabeum*-decayed spruce. The increased reflectance (decreased absorbance) has been attributed to a decrease in hydroxyl vibrations and to changes in the wood hydroxyl and hydrogen bonded water associated with lignin (Kelley *et al.*, 2002). Ferraz *et al.*

(2004) have observed the opposite trend in loblolly pine samples decayed by a white-rot fungus, likely due to an increase in hydroxyl groups.

Correlations between measured and predicted caustic solubility and buffering capacity were strong (Figure 3.14 and 3.15). The RMSECV and RMSEP indicate that the data were accurately modeled and that the NIR models were of similar quality to FTIR models. However, the caustic solubility model (Figure 3.14) does indicate a bias towards under-estimating caustic solubility at high levels. Presently the causes to this apparent bias remain unclear, however, since the bias is small and only occurs at over 30% caustic solubility it is unlikely to have a significant impact. Despite this potential shortcoming, the NIR spectra were easier and faster to obtain the FTIR spectra. Furthermore, NIR spectroscopy is more amenable to online analysis than FTIR.

Table 3.11 PLS Models of Caustic Solubility and Buffering Capacity with NIR Dataset

Constituent	# of factors	r^2	RMSECV	RMSEP
Caustic Solubility	10	0.82	4.4 %	4.3 %
Buffering Capacity	10	0.80	0.026 mol/g	0.026 mol/g

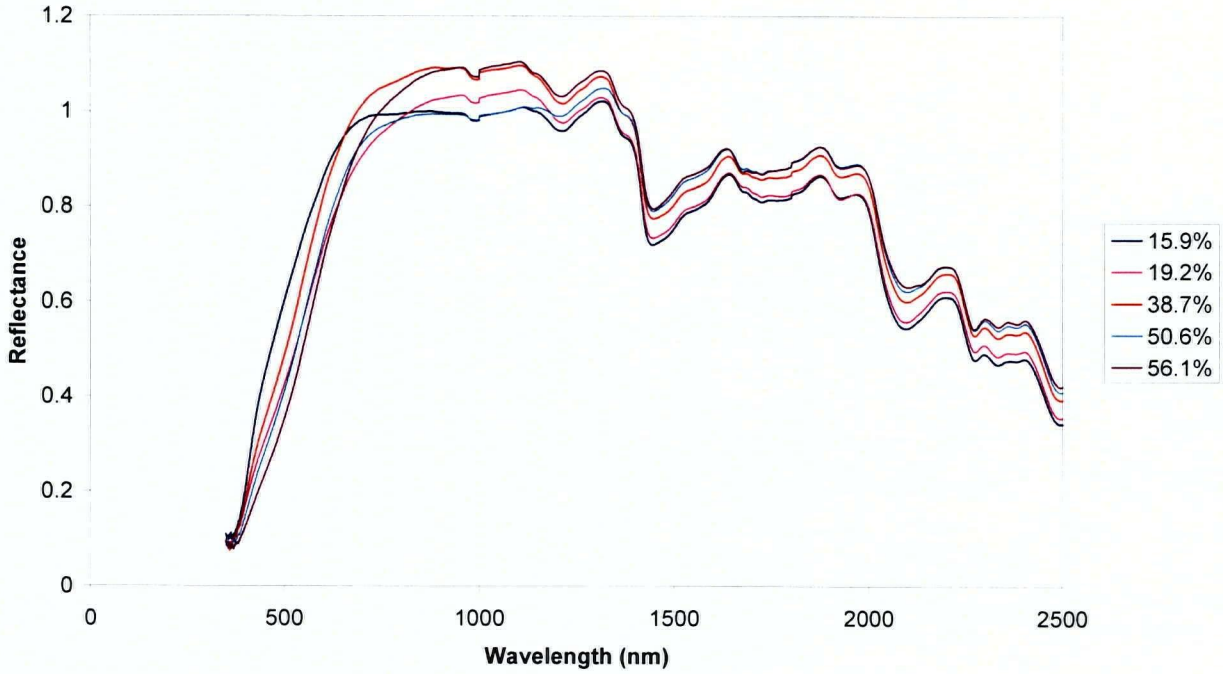

Figure 3.12 Visible/NIR spectra of Lodgepole pine with varying caustic solubility.

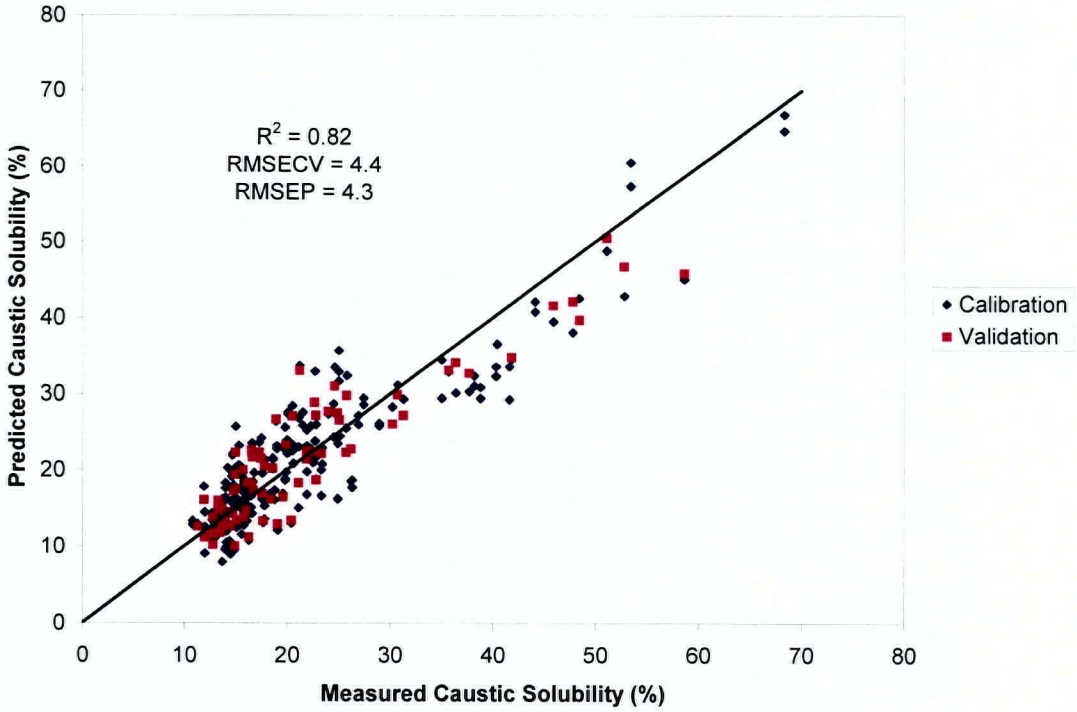

Figure 3.13 NIR-based Model: PLS-Predicted vs. Measured Caustic Solubility

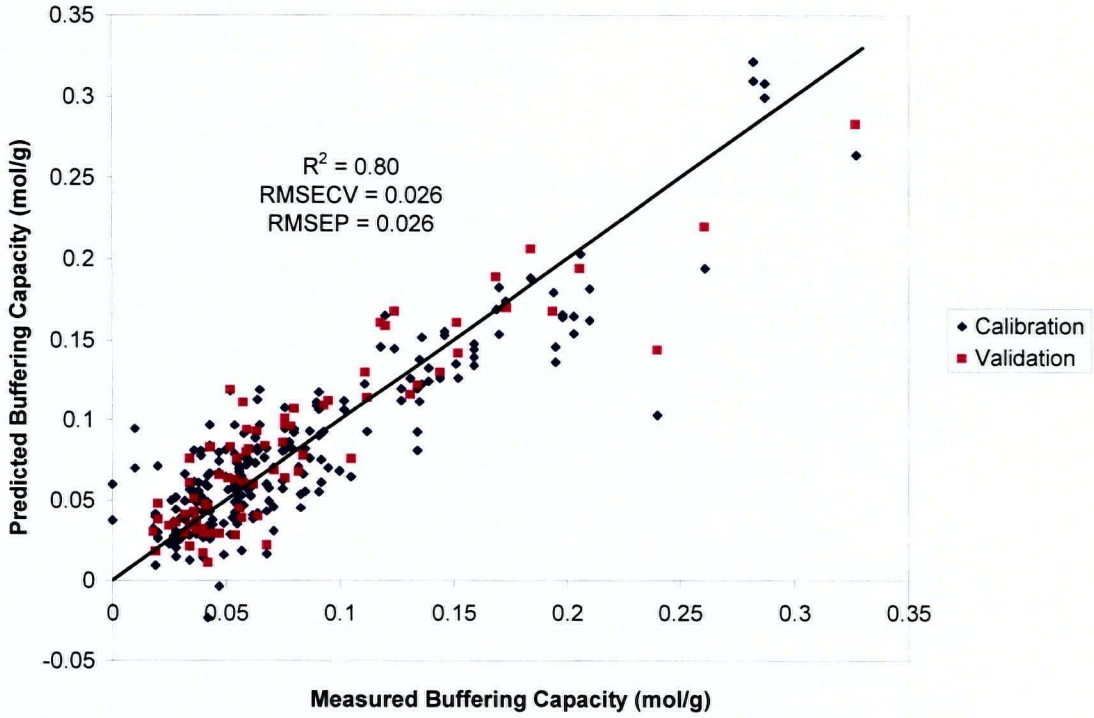

Figure 3.14 NIR-based Model: PLS-Predicted vs. Measured Buffering Capacity

3.3.4 Raman Modeling

Raman spectra of wood samples had very high laser induced fluorescence (LIF), as expected (Agarwal and Ralph, 1997). When SERDS spectra were obtained on the wood samples, LIF was significantly reduced but the quality of the spectra was also reduced by numerous spectral anomalies. The subtraction involved in the SERDS method resulted in negative peaks (Figure 3.15). The SERDS spectra did provide some qualitative chemical information. Peaks at 1096 and 1123 cm^{-1} are attributable to cellulose, the peak at 1335 cm^{-1} is attributable to aliphatic OH bending, and the peaks at 1606 and 1659 cm^{-1} correspond to symmetric aryl ring stretching in lignin (Agarwal and Ralph, 1997, Sun *et al.*, 1997). Since the y-axis is measured in Counts, this should not be observed. Nonetheless, the SERDS spectra showed a weak correlation to caustic solubility and buffering capacity around the peaks at 1105, 1140, 1610 and 1670 cm^{-1}. Attempts to develop PLS models around these peaks were unsuccessful (Table 3.12, Figures

3.16, 3.17). The loss of spectral quality due to extensive LIF reduced the quality of the models. The best models developed showed weak correlations between the predicted and measured data and had a RMSECV approximately five times greater than the standard deviation of the caustic solubility and buffering capacity methods.

Table 3.12 PLS Modeling Statistics for Raman Spectra

Constituent	# of factors	r^2	RMSECV
Caustic Solubility	10	0.44	9.6 %
Buffering Capacity	7	0.28	0.054 mol/g

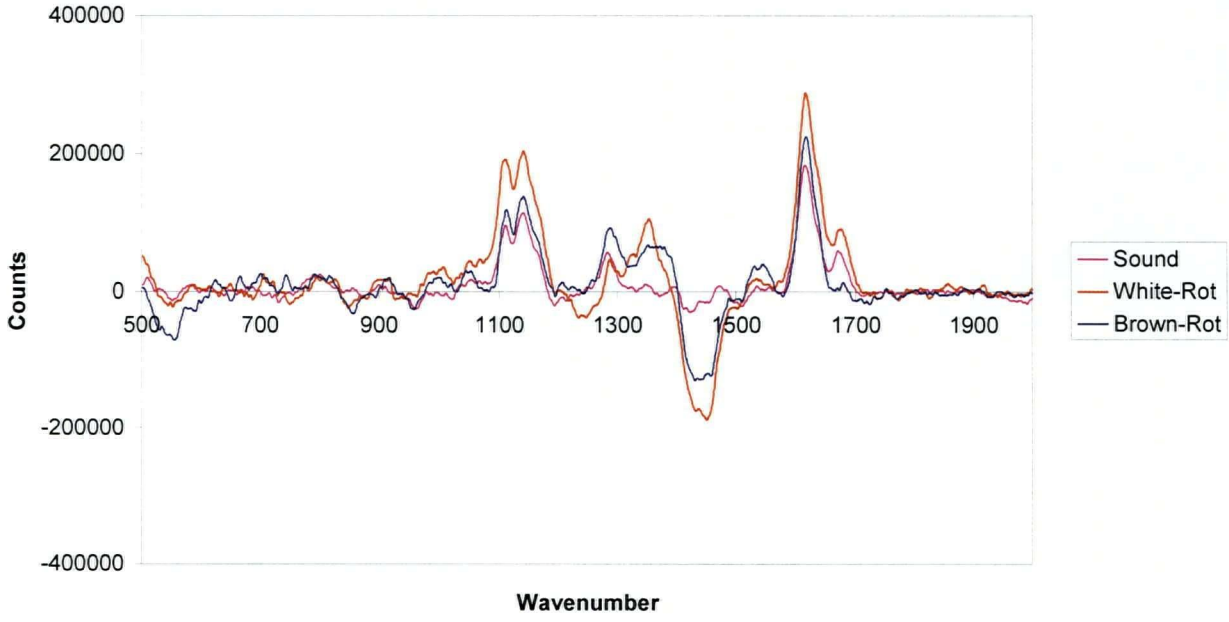

Figure 3.15 SERDS spectra of sound, white-rot, and brown-rot decayed spruce samples.

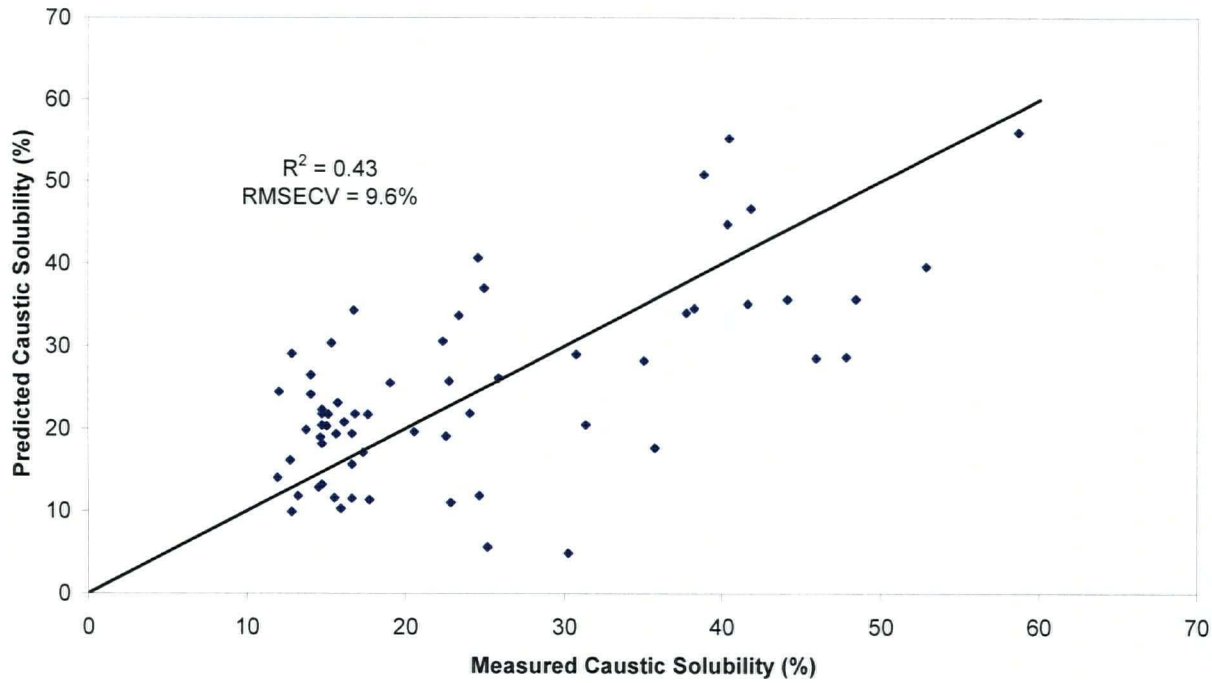

Figure 3.16 Raman-based Model: PLS-Predicted vs. Measured Caustic Solubility

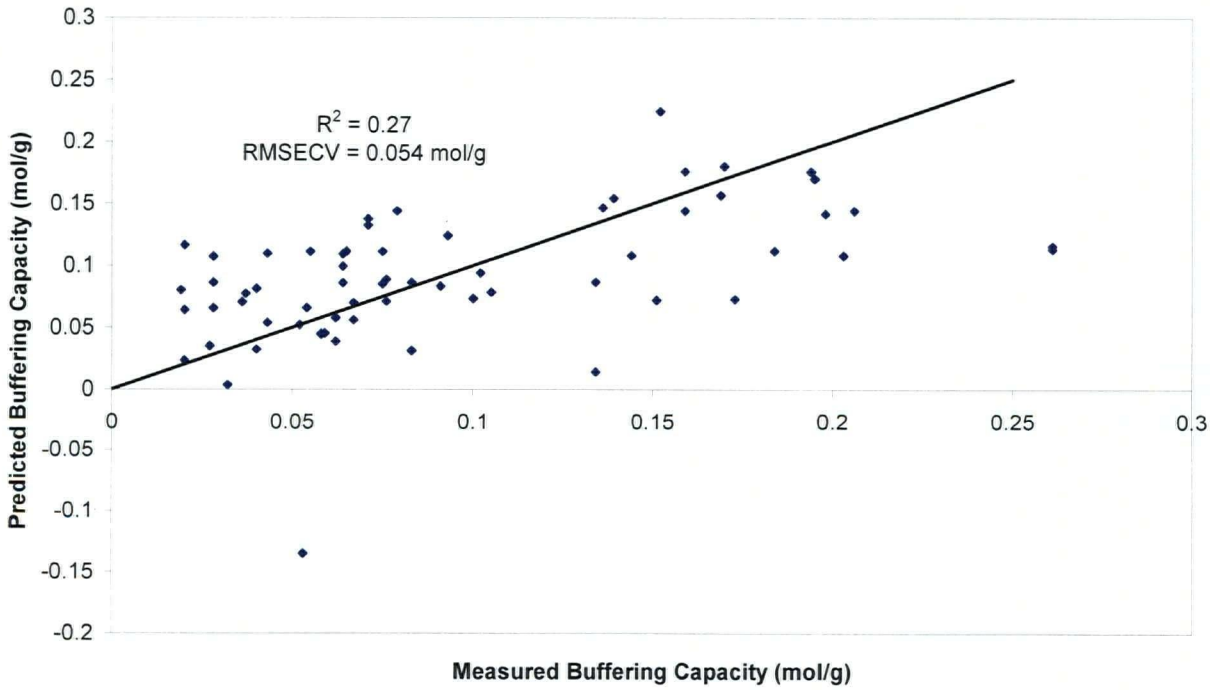

Figure 3.17 Raman-based Model: PLS-Predicted vs. Measured Buffering Capacity

3.3.5 Basic Wood Density

In order to rapidly decay the samples, a smaller sample size than recommended by Tappi method T258 om-02 for measuring density was required. The scaled-down method used to measure wood chip density yielded very precise data with a pooled standard deviation from all density measurements of 0.0071 g/mL. This is only slightly higher than the reported repeatability of the standard method, 0.00556 g/mL (TAPPI, 2002). The basic wood density of the calibration dataset ranged from 0.249 to 0.424 g/mL, with a median density of 0.375 g/mL. Sound, high-density samples dominated.

3.3.5.1 FTIR Modeling of Wood Density

Using a correlogram based on basic wood density and FTIR spectral datasets (Appendix IV) the region between 1842 cm^{-1} and 1486 cm^{-1} was determined to be best able to model basic wood density. This region encompasses a number of peaks including, carboxyl stretching of acetyl groups, carbonyl stretching of ketones, carbonyl and ester groups and aromatic skeletal vibrations (Baeza and Freer, 2001). As with the caustic solubility and buffering capacity models, the optimum number of factors to model each constituent was chosen based on a predicted residual error sum of squares (PRESS) diagram (Appendix V). Descriptions of these PLS models are shown in Table 3.13. The r^2 values for the density dataset are influenced by the bias towards sound samples present in the density dataset, and thus may be over-estimated.

Figure 3.18 shows the basic wood density predicted from FTIR spectra as a function of the measured basic wood density. Despite the poor correlation between predicted and measured basic wood density data, the RMSEP remained low; approximately three times greater than the standard deviation of the scaled-down standard method (Appendix IV). While this level of precision is poorer than that of the reference method, the ease of this method makes it attractive for mill applications that require speed over precision.

Table 3.13 PLS Models of Basic Wood Density

Population	Spectra	Factors	r^2 (calibration)	RMSECV (n=47)	RMSEP (n=23)
Pine - all	FTIR	5	0.65	0.022	0.020
Pine - all	NIR	3	0.82	0.016	0.024
Pine - field samples	FTIR	3	0.25	0.023	
Pine - field samples	NIR	5	0.40	0.017	

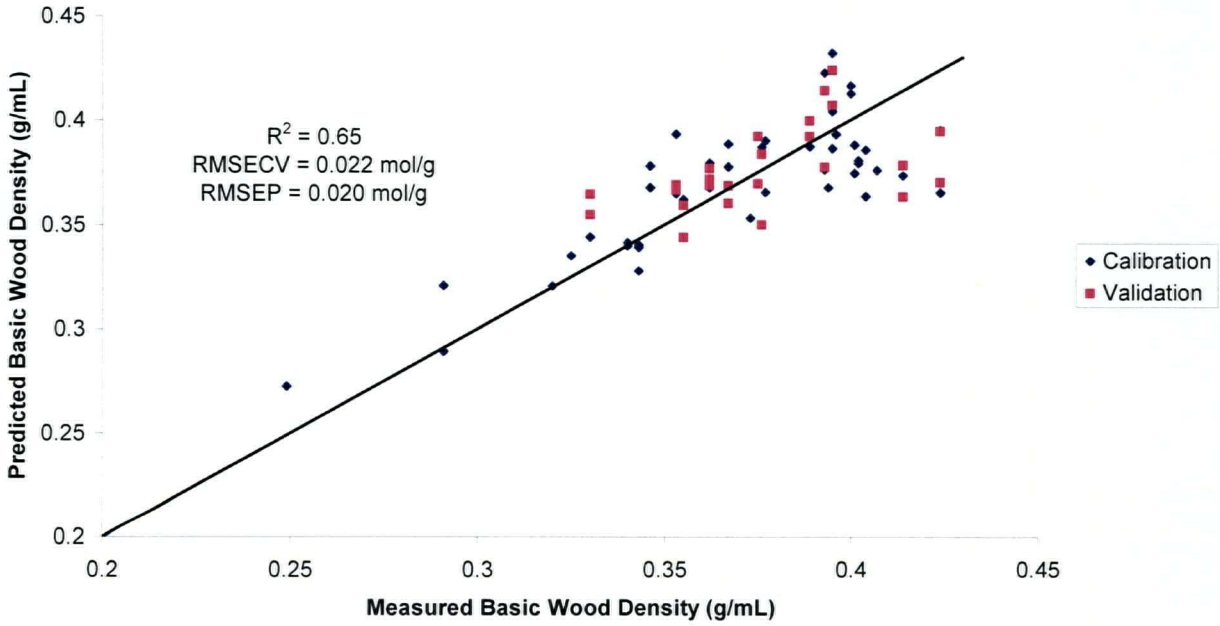

Figure 3.18 FTIR-based Model: PLS-Predicted vs. Measured Basic Wood Density in Lodgepole Pine

3.3.5.2 NIR Modeling of Wood Density

Constituents were modeled from 23-point Savitzky-Golay 1st derivative NIR spectra in the same manner as from FTIR spectra. The 1563 to 1718 and 2117 to 2316 nm regions were

used to develop all models. The first region corresponds to O-H stretching in cellulose, hemicellulose and lignin, and the second region to O-H, C-H and C-C stretching and deformation in cellulose and C-H and C=C stretching in lignin (Ali *et al.*, 2001, Fourty *et al.*, 1996, Kelley *et al.*, 2004). Descriptions of the NIR-based PLS models are shown in Table 3.13. Figure 3.19 shows the 1st derivative NIR spectra of Lodgepole pine samples with varying density. The use of 1st derivative spectra reduces the effects of baseline and particle size. Variation in baseline is related to density differences; however, in milled wood this may be confounded by other variables (Schimleck *et al.*, 1999, So *et al.*, 2004). Variation in particle size is not related to variation in density (Schimleck *et al.*, 1999).

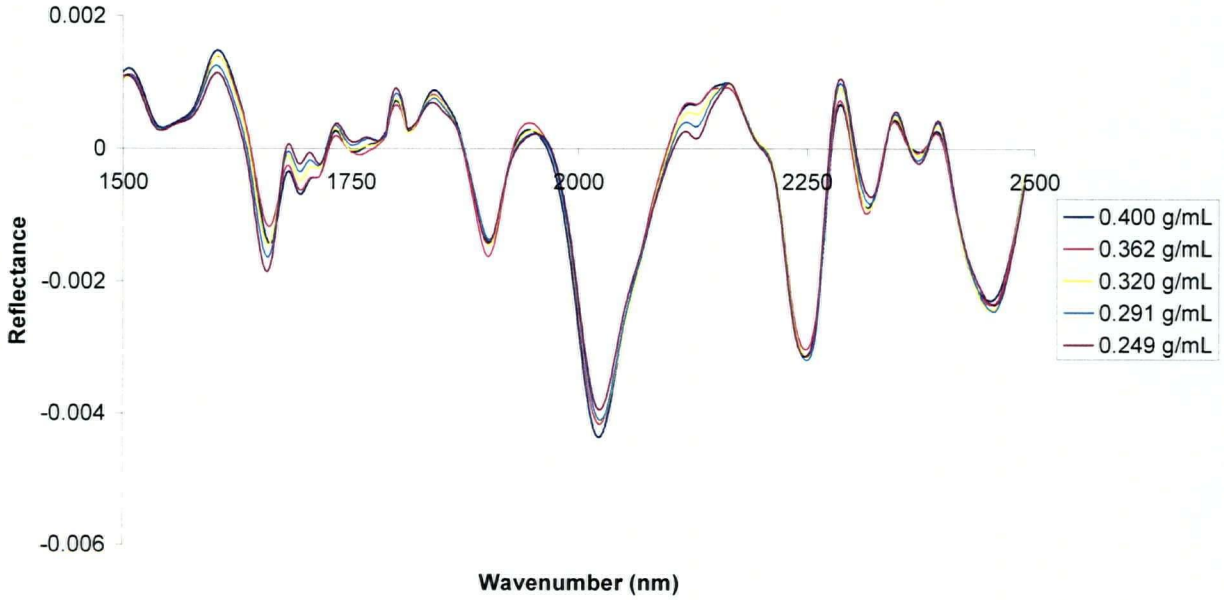

Figure 3.19 First Derivative (23 point Savitzky Golay) NIR Spectra of Lodgepole Pine Samples with Varying Density

Figure 3.20 shows the data predicted from NIR spectra as a function of the measured data. Two samples were identified as outliers based on very high spectral residuals and high concentration residuals in combination with high leverage and were removed from the NIR calibration dataset, resulting in a calibration dataset with two fewer spectra than that used in the

FTIR models (Beebe *et al.*, 1998). The same samples randomly chosen as the validation dataset in the FTIR models were used as a validation dataset in the NIR models. Overall the NIR-based PLS models performed very similar to the FTIR models. However, the NIR spectra required less sample preparation, as they could be obtained in glass sample bottles, and could be obtained in less than one minute. NIR spectroscopy can thus be used to develop models or make predictions more rapidly than FTIR spectroscopy.

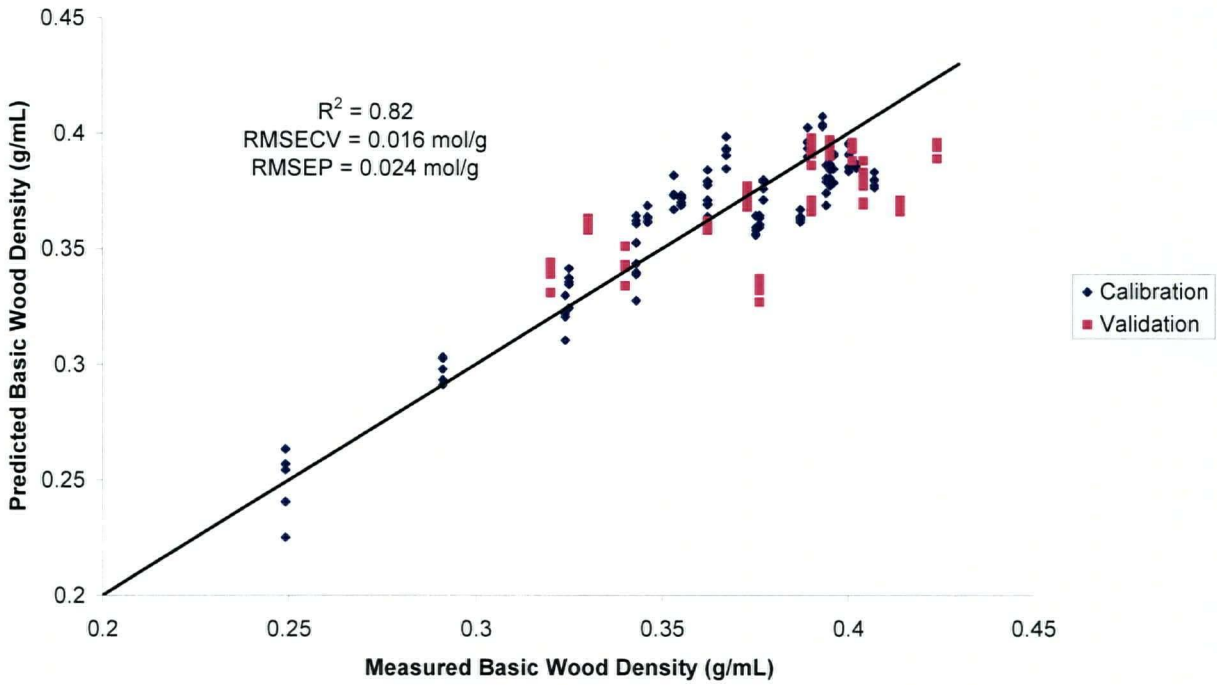

Figure 3.20 NIR-based Model: PLS-Predicted vs. Measured Basic Wood Density in Lodgepole Pine

3.3.5.3 Field Samples

The FTIR and NIR spectra of Lodgepole pine field samples were modeled without the laboratory-prepared samples to investigate the model's ability to predict wood density in the absence of decay (Table 3.13). The FTIR-based models had poor correlations between predicted and measured data, but low RMSECV due to the small range in constituent values (Appendix I). Without the presence of decay, the variations in density, caustic solubility and buffering capacity were small. The NIR-based models were superior to the FTIR-based models. Correlations

between measured and PLS-predicted data were higher than the overall models. The RMSECV was very low in part because of the small range and in part because of the very precise predictions.

3.3.5.4 Leachate COD

COD measurements of the leachate from the basic wood density test of the laboratory-prepared samples were predicted from the FTIR and Visible/NIR spectra (Table 3.14). Three of the most decayed samples had COD values that were erroneously high due to contamination from fungal hyphae in the leachate. When these samples were removed, strong negative correlations were found between leachate COD and basic wood density ($r^2 = 0.66$). This enabled the leachate COD to be modeled from the FTIR and NIR spectra of the wood.

Table 3.14 PLS Models of Leachate COD from the Basic Wood Density Test

Spectra	Factors	r^2	RMSECV (ppm)
FTIR	9	0.80	2158
NIR	11	0.89	1380

Although the PLS-predicted leachate COD was strongly correlated with the measured data, the RMSECV was very high. PLS models of COD based on Visible/NIR spectra of bleach plant effluents have accurately modeled COD (Sparen *et al.*, 2003). PLS models based on the spectra of wood are less able to model COD than models based on leachate/effluent as they are not based directly on the chemicals that contribute to COD.

3.4 Discussion

PLS models based on FTIR, NIR and Raman spectroscopy were developed to estimate indicators of decay. FTIR and NIR models were able to accurately estimate caustic solubility, buffering capacity and basic wood density. Raman spectra were heavily influenced by LIF and could not be used to estimate indicators of decay.

Visual classification of decay by hand-sorting was found to poorly represent the extent of decay present in chip samples. Despite being able to reliably identify visibly decayed wood, hand-sorting fails to account for variation in extent of decay. Chips identified as decayed may exhibit incipient or advanced decay characteristics. Since the variation in extent of decay can have significant impacts on pulping (Hunt, 1978b), this method of measuring decay is inadequate. Consequently, the visual method can lead to false-positives, where stained wood is identified as decayed, and false-negatives, where incipient decay is identified as sound. If mills were to make fibre management decisions based on hand-sorting estimates of decay, they would often discard good quality chips and accept (or pay too much for) poor quality chips. Both caustic solubility and buffering capacity, as well as the PLS predictions of these variables, measure the degree of decay present in a chip sample, not simply the proportion of visibly decayed chips. Thus, for an accurate estimate of extent of decay present in chip samples, caustic solubility or buffering capacity should be used in place of visual detection.

The strong correlation between caustic solubility and buffering capacity is in agreement with Katuscak and Katuscakova (1987), who showed a relationship between pH and 1% caustic solubility. This, along with the very similar ANOVA analyses for caustic solubility and buffering capacity shown by the present research, suggests that although independent, caustic solubility and buffering capacity are measuring a similar phenomenon. Due to the action of fungal enzymes, brown-rot decayed wood has increased caustic solubility and increased acidity. This underlying relationship between caustic solubility and buffering capacity explains why the

correlograms and PLS models are so similar. The underlying chemical changes in decayed wood that facilitate these models are discussed in Chapter 4.

Buffering capacity and caustic solubility suffer from low precision, relative to other wood chemistry methods (PAPTAC, 2000, Tappi, 2002). This is an inherent property of the tests and also a reflection of the natural variability of wood, as acknowledged by the PAPTAC Standard for 1% Caustic Solubility (PAPTAC, 2000). Unfortunately, this low precision carries through to the spectroscopic models because a model's validity is limited by the precision of the data upon which it is based (Schwanninger and Hinterstoisser, 2002). Thus, the aim of modeling these indicators of decay is to produce a simple and rapid method with comparable, but not improved precision. The advantages of spectroscopic modelling are increased speed and the ability to measure multiple constituents simultaneously.

The comparison of spectral variance between acetone-extracted and unextracted samples showed that the wood extractives had little effect on the FTIR spectra. As a result of this, as well as the time and expense of acetone-extraction, it was not included in standard sample preparation. However, the extractives content of the Western redcedar field sample did have an impact on the PLS-predictions of that sample. Western redcedar is known to contain large amounts of acidic extractives that are likely to impact the spectral predictions. A spectral dataset based on acetone-extracted wood samples may thus be beneficial for some species, but would require significantly more time and labour, putting the FTIR-based method at a disadvantage to the wet methods. Further research is needed to extend these PLS models to Western redcedar. Removing acetone-extractives may not be sufficient to enable accurate predictions on Western redcedar samples.

The comparison of spectral variance between samples prepared in a KCl mull and neat samples provided insight into the relative effects of sample concentration (increased signal) and uniformity (reduction of specular reflectance). Increased signal has more of an impact than the

elimination of specular reflectance on spectral reproducibility. However, independent of specular reflectance concerns, it is clear that small particle size is necessary to ensure sample homogeneity.

In conjunction with the effects of particle size, the effects of oven-drying and autoclaving underscore the need for a consistent sample preparation procedure. The actual sterilization/drying procedure is likely not as important as is the consistency of its application. FTIR spectra of samples freeze-dried or oven-dried under different conditions could be used to develop a PLS model. However, the ability of these spectra to be used to model decay is uncertain because it is not known how the predictive properties of the spectra change in relation to one another as conditions change.

The impact of fungus type (brown-rot vs. white-rot) on the wood, and its spectra is clear. Brown-rot fungi result in much more significant changes in caustic solubility and buffering capacity than white-rot fungi. These changes in caustic solubility were observed by Hunt (1978b) and are confirmed by the ANOVA results, which show fungal type as the most significant factor affecting caustic solubility. PLS models developed using only brown-rot samples were more accurate than those produced on white-rot samples because of the significantly larger range in caustic solubility and buffering capacity values with brown-rot fungi. This suggests that the models are most suitable to identify brown-rot decay. The improved prediction of brown-rot decay is significant as brown-rot decay has the greatest negative effects on pulping and pulp properties (Hunt, 1978b).

The impact of wood species on the PLS models was for the most part insignificant. The exceptions were the Western redcedar samples, which were poorly predicted by the models. The ANOVA of the caustic solubility and buffering capacity datasets indicate that wood species did not have a significant impact. The difference spectra of sound and decayed wood for each wood species shows similar spectra in all wood species; all with major variations in the PLS-predictive

region. However, the PLS models produced on only aspen were poorer than those produced on only softwoods. When a random selection of softwood samples was taken, the models produced were still superior to the model produced on the aspen samples. This suggests that the PLS models produced are best for softwoods. Despite this species effect, the overall model accurately predicted the decay content of aspen samples. Since increasing the size of a calibration dataset and increasing its reflection of natural variations, a large calibration dataset based on many different hardwood species may be better able to model caustic solubility and buffering capacity in hardwood species.

The PLS predictions of the sample mixtures demonstrated three things: mixtures of the same wood species with different decay contents were accurately predicted, mixtures of different sound woods were accurately predicted and mixtures of sound and decay wood of different species were accurately predicted. This is an important finding as chip supplies often contain mixtures of wood species with sound and decayed chips present. The study of these mixtures was limited to spruce, pine, and fir (SPF), as this fibre mixture is commonly used by mills in BC. Mixtures of various softwoods and hardwoods or mixtures including Western redcedar, may yield less precise or potentially biased data with the current model. To be confident in a PLS prediction of caustic solubility or buffering capacity, new species mixtures should be scrutinized by also determining these parameters by their wet methods. Further research should focus on validating other common species mixtures.

Field samples, present in both the calibration and external validation datasets, were obtained from as many different sites as possible so that the natural variability of wood would be captured. Differences between laboratory-prepared decayed wood and field samples were not observed in the model's ability to accurately predict the sample. Since so many of the field samples were sound wood, the model was biased in favour of sound wood. However, since most wood chips are sound, the excessive number of sound samples probably mimics what would be

found when sampling at a mill. Nevertheless, the field samples were not obtained randomly, and thus cannot be used to suggest the prevalence of decay. More robust models could be developed by obtaining an even more diverse dataset.

The effect of staining fungi on 1% caustic solubility was minimal. However, small decreases (likely due to utilization of extractives and soluble sugars) were observed in some samples. The PLS models did not show any bias with respect to estimating extent of decay in samples with varying extents of stain and decay (either prepared in the lab, or obtained from the field). This demonstrates the models' specificity for decay as it is not influenced by either the presence of a non-decay fungus or by the staining pigments. As a consequence this method may be useful in determining decay in trees attacked by the mountain pine beetle. Trees killed by the mountain pine beetle will exhibit both stain and decay as the beetle is associated with staining fungi and sometimes with decay fungi that infest Lodgepole and Ponderosa pine. It is currently a major problem in British Columbia with over 160 million m^3 of timber affected (BC Ministry of Forests, 2003). Since the PLS models were not influenced by staining fungi, they show utility in determining the extent of decay in chips, and thus their potential value for pulping.

PLS models of caustic solubility, buffering capacity and basic wood density were successfully developed based on NIR spectra. These models were of similar quality to those developed on FTIR spectra. The principal advantage of using NIR, instead of FTIR spectroscopy, is that spectra can be obtained more quickly, since fewer scans are required because of the improved S/N, and with less sample preparation, since NIR spectra can be obtained through glass sample vials. The faster acquisition of spectra means that more samples can be analyzed to improve PLS predictions. Models that can simultaneously predict caustic solubility, buffering capacity and basic wood density, as well as other parameters, such as lignin and polysaccharide content (Raymond and Schimleck, 2002, Yeh *et al.*, 2004), would be

extremely useful to mills. Since NIR is fast and easy to use, it is often used in various production facilities for quality control. Thus, NIR is an important area for future study in chip analysis.

In contrast to the PLS models based on FTIR and NIR spectra, models based on Raman spectra were of poor quality due to overwhelming LIF. Although models showed some correlation between spectral and concentration datasets, the precision was too low for the models to be useful. SERDS spectra were of qualitative value, exhibiting many peaks characteristic of wood. However, their quantitative value was limited due to the anomalies produced by subtracting spectra with very high LIF. FT-Raman may provide improved spectra for PLS modeling of decay.

Either FTIR or NIR spectra can be used to model wood density as well as caustic solubility and buffering capacity. Models based on NIR spectra may be preferable in a commercial operation to those based on FTIR, even though models are of similar quality, because the spectra are easier to obtain. The RMSEP of the NIR-based model of basic wood density was 0.019 g/mL; about three times greater than the standard deviation of the scaled-down standard method. Wood density was more precisely modeled than caustic solubility and buffering capacity. This is attributable to the scaled-down density method having greater precision than the caustic solubility and buffering capacity methods. However, the wood density models were also confounded by the variable extractives content in the calibration dataset. The low-density samples leached more extractives into the water than the high-density samples, which likely resulted in underestimating the density in the low-density samples. This problem could be addressed by extracting the wood chips prior to soaking. Unfortunately, extraction of wood chips prior to obtaining spectra would remove the method's principal advantage of increased speed. Models of basic wood density could be made more robust by developing a calibration dataset with more low-density samples.

Since the NIR spectra were obtained on milled wood, as opposed to solid wood, predictions of wood density were based on C-C, C-O and C-H stretching in the polysaccharides and lignin, and not on deviations in the gross physical structure of the wood. However, the physical structure of the fibres may have influenced the spectra because the samples were only milled to pass through a 0.5 mm screen. This diameter is much larger than that of a typical fibre, and thus the structure of the fibre walls may have influenced the spectra. Schimleck and Evans (2003) report PLS models of similar quality based on NIR spectra taken on increment cores of solid wood. The exact nature of the relationship between wood density and NIR spectra of the milled wood is not fully understood.

The overall NIR-based models developed for basic wood density had the same predicted error (RMSEP) as models reported on solid *Picea abies*, however, the r^2 values were lower (Hoffmeyer and Pedersen, 1995). The developed models compared favourably to models developed on milled *Eucalyptus globulus*, which had slightly higher predicted error and a bias that underestimated high-density samples and overestimated low-density samples (Schimleck *et al.*, 1999). Although the datasets are different in scope and size, this may suggest that the density of softwoods is easier to model than that of hardwoods, likely due to the absence of vessel elements (Schimleck *et al.*, 1999).

The leachate from the basic density test has some implications for mills. As measured by COD under standard conditions, leachate from decayed wood has increased COD. Thus, storing decayed chips could have negative environmental consequences, as some wood chip leachates have been found to be harmful to aquatic life (Peters *et al.*, 1976).

The new FTIR- and NIR-based methods for predicting caustic solubility and buffering capacity are significantly faster than the wet methods and have only slightly poorer precision. Excluding drying time, caustic solubility and buffering capacity take 2 to 3 hours of labour-intensive work. With the new PLS models, caustic solubility and buffering capacity can be

predicted in minutes with only slightly higher error. The NIR-based method is faster than the FTIR-based method because spectra can be obtained through glass sample vials and scanning is much more rapid. These methods have the potential to quantify the extent of decay in pulp and paper fibre supplies, which could lead to improved fibre management.

As forest practices dictate that more poor quality fibre should be utilized, the pulp and paper industry can expect a greater proportion of decayed wood in its fibre furnish. The developed methods have many applications and should significantly accelerate the assessment of decay in wood chips. They should also facilitate a means for mills to evaluate the decay content in their incoming fibre supply, either under the current batch sampling procedures, or as the method is amenable to on-line analysis, on a continuous basis. The PLS models will enable mills to assess the quality of defective wood chips from areas affected by beetle attack, and fungal decay and from over-mature stands. The value of chips decayed while in storage will also be able to be rapidly determined. The rapid prediction of 1% caustic solubility in their fibre supply should help mills to predict improve pulp uniformity and reduce chemical consumption.

CHAPTER 4

Analysis of Decay Indicators

4.1 Introduction

The Partial Least Squares (PLS) models described in Chapter 3 are based on a relationship between the spectroscopic characteristics of wood and caustic solubility and buffering capacity. This relationship is mediated through physical and chemical changes in the wood, which result in changes in spectral and concentration datasets. The relationship between FTIR spectra and wood chemistry will be investigated to show how decay fungi affect wood structure and chemistry, and how this affects caustic solubility, buffering capacity and FTIR spectroscopic properties.

4.1.1 One Percent Caustic Extracts

The 1% caustic solubility method (PAPTAC standard G.6 and G.7) fractionates wood into soluble and insoluble fractions (PAPTAC, 2000). The solubility of the wood has been correlated with extent of decay (Procter and Chow, 1973). However, the components of the fractions and qualitative differences in fractionation as a function of decay extent are not well understood.

Previous work conducted at Paprican by K. Hunt and J.V. Hatton (unpublished) has indicated that the 1% caustic extracts of brown-rot decayed wood differ from those of sound wood. Klason lignin content was largely unaltered after extraction in both sound and decayed samples. All sugars were partially solubilized in the sound sample and solubilized to a greater extent in the decayed sample. Carboxylic acid content was greater in the decayed fractions after caustic extraction. Acetyl groups bound to hemicelluloses are saponified under these conditions (Zanuttini *et al.*, 1998). Lignin and xylan from aspen decayed by the white-rot fungus *Phellinus igniarius* have increased caustic solubility (Kosikova *et al.*, 1992).

With renewed focus on 1% caustic solubility as a method of predicting decay, the nature of these extracts is once again an important question. Instead of searching for compounds unique to decayed wood, compounds responsible for changes in FTIR spectra that lead to the predictive ability of the PLS models are sought.

4.1.2 FTIR Spectra of Decay

The correlation between IR absorbance and caustic solubility and buffering capacity is based primarily on fundamental changes in the chemistry of the wood but may be influenced by some physical changes within fibres (large structural changes were not considered because the wood was milled). In order to understand why FTIR spectroscopy is predictive of 1% caustic solubility and buffering capacity, it is necessary to determine which components of the sample are responsible for absorption in the predictive region.

The PLS models of caustic solubility and buffering capacity were based on the 1872 cm^{-1} to 1672 cm^{-1} region of the FTIR spectra of milled wood (Chapter 3). This region contains two absorbance maxima at 1736 cm^{-1} and 1662 cm^{-1} and is known to correlate with a number of different wood components (Michell, 1988). These include water adsorbed to cellulose (1635 cm^{-1}), acetyl groups bound to hemicelluloses (1735 cm^{-1}), carbonyl stretching from unconjugated ketones, ester groups in lignin (1722 cm^{-1}), and carbonyl stretching from conjugated *p*-substituted aryl ketones in lignin (1663 cm^{-1}, Baeza and Freer, 2001, Faix, 1991, Zanuttini *et al.*, 1998). Since decay can affect all of these constituents, each must be examined to determine if decay affects FTIR spectra in the predictive region.

The characteristic carbonyl and lignin stretching frequencies of wood from various species may vary by several wavenumbers (Moore and Owen, 2001). Diffuse reflectance FTIR spectra of various tropical hardwoods exhibit significant variation in absorbance maxima between 1740 and 1240 cm^{-1} (Pandey and Theagarajan, 1997). The PLS models reduce the effect

of this variation by looking at a range of values and not just the absorbance maxima. However, one must be careful when predicting decay content in new wood species.

The effect of fungal type on the FTIR spectra of decayed wood varies between fungal species, and most significantly between white- and brown-rot fungi. Fungal decay has been shown to cause changes in the ratios of polysaccharide bands between 1200 and 1000 cm^{-1} (Kacurakova *et al.*, 2000). These changes have been correlated with glucan content (Ferraz *et al.*, 2000). The increase in the peak at approximately 1740 cm^{-1}, which corresponds to C=O stretching of carbonyl and acetyl groups in hemicellulose, has been correlated with an increase in the cleavage of lignin-carbohydrate bonds, and bonds within the lignin macromolecule due to decay (Roy *et al.*, 1992). Changes in absorbance at 1635 cm^{-1} have been attributed to white-rot fungi disrupting adsorbed water in the non-crystalline regions of cellulose (Roy *et al.*, 1992). The intensity of the peak at 1660 cm^{-1} has been correlated with the formation of new conjugated and unconjugated acid substructures in the side chains of lignin in brown-rot samples (Ferraz *et al.*, 2000).

The extent of decay, as indicated by PLS-predicted caustic solubility and buffering capacity, increases with fungal incubation time. The success of the PLS models for caustic solubility and buffering capacity indicates that the models were able to focus only on the intensity of decay, as measured by 1% caustic solubility and buffering capacity (Chapter 3). The chemical changes associated with decay will be investigated to better understand the IR spectroscopic properties of decayed wood.

4.1.3 Fungal Damage to Fibres

In addition to altering wood chemistry, decay fungi also cause physical fibre damage. In the case of white-rot fungi, changes in chemistry may not be detected but fibre damage can still occur, reducing fibre strength. These changes in wood chemistry can result in poorer pulp yields,

as well as changes in the physical properties of wood fibres, which can result in poorer pulp properties. These two effects of decay are related since removal of a specific portion of a fibre will alter the chemistry of the fibre as a whole (Curling *et al.*, 2002, Nilsson *et al.*, 1989).

Decayed hemlock has reduced length-weighted fibre length, but similar fibre coarseness to sound hemlock (Mischki *et al.*, 2005). Fibre length and coarseness have major impacts on pulp properties. In a well-bonded sheet, fibre length affects strength properties, including tensile strength, stretch, bursting strength, tearing resistance and folding endurance (Seth, 1990). It also affects sheet formation (Hurst and Sutton, 1999). Coarseness, the mass of fibres per unit length, affects sheet structure and optical properties, as well as strength (Seth, 1990a).

Since white-rot fungi cause little change in caustic solubility or buffering capacity, they require other means of quantification. Extent of decay by white-rot fungi can be quantified by microscopy or with a Fiber Quality Analyzer (FQA). Light microscopy can show major changes in wood due to decay (Kuo *et al.*, 1988). The Basic Green Stain can be used to identify wood decayed by white-rot fungi (PAPTAC standard B. 3P). The FQA measures fibre length and coarseness, which can be indicative of damage due to decay. Both methods will be used to determine the physical damage caused by decay.

In order to determine the effect of decay on fibre properties, samples of sound and decayed wood were examined by microscopy and fibre quality analysis. PLS-predicted extent of decay were compared with extent of decay by microscopic examination in both white- and brown-rot decayed samples.

4.2 Methods

Samples of spruce (*Picea glauca* (Moench) Voss) chips were decayed by *Phellinus igniarius* CBS 512.63 (a white-rot fungus) and *Gloeophyllum trabeum* 61750M (a brown-rot fungus) for 60 days following the method described by Ferraz *et al.* (2000). These samples,

along with sound spruce chips, were used as models for investigating the effects of decay on wood chemistry, 1% caustic solubility, FTIR spectra and fibre quality.

4.2.1 One Percent Caustic Solubility Fractionation

Wood samples were tested for 1% caustic solubility by the standard method and a modified version of PAPTAC method G.6 and G.7 (PAPTAC, 2000). To prevent acetate contamination in the caustic soluble fraction, 3 M HCl was used to wash the sample, instead of the standard 10% acetic acid. This left the caustic soluble fraction in an IR-transparent matrix, sodium chloride, instead of sodium acetate, which is a strong IR absorber. The 1% caustic soluble and insoluble fractions were retained for further testing. The soluble fractions were neutralized with NaOH and made up to 500 mL. Two hundred millilitres of these samples were freeze-dried for FTIR analysis.

4.2.2 Chemical Analyses

The wood, caustic-insoluble and freeze-dried caustic-soluble fractions were tested for acid-soluble lignin, Klason lignin and carbohydrates (method described in Chapter 2). The acetone-extractives of the wood and caustic-insoluble fraction were determined. The caustic soluble fraction was tested for acetyl groups and caustic degradation products of polysaccharides. The acetyl groups were converted to acetic acid in solution and were quantified by GC/MS as their benzyl esters according to the method of Feng *et al.* (2001). Peaks were identified by comparison of retention times with an authentic standard and by a NIST library search of the mass spectra. Caustic degradation products were determined by GC/MS by the method of Alen *et al.* (1984) using a DB1 column. The NIST Mass Spectral Search Program version 1.7a (National Institute of Standards and Technology, USA) was used to identify some components by their mass spectra.

4.2.3 FTIR Analyses

A number of experiments were conducted to elucidate the cause of variations in the spectra attributable to decay. Spectra of wood, caustic soluble and insoluble fractions were obtained to monitor how functional groups changed as a result of the caustic extraction. The following samples were also analysed by FTIR spectroscopy: Klason lignin, delignified wood, acetylated wood and acetylated-delignified wood.

Wood samples were delignified based on the methods of Wise *et al.* (1946) and Maekawa and Koshijima (1983). One gram of milled wood was added to an Erlenmeyer flask with 50 mL of 10% sodium chlorite and 33 mL of acetic acid/sodium acetate buffer and heated for 7 hours at 70°C. Samples were suction filtered, washed with water and acetone, oven-dried, and analyzed by FTIR.

Samples of wood and delignified wood were reduced by adding 5 mL of 3 M sodium borohydride in ammonium hydroxide and heating in a water bath at 40°C for 90 minutes. Two hundred microlitres of glacial acetic acid was added to stop the reduction. Samples were filtered, washed with 50 mL of water, oven-dried and analyzed by FTIR.

Wood was acetylated by reacting milled or delignified wood with 100 μL of acetic acid, 0.5 mL of methylimidazole and 2 mL of acetic anhydride for ten minutes. Excess acetic anhydride was removed by adding 4 mL water. Samples were filtered, washed with 80 mL water, oven-dried and determined by FTIR.

4.2.4 Microscopic and Fibre Quality Analyses

Lodgepole pine wood chips were placed in Petri dishes containing fungi growing on malt extract agar. The chips were incubated until hyphae reached half way across the wood chip surface. The chips were then cut along the hyphal front, dried, milled, and analyzed by FTIR. These chips, and heavily decayed spruce chips, were cut into approximately 2 x 2 x 4 mm blocks

and dehydrated with acetone overnight. Samples were air-dried and impregnated with Spurr epoxy resin. Fresh resin was added to the wood blocks and cured at 70°C overnight. Two-micron sections were cut from the embedded wood blocks using a Reichert Ultracut E Ultramicrotome. The sections were stained with basic green dye (PAPTAC standard B. 3P) and viewed with a light microscope.

Wood chips were split into match stick-sized pieces with a chisel and placed in test tubes. The wood was heated in water at 120°C for four hours and then with a 1:1 (v/v) mixture of acetic acid and 34-37% hydrogen peroxide at 70°C for 48 hours. Samples were rinsed and disintegrated in a blender for 2 to 3 minutes. Disintegrated samples were washed over a 150-mesh screen to remove fines, dewatered, and conditioned at constant temperature and humidity (23°C and 50% relative humidity). Moisture was determined by oven drying. The samples were diluted and the fibre length measured by FQA (Optest, Hawkesbury, ON). The arithmetic fibre length was length-weighted to correct for a bias towards shorter fibres (Schimleck *et al.*, 2004). Length weighted fibre length is determined by Equation 4.1 (Ring and Bacon, 1997). Eight replicates were run for each sample.

Equation 4.1 Length-Weighted Fibre Length

$$LWFL = \frac{\sum(n_i l_i^2)}{\sum(n_i l_i)}$$

Where l_i = fibre length in class i and n_i = the number of fibres in length class i

4.3 Results

4.3.1 Chemical Analyses

The slight increase in caustic solubility and buffering capacity caused by the white-rot fungus and the massive increase caused by the brown-rot fungus is typical of wood heavily decayed by these fungi (Table 4.1). Staining fungi were not considered.

Table 4.1 One Percent Caustic Solubility and Buffering Capacity of Sound, White-rot, and Brown-rot Decayed Spruce Samples (Standard Deviation in parentheses)

Spruce Samples	1% Caustic Solubility (%)	Buffering Capacity (mol/g)	Buffering Capacity of Acetone Extracted Wood (mol/g)
Sound	10.9 (0.1)	0.064 (0.004)	0.046 (0.004)
P. igniarius (WR)	15.4 (0.3)	0.083 (0.004)	0.071 (0.004)
G. trabeum (BR)	48.9 (1.1)	0.184 (0.006)	0.140 (0.007)

WR = White-rot, BR= Brown-rot

The actual wood substance loss due to decay was not measured. Individual wood constituents reported show the relative changes in wood components. The summative analysis of the sound and decayed samples (Table 4.2, Figure 4.1) was consistent with previous analyses of spruce and previous analyses of the effects of white- and brown-rot fungi (Hatton and Hunt, 1972, Zabel and Morrell, 1992). Relative to the mass of wood, lignin content decreased slightly in the white-rot decayed sample, as the fungus degraded and consumed the lignin, and increased in the brown-rot decayed sample, as the polysaccharide fraction was consumed.

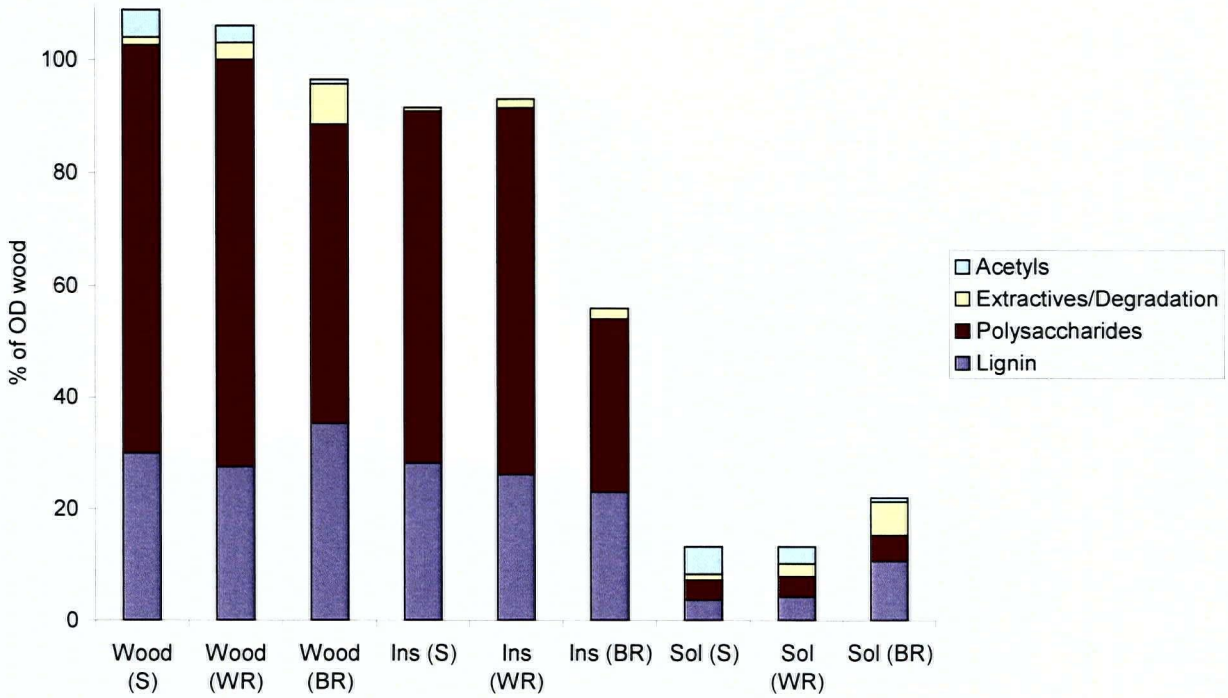

Figure 4.1 Constituents of Spruce Samples and 1% Caustic Fractions (S = Sound, WR = White-rot, BR = Brown-rot, Ins = Insoluble, and Sol = Soluble)

Monosaccharide concentrations were consistent with the consumption of hemicellulose by the fungi. Losses of arabinose, xylose and galactose were observed in both decayed samples, as well as a significant drop in mannose content in the brown-rot sample (Table 4.2, Appendix V). The proportion of glucose content increased slightly in the decayed samples due to the resistance of crystalline cellulose to decay (Blanchette, 1995). The degradation of hemicelluloses by the fungi can be examined by ratioing the amounts of the constituent sugars. Arabinose/xylose ratios show a loss of arabinose relative to xylose in the sample decayed by *G. trabeum*, suggesting that the fungus is degrading the arabinose side-chains more rapidly than the xylose backbone. Galactose/mannose ratios are lower in both decayed samples, suggesting that both fungi are able to degrade galactose side chains faster than the glucomannan backbone. The loss of hemicelluloses resulted in acetyl contents dropping significantly in the decayed samples. Despite good chromatography (Appendix VI), the alditol-acetate method of sugars analysis had a

poor level of precision, possibly due to variable levels of acetylation. This limits the conclusions that can be drawn from these data. Alternate methods of quantifying sugars are based on no derivatization and HPLC analysis (DeJong *et al.*, 1997a).

Table 4.2 Summative Analysis of Spruce Samples

Test	N	Sound (Std. Dev.)	*P. igniarius* (WR) (Std. Dev.)	*G. trabeum* (BR) (Std. Dev.)
Klason lignin (%)	2	29.6 (0.2)	27.1 (0.2)	34.4 (0.2)
Acid-soluble lignin (%)	2	0.44 (0.03)	0.5 (0.2)	0.8 (0.1)
Total lignin (%)	2	30.0 (0.2)	27.6 (0.2)	35.2 (0.1)
Arabinan (%)	4	1.5 (0.7)	1.3 (0.7)	0.45 (0.03)
Xylan (%)	4	8 (2)	7 (2)	5 (1)
Mannan (%)	4	17 (1)	17 (5)	4 (2)
Galactan (%)	4	2.5 (0.4)	1.4 (0.8)	0.3 (0.5)
Glucan (%)	4	42.8 (0.9)	46 (2)	43 (3)
Total polysaccharides (%)	4	73 (5)	72 (9)	53 (6)
Extractives – by mass (%)	1	1.4	3.1	7.1
Acetyl (%)	5	4.9 (0.2)	3.0 (0.7)	0.7 (1)
Sum (%)		109 (7)	106 (10)	96 (7)

Acetone extractives, determined gravimetrically, increased in both decayed samples on a relative mass basis (Table 4.2). Yield after acetone extraction was not determined. Figure 4.2 shows the gas chromatograms of the acetone extractives from each sample. The chromatograms from the decayed samples show major reductions in all of the extractives classes identified in the chromatogram of sound spruce. Fatty acids identified in the sound sample were absent in the

decayed samples. Resin acids and sterols found in the sound sample were present in much smaller quantities in the decayed samples. The sound sample has the greatest amount of identified extractives, as determined by GC, suggesting that the higher values determined gravimetrically (and reported in Table 4.2) are a result of acetone-soluble degradation products that are not detected by this GC procedure. This increase in acetone-soluble degradation products may be attributable to degraded lignin compounds or oligosaccharides that the fungus was unable to consume and to components of the fungal hyphae.

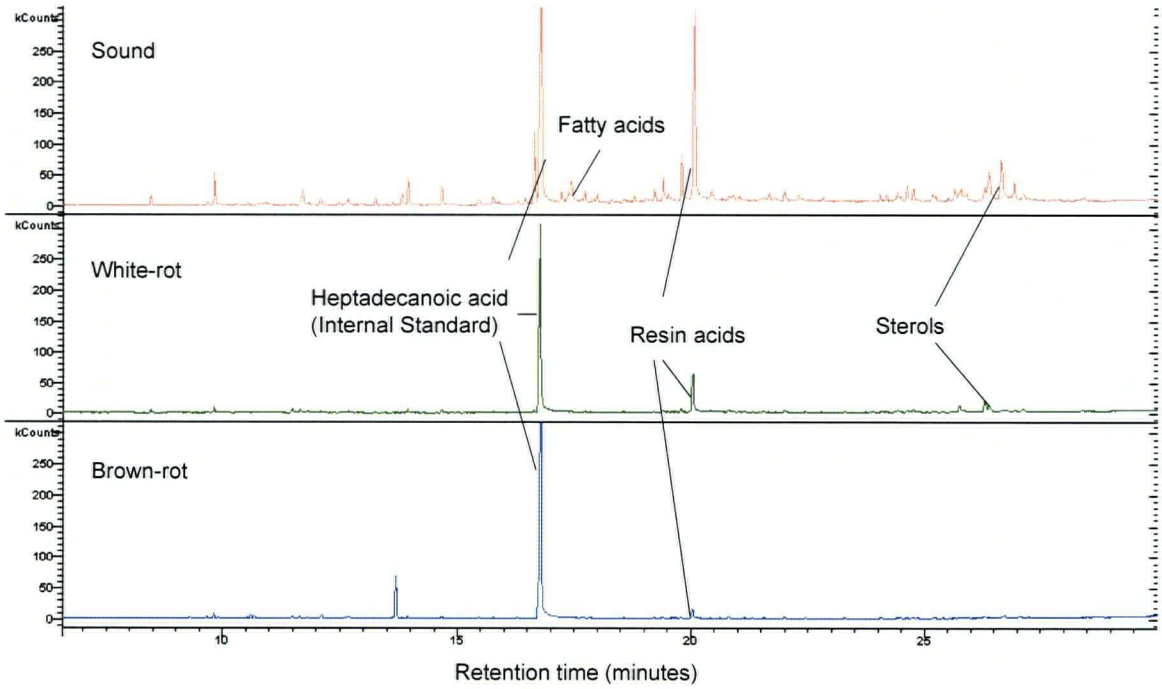

Figure 4.2 Gas Chromatograms of Acetone Extractives from Sound, White-rot, and Brown-rot Decayed Spruce Samples

4.3.1.1 Caustic Extraction

These spruce samples were fractionated by the 1% caustic solubility test, resulting in a soluble and an insoluble fraction. The analysis of the wood and its fractions are shown in Figure 4.1. For simplicity, only lignin, polysaccharides, acetyl groups and extractives/degradation

products, as a percentage of the original material, have been shown. The sum of the insoluble and soluble fractions was similar to that of the original wood, with the exception of the *G. trabeum* decayed sample, which showed significant mass loss from the caustic extraction.

Acetyl groups were liberated from the wood by the 1% caustic extraction. Zanuttini *et al.*, (1998) showed that wood contained only 0.01% acetyl groups after 1% caustic extraction under the same conditions. Removal of acetyl groups by the 1% caustic extraction was thus considered quantitative. Figure 4.3 shows the chromatograms of the acetyl benzyl esters (mass spectra are found in Appendix VII). Acetyl contents decreased in both the white- and brown-rot decayed samples (Figure 4.1). This is likely due to enzymatic removal by the decay fungi.

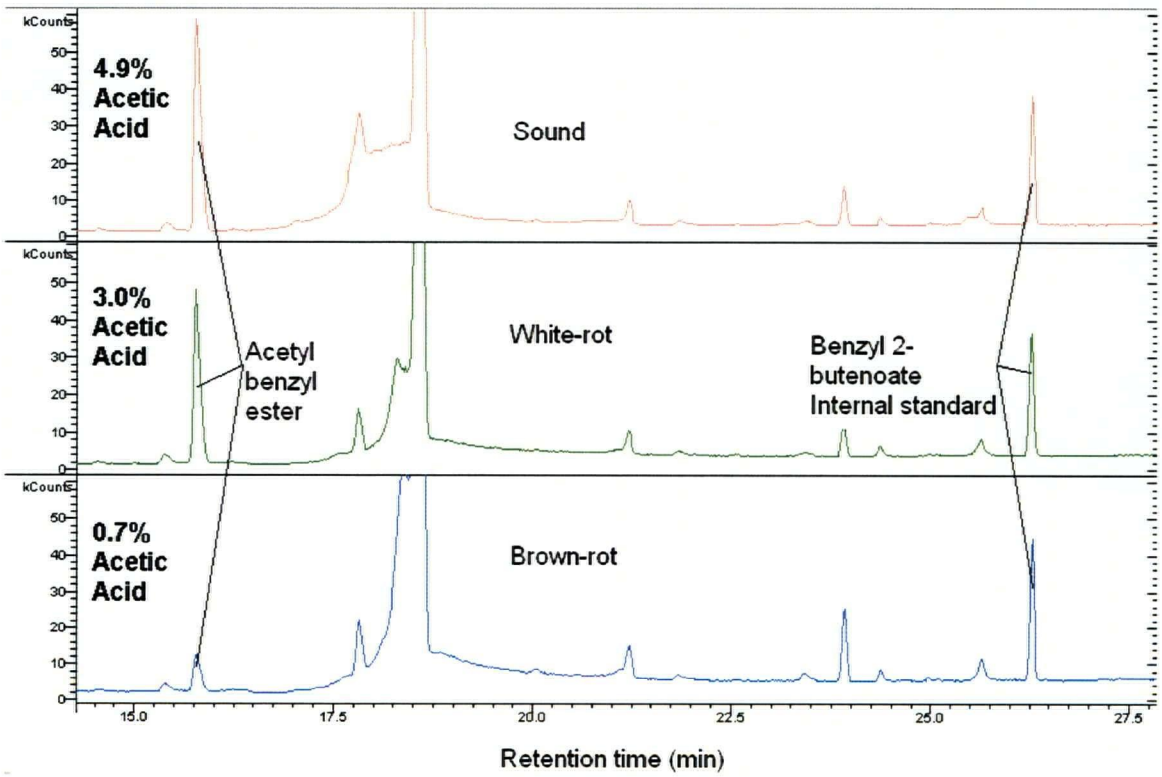

Figure 4.3 Gas Chromatograms of Benzylated Acetic Acid and Crotonic Acid (Internal Standard) from the 1% Caustic Extracts of Sound, White-rot, and Brown-rot Decayed Spruce

Table 4.3 shows the Klason and acid-soluble lignin data (average of two replicates) for the sound and decayed samples and their 1% caustic fractions. Ninety four percent of the total

lignin remained in the insoluble fraction of the sound and white-rot decayed samples, while only 65% remained in the insoluble fraction of the brown-rot decayed sample. This suggests that while *P. igniarius* is degrading lignin, it is not likely changing the caustic solubility of the lignin. In contrast, *G. trabeum* modifies the lignin in a way that increases its caustic solubility.

The percentage of acid soluble lignin in the wood and the caustic insoluble fraction ranged from 1 to 2.5% (Table 4.3). In the caustic soluble fraction, acid soluble lignin accounted for between 16 and 32% of the total lignin (Table 4.3). Acid soluble lignin has a greater caustic solubility than Klason lignin. Between 8 and 25% of the Klason lignin was caustic soluble, while the majority of acid soluble lignin was also caustic soluble. Table 4.3 shows that the make up of the caustic soluble fraction is dependent on the type of decay present.

Table 4.3 Fractionation of Lignin in Sound, White-rot, and Brown-rot Decayed Spruce Samples and Their 1% Caustic Soluble and Insoluble Fractions. Determined in Duplicate. Standard Deviations in Parentheses.

Fungus	Fraction	Klason lignin (% of wood)	Acid soluble lignin (% of wood)	Total lignin (% of wood)	% of acid soluble lignin in total lignin
Sound wood	W	29.6 (0.2)	0.4 (0.03)	30.0 (0.2)	1.5
P. igniarius (WR)	W	27 (2)	0.5 (0.2)	28 (2)	1.9
G. trabeum (BR)	W	34.4 (0.2)	0.8 (0.1)	35.2 (0.1)	2.3
Sound wood	I	27.8 (0.2)	0.5 (0.2)	28.3 (0.1)	1.7
P. igniarius (WR)	I	25.8 (0.2)	0.5 (0.1)	26.2 (0.3)	1.8
G. trabeum (BR)	I	23 (2)	0.3 (0.1)	23 (2)	1.2
Sound wood	S	3.0 (2)	1.2 (0.5)	4 (2)	31.8
P. igniarius (WR)	S	3.3 (0.2)	1.0 (0.6)	4.3 (0.4)	24.1
G. trabeum (BR)	S	8.9 (0.3)	1.8 (0.02)	10.7 (0.3)	16.4

W = wood, I = caustic insoluble fraction, S = caustic soluble fraction

The 1% caustic fractionation of the polysaccharides is shown in Figure 4.4. It is clear that the majority of the polysaccharides remain insoluble under 1% caustic conditions. Xylose and glucose were the only sugars detected in the 1% caustic soluble fraction of the sound and white-rot samples. Arabinose and mannose were detected in small amounts in the brown-rot samples.

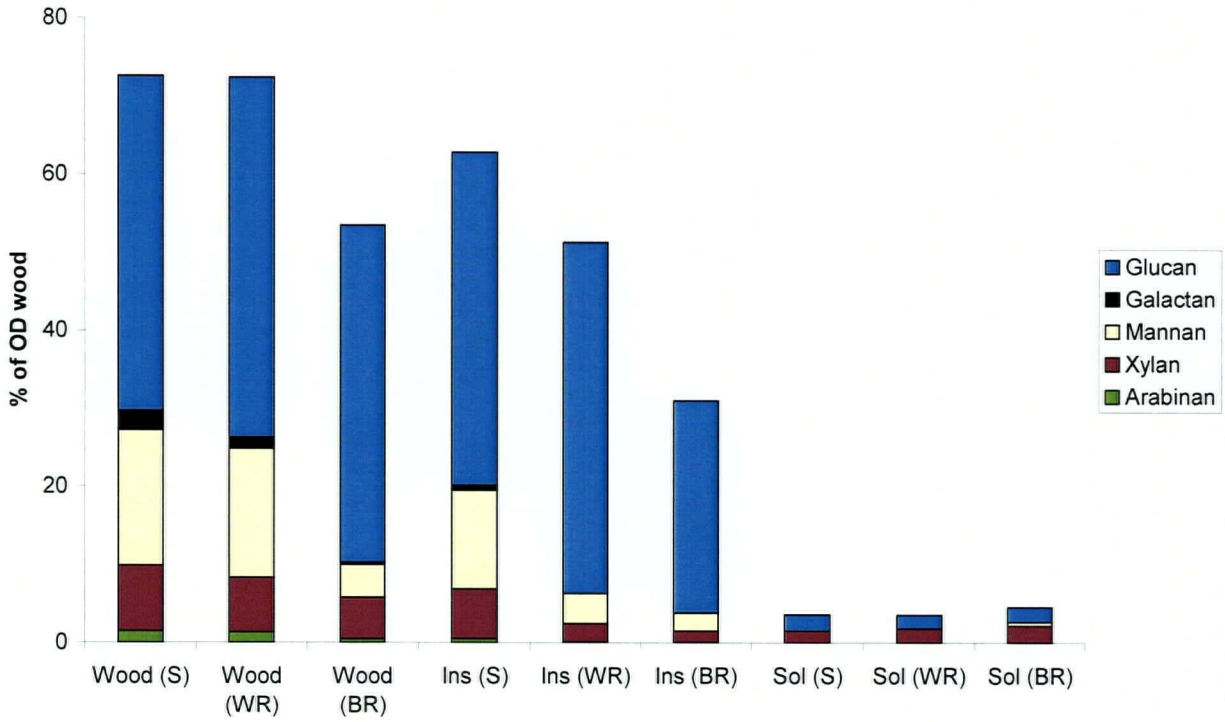

Figure 4.4 Fractionation of Carbohydrates by 1% Caustic Extraction of Sound and White- and Brown-Rot Decayed Wood (S = Sound, WR = White-rot, BR = Brown-rot, Ins = Insoluble, and Sol = Soluble)

Acetone extractives and caustic degradation products have been grouped together to allow for a comparison of soluble and insoluble fractions. These groups were measured independently and contain some of the same compounds. The wood and insoluble fractions report only extractives, while the soluble fraction reports caustic degradation products. The majority of the extractives were 1% caustic soluble, although a significant amount remained insoluble. The extractives were determined quantitatively by mass, but were qualified using GC/MS (Figure 4.2). The caustic degradation products, also determined by GC/MS, are shown

in Figure 4.5 (chromatographic data listed in Appendix VII). Many of these compounds were identified by a mass spectral library search as being carbohydrate degradation products and quantified by comparison with the internal standard, xylitol. The TMS-esters of propanoic, butanoic, and pentanoic acids were determined based on a library search of the mass spectra (Appendix VII).

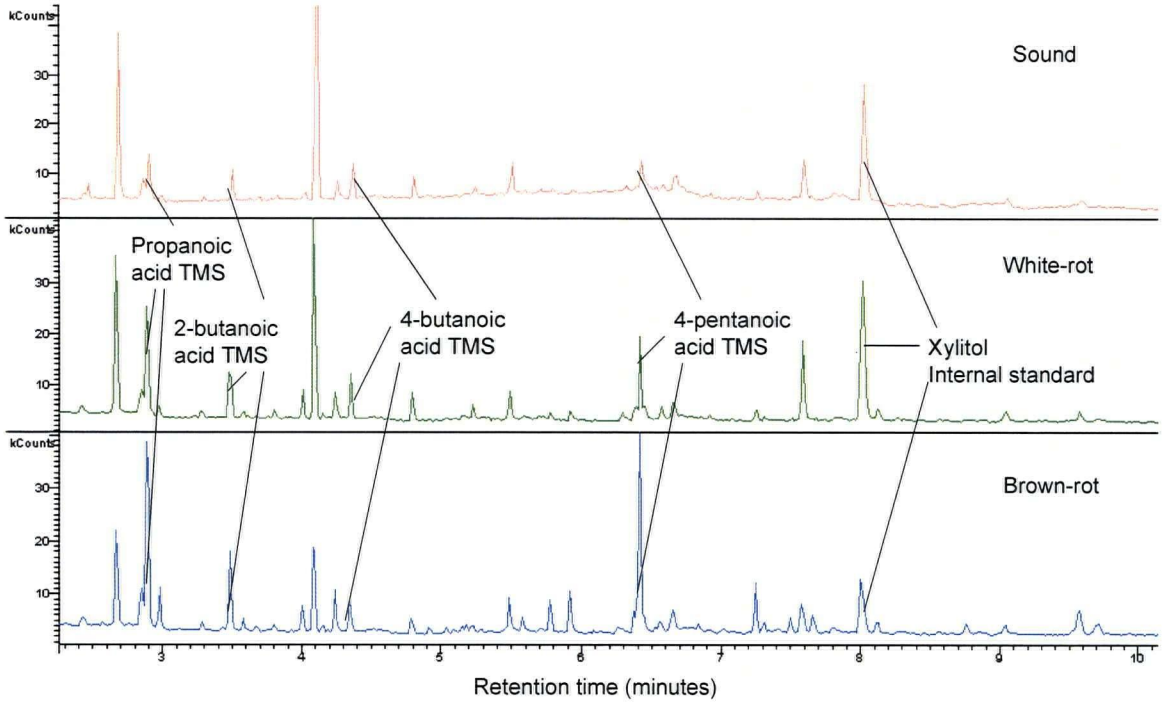

Figure 4.5 Gas Chromatograms of the Caustic Degradation Products of Sound, White-rot and Brown-rot Decayed Spruce Samples

The quantity of the wood components in caustic extracts varies between sound, white-rot and brown-rot decayed wood (Table 4.4). The most significant changes in the components of the caustic soluble fraction are the decrease in acetyl content and increase in lignin content.

Table 4.4 Percent Composition of Caustic Extracts from Sound, White-rot and Brown-rot Decayed Spruce Samples

Constituent	Sound (%)	*P. igniarius* (WR, %)	*G. trabeum* (BR, %)
Acetyls	37	23	3
Extractives/ Degradation products	8	18	27
Polysaccharides	27	27	21
Lignin	28	32	49

4.3.1.2 Buffering Capacity Fractionation

The spruce samples were analyzed to determine the effect of wood components on buffering capacity. By comparing the buffering capacity of untreated and acetone-extracted wood, extractives were found to account for between 15 and 30% of the buffering capacity (Table 4.1). Acetyl groups were calculated to account for less than 2% of the buffering capacity. The buffering capacities of the lignin and polysaccharides were not determined directly. Care must be taken not to form new acid groups when separating lignin and polysaccharides. This could be achieved by ball-milling the wood samples, isolating the holocellulose with chlorine dioxide, and isolating the lignin with enzymatic degradation of the polysaccharides. Phenolic groups found in lignin and carboxyl groups bound to xylans would likely both contribute to the buffering capacity of wood (Sjöström, 1989).

4.3.2 FTIR Spectroscopy

The predictive region of the FTIR spectra of the sound and decayed woods were compared (Figure 4.6, Table 4.5). The results clearly demonstrate three peaks at 1596, 1660 and 1736 cm^{-1}, which correspond to the aromatic skeletal vibration plus carbonyl stretching, carbonyl

stretch on conjugated *p*-substituted aryl ketones and acetyl stretching, respectively (Faix, 1991, Zanuttini *et al.*, 1998). The only noticeable differences between the *G. trabeum*-decayed and the sound sample were a shift in the 1660 cm^{-1} peak to 1668 cm^{-1} and broadening at 1736 cm^{-1}. Spectra of sound and *P. igniarius*-decayed spruce were almost identical in the predictive region. The entire FTIR spectrum did not show major differences between the sound and decayed samples (Appendix VIII). First derivative spectra were also very similar and did not highlight any other changes (Appendix VIII). These changes are consistent with loss of acetyl groups and changes in the lignin being responsible for the predictive ability of the PLS models.

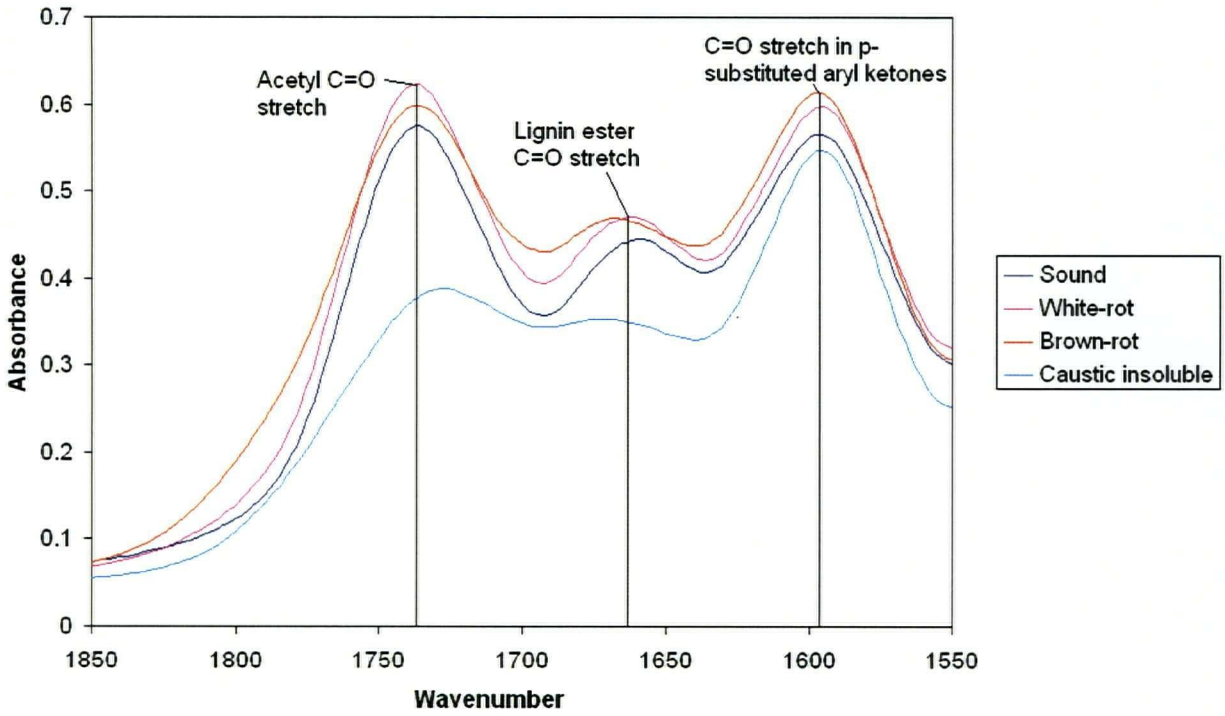

Figure 4.6 Normalized FTIR Spectra (31 point Savitzky-Golay Smoothed) of Sound, White-rot and Brown-rot Decayed Spruce Samples from 1850 to 1550 cm^{-1}. Spectral Assignments (Faix, 1991).

The effect of modifications to acetyl groups on the FTIR spectra was determined by comparing the spectra of wood with acetyl groups removed and of wood with acetyl groups added. Acetyl groups were removed by the 1% caustic extraction along with other wood

components. The most significant change was that of the peak at 1736 cm^{-1}, which was significantly reduced and shifted to 1728 cm^{-1} (Figure 4.6). As Zanuttini *et al.* (1998) have shown, the peak at 1728 cm^{-1} corresponds with acetyl content. Also of interest is the shift and decreased intensity of the 1660 cm^{-1} peak, which suggests that some of the *p*-substituted aryl ketones in the lignin were caustic soluble.

Acetylated wood (Figure 4.7) and acetylated-delignified wood show a major increase in the intensity of the peak at 1736 cm^{-1}. FTIR spectra of the acetylated wood and acetylated-delignified wood show a concurrent decrease in OH stretching at 3400 cm^{-1} which indicate partial acetylation (Appendix VIII). The increase in the delignified wood demonstrates that the acetyl groups are associated with the polysaccharide fraction. This does not indicate where the acetyl groups have been attached, only that they were somewhere on the polysaccharide fraction.

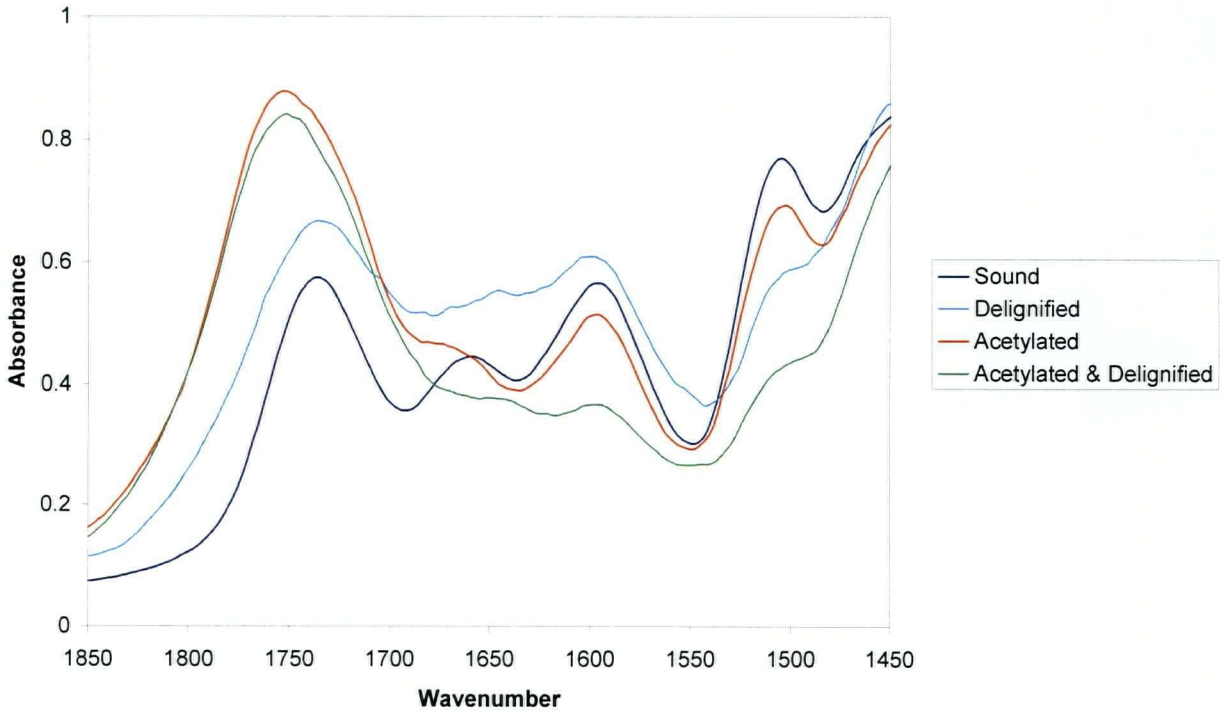

Figure 4.7 FTIR Spectra (31 point Savitzky-Golay Smoothed) of Sound Spruce, Delignified, Acetylated and Delignified and Acetylated from 1850 to 1450 cm^{-1}

The spectrum of delignified wood shows the loss of the peak at 1504 cm^{-1}, which is known to be a "pure" lignin peak (Ferraz *et al.*, 2000). This confirms the visual observations of delignification. Klason lignin content of the delignified samples was not determined. The peak at 1596 cm^{-1}, which is attributed to the aromatic stretching of lignin, as well as carbonyl stretching, did not diminish, and suggests that the carbonyl stretching component is significant and is not contained in the lignin (Faix, 1991).

FTIR spectra of Klason lignin are not an accurate representation of native lignin because of condensation reactions induced by the acid hydrolysis. Nonetheless, FTIR spectra do offer some insight into the, albeit modified, structure of the lignin (Table 4.5). Peaks were observed at 1716 and 1598 cm^{-1}. The peak at 1598 cm^{-1} is attributed to the aromatic skeletal vibrations and carbonyl stretching of the lignin (Faix, 1991). The peak at 1716 cm^{-1} is attributable to the carbonyl stretching of functional groups bound to the lignin formed by condensation reactions. FTIR spectra of native lignins do not report a peak in this area (Faix, 1991).

Table 4.5 Absorbance Maxima and Relative Intensities in FTIR Spectra of Sound, White-rot and Brown-rot Decayed Spruce Samples and Wood Fractions

Sample	Peak 1	Peak 2	Peak 3	Peak 4
Sound spruce	1736 m	1660 m	1596 m	1504 m
P. igniarius	1736 m	1662 m	1596 m	1504 m
G. trabeum	1736 m	1668 m	1596 m	1506 m
Sound spruce – Caustic insoluble	1728 w	1670 w	1596 m	1506 m
Sound spruce – Delignified	1736 m		1600 m	
Sound spruce – Acetylated	1752 s		1598 m	1502 m
Sound spruce – Delignified and Acetylated	1752 s		1598 w	
Sound Spruce – Klason lignin	1716 m		1598 s	1500 s

s = strong, m = medium and w = weak absorbance

4.3.3 Microscopy and Fibre Quality Analysis

To monitor the progress of decay in individual chips, *P. igniarius* and *G. trabeum* were grown on one side of a wood chip to yield single chips with decay on only one half of the chip. The chips were then cut at the hyphal front. FTIR spectra were obtained on each side of the portion of the chip and caustic solubility and buffering capacity were determined (Table 4.6).

Table 4.6 PLS-Predicted Caustic Solubility and Buffering Capacity of a Single Wood Chip, Half Covered with either White- or Brown-rot Fungi

Sample	PLS-Predicted Caustic Solubility	PLS-Predicted Buffering Capacity
P. igniarius (WR) – sound	12.3	0.034
P. igniarius (WR) – decay	18.4	0.048
G. trabeum (BR) – sound	11.4	0.034
G. trabeum (BR) - decay	15.8	0.041

Figure 4.8 shows light micrographs of cross-sections of incipient white- and brown-rot decay in pine and advanced white- and brown-rot decay in spruce. The basic green stain dyes lignin green and cellulose yellow. Thus, the yellow areas represent regions of delignification, indicative of decay. The sensitivity of the stain to over-staining was not determined. Although incipient decayed samples had increased caustic solubility, hyphae, cell wall damage and delignification were not evident in the micrographs. The heavily decayed samples confirmed the presence of hyphae in the lumina and cell walls that were damaged. The heavily decayed white-rot sample had clear zones of delignification, not present in the brown-rot sample.

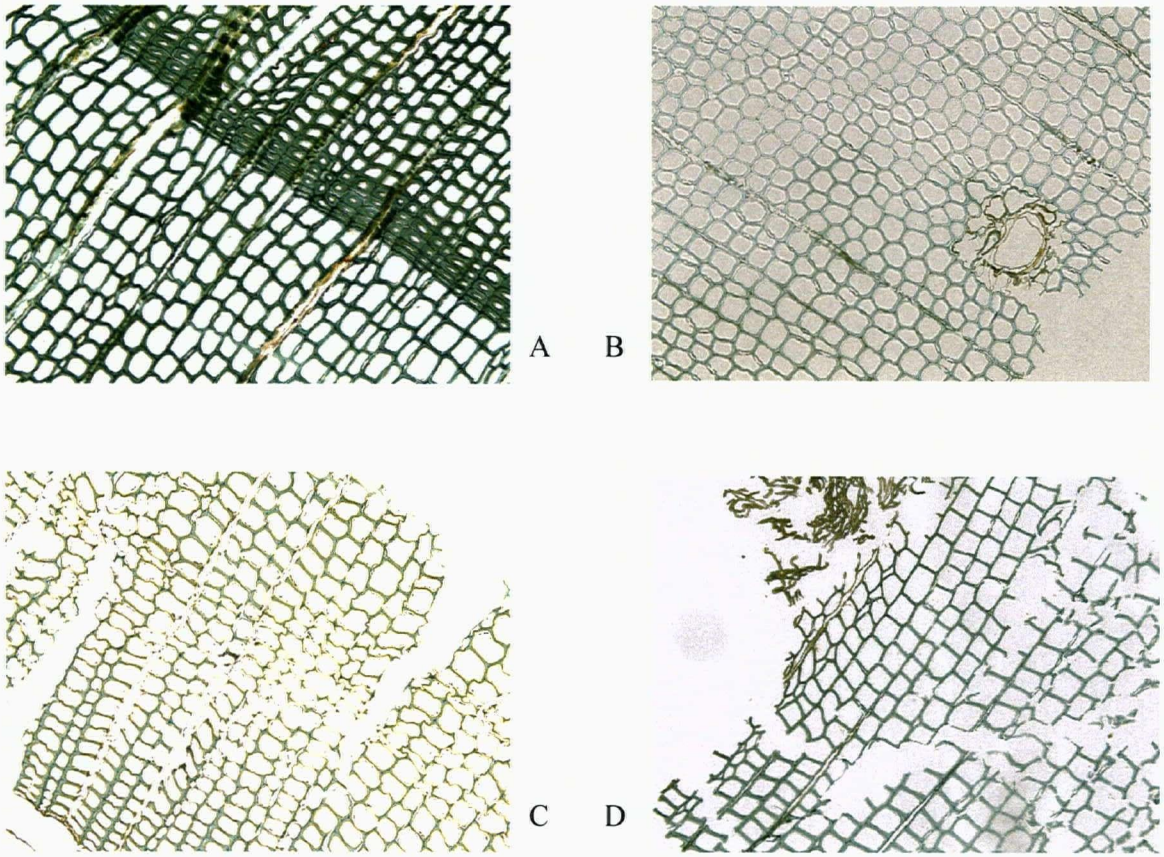

Figure 4.8 Micrographs of Decayed Wood Taken Through a 20X Lens (A) Incipient Decay by *P. igniarius* in Lodgepole Pine, (B) Incipient Decay by *G. trabeum* in Lodgepole Pine, (C) Advanced Decay by *P. igniarius* in White Spruce, (D) Advanced Decay by *G. trabeum* in White Spruce.

Brown-rot decayed chips had different fibre lengths than sound and white-rot decayed samples (Table 4.7). All samples had the same coarseness. These results are consistent with those obtained by Mischki *et al.* (2005) on Western hemlock. Brown-rot fungi lower cellulose D.P. and, thus, can severely weaken fibres to the point that they are easily broken. The increase in fibre length in white-rot decayed wood may be an indication that the fungus had made the fibres easier to separate, but do not appreciably affect fibre strength, and thus helped to preserve fibre length.

Table 4.7 Fibre Quality Analysis of Sound, White-rot and Brown-rot Decayed Spruce Samples, Std. Dev. in Parentheses (n = 8)

Sample	Sound	*P. igniarius*	*G. trabeum*
Coarseness (mg/m)	0.20 (0.01)	0.20 (0.01)	0.19 (0.01)
Length-weighted fibre length (mm)	2.56 (0.03)	2.69 (0.07)	1.9 (0.4)

4.4 Discussion

Lignin, acetyl groups and extractives were found to underlie the predictive ability of the PLS models of caustic solubility and buffering capacity. Brown-rot decayed wood contained more lignin, relative to the other wood components, than the sound wood, and had increased lignin solubility and decreased acetyl content. These chemical changes resulted in small changes in the IR spectra in the region used to predict caustic solubility and buffering capacity. The lack of major changes in the IR spectra make PLS modeling necessary. Since white-rot decayed wood did not exhibit the same chemical changes as brown-rot, it was more poorly estimated by the PLS models. Therefore, a more accurate method of estimating the extent of white-rot decay is by using the microscopic method outlined in PAPTAC standard B.3P (PAPTAC, 2000). Unfortunately, microscopic analysis of wood is too expensive and time-consuming to be regularly used by mills. NIR spectroscopy may be better able to estimate extent of white-rot decay (this was not determined in this thesis).

The precision of the methods used to determine the wood components was influenced by many factors. The sum of components in the wood samples did not equal 100% because some constituents are measured twice and some, such as ash or protein, were not measured. Baeza and Freer (2001) report that sums deficient or in excess by 10% are frequently obtained. In the analysis of acid-soluble lignin, an extinction coefficient of 110 L g^{-1} cm^{-1} was used. Since the extinction coefficient is dependent on the composition of the acid-soluble lignin, this is only an

estimate. The loss of water from the lignin condensation and methanol liberated from the demethoxylation of the polysaccharides was not accounted for. Also, uronic acids were reduced to their corresponding neutral sugars because of the reduction step required for sugars analysis by GC (Baeza and Freer, 2001). However, all of these sources of error are small (Baeza and Freer, 2001). The remainder of the error is attributed to the level of precision of the methods.

Decay by either *P. igniarius* or *G. trabeum* modifies the lignin and results in increased acid solubility. The decrease in Klason lignin in the white-rot sample is consistent with white-rot fungi utilizing the lignin, and the increase in the brown-rot sample is consistent with losses of carbohydrates.

Some fungi are known to produce acetyl esterases, which remove acetyl groups from hemicelluloses and facilitate the activity of endoglucanases or xylanases (Altaner *et al.*, 2003). These enzymes contribute to the removal of acetyl groups from decayed wood. The literature does not report whether the species used in this experiment, *P. igniarius* or *G. trabeum*, produce these enzymes. Alternatively, acetyl groups may be removed by non-enzymatic reactions or by removing the hemicellulosic sugars to which the acetyl groups are bound.

The mannose content in the decayed samples suggests that *G. trabeum* was able to effectively remove and metabolize mannans. The glucose content in the decayed samples suggests that the cellulose was degraded at a lower rate than the hemicelluloses, which were severely affected. In softwoods the dominant hemicellulose is galactoglucomannan with only small amounts of arabinoglucuronoxylans. The carbohydrate data suggest that xylan is being solubilized. The glucose detected could be from the reduction of the glucuronic acids, though this was not tested. The brown-rot sample was much more extensively damaged by the fungus and resulted in the increased liberation of sugars. There is some carbohydrate loss due to the caustic extraction in each sample; however, this is most significant in the brown-rot sample where one third of the carbohydrate fraction is lost during the extraction. This, in combination

with the lowered D.P. of cellulose and hemicelluloses, explains the large caustic solubility of the brown-rot samples. This suggests that under kraft pulping conditions, brown-rot decayed wood will reduce pulp yield. Moreover, the lower D.P. of carbohydrates will reduce the strength properties of the fibres produced from brown-rot decayed wood. These findings are consistent with research on kraft pulping brown-rot decayed wood (Hunt, 1978b).

The 1% caustic solubility test is a measure of changes in several different wood components. Polysaccharides, lignin and extractives were all partially soluble under the conditions of the 1% caustic solubility test. As in kraft pulping, cellulose was much more resistant to alkaline degradation than the hemicelluloses (Gustavsson and Al-Dajani, 2000). Xylans were more soluble than glucomannans under the conditions of the 1% caustic solubility test, despite the reported stability of xylans under these conditions (Gustavsson and Al-Dajani, 2000). The milder conditions of the 1% caustic solubility test meant that much less lignin was dissolved than in kraft pulping. The 1% caustic solubility test is thus influenced not just by one wood component but, to some extent, by all of them.

Buffering capacity, used to measure changes in acid groups, is based on the molar equivalents of sodium hydroxide neutralized and not on the mass of acid groups. Determining the effects of various wood fractions on buffering capacity is difficult because the fractionation process can affect the abundance of acid groups, such as in the cases of caustic insoluble and acid-chlorite delignified wood. The buffering capacity of the extractives was significant, but did not correlate with extent of decay. Acetyl groups were determined to be only minor contributors to the buffering capacity of wood. The most significant factors affecting buffering capacity were the polysaccharides and lignin. The polysaccharides in wood contain glucuronic acid residues, which may contribute to the buffering capacity of wood (uronic acids were not measured). Polysaccharides in decayed wood have increased carboxyl content (Blanchette, 1995). Lignin is known to contain a variety of acid functional groups, which will also likely contribute to

buffering capacity. After decay, lignin contains increased acid functional groups (Zabel and Morrell, 1992).

The measurement and prediction of buffering capacity is of particular relevance to kraft pulping where increases in the buffering capacity of incoming wood chips will cause an increase in the consumption of effective alkali (EA). Major increases in the buffering capacity of wood chips will increase chemical usage and place extra demand on recovery systems.

The absorbance in the predictive region of the FTIR spectra came from functional groups on the lignin and hemicellulose fractions. The relative spectral contributions of the lignin and acetyl groups will vary with the nature and extent of decay. Since the changes in IR spectra that result from decay are subtle and occur over a range of frequencies, multivariate modeling was required.

Abbott *et al.* (1988) found that wood extracted with 12% NaOH was chemically changed and that component spectra could not be reconstructed. The same applies for wood extracted with 1% NaOH. The primary difference is the loss of the peak at 1736 cm^{-1}. The acetyl groups have been liberated by the caustic extraction and have formed sodium acetate, which absorbs at lower frequencies.

Histological analysis of incipient and advanced white- and brown-rot decay confirmed that the basic green stain is an effective way to monitor delignification from white-rot fungi (PAPTAC, 2000). Moreover, there was no microscopic evidence of fungal decay in the incipient decay samples despite higher caustic solubility. This suggests that the PLS models are capable of identifying decayed wood, even when light microscopy cannot. Changes in wood chemistry may take place before hyphae are visible inside the lumen and before changes in cell wall structure occur. As a result IR spectra and PLS modeling could be used to measure decay in very controlled studies.

The reduction of fibre length and constant coarseness suggests that the brown-rot decayed fibres were cleaved and not eroded. Microscopic and FQA data support the presumed correlation between changes in wood chemistry and fibre damage due to decay fungi.

In summary, IR predictive ability due to loss of acetyl groups from hemicellulose and modifications to lignin. Microscopic analysis is preferable for detecting white-rot decay; IR is better for detecting brown-rot decay.

PLS modeling of FTIR spectra could be applied to many other research areas. Changes in lignin and acetyl groups are not unique to decay. Phenotypic variation in lignin content could be predicted with IR spectroscopy and PLS modeling (Poke *et al.*, 2004). Similarly, the weathering of wood could be modeled based on IR spectroscopy (Nuopponen *et al.*, 2003, Sudiyani *et al.*, 2003) as well as lignin modification by chemicals, enzymes or fungi (Gonçalves *et al.*, 1998, Jin *et al.*, 1990). IR spectroscopy can be focussed on small regions of wood and collected at different time intervals. This would enable one to monitor changes in lignin and acetyl groups as fungal hyphae grow through a wood sample or as their enzymes diffuse into a wood sample. Coupled with traditional microscopic techniques, one could view the growth of hyphae and monitor the associated chemical changes using IR spectroscopy on the same sample at the same time.

PLS modeling of FTIR spectra has been found to correlate with caustic solubility and buffering capacity. In turn, FTIR spectra of wood have been correlated with the chemical changes in wood that underlie these methods - the concentration of acetyl groups and lignin in wood. In order to fully understand the relevance of the FTIR-based predictions of decay, pulps must be prepared from wood that has been measured by the developed methods. This will show the relationship between predictions of extent of decay in wood chips and the resulting pulp properties.

CHAPTER 5

Chemical and Mechanical Pulping of Decayed Wood

5.1 Introduction

As discussed in Chapter 1, decayed wood is currently pulped at many mills. It enters the fibre supply from harvesting diseased wood or over-mature stands, and from decay occurring while in storage. Wood chip piles, the most common means of fibre storage, offer an ideal environment for decay fungi to thrive (Fuller, 1985). Many factors contribute to the decay of wood chip piles including the length of storage, wood species, location, fungal ecology, moisture, oxygen levels, and pH (Nicholas and Crawford, 2003, Saunders and Singh, 1988). Decay fungi may enter wood chip piles from spores that are transported to the wood, by wind, rain, and insects, or by direct contact with mycelia present in soil. Wood chips are also inoculated when sound and decayed chips are mixed. Thus, the rate of mixing and size of inoculum will also impact the rate of decay. Understanding the significance of inoculum size on the rate of wood chip decay is an important step to determine better ways of preserving wood chip value.

The initial and most dramatic effect of decay is the direct loss of wood substance (Feist *et al.*, 1971, Hunt and Hatton, 1979). This can be minimized by proper wood chip procurement and storage procedures. When decayed wood is to be pulped, the adverse effects can be minimized by either pulping sound and decayed wood chips in a uniform ratio or by pulping them separately to avoid swings in the energy and chemical consumption of mechanical and kraft pulps, respectively (Hunt and Hatton, 1979). The decision of the quantity of wood chips to use when mixing sound and decayed wood chips will depend on the extent of decay, quantity of decayed chips, and the effect on final pulp properties.

The many effects of decay on mechanical pulps are often overshadowed by the loss of brightness. Brightness can be significantly reduced by decay, with a maximum loss of 17 ISO

points reported (Jackson *et al.*, 1985), and it has been estimated that a one ISO point drop in brightness occurs for every 4% increase in decay content (Christie, 1979). In addition, significant costs can be incurred brightening pulps produced from stained or decayed wood. Pulps may be easier or more difficult to bleach depending on the fungi involved in the decay process and the bleaching method used (DeJong *et al.*, 1997). In addition to having lower brightness, chemithermomechanical pulps produced from decayed aspen have higher scattering coefficients, and lower tear resistance than pulps made from sound wood (Jackson *et al.*, 1985, Whitty *et al.*, 1991).

The effects of kraft pulping decayed wood have been well documented (Becker and Briggs, 1983, Hunt, 1978a, Hunt, 1978b, Mischki *et al.*, 2005, Procter, 1973). In short, losses in pulp yield and increased alkali consumption are associated with decay, and adverse properties include burst, tear, tensile and indices, folding endurance and brightness (Hatton, 1978a, Hunt, 1978a, Hunt, 1978b, Procter, 1973). The extent of yield loss and the degree to which pulp properties are affected depend on the type and degree of decay (Procter, 1973).

Since Lodgepole pine is an abundant and economically important species in BC, and because the current Mountain Pine Beetle infestation increases the wood supply available, Lodgepole pine was chosen for use in this study. The first objective of this chapter was to quantify the effects of inoculum size on the rate of decay and on the properties of pulps produced by Thermomechanical Pulping (TMP). Although white-rot and staining fungi have significant effects on wood in storage that are of particular interest for biopulping, only brown-rot decay was considered since it is known to cause the largest drops in pulp quality. The purpose of this study was to investigate the worst-case scenario of a decayed fibre supply, not to study the potential benefits of fungal treatment of wood.

The second objective of this chapter was to further validate the PLS models of caustic solubility and buffering capacity, described in Chapter 3. This was achieved by periodically

testing the wood chips stored with varying inoculum size extent of decay over time. Changes in PLS-predicted caustic solubility or buffering capacity was used as indicators of extent of decay. The accuracy of these predictions was determined once the samples were pulped. If samples with high PLS-predicted caustic solubility and buffering capacity have poor pulp properties, and samples with low PLS-predicted caustic solubility and buffering capacity have better pulp properties, then the models are accurately measuring decay, as it affects pulping. To provide a suitable range of decay and to compare chemical and mechanical pulps, RMP and kraft pulps were prepared from samples of sound, discoloured, intermediate, and advanced brown-rot decayed wood chips. This also enabled for a direct comparison between the effects of brown-rot decay on kraft and mechanical pulps.

5.2 Methods

5.2.1 Wood Chip Preparation

Lodgepole pine (*Pinus contorta* Dougl. var. *latifolia* Engelm.) was obtained from 25 randomly harvested trees from an overstocked, small diameter site near Kamloops, BC. Trees ranged in age from 50 to 80 years and had a mean diameter-at-breast-height of 11.5 cm. Harvested trees were cut to manageable lengths, debarked by hand with a draw-blade, and chipped using a 36-inch CM&E 10-knife disc chipper. Wood chips were mixed and, since the wood chips were not sterilized, stored in plastic bags at -6°C to prevent fungal growth prior to being used.

In order to investigate the effect of inoculum size on rate of decay a bench-scale experiment was conducted. First, the optimum growth temperature of the brown-rot fungus, *Gloeophyllum trabeum* 61750M on MEA, was determined. *G. trabeum* was grown on 1% MEA (Difco, Sparks, MD) plates. Plug samples (5 mm diameter) of mycelia and agar were taken from the edge of a young colony and sub-cultured to the centre of a fresh 1% MEA plate and

incubated at 23, 30, 33, 35, 37 or 40°C. Growth curves were determined by measuring colony diameter over time.

G. trabeum was incubated with Lodgepole pine chips at optimum growth temperature. Lodgepole pine wood chips were first screened to obtain the fraction retained on a 7 mm screen. The inoculum was prepared by cutting these chips along the fibre axis with a chisel to produce "pins" from accept-quality chips. These pins were then inoculated with *G. trabeum* and incubated for 23 days, according to the method of Ferraz *et al.* (2000). Eighty-five grams of sound wood chips (50% OD) were added to a 1L Erlenmeyer flask and 0, 5, 10, 20, 40 or 80 decayed pins were added. Flasks were incubated for 70 days at 34°C with filtered, moist air continually passed over the samples. Wood chips were sampled periodically for FTIR analysis and prediction of 1% caustic solubility and buffering capacity using the models described in Chapter 3. Pin chips, known to be the inoculum, were excluded from these samples.

Four samples of unsterilized pine chips were prepared and stored at 34°C for 115 days prior to TMP. The pine samples included one bag of sound chips and three bags with small, medium and large inoculations of *G. trabeum*-decayed chips. All wood chips samples were periodically tested for moisture content and analyzed by FTIR to predict caustic solubility and buffering capacity.

In order to assess the impact of decay on kraft and refiner mechanical pulping (RMP) over a wide range of decay, four samples of Lodgepole pine chips were obtained. Wood chips were inoculated with *G. trabeum* for RMP and kraft pulping, and selected for the extent of decay, based on PLS-predicted caustic solubility and buffering capacity. This produced four categories: sound, discoloured (wood chips containing mould but no decay), intermediate decayed and advanced decayed wood chips. These samples were analyzed for moisture content, basic wood density, packing density, extractives, and Klason and acid soluble lignin by PAPTAC standards (PAPTAC, 2000), or methods outlined in Chapter 2.

5.2.2 Mechanical Pulping

Using Paprican facilities, RMP pulp was prepared from four Lodgepole pine chip samples: sound, chips stored at room temperature, and chips moderately and severely decayed by *G. trabeum*. Pulps were prepared using a Sprout Waldron open-discharge laboratory refiner equipped with type D2A507 plates. Each sample was refined to three energy levels, with the exception of the advanced decayed sample, which, due to limited sample size, was only refined to two points.

TMP pulp was prepared using a Sunds Defibrator TMP 300 single-disc laboratory refiner for first-stage refining (Table 5.1). A Labview PC system was used to control and/or monitor the refining variables. A high freeness pulp sample from each of the four primary thermomechanical (TMP) pulps was given one or more further passes in 30.5 cm Sprout Waldron open-discharge laboratory refiner equipped with type D2A507 plates at 17-25% refining consistency. Each sample was refined at three or four energy levels to give TMP pulps in the freeness range from 78 to 230 mL Canadian Standard Freeness (CSF).

Table 5.1 TMP Conditions

Plates	Rotor, No. 3809 modified
	Stator, No. 3804 modified
Preheater pressure	152 kPa
Refiner housing pressure	172 -179 kPa
Chip presteaming time	7 min (atmospheric pressure)
Preheater residence time	7 min
Pulp consistency	20 to 24 % od pulp (cyclone exit)
Prex compression ratio	3:1

After latency removal with boiling water, mechanical pulp samples were screened on a 6-cut laboratory flat screen and screen rejects determined. Bauer-McNett fibre classifications were also determined on the screened pulps, while fibre lengths were determined using a Fibre Quality Analyzer (FQA). Standard handsheets were prepared for testing physical and optical properties with white water recirculation to minimize the loss of fines.

5.2.3 Kraft Pulping

The same wood chip samples used to prepare RMP pulps were also used to prepare kraft pulps. First, these samples were air-dried and screened. Next, fifty-gram (OD equivalent) samples from the "accepts" fraction (2 – 6mm) were added to bombs and cooked within a B-K micro-digester assembly. The cooking conditions of the exploratory cook are shown in Table 5.2.

Table 5.2 Kraft Pulping Conditions (Constant H-factor)

Time to maximum temperature (min)	135
Maximum cooking temperature (°C)	170
Effective alkali (EA, %)	16
Sulphidity (%)	25
Liquor to wood ratio	4.5 to 1
H-factor	1290

Based on the results of these exploratory cooks, pulps were produced with a target kappa number of 30 by varying the H-factor and EA. All pulps were disintegrated, washed, and screened through an 8-cut screen plate. Fibre properties were determined using a Fibre Quality Analyzer (FQA). Fibre length distributions were determined using a Bauer McNett classifier.

Beating curves were prepared using PFI mill runs of 0, 3000, 6000 and 12000 revolutions for sound and discoloured samples and 0, 6000 and 12000 revolutions for decayed samples, according to PAPTAC standard C.7 (PAPTAC, 2000). Canadian Standard Freeness was determined for each point according to PAPTAC standard C.1 (PAPTAC, 2000). Handsheets were prepared for testing optical and physical properties according to PAPTAC standard C.4 (PAPTAC, 2000).

Black liquors were analyzed for residual effective alkali (REA) by auto-titration with 0.5N HCl to an endpoint of 11.38 (Milanova and Dorris, 1994). Solids and ash content were determined gravimetrically by heating at 105 and 775°C, respectively. The ratio of organics to inorganics was determined by comparing the solids content minus the ash content, to the ash content.

5.2.4 Pulp Testing

Kappa number, brightness, opacity, scattering coefficient, caliper, roughness, air resistance, basis weight, moisture content, zerospan, and burst, tear and tensile indices were all determined according to PAPTAC standard methods (PAPTAC, 2000). Data reported at constant freeness were linearly interpolated or extrapolated from the two data points closest to the freeness target.

5.3 Results

5.3.1 The Effects of Inoculum Size and Wood Chip Storage

The temperature at which the optimal growth of *G. trabeum* occurred on MEA was 35°C (Table 5.3). Growth at 33°C was comparable, while growth at 37°C was much slower. Since higher temperatures severely limited the growth of the fungus and the incubator temperature was

known to fluctuate by a few degrees, 34°C was used to incubate all subsequent wood chip samples.

Table 5.3 Colony diameter of *G. trabeum* on Malt Extract Agar after 7 days of incubation at varying temperatures

Incubation Temperature (°C)	Colony Diameter (mm) (Std. Dev. = 2 mm)
23	25
30	53
33	54
35	66
37	14
40	6

The PLS-predicted caustic solubility of bench-scale wood chip samples with varying inoculum concentration was plotted as a function of incubation time and inoculum size (Figure 5.1). When inoculum concentration was low, caustic solubility dipped slightly but did not change significantly over time. When inoculum concentration was high, caustic solubility increased with time. The precision of the PLS-predicted caustic solubility limits the ability of this method to differentiate small changes in decay content. However, these data suggest that using this method of inoculation, an intermediate level of decay will be reached after 70 days of incubation with a minimum of 7% inoculum.

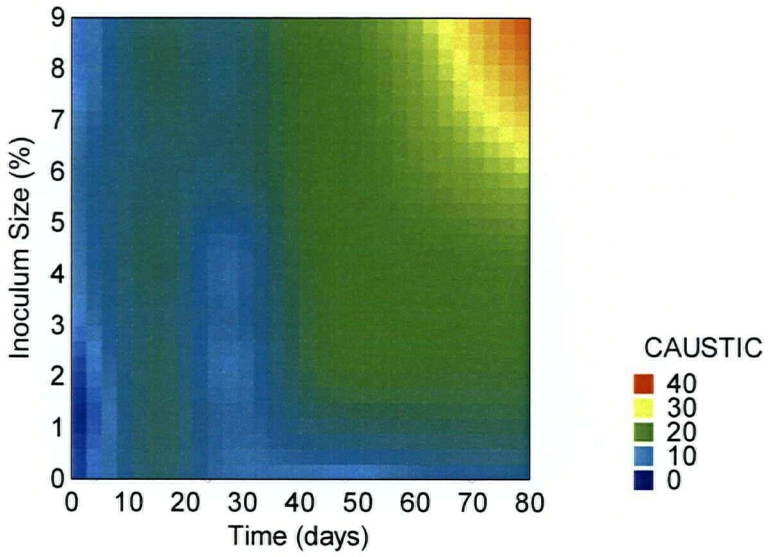

Figure 5.1 PLS-Predicted Caustic Solubility as a Function of Inoculum Concentration and Time (Bench-Scale).

Table 5.4 shows the analysis of variance for the caustic solubility of pine samples inoculated with *G. trabeum*. Results from the ANOVA indicated that both time and inoculum size were significant contributors to caustic solubility and buffering capacity ($\alpha = 0.05$). Eta-squared correlation ratios showed that time accounted for more of the variance in caustic solubility than did inoculum size. However, the majority of the variance was not accounted for by either time or inoculum size. This suggests that, although statistically significant, inoculum size did not have a major impact on caustic solubility or buffering capacity.

Table 5.4 Caustic Solubility Bench Scale Analysis of Variance (N = 80, α = 0.05) for Lodgepole Pine Chips Inoculated with *G. trabeum*. Time was specified as a covariate.

Variables	SS	df	Mean Square	F ratio	P value	Eta squared (%)
Inoculum	463.7	5	92.7	2.867	0.020	13.0
Time	740.4	1	740.4	22.885	0.000	20.8
Error	2361.6	73	32.4			66.2

Where SS = Sum of Squares and df = Degrees of Freedom

The experiment described above, to investigate the effects of inoculum size on extent of decay, was scaled up to 15 kg OD of wood chips to provide enough chips for TMP. The Lodgepole pine chips with *G. trabeum* that served as an inoculum had a caustic solubility of 31.9%. The caustic solubility and buffering capacity of the pine samples vary with the sample's inoculum concentration because the chips used as inoculum could not be distinguished from the fresh wood chips. Caustic solubility and buffering capacity of the pine chips before and after storage are presented in Table 5.5.

The moisture content of these samples remained stable throughout the incubation period, between the limits of 40 to 80% (as a percentage of wet weight) that is optimal for fungal growth (Nicholas and Crawford, 2003). After storage, the caustic solubility and buffering capacity decreased or stayed roughly the same in most samples, indicating that the wood chips were not significantly decayed. The major variations in caustic solubility are attributable to the initial caustic solubility of the inoculum. After storage, only the high-inoculum sample had significantly higher caustic solubility and buffering capacity that the control sample. The apparent loss in caustic solubility in the control sample after storage is likely due to the loss of volatile extractives. The lack of decay in these chips was likely due to antagonistic interactions with moulds present on the chips (the chips were not sterilized) and to uncontrolled relative

humidity. Since there were only minor changes in PLS-predicted caustic solubility and buffering capacity, there should only be minor changes due to decay in the TMP pulps.

Table 5.5 Caustic Solubility and Buffering Capacity in Lodgepole Pine Chips before and after 115 Days Storage. Standard Deviation in Parentheses.

			Initial Conditions		Final Conditions	
Sample	Inoculum size (%)	Storage time (days)	1% Caustic solubility (%) n = 3	Buffering Capacity (mol/g) n = 1	1% Caustic solubility (%) n = 3	Buffering Capacity (mol/g) n = 1
Pine stored sound	0	115	16.2 (0.4)	0.037	13.1 (0.3)	0.047
Pine low decay	8.9	115	17.6 (0.5)	0.041	13.0 (0.9)	0.065
Pine medium decay	16.6	115	18.8 (0.5)	0.045	16.7 (0.3)	0.069
Pine high decay	29.8	115	20.9 (0.6)	0.051	19.9 (0.9)	0.070

In order to compare the resulting physical and optical pulp properties, appropriate baseline values of pulp freeness were selected. Raw data were standardized by interpolation or extrapolation to a freeness of 100 mL CSF. Table 5.6 shows the pulp properties of pine TMP pulps (raw data are presented in Appendix IX). Less than 0.1 % screen rejects were produced for all TMP pulps.

Incubation with white-rot fungi has been shown in biomechanical pulping to reduce energy requirements (Ahktar *et al.*, 2000). However, in the current study *G. trabeum* did not consistently improve energy consumption over a range of freeness (Figure 5.2). The differences in specific refining energy at any given freeness between samples were small - typically less than 10% of the energy required to pulp the sound wood. This small difference in refining energy corresponded to the small differences observed in decay extent.

Table 5.6 Lodgepole Pine TMP Pulp Properties Interpolated or Extrapolated to 100 mL CSF

Sample	Sound	Stored-Sound (Control)	Low Inoculum	Medium Inoculum	High Inoculum
1% Caustic Solubility (%)	16.2	13.1	13.0	16.7	19.9
Specific Refining Energy (MJ/kg)	12.8	12.3	13.2	11.5	12.1
Apparent Sheet Density (kg/m3)	362	348	337	333	348
Burst Index (kPa•m2/g)	2.1	2.2	2.3	2.3	2.4
Tensile Index (N•m/g)	35	39	37	36	42
Stretch (%)	1.3	1.5	1.4	1.5	1.7
Tear Index (mN•m2/g)	6.2	6.6	6.5	6.4	6.6
Sheffield Roughness (SU)	181	184	214	229	209
Brightness (%)	56	49	46	46	44
Opacity (%)	96.0	97.6	97.9	98.0	98.1
Scattering Coefficient (cm2/g)	592	572	562	569	536
Length Weighted Fibre Length (mm)	1.17	1.21	1.29	1.27	1.39
Bauer McNett R-14 (%)	1.1	1.9	1.5	1.7	2.8
Bauer McNett 14/28 (%)	21.1	24.9	26.1	26.4	28.0
Bauer McNett 28/48 (%)	26.0	23.3	23.7	23.5	22.3
Bauer McNett 48/100 (%)	18.1	18.2	14.7	14.4	13.0
Bauer McNett 100/200 (%)	9.0	7.9	7.8	7.3	6.1
Bauer McNett P200 (% fines)	24.9	24.5	26.5	27.4	27.9

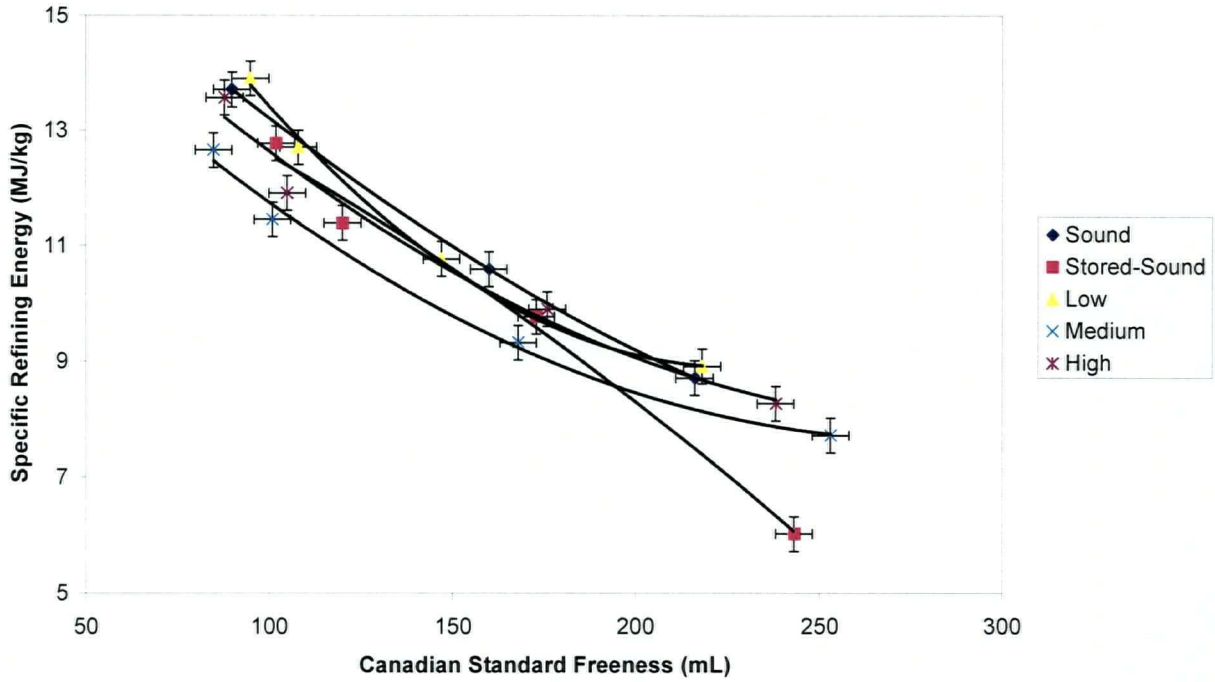

Figure 5.2 Specific Refining Energy vs. Canadian Standard Freeness for Thermomechanical Pulps

Since the wood chip samples were only slightly decayed (as indicated by the PLS-predicted caustic solubility and buffering capacity), with only the most heavily decayed sample falling into the incipient decay category (as defined by Hunt (1978)), changes in pulp properties were small. Length-weighted fibre length at 100mL CSF showed an increase with inoculum size (Table 5.6). Bauer McNett classification showed increases in the long fibre fractions and fines with inoculum size (Table 5.6). Increased fibre length in pulps produced from decayed wood can be attributed to fibres being less strongly bonded together prior to refining (DeJong *et al.*, 1997). Samples that required less energy to reach a given freeness, were thus able to retain increased amounts of long fibres. Although small, the changes in refining energy were large enough to impact the fibre development, resulting in the preservation of more long fibres and the production of more fines.

Bulk properties of the sheet are affected by the amount of long fibres and fines present in the sheet (Seth, 1990). If only the long fibre fractions increased with inoculum size then the

apparent sheet density should decrease (Corson, 1996). However, the fines content also increased with inoculum size, so there is little change in apparent sheet density with increasing inoculum size. The concurrent increase in fines and long fibres led to little variation in the bulk properties in pulps produced from sound and inoculated wood.

Increased fibre length has a direct impact on the mechanical properties of the pulps (Seth, 1990). Increased long fibre content is known to increase tensile and burst indices independent of formation, and increase tear resistance, in a weakly bonded sheet (Seth, 1990). Tensile strength is dependent upon fibre strength and bonding (Page, 1969). Burst index is largely affected by fibre bonding (Howard *et al.*, 1994). The factors affecting tear index are controlled by how well a sheet is bonded. In weakly bonded sheets, fibre length dominates because more fibres pull out than break in the tear zone. Conversely, in well-bonded sheets, fibre strength dominates because more fibres break than pull out in the tear zone (Seth, 1990). However, the increase in fibre length in the high-inoculum sample was very small and as a result, improvements in tear, tensile, and burst indices were also small.

The most significant effect on pulp properties was the loss of ISO brightness. This is attributable to the discolouration of the wood chips by the moulds found on the chips after incubation (the fungi present on wood chips after storage were not identified). If preparing a bleached pulp, additional bleaching chemicals might be required to make up for this loss in brightness.

The effects of wood chip storage were determined by comparing the sound and the stored-sound pine TMP pulp samples (Table 5.6). Moulds and non-decay fungi, which utilize extractives but do not affect the structural integrity of wood, grew on the stored wood chips, and resulted in a small drop in caustic solubility and a small rise in buffering capacity (Table 5.5). The discolouration of the stored wood chips directly contributed to a 7% ISO drop in brightness. Bauer McNett classifications indicated an increase in the long fibre fractions in the stored

sample, which corresponds to the small decrease in specific refining energy in the stored sound sample (Table 5.6). As a result of the longer fibres, at 100mL CSF, there were minor increases in tensile strength.

5.3.2 Refiner Mechanical Pulping

The wood properties of the four chip samples prepared for RMP and kraft pulping are shown in Table 5.7 (RMP was used instead of TMP due to limited sample size). Based on the caustic solubility data, the samples were classified as: sound, sound (discoloured), intermediate decay, and advanced decay. The discoloured wood chips had been stored at room temperature for eight months, and showed little evidence of decay but were very mouldy and discoloured (Figure 5.3). The range of caustic solubility, buffering capacity, and packing and basic wood density was consistent with brown-rot decay in the intermediate and advanced decayed samples. Acetone extractives, determined gravimetrically, increased significantly in the advanced decay sample indicating that compounds previously insoluble had become soluble. Further evidence of brown-rot decay included an increase in lignin content (an indication that polysaccharides have been preferentially removed). Decayed wood chips were visibly darker than sound chips (Figure 5.3) and were more easily broken.

Table 5.7 Properties of Lodgepole Pine Chips Used for RMP and Kraft Pulping. Standard Deviations in Parentheses.

Sample*	Sound	Discoloured	Intermediate Decay	Advanced Decay
Moisture (%) n =2	49.6 (0.1)	51.5 (0.1)	54.2 (0.2)	48.9 (0.2)
Caustic Solubility (%) n = 3	15.3 (0.5)	14.5 (0.1)	26.3 (0.2)	36 (1)
Buffering Capacity (mol/g) n = 1	0.057	0.054	0.087	0.118
Packing Density (g/L) n = 1	180.4	156.3	153.8	133.6
Wood Density (g/mL) n = 3	0.41 (0.02)	0.390 (0.007)	0.387 (0.002)	0.376 (0.007)
Extractives (%) n = 1	2.3	2.7	2.5	4.3
Klason lignin (%) n = 2	24.5 (0.1)	23.4 (0.1)	26.9 (0.2)	30.8 (0.4)
Acid-soluble lignin (%) n = 2	0.4 (0.01)	0.4 (0.01)	0.6 (0.02)	0.7 (0.01)
Total lignin (%) n = 2	24.9 (0.1)	23.8 (0.1)	27.5 (0.2)	31.5 (0.4)

* Samples were classified as Sound, Discoloured, Intermediate Decay and Advanced Decay based on visual observations and decay categories based on 1% Caustic Solubility (Hunt, 1978)

RMP pulp was prepared targeting a freeness of 100mL (Table 5.8). Figure 5.4 shows the specific refining energy as a function of Canadian Standard Freeness (CSF) for the RMP pulp samples. Despite only having two data points (due to limited sample), the advanced brown-rot decayed sample showed a major decrease in specific refining energy. Screen rejects at a given freeness were not consistently impacted by the level of decay in the sample (as indicated by PLS-predicted caustic solubility and buffering capacity).

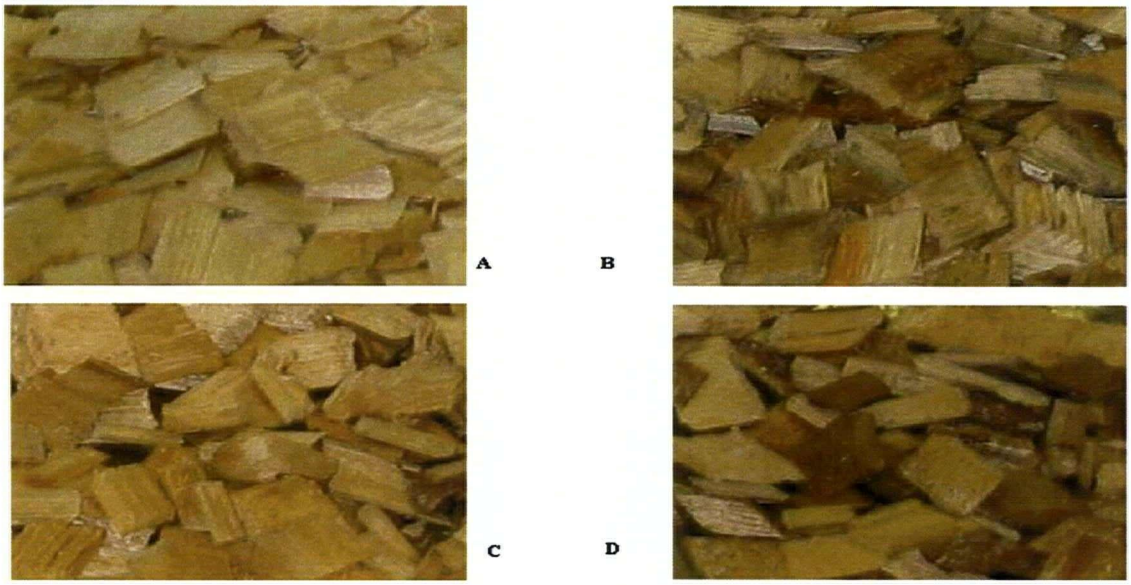

Figure 5.3 Photographs of Lodgepole Pine chips Used for RMP and Kraft Pulping (A) Sound, (B) Discoloured (Stored at room temperature for 8 months), (C) Intermediate Decay (*G. trabeum*), (D) Advanced Decay (*G. trabeum*)

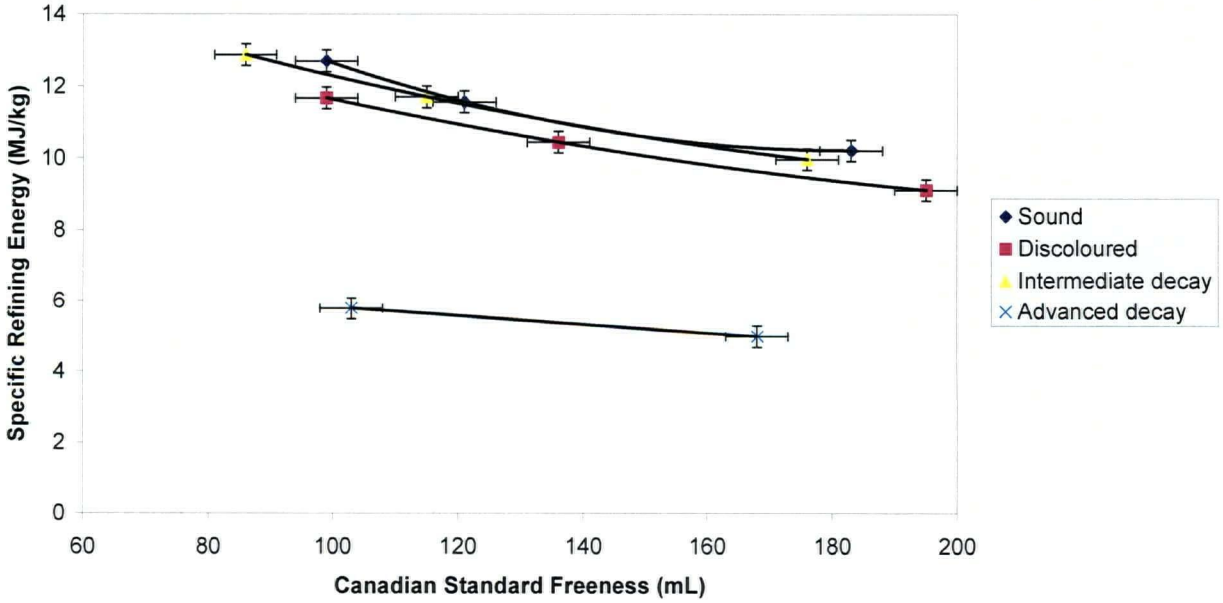

Figure 5.4 Specific Refining Energy of Lodgepole Pine Chips vs. Canadian Standard Freeness for Refiner Mechanical Pulps.

Table 5.8 RMP Properties of Lodgepole Pine Interpolated to 100 mL CSF

Property	Sound	Discoloured	Intermediate	Advanced
Specific Refining Energy (MJ/kg)	12.6	11.6	12.3	5.8
Apparent Density (kg/m^3)	296	280	327	311
Burst Index (kPa·m^2/g)	2.0	1.8	2.2	1.4
Tensile Index (N·m/g)	31.0	27.4	31.2	24.8
Stretch (%)	1.65	1.45	1.40	0.98
Tear Index (mN·m^2/g) (4 Ply)	6.2	5.1	6.3	4.5
Zero Span Breaking Length (km)	8.0	7.5	8.2	6.6
Air Resistance (Gurley) (sec/100 mL)	49.4	40.5	79.7	90.4
Sheffield Roughness (SU)	258	277	213	292
Brightness (%)	56.5	49.0	45.3	36.5
Opacity (%)	96.4	97.6	98.1	99.4
Scattering Coefficient (cm^2/g)	560	549	533	467
Length Weighted Fibre Length (mm)	1.23	1.58	1.67	1.68
Bauer McNett R-14 (%)	2.79	1.89	1.90	3.98
Bauer McNett 14/28 (%)	29.55	25.21	28.88	24.25
Bauer McNett 28/48 (%)	24.14	25.70	24.31	20.02
Bauer McNett 48/100 (%)	13.04	14.08	13.14	11.68
Bauer McNett 100/200 (%)	3.31	4.30	3.95	5.05
Bauer McNett P200 (% fines)	26.93	28.58	24.60	35.92

Physical and optical properties for RMP pulps were interpolated to 100mL CSF (Table 5.8, Appendix X). The major decrease in specific refining energy and brightness are the most

significant effects of decay on RMP pulps. While a mill will save energy by refining heavily decayed wood chips, it will also produce a much darker pulp with inferior strength properties.

Changes in pulp properties between the sound and intermediate decay sample were small. This suggests that the mechanical pulping process may tolerate low levels of brown-rot decay. However, when advanced brown-rot decayed wood was mechanically pulped, there were significant impacts. The most significant difference was the decrease in porosity, which could be attributed to the increased fines content. There was also a major gain in length-weighted fibre length, which was substantiated by increases in long fibre fractions determined by Bauer McNett fractionation. Despite this increase in fibre length, the tear, tensile and burst indices decreased. This was in part due to the decrease in individual fibre strength, as measured by zerospan breaking length. The increased fibre length in the mechanical pulp samples altered the formation properties of the sheet, which resulted in lower density and higher scattering coefficient in the advanced decayed sample.

Brightness is an important factor in mechanical pulping. Based on the major loss of brightness observed in the advanced decay sample it is likely that increased bleaching costs would be accrued. However, this may be partially offset by an improved bleaching response. The losses in packing density, strength properties, and brightness negate the potential energy savings from pulping advanced brown-rot decayed wood.

5.3.3 Kraft Pulping

Kraft pulps were first prepared at constant EA and H-factor. Yield, screen rejects and kappa number were determined. These data show the negative effects of kraft pulping decayed wood and are in agreement with previous research (Hatton, 1978a, Hunt 1978a, Hunt, 1978b). Figure 5.5 shows that as decay increases yield decreases and kappa number increases. When pulping sound wood, yield normally decreases when kappa number decreases, since more lignin

has been removed from the pulp. Thus, the increased lignin content found in the decayed wood (Table 5.7) contributes to a higher kappa number. Screen rejects were also greater in decayed samples.

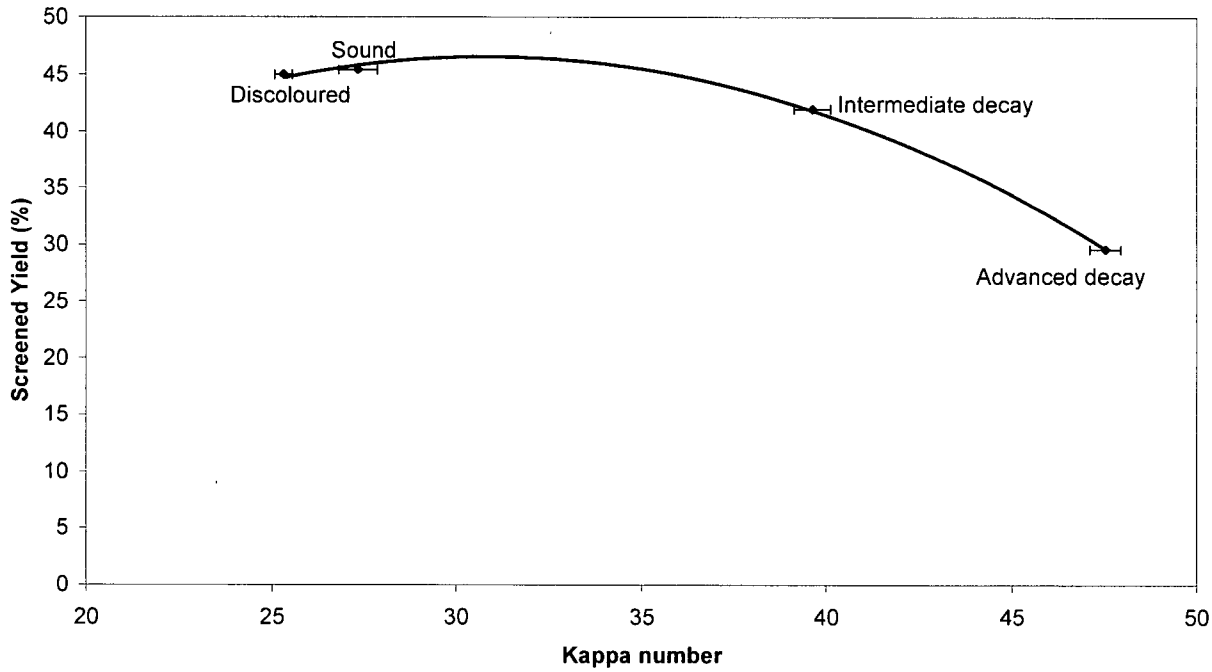

Figure 5.5 Screened Yield vs. the Kappa Number of Pulps Produced at 16% EA and 1290 H-factor. Error bars represent the standard deviation of the kappa number determination (n = 4).

Figure 5.6 shows some of the kraft pulping characteristics of the sound wood. H-factor is a measure of the rate of delignification, with respect to time and temperature applied to the chips in kraft pulping (Sjöström, 1993). As H-factor increases and more lignin is removed, both yield and kappa number decrease. This confirms that the kraft pulping of Lodgepole pine followed expected trends (Kumar *et al.*, 2004).

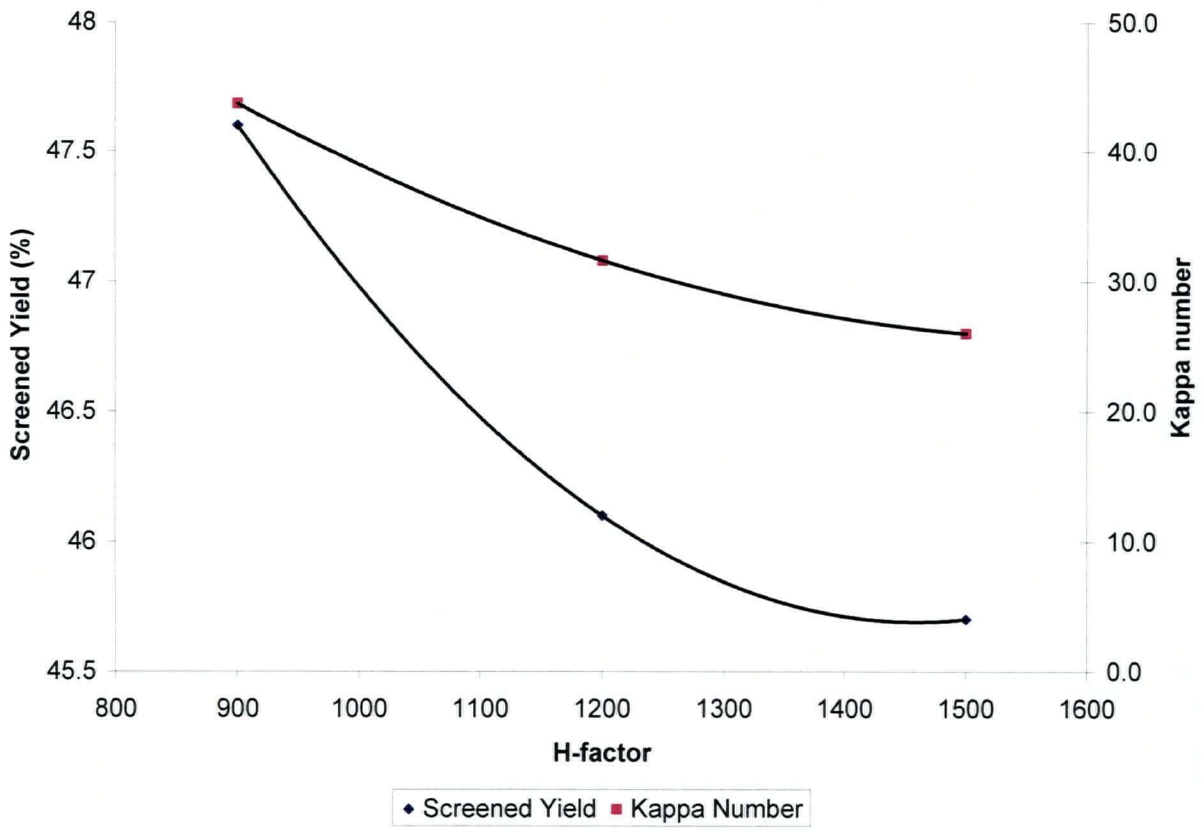

Figure 5.6 Screened Yield and Kappa Number as a Function of H-Factor for Kraft Pulps Produced from Sound Lodgepole Pine Chips (EA = 16%)

The black liquor produced from pulps prepared at constant EA and H-factor was measured for residual effective alkali (REA), black liquor solids and the ratio of organic to inorganic solids (Table 5.9). REA decreased with increased decay, indicating that the decayed wood had increased chemical consumption, despite also having a higher kappa number. Figure 5.7 shows EA consumption as a function of kappa number. Normally with sound wood when EA consumption increases, kappa number decreases. However, with brown-rot decayed wood the increased lignin content and decreased cellulose content results in increased EA consumption and a higher kappa number than corresponding sound wood. When decayed wood is kraft pulped, more chemicals are required to produce less pulp with a higher kappa number. To account for the higher kappa number either a larger loss of yield and increased chemical

consumption are required, or the pulp will have lower brightness or require more bleaching than equivalent pulp produced from sound wood.

Table 5.9 Lodgepole Pine Kraft Pulp and Black Liquor Properties (EA = 16%, H-factor = 1290)

Sample	Unscreened yield (%)	Screen rejects (%)	Kappa number	REA (%)	Black Liquor Solids (%)	Organic/ Inorganic ratio
Sound	45.4	trace	27.3	5.40	13.8	1.55
Discoloured	45.0	trace	25.3	5.64	13.7	1.50
Intermediate decay	42.1	0.1	39.6	3.29	13.7	1.70
Advanced decay	30.7	1.1	47.5	2.63	15.7	1.81

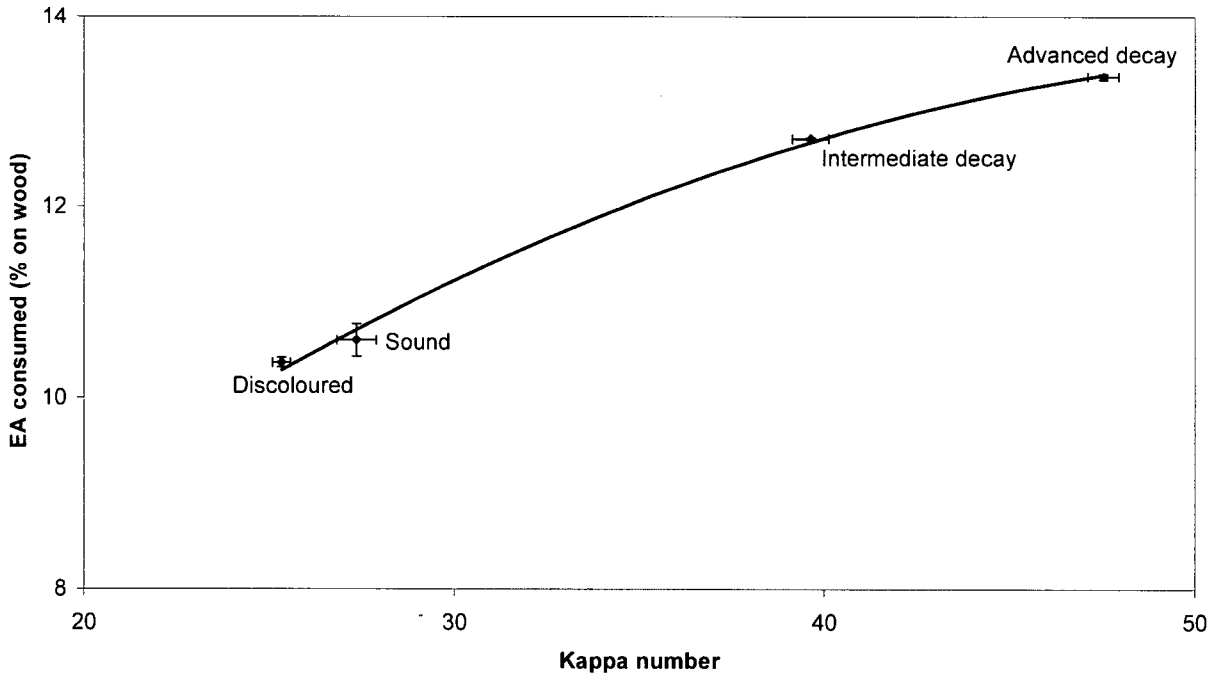

Figure 5.7 Effective Alkali Consumed vs. Kappa Number for Sound, Discoloured, Intermediate and Advanced Decay Samples Pulped to a Constant H-factor (1290) and EA (16%). Error bars represent the standard deviation of EA consumed and kappa number (n = 4).

The increased EA consumption can also be related to the increased buffering capacity of the decayed wood chips. With increased acid groups present in the decayed wood, the EA consumed increases (Figure 5.8). Thus, if incoming wood chips have increased decay content, as measured by buffering capacity, mills can expect an increase in EA consumption. Figure 5.8 also shows that at high buffering capacities, EA consumption levels off, indicating that the greatest loss of EA, relative to buffering capacity, will occur at incipient levels of decay.

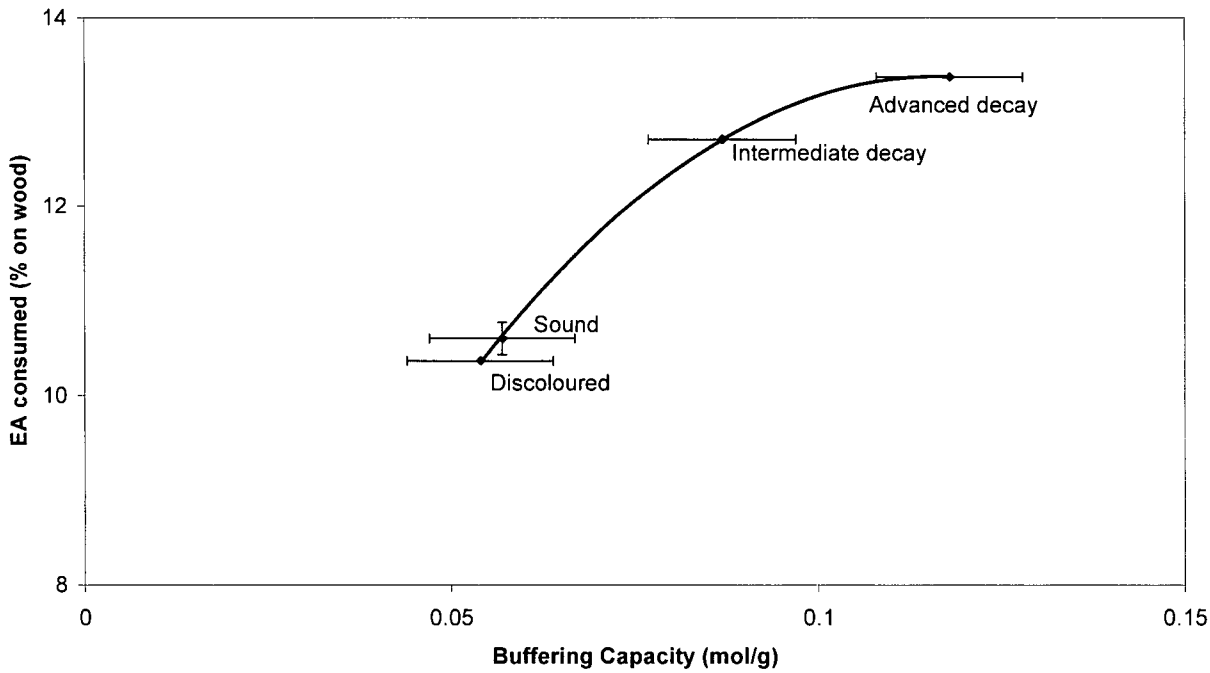

Figure 5.8 Effective Alkali Consumed during the Kraft Pulping of Lodgepole Pine to an H-factor of 1290 vs. Buffering Capacity of the Wood Chips

Pulping decayed wood chips can also have significant impacts on recovery systems. Decayed wood chips consume more alkali than equivalent sound chips, and increase the amount of organic matter in black liquor (Table 5.9). As expected, the increased decay results in higher black liquor solids content (Hunt, 1978). The increase in the ratio of organic to inorganic matter may affect the rate of black liquor evaporation and should be considered by mills when pulping decayed wood.

Each wood chip sample was kraft pulped again with varying EA and H-factor targeting a kappa number of 30. Kappa number is affected by the amount of EA applied to the wood chips, H-factor, which is a combined measure of time and temperature, and wood chip properties (Sjöström, 1993). It is necessary to have pulps of comparable kappa number in order to compare their properties (MacLeod, 1991). The pulping of these wood chips is described in Table 5.10. The sound and discoloured samples were pulped under the same conditions and had similar kappa number and REA, suggesting that the effect of discolouration on kraft pulping is minor. The decayed samples were pulped with higher EA since the REA was very low when pulped at constant H-factor (Table 5.10). For the intermediate decay sample, a lower H-factor was used to compensate for the increased EA; however, for the advanced decay sample the H-factor was increased. Despite the increased EA and H-factor, the advanced decay sample still had a higher than expected kappa due to the impact of decay on the wood chips. Due to limited sample, this was not repeated.

Table 5.10 Kraft Pulping of Lodgepole Pine Samples (Target Kappa = 30)

Sample	EA (%)	H-factor	Kappa number	REA (%)
Sound	16	1290	31.1	5.60
Discoloured	16	1290	28.8	5.46
Intermediate decay	17	1150	31.2	5.23
Advanced decay	17	1350	39.2	2.98

Physical and optical properties for kraft pulps were interpolated to 300mL CSF (Table 5.11, Appendix XI). Decayed wood chips required less energy to reach a freeness of 300mL, as indicated by PFI revolutions (Table 5.11). The decreased fibre length and lower zerospan breaking length (an indication of fibre strength) contributed to lower tear, tensile and burst

indices. The increased fines content contributed to increased roughness and air resistance. However, sheet density was relatively unaffected.

Table 5.11 Kraft Pulp Properties of Lodgepole Pine Interpolated to 300 mL CSF

Property	Sound	Discoloured	Intermediate	Advanced
Calculated PFI Revolutions at 300 mL CSF	14750	15035	12130	7182
Apparent Density (kg/m^3)	706	704.8	707.7	695.5
Burst Index ($kPa \cdot m^2/g$)	11.3	11.2	11.3	9.1
Tensile Index ($N \cdot m/g$)	133	131.4	123.5	97.1
Stretch (%)	3.7	4.1	3.5	3.2
Tear Index ($mN \cdot m^2/g$) (4 Ply)	10.4	9.5	9.4	8.1
Zero Span Breaking Length (km)	15.8	15.1	15.0	14.6
Air Resistance (Gurley) (sec/100 mL)	72	69.3	106.3	105.5
Sheffield Roughness (SU)	67	82.4	75.0	74.7
Opacity (%)	91	90.5	92.0	96.7
Scattering Coefficient (cm^2/g)	145	139.2	161.1	173.3
Length Weighted Fibre Length (mm)	2.07	2.05	2.03	1.74
Coarseness (mg/m)	0.120	0.163	0.141	0.124
Bauer McNett R-14 (%)	33.51	30.03	31.59	22.13
Bauer McNett 14/28 (%)	40.83	39.92	39.57	44.61
Bauer McNett 28/48 (%)	20.89	22.09	18.91	20.99
Bauer McNett 48/100 (%)	5.72	5.85	4.59	5.46
Bauer McNett 100/200 (%)	0.75	1.18	1.25	2.04
Bauer McNett P200 (% fines)	0.00	0.95	4.09	4.76

The length-weighted fibre length and fibre length distribution of the kraft pulps were determined by the FQA and Bauer McNett fractionation (Table 5.11). The kraft fibres decreased in length with extent of decay. This is in agreement with Mischki *et al.* (2005) who found that fibre length decreased with increasing decay in Western hemlock. The Bauer McNett distributions shown for the kraft pulps were determined from the zero-point samples (Table 5.11). The effects of decay were seen most clearly in the long fibre and fines fractions. The R14 fraction decreases with decay, while the R14/28 fraction increases. The R14 fibres have been shortened leaving increased R14/28 and fines fractions.

The losses in pulp properties were overshadowed by the loss of yield and increased chemical consumption. Increased EA consumption due to the use of decayed wood would require mills to increase EA charge, increase H-factor or increase both. Increasing H-factor will slow production and consume more energy. In addition the decrease in packing density and pulp yield would significantly increase a mill's fibre requirements. These data are in agreement with previous research (Hunt, 1978b, Mischki *et al.*, 2005).

5.4 Discussion

The first part of the pulping experiments investigated the effects of inoculum size on TMP. There were only minor changes in the wood chips, likely due to antagonistic interactions between *G. trabeum* and moulds. Since there were only minor changes in the wood chips, there were only minor changes in the resulting pulp properties. The most significant change was in the loss of brightness, which occurred in the control and in the inoculated chips, and was thus attributable to the action of the moulds. This may result in increased bleaching demand. However, DeJong *et al.* (1997) found that mould (*Penicillium simplicissimum*) grown on wood chips for seven days had a negligible effect on brightness both before and after bleaching. The effect of moulds on wood chips stored for a longer period of time on bleaching chemical demand

remains unclear. To more accurately characterize the effects of inoculum size on rate of decay and changes in pulp properties, sterilized wood chips should be used.

Since the magnitude of the difference in pulp properties was small, the advantages of separating decayed wood chips from sound ones would be minimal. A different management strategy would only be worthwhile if significant quantities of decayed wood chips were to be pulped and were separate from the remaining fibre supply. Such a strategy could involve either pulping decayed wood chips in a constant ratio with sound wood chips or pulping sound and decayed wood chips separately. In most cases the best approach would be to follow established wood chip management procedures and to regularly monitor wood chip quality, possibly including the use of caustic solubility and buffering capacity tests.

Although in this experiment storing sound Lodgepole pine chips did not result in a significant reduction in refining energy to reach target freeness, other authors have shown that the effects of storage can be significant (Behrendt *et al.*, 2000, Fischer *et al.*, 1994). Colonization by fungi endemic in wood chip piles can reduce extractives and attack structural polymers, which lowers the amount of energy required to refine wood chips to a given freeness (Fischer *et al.*, 1994). Applying less energy to the wood chips results in the preservation of fibre length, which can improve strength properties. The gains in tensile strength and stretch after storage are consistent with those observed by Fischer *et al.* (1994) who evaluated *O. piliferum*-treated wood chips.

The second part of the pulping experiments investigated the RMP and kraft pulp properties of sound, discoloured, and intermediate and advanced brown-rot decayed wood chips. The wood chips used to prepare the RMP pulps were much more heavily decayed (as indicated by the much higher 1% caustic solubility) than those used to produce the TMP pulp. This showed more clearly the effects of mechanically pulping moderately and heavily brown-rot decayed wood chips. RMP of decayed wood chips required less energy and produced a darker

pulp. The reduction in specific refining energy preserved more of the long fibres; however, the weakness of the decayed fibres resulted in the generation of more fines. The increased fines content contributed to an increased air resistance, which can impact papermaking properties. The weakened fibres also resulted in poorer strength properties, despite the preservation of the long fibre fraction. RMP pulp produced from decayed Lodgepole pine had pulp properties that were inferior to those produced from equivalent sound pine.

The effect of *G. trabeum* on kraft pulping of Lodgepole pine was deleterious (Hunt, 1978a, Procter, 1973). In addition to the negative effects on yield and pulp properties, the black liquor was significantly altered by decay. The increase in black liquor solids may make recovery more difficult, and the change in the ratio of organic to inorganics may change the viscosity of the liquor, resulting in significant impacts on the recovery operation.

In both kraft and mechanical pulping the most significant differences are in the effect of decay on the process. In mechanical pulping decayed wood results in an energy savings and a potential increase in bleaching chemical consumption, while in kraft pulping yield is reduced, and pulping and bleaching chemical consumption is increased. The effects of decay on pulp properties vary because mechanical pulping is better able to preserve long fibre fractions. Despite this, strength properties decreased in advanced brown-rot decay samples in both kraft and mechanical pulps.

Since the impacts of advanced decay on RMP and kraft pulping are so deleterious, brown-rot decayed wood should be avoided where possible. Mills should either avoid advanced decayed wood or manage it a way that minimizes its impact. This can be accomplished either by pulping similarly decayed wood all at once and producing a lower quality product or by adding decayed wood to sound wood in a constant ratio. Either method will avoid the large swings in pulp quality that are possible when the level of decay is not controlled. This highlights the need

for rapid methods to identify decayed wood. Once wood is determined to be decayed, appropriate measures can then be taken to circumvent any deleterious effects that may result.

The final objective of this chapter was to further validate the PLS models of caustic solubility and buffering capacity. Estimates of caustic solubility and buffering capacity showed only minor changes in the samples with varying inoculum size that were thermomechanically pulped. This was consistent with the minor changes observed in pulp properties. Estimates of caustic solubility and buffering capacity increased significantly in the "intermediate" and "advanced" decayed samples that were refiner mechanically and kraft pulped. This closely paralleled kraft pulp quality. The RMP quality was not significantly compromised in the "intermediate" decay sample, which suggests that while the models are detecting changes due to decay, these changes do not result in poorer RMP pulp quality. Thus, mechanical pulping has a higher tolerance for brown-rot decayed wood than kraft pulping. Furthermore, the changes in PLS-predicted caustic solubility and buffering capacity may not correspond directly with mechanical pulp properties. Only at the highest predicted caustic solubility and buffering capacity would RMP pulps be of poorer quality.

The measured and predicted caustic solubility and buffering capacity of Lodgepole pine chip samples can be related to subsequent pulping and pulp properties. However, with only four data points obtained from one wood species, decayed by one fungal species, these correlations are of a limited scope. Many more samples would have to be analyzed to make quantitative models of pulp properties from spectral data. However, of significance is the qualitative relationship between data collected from wood chips and the subsequent pulp properties. Since caustic solubility and buffering were so highly correlated with each other, there was little variation between pulp property correlations with them. The caustic solubility of the wood chips used to make kraft pulps had strong ($r^2 > 0.8$) correlations with tensile index, stretch, air resistance, opacity, scattering coefficient, length weighted fibre length and pulp yield. The

caustic solubility of the wood chips used to make RMP pulp had strong correlations with stretch, air resistance, brightness, opacity and scattering coefficient. In general, correlations between caustic solubility and kraft pulp properties were greater than those with RMP pulp properties.

There are undoubtedly strong quantitative relationships between caustic solubility and various pulp properties. However, for these relationships to be exploited and used to predict pulp properties from the spectroscopy of wood, many variables have to be considered. Changes at any stage of the process from wood chip storage to brownstock washing would affect these predictions. These correlations will not be of direct use to mills without considerable investments in spectrometers, model development and process control. The qualitative and quantitative nature of these effects depends too much upon other factors. Future work aimed at implementing spectroscopic techniques in pulp mills to address process control problems should thus focus on accurately predicting wood or fibre properties. Since the relationship between fibre properties, process conditions and pulp properties is somewhat mill-specific, this relationship will need to be determined for each mill. By using spectroscopy to predict only wood properties, the developed methods will be generally applicable.

CHAPTER 6

Conclusions and Future Work

6.1 Conclusions

The work described in this thesis was aimed at providing solutions to the problem of fungal decay in pulp and paper fibre supplies. Decayed wood chips can result in significant economic penalties for pulp mills, direct wood substance losses, and increased fines production when chipped (Hunt, 1978). When kraft pulped, brown-rot decayed wood will result in lower yields, increased chemical consumption, and poorer strength and optical properties of the paper, relative to sound wood (Hunt, 1978b, Hunt and Hatton, 1979, Procter, 1973). When mechanically pulped, brown-rot decayed wood can reduce specific refiner energy consumption, but requires increased amounts of bleaching chemicals and has poorer strength properties (Whitty *et al.*, 1991). The work described in this thesis confirmed and expanded upon these findings and identified other issues pertinent to the management of decayed wood.

In order to address these issues, the first objective of this research was to develop an improved method of estimating extent of decay. The hand-sorting method of decay detection was evaluated and shown to be an unreliable indicator of decay. Previous research had established the 1% caustic solubility test as a pulp-and-paper-specific indicator of decay (PAPTAC, 2000, Procter and Chow, 1973). However, this method is time-consuming and laborious, and not amenable to automation. The present work developed and evaluated rapid methods of estimating the extent of decay in wood chips that may be applied in an industrial setting. As part of this work, several new methods of estimating the extent of decay in wood chips were developed. The present research showed that extent of decay can be estimated from both FTIR and NIR spectra, using 1% caustic solubility, buffering capacity, and basic wood density as decay indicators. These models were able to predict traditional indicators of decay (1% caustic solubility,

buffering capacity, and basic wood density) with much greater speed and ease than the wet methods.

One limitation of the spectroscopic models of extent of decay is that currently there is no perfect standard for estimating decay, and thus the standard methods upon which the PLS models were based contain error. As such, the precision of the PLS models was hindered by the unreliability of the traditional laboratory methods (1% caustic solubility and buffering capacity). Nevertheless, the precision was high enough for the models to be of value to researchers and industry, as suggested by the pulping data presented in this thesis. To better characterize the nature and validity of the PLS models, a number of different validations were preformed. Samples not included in the calibration data set, field samples, and mixtures were all successfully modeled. Moreover, separate wood species, fungal species, and field sample models were developed to understand the effects of natural variations on the models. In addition, the effects of oven drying and autoclaving samples on the PLS predictions were determined.

Overall, the developed models of extent of decay were shown to be robust and reliable. They are well suited for use in mills to estimate extent of decay and should be able to handle most of the variation observed in field samples. In their present state, the models could be used to monitor extent of decay from spectra obtained in a mill laboratory (the models are not currently able to handle the variation from spectra obtained over chips). This could be used to estimate the extent of decay of wood chips entering the wood yard, wood chips in storage, and wood chips obtained prior to entering digesters or refiners. By identifying decayed chips when they enter the wood yard, mills could then reject the shipment of chips, downgrade the price, or segregate them from sound chips. Ultimately, this could save mills money by rejecting fibre that would cause significant problems to their pulping processes, paying less for fibre of lower value, or from improved pulp uniformity. Losses due to wood chip storage could be determined using the developed models, which may suggest improved chip storage methods. Monitoring the extent

of decay in wood chip samples entering a digester or refiner, in combination with other data, could help to improve process control and lead to improved product uniformity, and reduced energy and chemical consumption.

The second objective of the work presented in this thesis was to determine the changes in decayed wood that underpin the successful modeling from FTIR spectra (the underlying chemistry behind the NIR models were not considered in this thesis). Through chemical and spectral analyses of sound and brown-rot decayed wood, changes in the acid substituents of lignin and in acetyl groups bound to polysaccharides were found to contribute to the changes in the FTIR spectra. These analyses also showed that the decay type was an important moderator of the predictive models. Changes in the concentration of acetyl groups and lignin in white-rot decayed wood were much smaller than in brown-rot decayed wood. Thus, the FTIR spectrum of the white-rot decayed wood was more similar to the spectra of sound wood than the brown-rot spectra. The spectroscopic models were therefore better able to predict brown-rot, than white-rot decay. Since brown-rot decay has a significantly greater impact on pulp properties (Hunt, 1978b), this actually represents a strength of the present method. The extent of white-rot decay is best determined by existing microscopic methods (PAPTAC, 2002).

The ability to determine changes in wood chemistry, such as loss of acetyl groups and modification of lignin, suggest a number of potential applications. For example, changes in wood chemistry due to the action of fungal enzymes could be monitored *in vivo* by FTIR spectroscopy. Since FTIR can be non-destructive, kinetics experiments could be conducted to determine rates of substrate modification. Also, chemical treatment of wood with preservatives or stains could potentially be measured and controlled by FTIR spectroscopy.

Finally, the work sought to explore the relationship between these indicators of decay and mechanical and kraft pulping. The first pulping experiment investigated the effect of inoculum size on rate of decay in stored wood chips. It was found that although inoculum size was a

statistically significant factor affecting rate of decay, it was not the major determinant of decay. With low modern storage times (McDonald and Twaddle, 2000), this suggests that decay in storage is much less significant than decay which already exists in incoming chips. PLS-predictions of caustic solubility and buffering capacity accurately determined that there was very little decay in these samples. The second pulping experiment investigated mechanical and chemical pulps prepared from sound, discoloured, and intermediate and advanced decayed wood chips to investigate the effects of decay at various levels. RMP pulp produced from advanced decayed wood had significantly reduced strength and optical properties, including a 20-point ISO drop in brightness, and an increase in long fibres as well as fines. Kraft pulps prepared from advanced decayed wood were produced with much lower yields, and greater chemical consumption. The physical and optical properties and long fibre fractions of kraft pulps were significantly reduced, while fines content increased. PLS-predictions of caustic solubility and buffering capacity were significantly correlated with resulting pulp properties. Thus the PLS models are able to capture the variations in the wood that correspond with changing pulp properties due to brown-rot decay.

With an improved understanding of the effects of pulping decayed wood, mills will be better able to make more prudent fibre management decisions. For example, if high-grade pulp is being produced, a mill may wish to exclude decayed chips from their furnish. Conversely, if low-grade pulp is being produced with better than required properties, decayed chips could be added to the chip furnish. To take advantage of potential energy savings and manage fibre properties when mechanically pulping decayed wood, mills may wish to separate decayed wood, refine it separately, and then add it in a controlled ratio to pulps produced from sound wood.

The work presented in this thesis also has many practical implications; PLS models of decay indicators provide industry with new tools to rapidly identify decayed wood. In combination with the evidence presented against the hand-sorting method of decay detection,

this will help to provide mills with reliable data on extent of decay in their chip furnishes. By enhancing our ability to identify decayed wood and quantify the extent of decay, mills will be able to make improved fibre management decisions. The effects of storing and mechanical and kraft pulping decayed wood shown in this thesis provide mills with an understanding of the effects of decay on their operations. Improved use of decayed wood chips will result in reduced fibre losses and improved pulp uniformity.

6.2 Future Directions

Future work derived from the research presented in this thesis should focus on three principal areas: broadening the understanding of the fundament effects of decay on wood and pulp spectral properties, improved multivariate statistical modeling of wood quality traits, and applying the models presented in this thesis to industrial settings.

Fungal decay of wood should be investigated to improve our understanding of its effects on the FTIR and NIR spectroscopic properties of wood. Specifically, there exist significant variations in spectra that occur as a function of wood species (Moore and Owen, 2001). The work presented in this thesis noted variations that occurred within the predictive regions, but did not attempt to categorize the variations between wood species across the entire spectrum. A systematic examination of these variations may facilitate the development of improved single-species models and provide a better explanation for why certain species, such as Western redcedar, were poorly estimated by the PLS models. There are also significant spectral variations in wood decayed by different fungal species. Although six decay fungi were used to prepare the calibration dataset, only one white-rot fungus and one brown-rot fungus were examined in detail. Further work should examine more species to better understand spectral variation attributable to fungal species, within white-, brown- and soft-rot groups. This may allow for model

development of extent of decay in white- and soft- rot fungi, which could be of use in bio-pulping applications.

A number of options exist to improve the developed PLS models. Working with existing data, a more comprehensive examination of the factors used to estimate extent of decay should be conducted to improve our understanding of what each factor represents. With this more complete understanding, improved models may be developed. A more complete investigation of Orthogonal Signal Correction may also yield improved models. One of the greatest limitations of the present research was the absence of a precise method of estimating extent of decay. Improving the precision of caustic solubility or buffering capacity would be beneficial, as would finding an alternative method with a high specificity for extent of decay. One such method might involve directly correlating spectral data of wood to subsequent pulp properties. Since the research described in this thesis was begun, commercial NIR spectrometers and chemometrics software have been significantly improved. Using these new tools will greatly facilitate the rapid collection of high-quality spectra and their subsequent analysis.

Further research should also focus on integrating the PLS models into a mill environment. Spectra obtained in this thesis were obtained under laboratory conditions. Therefore, it would be salient to determine the effects of mill conditions on spectral properties and their subsequent impacts on PLS predictions of extent of decay. Specifically, research should focus on developing a system that allows spectra to be reproducibly obtained from wood chips on a conveyer. This would enable continuous monitoring and feed-forward process control, which could be used to optimize refiner or digester conditions. To gain a more complete understanding of the effects of decay, a thorough analysis of its effects on black liquor recovery and on pulp bleaching would also be beneficial.

Future research must also look at other applications of this technology. Within the mill, spectroscopic methods have the potential to be used to monitor pulp, liquor and effluent

properties. Such methods could be used to automate many tests, reducing labour costs, and provide mills with the opportunity for better process control, which could lead to a more uniform product, lower chemical costs and improved environmental compliance. Outside the mill, spectroscopic methods could be used to estimate wood quality in plantations. The spectroscopic methods developed for use on wood chips can be adapted to work on increment cores. However, of greater interest is the use of portable NIR spectrometers (such as the one illustrated by So *et al.*, 2004) to collect spectra at any point in the field. It is in this capacity that the methods will prove most cost effective. While rapid DNA-based techniques may be able to determine the genetic components that lead to altered fibre traits, spectroscopy-based techniques will be able to determine the trees that actually grow these fibres.

In summary, future work should aim to advance the PLS modeling of extent of decay from FTIR and NIR spectra. This will be achieved by improving our understanding of the fundamentals underlying the models, making better models, and advancing their application to industrial settings.

REFERENCES

Abbott, T.P., Palmer, D.M., Gordon, S.H., Bagby, M.O., 1988. "Solid State Analysis of Plant Polymers by FTIR." *Journal of Wood Chemistry and Technology*. 8(1): 1-28.

Adair, S., Kim, S.H., Breuil, C., 2002. "A molecular approach for early monitoring of decay basidiomycetes in wood chips." *FEMS Microbiology Letters*. 211: 117-122.

Agarwal, U.P., Atalla, R., 1995. "FT Raman Spectroscopy: What it is and what it can do for research on lignocellulosic materials." *Int. Symp. Wood Pulping Chem., 8th*. 67-72.

Agarwal, U.P., Ralph, S.A., 1997. "FT-Raman Spectroscopy of Wood: Identifying Contributions of Lignin and Carbohydrate Polymers in the Spectrum of Black Spruce (*Picea mariana*)." *Applied Spectroscopy*. 51(11): 1648-1655.

Agarwal, U.P., Weinstock, I.A., Atalla, R.H., 2003. "FT-Raman spectroscopy of direct measurement of lignin concentrations in kraft pulps." *Tappi Journal*. 2(1): 22-26.

Akhtar, M., Scott, G.M., Swaney, R.E., Shipley, D.F., 2000. "Biomechanical pulping: A mill-scale evaluation." *Resources, Conservation and Recycling*. 28(3): 241-252.

Alen, R., Niemela, K., Sjöström, E., 1984. "Gas-liquid chromatographic separation of hydroxyl monocarboxylic acids and dicarboxylic acids on a fused-silica capillary column." *Journal of Chromatography*. 301: 273-276.

Ali, M., Emsley, A., Herman, H, Heywood, R., 2001. "Spectroscopic studies of the aging of cellulose paper." *Polymer*. 42: 2893-2900.

Allen, E., Morrison, D., Wallis, G., 1996. Common Tree Diseases of British Columbia. Canadian Forest Service, Victoria.

Altaner, C., Saake, B., Puls, J., 2003. "Specificity of an *Aspergillus niger* esterase deacetylating cellulose acetate." *Cellulose*. 10(1): 85-95.

Anagnost, S.E., Smith, W.B., 1997. "Hygroscopicity of Decayed Wood: Implications for Weight Loss Determinations." *Wood and Fiber Science*. 29(3): 299-305.

Anderson, T.H., Weaver, F.W., Owen, N.L., 1991. "Anomalies in diffuse reflectance infrared spectra of wood and wood polymers." *Journal of Molecular Structure*. 249: 257-275.

ASTM, 1998. "Standard Method of Accelerated Laboratory Test of Natural Decay Resistance of Wood." Standard D 2017-94. Annual Book of ASTM Standards, 4.10. American Society of Testing and Materials, Philadelphia, PA.

Atalla, R.H., 1987. "Raman Spectroscopy and the Raman Microprobe: Valuable New Tools for Characterizing Wood and Wood-Pulp Fibres." *Journal of Wood Chemistry and Technology*. 7(1): 115-131.

Axrup, L., Markides, K., Nilsson, T. 2000. "Using Miniature Diode Array NIR Spectrometers for Analysing Wood Chips and Bark Samples in Motion." *J. Chemometrics*. 14: 561-572.

Backa, S., Brolin, A., Nilsson, T., 2001. "Characterisation of Fungal Degraded Birch Wood by FTIR and Py-GC." *Holzforschung*. 55(3): 225-232.

Baeza, J., Freer, J., 2001. "Chemical Characterization of Wood and Its Components." In Hon, D.N.-S., Shiraishi, N., "Wood and Cellulosic Chemistry, 2nd Edition, Revised and Expanded." Marcel Dekker, New York.

Baldwin, R.C., Streisel, R.C., 1985. "Detection of fungal degradation at low weight loss by differential scanning calorimetry." *Wood and Fiber Science*. 17(3): 315-326.

Barnes, E.T., 1979. "Chip Screening." In Hatton, J.V. "Chip Quality Monograph." Joint Textbook Committee of the Paper Industry, Montréal.

Baulsir, C.F., Tague, T.J., 2000. "Introduction to Diffuse Reflectance Infrared Fourier Transform Spectroscopy." Technical Note. Spectra-Tech, Shelton, CT.

Basham, J.T., 1984. "Degradation and Loss of Wood Fibre in Spruce Budworm-killed Timber, and Effects on Utilization." *Forestry Chronicle*. 60(1):10-14.

BC Ministry of Forests, 2003. Mountain Pine Beetle in B.C. BC Ministry of Forests, Victoria.

Beall, F.C., Merrill, W., Baldwin, R.C., Wang, J.-H., 1976. "Thermogravimetric Evaluation of Fungal Degradation of Wood." *Wood & Fiber*. 8(3): 159-167.

Becker, E.S., Briggs, S.R., 1983. "A Comparison of CTMP and Kraft Pulping of Stained and Decayed Aspen." *Proc. TAPPI Pulp. Conf.*, Houston, Texas. 261-268.

Beebe, K.R., Kowalski, B.R., 1987. "An Introduction to Multivariate Calibration and Analysis." *Anal. Chem.* 59(17): 1007A-1017A.

Beebe, K.R., Pell, R.J., Seasholtz, M.B., 1998. Chemometrics A Practical Guide. John Wiley & Sons, New York.

Bennett, S., 1997. "Future Woodyard to Focus on Seamless Quality Operation." *Pulp & Paper*. 71(7): 77-78, 81.

Behrendt, C.J., Blanchette, R.A. Akhtar, M., Enebak, S., Iverson, S., Williams, D., 2000. "Biomechanical pulping with *Phlebiopsis gigantean* reduced energy consumption and increased paper strength." *Tappi*. 83(9): 65.

Bharati, M.H., MacGregor, J.F., Champagne, M., 2004. "Using near-infrared multivariate image regression to predict pulp properties." *Tappi Journal*. 3(5): 8-13.

Bioscience, 2003. "The Micro-COD Test Method accu-Test Standard Range." Bioscience Inc., Bethlehem, PA.

Birkett, M.D., Gambino, M.J.T., 1989. "Estimation of Pulp Kappa Number with Near-Infrared Spectroscopy." *Tappi*. 72(9): 193-197.

Bjurman, J., 1999. "Fungal and Microbial Activity in External Wooden Panels as Determined by Finish, Exposure and Construction Techniques." *International Biodeterioration and Biodegradation.* 43: 1-5.

Blanchette, 1980. "Wood Decomposition by *Phellinus* (*Fomes*) *pini*: A Scanning Electron Microscopy Study." *Canadian Journal of Botany*. 58(13): 1496-1503.

Blanchette, R.A. 1995. "Degradation of the lignocellulose complex in wood." *Canadian Journal of Botany*. 73(Suppl. 1): S999-S1010.

Bonnarme, P., Jeffries, T.W., 1990. "Mn(II) Regulation of Lignin Peroxidases and Manganese-Dependent Peroxidases from Lignin-Degrading White Rot Fungi." *Applied and Environmental Microbiology*. 56: 210-217.

Boyle, C.D., Kropp, B.R., 1992. "Development and comparison of methods for measuring growth of filamentous fungi on wood." *Canadian Journal of Microbiology*. 38(10): 1053-1060.

Bowyer, J.L., Shmulsky, R., Haygreen, J.G., 2003. Forest Products and Wood Science. Iowa State Press, Ames, Iowa.

Bruce, A., 1998. "Biotechnology in the Study of Brown- and White-Rot Decay." In Bruce, A., Palfreyman, J.W. "Forest Products Biotechnology." Taylor and Francis, Bristol, PA.

Brush, T.S., Farrell, R.L., Ho, C., 1994. "Biodegradation of Wood Extractives from Southern Yellow Pine (*Pinus*) by *Ophiostoma piliferum*." *Tappi*. 77(1): 155-159.

Bucur, V., Garros, S., Navarrete, A. de Troya, M.T., Guyonnet, R., 1997. "Kinetics of wood degradation by fungi with x-ray microdensitometric technique." *Wood Science and Technology*. 31: 383-389.

Cao, B., Tschirner, U., Ramaswamy, S., Webb, A., 1997. "Rapid Modified Gas-Chromatographic Method for Carbohydrate Analysis of Wood Pulps." *Tappi*. 80(9): 193-197.

Champagne, M., Meglan, B., Wold, S., Kettaneh-Wold, N., 2001. "The use of orthogonal signal correction to improve NIR readings of pulp fibre properties." *Pulp & Paper Canada*. 102(4): T99-T101.

Chong, T.K., Jones, N., 1982. "Fast Growing Hardwood Plantations on Logged-Over Forest Sites in Sabah." *Malay Forester*. 45(4): 558-575.

Christie, R.D., 1979. "The Use of Decayed Wood in Pulping Processes." In Hatton, J.V. "Chip Quality Monograph." Joint Textbook Committee of the Paper Industry, Montréal.

Clausen, C.A., 1997. "Immunological Detection of Wood Decay Fungi – An overview of Techniques developed from 1986 to the Present." *International Biodeterioration and Biodegradation*. 39(2/3): 133-143.

Corson, S.R., 1996. "Development of TMP Fibre and Pulp Quality." *Appita*. 49(6): 309-312, 324.

Costa e Silva, J., Nielsen, B.H., Rodrigues, J., Pereira, H., Wellendorf, H., 1999. "Rapid Determination of the Lignin Content in Sitka Spruce (*Picea sitchensis* (Bong.) Carr.) Wood by Fourier Transform Infrared Spectroscopy." *Holzforschung*. 53(6): 597-602.

Côté, W. 1976. "Wood Ultrastructure in Relation to Chemical Composition." In Loewus, F.A. and Runeckles, V.C., "Recent Advances in Phytochemistry: Volume 11, The Structure, Biosynthesis, and Degradation of Wood." Plenum Press, New York.

Creed, I.F., Webster, K.L., Morrison, D.L., 2004. "A comparison of techniques for measuring density and concentrations of carbon and nitrogen in coarse woody debris at different stages of decay." *Can. J. For. Res.* 34: 744-753.

Curling, S.F., Clausen, C.A., Winandy, J.E., 2002. "Relationships between Mechanical Properties, Weight Loss and Chemical Composition of Wood During Incipient Brown-Rot Decay." *Forest Products Journal*. 52(7/8): 34-39.

Daniel, G., Nilsson, T., 1998. "Developments in the Study of Soft Rot and Bacterial Decay." In Bruce, A., Palfreyman, J.W. "Forest Products Biotechnology." Taylor & Francis, Bristol, PA.

Dass, S.B., Dosoretz, C.G., Reddy, C.A., Grethlein, H.E., 1995. "Extracellular proteases produced by the wood-decaying fungus *Phanerochaete chrysosporium* under ligninolytic and non-ligninolytic conditions." *Archives of Microbiology*. 163(4): 254-258.

Davis, M.F., Schroeder, H.A., Maciel, G.E., 1994. "Solid-State ^{13}C Nuclear Magnetic Resonance Studies of Wood Decay." *Holzforschung*. 48(4): 301-307.

DeJong, E., Chandra, R.P., Saddler, J.N., 1997. "Effects of Fungal Treatment on the Brightness and Strength Properties of a Mechanical Pulp from Douglas Fir." *Bioresource Technology*. 61(1): 61-68.

DeJong, E., Wong, K.K.Y., Saddler, J.N., 1997a. "The Mechanism of Xylanase Prebleaching of Kraft Pulp: An Examination Using Model Pulps Prepared by Depositing Lignin and Xylan on Cellulose Fibers." *Holzforschung*. 51(1): 19-26.

Eriksson O.E., Winka K., 1998. "Families and higher taxa of Ascomycota." *Myconet* 1(2): 17-24.

Eklund, E., Schneitz, C., Soila, R., 1973. "Effect of Storage Time on Wood Losses Caused by Various Fungi Isolated from Outside Stored Wood Chips." *Paperi Puu*. 55(10): 751-759.

Eslyn, W.E., 1979. "Utility Pole Decay." *Wood Sci. Technol.* 13: 117-126.

Espejo, E., Agosin, E., 1991. "Production and Degradation of Oxalic Acid by Brown Rot Fungi." *Applied and Environmental Microbiology*. 57: 1980-1986.

Evans, R., Kibblewhite, R.P., Lausberg, M., 1999. "Relationships between wood and pulp properties of twenty-five 13 year old radiate pine trees." *Appita*. 52(2): 132-138.

Faix, O, 1991. "Classification of Lignins from Different Botanical Origin by FTIR Spectroscopy." *Holzforschung*. 45(suppl.): 21-27.

FAO, 2001. "Global Forest Resources Assessment 2000." FAO Forestry Paper 140, Rome.

Farrell, R.L., Brush, T.S., Fritz, A.R., Blanchette, R.A., Iverson, S., 1994. "Cartapip ®: A Biological Product for Control of Pitch and Resin Acid Problems in Pulp Mills." *1994 Biological Sciences Symposium: Proceedings*. 85-88.

Favis, B., Goring, D. 1983. "High Temperature Leaching of Lignin form Unbleached Kraft Pulp Fibers." *J. Wood Chem. & Technol.* 3(1): 1-7.

Feist, W.C., Eslyn, W.E., Springer, E.L., Hajny, G.J., 1971. "Determining Loss of Wood Substance After Fungal Attack." *Tappi*. 54(8): 1271-1273.

Feist, W.C., Hajny, G.J., Springer, E.L., 1973. "Effect of Storing Green Wood Chips at Elevated Temperatures." *Tappi*. 56(8): 91-95.

Feng, Z., Alen, R., Louhelainen, J., 2001. "Characterisation of black liquors from soda-AQ pulping of wheat straw." *Appita*. 54(2): 234-238, 244.

Fernandez, M.P., 2000. "The identification and natural clonal variation of important wood extractives in *Populus tremuloides*." M.Sc. Thesis. University of British Columbia. Faculty of Forestry.

Fernandez, M.P, Watson, P.A, Breuil, C., 2001. "Gas Chromatography-Mass Spectrometry Method for the Simultaneous Determination of Wood Extractive Compounds in Quaking Aspen." *Journal of Chromatography A*. 922(1/2): 225-233.

Ferraz, A., Baeza, J., Rodriguez, J., Freer, J., 2000. "Estimating the chemical composition of biodegraded pine and eucalyptus wood by DRIFT spectroscopy and multivariate analysis." *Bioresource Technology*. 74: 201-212.

Ferraz, A., Mendonca, R., Guerra, A., Ruiz, J., Rodriguez, J., Baeza, J., Freer, J., 2004. "Near-Infrared Spectra and Chemical Characteristics of *Pinus taeda* (Loblolly Pine) Wood Chips Biotreated by the White-Rot Fungus *Ceriporiopsis subvermispora*." *Journal of Wood Chemistry and Technology*. 24(2): 99-113.

Fischer, K., Akhtar, M., Blanchette, R.A., Burnes, T.A., Messner, K., Kirk, T.K., 1994. "Reduction of Resin Content in Wood Chips during Experimental Biological Pulping Processes." *Holzforschung*. 48(4): 285-290.

Fourty, T., Baret, F., Jacquemound, S., Schmuck, G., Verdebout, J., 1996. "Leaf Optical Properties with Explicit Description of its Biochemical Composition: Direct and Inverse Problems." *Remote Sensing and Environment*. 56: 104-117.

Fuhr, B.J., Henry, D., Leary, G., Smith, G., 1998. "Seasonal variations at a mechanical newsprint mill." *Pulp & Paper Canada*. 99(2): T61-65.

Fujita, M., Harada, H., 2001. "Ultrastructure and Formation of Wood Cell Wall." In Hon, D.N.-S., Shiraishi, N., "Wood and Cellulosic Chemistry, 2nd Edition, Revised and Expanded." Marcel Dekker, New York.

Fuller, W.S., 1985. "Chip pile storage – a review of practices to avoid deterioration and economic losses. *Tappi*. 68(8): 48-52.

Gao, Y., Chen, T., Breuil, C., 1993. "Ergosterol – A Measure of Fungal Growth in Wood for Staining and Pitch Control Fungi." *Biotechnology Techniques*. 7(9): 621-626.

Geladi, P., Kowalski, B.R., 1986. "Partial Least-Squares Regression: A Tutorial." *Analytica Chimica Acta*. 185: 1-17.

Gibson, D.G., Krahmer, R.L., DeGroot, R.C., 1985. "Early Detection of Brown Rot Decay in Douglas-Fir and Southern Yellow Pine by Infrared Spectroscopy." *Wood and Fiber Science*. 17(4): 522-528.

Gonçalves, A.R., Esposito, E., Benar, P., 1998. "Evaluation of *Panus tigrinus* in the delignification of sugarcane bagasse by FTIR-PCA and pulp properties." *Journal of Biotechnology*. 66: 177-185.

Greaves, H., 1973. "Outside storage of tropical hardwood chips (III) Microbial Ecology of Chip Piles After Two and Four Months Storage." *Appita*. 27(1): 25-30.

Green, F., Larsen, M.J., Winandy, J.E., Highley, T.L., 1991. "Role of oxalic acid in incipient brown-rot decay." *Materials und Organismen*. 26: 191-211.

Gureyev, T.E., Evans, R., 1999. "New Method for rapid measurement of vessel-free density in hardwoods." *Appita*. 52(3): 226-230.

Gustavsson, C.A.-S., Al-Dajani, W.W., 2000. "The influence of cooking conditions on the degradation of hexenuronic acid, xylan, glucomannans and cellulose during kraft pulping of softwood." *Nordic Pulp and Paper Research Journal*. 15(2): 160-166.

Hajny, G.J., 1966. "Outside Storage of Pulpwood Chips A Review and Bibliography." *Tappi*. 49(10): 97A-105A.

Halttunen, M., Vyörykkä, J., Hortling, B., Tamminen, T., Batchelder, D., Zimmermann, A., Vuorinen, T., 2001. "Study of Residual Lignin in Pulp by UV Resonance Raman Spectroscopy." *Holzforschung*. 55(6): 631-638.

Hammel, K.E., Kapich, A.N., Jensen, K.A. Jr., Ryan, Z.C., 2002. "Reactive oxygen species as agents of wood decay by fungi." *Enzyme and Microbial Technology*. 30: 445-453.

Harris, D.C., 1995. Quantitative Chemical Analysis 4th Ed. W.H. Freeman and Co., New York.

Harris, G., Karnis, A., 1988. "A rapid method for characterizing decay in wood chips." *Pulp & Paper Canada*. 89(4): T137-T144.

Hartler, N., 1996. "Achievement and significance of optimal chip quality." *Tappi*. 79(2): 259-264.

Hatton, J.V., 1970. "Precise Studies on the Effect of Outside Chip Storage on Fiber Yield: White Spruce and Lodgepole Pine." *Tappi*. 53(4): 627-638.

Hatton, J.V., 1975. "WFPL chip quality analytical procedure: Effect of chipper, wood species and season on production of pin chips and fines." *Pulp & Paper Canada*. 76(8): 64-70.

Hatton, J.V., 1977. "Quantitative evaluation of pulpwood chip quality." *Tappi*. 60(4): 97-100.

Hatton, J.V., 1978. "Debarking wood losses and chip quality of deadwood." *Tappi*. 61(12): 43-46.

Hatton, J.V., 1978a. "Kraft pulping efficiency: The ratio of screened-pulp yield to effective alkali consumed." *Tappi*. 61(6): 51-54.

Hatton, J.V., 1985. "Kraft pulping in Canada: A survey of wood usage, and chip preparation, handling and quality evaluation." *Pulp & Paper Canada*. 86(10): T289-T297.

Hatton, J.V., 1987. "Debarking of frozen wood." *Tappi*. 70(2): 61-66.

Hatton, J.V., Hunt, K., 1972. "Effect of Prolonged Outside Chip Storage on Yield and Quality of Kraft Pulps From *Picea glauca* and *Pinus contorta* Chips." *Tappi*. 55(1):122-126.

Hatton, J.V., Johal, S.S., 1989. "Chemithermomechanical pulps from hardwood/softwood chip mixtures." *Pulp and Paper Canada*. 90(3): 90-98.

Hatton, J.V., Smith, R.S., Rogers, I.H., 1969. "Ideal chip pile in B.C. Interior: long, low, narrow and pine." *Canadian Pulp and Paper Industry*. 22(12): 32-33.

Hauksson, J.B., Bergqvist, G., Bergsten, U., Sjöström, M., Edlund, U., 2001. "Prediction of basic wood properties for Norway spruce. Interpretation of Near Infrared Spectroscopy data using partial least squares regression." *Wood Science and Technology*. 35: 475-485.

Hegarty, B., Steinfurth, A., Liese, W., Schmidt, O., 1987. "Comparative Investigations on Wood Decay and Cellulolytic and Xylanolytic Activity of Some Basidiomycete Fungi." *Holzforschung*. 41(5): 265-269.

Henningsson, B., 1967. "Microbial decomposition of unpeeled birch and aspen pulpwood during storage." *Studia Forestalia Suecica*. Nr. 54.

Highley, T.L., 1973. "Influence of Carbon Source on Cellulase Activity of White-rot and Brown-rot Fungi" *Wood and Fiber*. 5(1): 50-58.

Highley, T.L., Murmanis, L., Palmer, J.G., 1985. "Micromorphology of Degradation in Western Hemlock and Sweetgum by the Brown Rot Fungus *Poria placenta*." *Holzforschung*. 39(2): 73-78.

Highley, T.L., Dashek, W.V., 1998. "Biotechnology in the Study of Brown- and White-Rot Decay." In Bruce, A., Palfreyman, J.W. "Forest Products Biotechnology." Taylor & Francis, Bristol, PA.

Hoadley, R.B., 1990. Identifying Wood: Accurate Results with Simple Tools. Tauton Press, Newtown, CT.

Hocking, M.B., 1998. Handbook of Chemical Technology and Pollution Control. Academic Press, Toronto.

Hoffmeyer, P., Pedersen, J.G., 1995. "Evaluation of density and strength of Norway spruce by near infrared reflectance spectroscopy." *Holz als Roh- und Werkstoff*. 53: 165-170.

Horng, A.J., Chatwin, M.A., Wate, G.K., 1988. "Adverse effects of using rotten logs in kraft mills." *Pulp and Paper Canada*. 89(10): 65-70.

Howard, R.C., Poole, R., Page, D.H., 1994. "Factor Analysis Applied to the Results of a Laboratory Beating Investigation." *Journal of Pulp and Paper Science*. 20(5): J137-J141.

Hulme, M.A., 1979. "Outside Chip Storage – Deterioration During OCS." In Hatton, J.V. "Chip Quality Monograph." Joint Textbook Committee of the Paper Industry, Montréal.

Hulme, M.A, Shields, J.K., 1973. "Treatments to Reduce Chip Deterioration During Storage." *Tappi*. 56(8): 88-90.

Hulme, M.A., Hatton, J.V., 1978. "Silo-stored hardwood chips treated with sodium carbonate." *Tappi*. 61(12): 47-50.

Hunt, K., 1978. "Chipping western hemlock decayed by white-rot fungi." *Pulp & Paper Canada*. 79(6): T192-T193.

Hunt, K., 1978a. "Kraft pulping of decayed wood: western red cedar and alpine fir." *Pulp & Paper Canada*. 79(7): T229-T234.

Hunt, K., 1978b. "How rot-decayed wood affects chipping and kraft pulping." *Pulp & Paper Canada*. 79(8): T264-T267.

Hunt, K., Hatton, J.V., 1979. "Predicting the kraft pulping behavior of decayed pulpwood." *Pulp & Paper Canada*. 80(3): T72-T74.

Hurst, M., Sutton, P., 1999. "Fiber quality analyzer – a valuable mill tool." *Proceedings of the 1999 85th Annual Meeting of PAPTAC*. A81-A84.

Irbe, I., Andersone, I., Andersons, B., Chirkova, J., 2001. "Use of ^{13}C NMR, sorption and chemical analyses of characteristics of brown-rotted Scots pine." *International Biodegradation & Biodeterioration*. 47: 37-45.

Jackson, M., Falk, B., Akerlund, G., 1985. "High-yield pulp from North American aspen." *Tappi*. 68(11): 62-66.

Jasalavich, C.A., Ostrofsky, A., Jellison, J., 2000. "Detection and identification of decay fungi in spruce wood by restriction fragment length polymorphism analysis of amplified genes encoding rRNA." *Applied and Environ. Microbiol.* 66(11): 4725-4734.

Jellison, J., Goodell, B., 1988. "Immunological detection of decay in wood." *Wood Science and Technology*. 22: 293-297.

Jellison, J., Jasalavich, C., 2000. "Selected methods for the detection of degradative fungi." *International Biodeterioration and Biodegradation*. 46: 241-244.

Jensen, K.A., Houtman, C.J., Ryan, Z.C., Hammel, K.E., 2001. "Pathways for Extracellular Fenton Chemistry in the Brown Rot Basidiomycete *Gloeophyllum trabeum*." *Applied and Environmental Microbiology*. 67(6): 2705-2711.

Jin, L., Schultz, T.P., Nicholas, D.D., 1990. "Structural Characterization of Brown-rotted Lignin." *Holzforschung*. 44(2): 133-138.

Johnson, B.R., Chen, G.C., 1983. "Occurrence and Inhibition of Chitin in Cell Walls of Wood-Decay Fungi." *Holzforschung*. 37: 255-259.

Johnson, B.N., McGill, W.B., 1990. "Comparison of ergosterol and chitin as quantitative estimates of mycorrhizal infection and *Pinus contorta* seedling response to inoculation." *Can. J. For. Res.* 20: 1125-1131.

Jones, R.W., Meglen, R.R., Hames, B.R., McClelland, J.F., 2002. "Chemical Analysis of Wood Chips in Motion Using Thermal-Emission Mid-Infrared Spectroscopy with Projection to Latent Structures Regression." *Anal. Chem.* 74(2): 453-457.

Jones, T.G., Richardson, J.D., 2001. "Chemimechanical pulping of New Zealand-grown *Eucalyptus regnans*." *Appita*. 54(3): 265-271.

Jordan, C.R., Dashek, W.V., Highley, T.L., 1996. "Detection and Quantification of Oxalic Acid from the Brown-Rot Decay Fungus, *Postia placenta*." *Holzforschung*. 50(4): 312-318.

Kacurakova, M., Capek, P., Sasinkova, V., Wellner, N., Ebringerova, A., 2000. "FT-IR study of plant cell wall model compounds: pectic polysaccharides and hemicelluloses." *Carbohydrate Polymers*. 43: 195-203.

Kang, K.-Y., Jo, B.-M., Oh, J.-S., Mansfield, S.D., 2003. "The Effects of Biopulping on Chemical and Energy Consumption during Kraft Pulping of Hybrid Poplar." *Wood and Fiber Science*. 35(4): 594-600.

Karlsson, M., Wancke Stahl, C., 2000. "Hallsta installs NIR technology to optimise TMP quality." *Paper Technology*. 41(1): 25-27.

Katuscak, S., Katuscakova, G., 1987. "Means of Objective Identification of Spruce Wood Decay." *Holzforschung*. 41(5): 315-320.

Kelley, S.S., Jellison, J., Goodell, B., 2002. "Use of NIR and pyrolysis-MBMS coupled with multivariate analysis for detecting the chemical changes associated with brown-rot biodegradation of spruce wood." *FEMS Microbiology Letters*. 209(1): 107-111.

Kelley, S.S., Rials, T.G., Groom, L.R., So, C.-L., 2004. "Use of near infrared spectroscopy to predict the mechanical properties of six softwoods." *Holzforschung*. 58: 252-260.

Kelley, S.S., Rials, T.G., Snell, R., Groom, L.H., Sluiter, A., 2004a. "Use of near infrared spectroscopy to measure the chemical and mechanical properties of solid wood." *Wood Science and Technology*. 38: 257-276.

Kibblewhite, R.P., Evans, R., Riddell, M.J.C., 1997. "Handsheet property prediction from kraft-fibre and wood-tracheid properties in eleven radiate pine clones." *Appita*. 50(2): 131-138.

Kim, S.H., Uzunovic, A., Breuil, C., 1999. "Rapid Detection of *Ophiostoma piceae* and *O. quercus* in Stained Wood by PCR." *Applied and Environmental* Microbiology. 65(1): 287-290.

Kim, Y.S., Jellison, J., Goodell, B., Tracy, V., Chandhoke, V., 1991. "The Use of ELISA for the Detection of White and Brown Rot Fungi." *Holzforschung*. 45(6): 403-406.

Kim, Y.S., Newman, R.H., 1995. "Solid State ^{13}C NMR Study of Wood Degraded by the Brown Rot Fungus *Gloeophyllum trabeum*." *Holzforschung*. 49(2): 109-114.

Knoll, C.S., Wong, B.M., Roy, D.N., 1993. "The chemistry of decayed aspen wood and perspectives on its utilization." *Wood Science and Technology*. 27(6): 439-448.

Kosikova, B., Ebringerova, A., Micko, M., 1992. "Effect of Aspen and Oak Wood Rotting on the Solubility of Their Main Components." *Holzforschung*. 46(4): 289-291.

Krahmer, R.L., DeGroot, R.C., Lowell, E.C., 1982. "Detecting Incipient Brown Rot with Fluorescence Microscopy." *Wood Science*. 15(2): 78-80.

Kramer, R., 1998. Chemometric Techniques for Quantitative Analysis. Marcel Dekker, New York.

Kubler, H., 1982. "Heat Release in Thermally Disintegrating Wood." *Wood and Fiber*. 14(3): 166-177.

Kumar, S., Barbour, R.J., Gustafson, R.R., 2004. "Kraft pulping response and paper properties of wood from densely stocked small-diameter stands." *Forest Products Journal*. 54(5): 50-56.

Kuo, M.-L., Stokke, D.D., McNabb, H.S., 1988. "Microscopy of Progressive Decay of Cottonwood by the Brown-Rot Fungus *Gloeophyllum trabeum*." *Wood and Fiber Science*. 20(4): 405-414.

Levitin, N., 1967. "Review of Effect of Chip Storage on Wood Resins and Pulps." *Pulp and Paper Magazine of Canada*. 68(9): T454-T460.

Lindgren, R.M., Eslyn, W.E., 1961. "Biological Deterioration of Pulpwood and Pulp Chips During Storage." *Tappi*. 44(6): 419-429.

Logan, A.F., Phillips, F.H., Harries, E.D., 1987. "Effect of Growth Conditions, Bark, and Defective Wood on Sulfate Pulps from Plantation Growth Eucalyptus deglupta B1." *Appita*. 40(3): 176-180.

MacLeod, J.C., 1967. "Problems, problems, problems in forest protection." *Pulp and Paper Magazine of Canada*. 68(6): WR274-277.

MacLeod, J.M., 1991. "Is unbleached softwood kraft pulp strongest at 30 kappa number?" *Paperi ja Puu*. 73(8): 773-777.

Maekawa, E., Koshijima, T., 1983. "Effect of Acetate Buffer in Preparing Chlorite Hemicellulose from Woody Materials." *Tappi*. 66(11): 79.

Marcus, A., 1998. "Modern Times Reach the Woodroom." *European Papermaker*. 5(3): 20-21.

Mark, R.E., Gillis, P.P., 1973. "The relationship between fiber modulus and S2 angle." *Tappi*. 56(4): 164-167.

McDonald, T., Twaddle, A., 2000. "Industry Trends in Chip Storage and Handling." *Tappi Pulping/Process & Product Quality Conference*. Boston, MA, 2000.

McGovern, J.N., 1979. "Raw Material Variables in Chip Production." In Hatton, J.V. "Chip Quality Monograph." Joint Textbook Committee of the Paper Industry, Montréal.

Meder, R., Gallagher, S., Mackie, K.L., Bohler, H, Meglen, R., 1999. "Rapid Determination of the Chemical Composition and Density of *Pinus radiata* by PLS Modeling of Transmission and Diffuse Reflectance FTIR Spectra." *Holzforschung*. 53(3): 261-266.

Messner, K., 1998. "Biopulping." In Bruce, A., Palfreyman, J.W. "Forest Products Biotechnology." Taylor & Francis, Bristol, PA.

Michell, A.J., 1988. "Infra-red Spectroscopy Transformed – New Applications in Wood and Pulping Chemistry." *Appita*. 41(5): 375-380.

Michell, A.J. 1994. "Vibrational Spectroscopy – A Rapid Means of Estimating Plantation Pulpwood Quality?" *Appita*. 47(1): 29-37.

Milanova, E., Dorris, G.M., 1994. "On the Determination of Residual Alkali in Black Liquors." *Nordic Pulp Pap. Res. J.* 9(1): 4-9.

Millard, P.J., Roth, B.L., Thi, H.P.T., Yue, S.T., Haugland, R.P., 1997. "Development of the FUN-1 Family of Fluorescent Probes for Vacuole Labelling and Viability Testing of Yeasts." *Applied and Environmental Microbiology*. 63(7): 2897-2905.

Mischki, T., Bicho, P., Watson, P., Gee, W., Drummond, J., 2005. "The Effects of Decadent Western Hemlock on Pulping and Pulp Properties." *Pulp and Paper Canada*. 106(1): 49-56.

Montagu, K.D., Kearney, D.E., Smith, R.G.B., 2003. "The biology and silviculture of pruning planted eucalypts for clear wood production – a review." *Forest Ecology and Management*. 179: 1-13.

Moore, S.A., 1990. "Cell size specific binding of the fluorescent dye calcofluor to budding yeast." *Biochimica et Biophysica Acta*. 1035: 206-213.

Moore, A.K., Owen, N.L., 2001. "Infrared Spectroscopic Studies of Solid Wood." *Applied Spectroscopy Reviews*. 36(1): 65-86.

Mroz, W., Surewicz, W., 1986. "Effect of Microbiological Defects of Pinewood on the Yield of Byproducts from Kraft Mills." *Przeglad papier*. 42(10): 359-360.

Muller, U., Bammer, R., Teischinger, A., 2002. "Detection of Incipient Fungal Attack in Wood Using Magnetic Resonance Parameter Mapping." *Holzforschung*. 56(5): 529-534.

Nicholas, D.D., Crawford, D., 2003. "Concepts in the Development of New Accelerated Test Methods for Wood Decay." In Goodell, B., Nicholas, D.D., Schultz, T.P., 2003. "Wood Deterioration and Preservation: Advances in Our Changing World." American Chemical Society, Washington, DC.

Nilsson, K., Bjurman, J., 1990. "Estimation of Mycelial Biomass by Determination of the Ergosterol Content of Wood Decayed by *Coniophora puteana* and *Fomes fomentarius*." *Material und Organismen*. 25(4): 275-285.

Nilsson, T, 1965. "Mikroorganismer i flisstackar. *Svensk Papperstidning*. 68(15): 495-499.

Nilsson, T., 1973. "Micro-organisms in Chip Piles." *IUFRO Symp. Protection of Wood in Storage, Norway/Sweden, July 1972*. XIV: 1-23.

Nilsson, T., Daniel, G., Kirk, T.K., Obst, J.R., 1989. "Chemistry and Microscopy of Wood Decay by Some Higher Ascomycetes." *Holzforschung*. 43(1): 11-18.

NRC, 2003. Statistics and Facts on Forestry. Natural Resources Canada, Ottawa.

Nuopponen, M., Wikberg, H., Vuorinen, T., Maunu, S.L., Jämsä, S., Viitaniemi, P., 2003. "Heat-Treated Softwood Exposed to Weathering." *Journal of Applied Polymer Science*. 91: 2128-2134.

Olsen, K.K., Schmidt, E.L., 1994. "An Attempt to Quantify Relative Mycelial Development of *Phanerochaete chrysosporium* using the Fluorescein Diacetate Spectrophotometer Assay." *Mycologia*. 86(6): 741-742.

Olsson, R.J., Omani, P., Carlson, M., Josef son, T., Solberg, K., Borland, C. 1995. "Multivariate Characterization of Chemical and Physical Descriptors in Pulp using NIRR." *Tappi*. 78(10): 158-166.

Olszewski, J., 1968. "The Influence of Soft rot on the Suitability of Pinewood as a Raw Material for Kraft Pulp Manufacture." *Przeglad papier*. 24(4): 114-118.

Ona, T., Sonata, T., Ito, K., Shibata, M., Kato, T., Outtake, Y., Tami, Y., Kojima, Y. 2000. "Rapid Prediction of Native Wood Pulp Properties by Fourier Transform Raman Spectroscopy." *Journal of Pulp and Paper Science*. 26(2): 43-46.

Page, D.H., El-Hussein, F., Winkler, K, Bain, R., 1972. "The Mechanical Properties of Single Wood-Pulp Fibers. Part 1: A New Approach." *Pulp and Paper Magazine of Canada*. 73(8): 72-77.

Page, D.H., 1969. "A Theory for the Tensile Strength of Paper." *Tappi*. 52(4): 674-681.

Pandey, K.K., Theagarajan, K.S., 1997. "Analysis of wood surfaces and ground wood by diffuse reflectance (DRIFT) and photoacoustic (PAS) Fourier transform infrared spectroscopic techniques." *Holz als Roh- und Werkstoff*. 55: 383-390.

PAPTAC, 2000. Standard Methods. PAPTAC, Montréal.

Peters, G.B., Dawson, H.J., Hrutfiord, B.F., Whitney, R.R., 1976. "Aqueous Leachate from Western Red Cedar: Effects on Some Aquatic Organisms." *J. Fish. Res. Board Can.* 33(12): 2703-2709.

Pitts, S., Bicho, P., Watson, P., 2004. "Rapid Prediction of Fibre Properties: Opportunities Using Forest Site Classification Methods." *PAPTAC 90th Annual Meeting*, Montreal. A185-A191.

Pleasants, S., Batchelor, W.J., Parker, I.H. 1998. "Measuring the fibril angle of bleached fibres using micro-Raman Spectroscopy." *Appita*. 51(5): 373-376.

Poke, F.S., Wright, J.K., Raymond, C.A., 2004. "Predicting Extractives and Lignin Contents in *Eucalyptus globules* Using Near Infrared Reflectance Analysis." *Journal of Wood Chemistry and Technology*. 24(1): 55-67.

Preston, C.M., Trofymow, J.A., Niu, J., Fyfe, C.A., 1998. "^{13}C CPMAS-NMR spectroscopy and chemical analysis of coarse woody debris in coastal forests of Vancouver Island." *Forest Ecology and Management*. 111: 51-68.

Procter, A.R., 1973. "The Effect of Rot on Kraft Pulp Yield and Quality – A Review." *Pulp & Paper Magazine of Canada*. 74(4): 62-68.

Procter, A., Chow, W., 1973. "A Chip Quality Index for Rot." *Pulp & Paper Magazine of Canada*. 74(7): 97-100.

Raymond, C.A., Schimleck, L.R., 2002. "Development of near infrared reflectance analysis calibrations for estimating genetic parameters for cellulose content in *Eucalyptus globulus*." *Can. J. For. Res.* 32(1): 170-176.

Ring, G.J.F., Bacon, A.J., 1997. "Multiple Component Analysis of Fiber Length Distributions." *Tappi*. 80(1): 160, 167, 174, 224-231.

Rinn, F., Schweingruber, F.-H., Schar, E., 1996. "RESISTOGRAPH and X-Ray Density Charts of Wood Comparative Evaluation of Drill Resistance Profiles and X-Ray Density Charts of Different Wood Species." *Holzforschung*. 50(4): 303-311.

Rodden, G., Lees, D., Potter, J., Moohan, M., Rettman, A., Dixon, M., James, R., Toland, J., O'Brian, H., Roberts, J., 2003. International Fact and Price Book – 2003. Paperloop, Brussels.

Roy, A.K., Bag, S.C., Basak, M.K., Sen, S.K., 1992. "Infrared Spectra of Jute Stick Treated with White-Rot Fungus." *Journal of Applied Polymer Science*. 44: 1607-1613.

Rudder, G., 2002. Pulp and Paper North American Fact Book 2002. Paperloop, San Francisco.

Saariaho, A.-M., Hortling, B., Jääskeläinen, A.-S., Tamminen, T., Vuorinen, T., 2003. "Simultaneous Quantification of Residual Lignin and Hexenuronic Acid from Chemical Pulps with UV Resonance Raman Spectroscopy and Multivariate Calibration." *Journal of Pulp and Paper Science*. 29(11): 363-370.

Sachs, I.B., Leatham, G.F., Myers, G.C., 1989. "Biomechanical Pulping of Aspen (*Populus*) Chips by *Phanerochaete chrysosporium*: Fungal Growth Pattern and Effects on Wood Cell Walls." *Wood and Fiber Science*. 21(4): 331-342.

Sakakibara, A., Sano, Y., 2001. "Chemistry of Lignin." In Hon, D.N.-S., Shiraishi, N., "Wood and Cellulosic Chemistry, 2nd Edition, Revised and Expanded." Marcel Dekker, New York.

Saunders, C.B., Singh, A., 1988. "Wood Chip Deterioration During Outside Storage and Its Prevention." Radiation Applications Research Branch Report, Pinawa, Manitoba.

Savitzky, A., Golay, M.J.E., 1964. "Smoothing and differentiation of data by simplified least square procedures." *Anal. Chem.* 36(8): 1627-1639.

Schimleck, L.R., Evans, R., 2003. "Estimation of Air Dry Density of Increment Cores by Near Infrared Spectroscopy." *Appita*. 56(4): 312-317.

Schimleck, L.R., Jones, P.D., Peter, G.F., Daniels, R.F., Clark III, A., 2004. "Nondestructive estimation of tracheid length from sections of radial wood strips by near infrared spectroscopy." *Holzforschung*. 58(4): 375-381.

Schimleck, L.R., Michell, A.J., Raymond, C.A., Muneri, A., 1999. "Estimation of basic density of *Eucalyptus globules* using near-infrared spectroscopy." *Can. J. For. Res.* 29: 194-201.

Schimleck, L.R., Raymond, C.A., Beadle, C.L., Downes, G.M., Kube, P.D., French, J. 2000. "Applications of NIR Spectroscopy to Forest Research." *Appita*. 53(5): 458-464.

Schmidt, O., 2000. "Molecular methods for the characterization and identification of the dry rot fungus *Serpula lacrymans*." *Holzforschung*. 54: 221-228.

Schmidt, R.L., 1990. "The effect of wood chip inventory rotation policies on storage costs, chip quality, and chip variability." *Tappi*. 73(11): 211-216.

Schultz, T.P., Burns, D.A. 1990. "Rapid Secondary Analysis of Lignocellulose: Comparison of Near Infrared (NIR) and Fourier Transform Infrared (FTIR)." *Tappi*. 73(5): 209-212.

Schultz, T.P., Templeton, M.C., McGinnis, G.D., 1985. "Rapid Determination of Lignocellulose by Diffuse Reflectance Fourier Transform Infrared Spectrometry". *Analytical Chemistry*. 57(14): 2867-2869.

Schwanninger, M., Hinterstoisser, B., 2002. "Klason lignin: Modifications to improve the precision of the standard determination." *Holzforschung*. 56(2): 161-166.

Schwartze, F.W.M.R., Baum, S., Fink, S., 2000. "Resistance of fibre regions in wood of *Acer pseudoplatanus* degraded by *Armillaria mellea*." *Mycological Research*. 104(9): 1126-1132.

Seitz, L.M., Sauer, D.B., Burroughs, R., Mohr, H.E., Hubbard, J.D., 1979. "Ergosterol as a Measure of Fungal Growth." *Phytopathology*. 69(11): 1202-1203.

Seth, R., 1990. "Fiber Quality Factors in Papermaking (1) Importance of Fiber Length and Strength." *Materials Res. Soc. Symp. Proc.* 197: 125-141.

Seth, R., 1990a. "Fiber Quality Factors in Papermaking (2) Importance of Fiber Coarseness." *Materials Res. Soc. Symp. Proc.* 197: 143-161.

Shaw, M., 2000. "Extensive Wood Yard Upgrade Improves Chip Quality at Bowater Newsprint." *Pulp & Paper*. 74(10): 57, 59-61.

Shields, J.K., 1969. "Microflora in Eastern Canadian Wood Chip Piles." *Mycologia*. 61: 1165-1168.

Shields, J.K., Atwell, E.A., 1963. "Effect of a Mold, *Trichoderma viride*, On Decay of Birch by Four Storage-Rot Fungi." *Forest Products Journal*. 13(7): 262-265.

Shimada, M., Akamtsu, Y., Tokimatsu, T., Mii, K., Hattori, T., 1997. "Possible biochemical roles of oxalic acid as a low molecular weight compound involved in brown-rot and white-rot wood decays." *Journal of Biotechnology*. 53: 103-113.

Simula, M., 2002. "Fibre Supply: the Achilles heel of the global pulp and paper industry." *Paperi ja puu*. 84(1): 16-19.

Singh, P., 1993. "Research and management strategies for major tree diseases in Canada: Synthesis Part 1." *Forest Chronicle*. 69(2): 151-162.

Sjöström, E., 1989. "The origin of charge on cellulosic fibers." *Nordic Pulp and Paper Research Journal*. 4(2): 90-93.

Sjöström, E., 1993. Wood Chemistry Fundamentals and Applications, 2nd Ed. Academic Press, San Diego.

Skoog, D.A., Leary, J.J., 1992. Principles of Instrumental Analysis, 4th Ed. Saunders College Publishing, Orlando, FL.

Smith, R.S., Hatton, J.V., 1971. "Economic Feasibility of Chemical Protection for Outside Chip Storage." *Tappi*. 54(10): 1638-1640.

Smith, R.S. 1973. "Colonization and Degradation of Outside Stored Softwood Chips by Fungi." IUFRO Symposium on Protection of Wood in Storage, Norway/Sweden, 1972. 22.

Smith, R.S., 1974. "Destructive Agencies of Wood – Fungi." *Proceedings of the Annual Meeting of the American Wood Preservers' Association*. 81-88.

Smook, G.A., 2002. Handbook for Pulp & Paper Technologists, 3rd Ed. Angus Wilde Publications, Vancouver.

So, C.-L., Via, B.K., Groom, L.H., Schimleck, L.R., Shupe, T.F., Kelley, S.S., Rials, T.G., 2004. "Near Infrared Spectroscopy in the Forest Products Industry." *Forest Products Journal*. 54(3): 6-16.

Sparen, A., Renberg, L., Furusjo, E., Hillforth, C.A., Danielsson, L.-G., 2003. "Determination of kappa number reduction in pulp and COD in bleach plant effluents using multiwavelength spectrometry and multivariate calibration." *Tappi Journal*. 2(1): 16-21.

Springer, E.L., Feist, W.C., Zoch, L.L., Hajny, G.J., 1975. "Evaluation of five treatments to prevent deterioration of wood chips during storage in pile simulators." *Tappi*. 58(3): 128-131.

Springer, E.L., Hajny, G.J., 1970. "Spontaneous Heating in Piled Wood Chips." *Tappi*. 53(1): 85-86.

Srebotnik, E., Messner, K., Foisner, R., 1988. "Penetrability of White Rot-Degraded Pine Wood by the Lignin Peroxidase of *Phanerochaete chrysosporium*." 54: 2608-2614.

Stuart, W.B., Leary, P.S., 1992. "Factors affecting sawmill residue chip quality." *Tappi*. 75(7): 129-132.

Subramanian, R.V., Somasekharan, K.N., Johns, W.E., 1983. "Acidity of Wood." *Holzforschung*. 37: 117-120.

Sudiyani, Y., Imamura, Y., Doi, S., Yamauchi, S., 2003. "Infrared spectroscopic investigations of weathering effects on the surface of tropical wood." *Journal of Wood Science*. 49: 86-92.

Supinski, J., Dziurzynski, A., 1988. "Studies of the Chemical Composition of Wood on the Basis of Infrared Spectroscopy, II Determination of Holocellulose and Lignin Content with the Use of Various Base Lines of 1515 (1510) cm^{-1} Band." *Folia Forestalia Polonica, Seria B.* 18: 19-27.

Sun, Z., Ibrahim, A., Oldham, P.B., Schultz, T.P., Conners, T.E. 1997. "Rapid Lignin Measurement in Hardwood Pulp Samples by Near-Infrared Fourier Transform Raman Spectroscopy." *J. Agric. Food Chem.* 45(8): 3088-3091.

Svedman, M., Tikka, P., Luhtanen, M., 1998. "Effects of softwood morphology and chip thickness on pulping with a displacement kraft batch process." *Tappi.* 81(7): 157-168.

TAPPI, 2002. Tappi Test Methods. TAPPI Press, Atlanta.

ThermoElectron, 2003. "Spectroscopic Solutions Seminar Fall 2003." ThermoElectron, Madison, WI.

ThermoGalactic, 2002, "Grams/AI (7.01): Help Menu." ThermoGalactic Corp. Salem NH.

Umezawa, T., 2001. "Chemistry of Extractives." In Hon, D.N.-S., Shiraishi, N., "Wood and Cellulosic Chemistry, 2nd Edition, Revised and Expanded." Marcel Dekker, New York.

Wariishi, H., Valli, K., Gold, M.H., 1992. "Manganese(II) Oxidation by Manganese Peroxide from the Basidiomycete *Phanerochaete chrysosporium.*" *Journal of Biological Chemistry.* 267(33): 23688-23695.

Whitty, N.J., Lee, C.L., Roste, E., 1991. "The Effects of Stain and Rot Content on the Bleach Response and Strength Properties of Aspen Mechanical Pulp." Pacific Paper Expo. 85-91.

Wise, L.E., Murphy, M., D'Addieco, A.A., 1946. "Chlorite Holocellulose, Its Fractionation and Bearing on Summative Wood Analysis and on Studies on Hemicelluloses." *Tappi.* 29: 11-19.

Wolfaardt, F., Rabie, C., 2003. "Evaluation of the Microclimate in a Stored Softwood Chip Pile for Biopulping." *Holzforschung.* 57(3): 295-300.

Wolfaardt, F., Taljaard, J.L., Jacobs, A., Male, J.R., Rabie, C.J., 2004. "Assessment of wood-inhabiting Basidiomycetes for biokraft pulping of softwood chips." *Bioresource Technology.* 95: 25-30.

Yang, J.L., Evans, R., 2003. "Prediction of MOE of Eucalypt Wood from Microfibril Angle and Density." *Holz als Roh- und Werkstoff.* 61(6): 449-452.

Yeh, T.-F., Chang, H.-M., Kadla, J.F., 2004. "Rapid Prediction of Solid Wood Lignin Content Using Transmittance Near-Infrared Spectroscopy." *Journal of Agricultural and Food Chemistry.* 52(6): 1435-1439.

Zabel, R.A., Morrell, J.J., 1992. Wood Microbiology Decay and Its Prevention. Academic Press, San Diego.

Zanuttini, M., Citroni, M., Martinez, M.J., 1998. "Application of Diffuse Reflectance Infrared Fourier Transform Spectroscopy to the Quantitative Determination of Acetyl Groups in Wood." *Holzforschung*. 52(3): 263-267.

Zhao, J., Carrabba, M.M., Allen, F.S., 2002. "Automated Fluorescence Rejection Using Shifted Excitation Raman Difference Spectroscopy." *Applied Spectroscopy*. 56(7): 834-845.

Zielinski, M.H., 1988. "Synergism and Antagonism in the Interaction of Fungal Pathogens in Pinewood (*Pinus*)." *Pr. Inst. Technol. Drewna*. 35(1/4): 3-37.

Appendix I – Concentration Datasets
Caustic Solubility and Buffering Capacity Calibration Dataset

		Caustic Solubility		Buffering Capacity	
Species	Location/Fungus	Measured	Predicted	Measured	Predicted
Alaskan spruce	BC	10.8	15.7	0.039	0.070
Alaskan spruce	BC	15.8	12.3	0.036	0.045
Black spruce	Antigonish, NS	12.9	11.0	0.028	0.009
Black spruce	Donnacona, QC	14.1	13.1	0.026	0.048
Black spruce	Donnacona, QC	16.3	14.7	0.040	0.043
Black spruce	Donnacona, QC	19.6	21.6	0.082	0.106
Jack pine	Smooth Rock Falls, ON	11.3	13.8	0.018	0.044
Lodgepole pine	BC	18.8	20.5	0.056	0.085
Lodgepole pine	BC	16.0	17.7	0.056	0.076
Lodgepole pine	BC	17.6	15.4	0.056	0.052
Lodgepole pine	BC	18.4	16.2	0.084	0.063
Lodgepole pine	Enderby, BC	14.0	16.5	0.043	0.053
Lodgepole pine	Kamloops, BC	14.1	16.6	0.047	0.061
Lodgepole pine	Kamloops, BC	14.3	17.6	0.057	0.061
Lodgepole pine	*G. trabeum*	16.6	16.6	0.075	0.062
Lodgepole pine	*G. trabeum*	19.0	21.6	0.091	0.082
Lodgepole pine	*G. trabeum*	33.3	37.7	0.180	0.187
Lodgepole pine	*G. trabeum*	24.5	28.1	0.136	0.132
Lodgepole pine	*G. trabeum*	50.8	48.7	0.180	0.241
Lodgepole pine	*O. piliferum*	15.8	13.9	0.064	0.046
Lodgepole pine	*P. chrysosporium*	15.5	16.5	0.067	0.060
Lodgepole pine	*P. chrysosporium*	15.3	20.0	0.065	0.066
Lodgepole pine	*P. chrysosporium*	20.3	19.0	0.106	0.081
Lodgepole pine	*P. pini*	16.6	18.7	0.058	0.073
Lodgepole pine	*P. pini*	15.6	23.6	0.134	0.098
Lodgepole pine	*P. pini*	15.7	18.5	0.076	0.074
Lodgepole pine	*P. placenta*	35.0	37.9	0.203	0.166
Lodgepole pine	*P. placenta*	22.6	19.0	0.093	0.084
Lodgepole pine	Williams Lake, BC	18.9	18.4	0.111	0.072
Lodgepole pine	BC	15.9	18.4	0.060	0.065
Lodgepole pine	BC	14.9	17.0	0.060	0.063
Lodgepole pine	BC	15.7	15.3	0.056	0.046
Lodgepole pine	BC	18.6	21.6	0.080	0.090
Lodgepole pine	Williams Lake, BC	18.4	14.0	0.100	0.065
Lodgepole pine	*G. trabeum*	19.5	24.9	0.104	0.132
Lodgepole pine	*G. trabeum*	21.7	16.8	0.108	0.087
Lodgepole pine	*G. trabeum*	30.2	33.0	0.163	0.165
Lodgepole pine	*G. trabeum*	21.1	17.9	0.108	0.080
Lodgepole pine	BC	13.7	9.2	0.048	0.011
Lodgepole pine	BC	14.4	12.4	0.048	0.034
Lodgepole pine	BC	11.8	10.8	0.030	0.025
Lodgepole pine	BC	14.0	14.0	0.054	0.033
Lodgepole pine	BC	16.0	11.6	0.050	0.035
Lodgepole pine	BC	13.1	12.0	0.033	0.027
Mixed softwood	Taylor, BC	14.2	17.4	0.038	0.046

Sample	Location/Fungus	Caustic Solubility Measured	Caustic Solubility Predicted	Buffering Capacity Measured	Buffering Capacity Predicted
Mixed softwood	Quesnel, BC	14.8	17.6	0.034	0.069
Mixed softwood	Quesnel, BC	15.3	18.5	0.050	0.074
Mixed softwood	Quesnel, BC	13.7	15.5	0.059	0.053
Mixed softwood	Quevillon, QC	12.7	14.4	0.044	0.034
Mixed softwood	Quevillon, QC	14.0	14.6	0.047	0.035
Mixed softwood	Quevillon, QC	16.1	15.7	0.051	0.044
Mixed softwood	Quevillon, QC	12.7	15.3	0.034	0.036
Mixed softwood	Taylor, BC	13.1	15.5	0.061	0.069
Mixed softwood	Taylor, BC	13.6	15.1	0.041	0.047
Mixed softwood	Taylor, BC	13.5	13.1	0.040	0.045
Mixed softwood	Taylor, BC	15.6	13.8	0.044	0.043
Mixed softwood	Taylor, BC	13.1	11.6	0.040	0.041
Mixed softwood	Southern USA	14.0	26.8	0.091	0.103
Mixed softwood	Taylor, BC	14.2	14.2	0.039	0.036
Poplar	BC	21.1	10.1	0.019	0.000
Sub-alpine fir	BC	15.8	10.5	0.037	0.033
Sub-alpine fir	*G. trabeum*	16.0	14.9	0.040	0.045
Sub-alpine fir	*G. trabeum*	15.1	14.6	0.036	0.060
Sub-alpine fir	*G. trabeum*	38.1	34.5	0.200	0.164
Sub-alpine fir	*P. chrysosporium*	12.8	12.7	0.020	0.039
Sub-alpine fir	*P. pini*	13.7	12.6	0.019	0.042
Sub-alpine fir	*P. igniarius*	14.7	12.3	0.028	0.030
Sub-alpine fir	*P. igniarius*	14.5	10.9	0.020	0.031
Sub-alpine fir	*P. placenta*	14.7	12.4	0.043	0.038
Trembling aspen	Fort Nelson, BC	21.1	17.0	0.030	0.034
Trembling aspen	Fort Nelson, BC	21.9	25.6	0.025	0.077
Trembling aspen	Fort Nelson, BC	17.5	20.6	0.034	0.045
Trembling aspen	Fort Nelson, BC	26.9	36.0	0.092	0.136
Trembling aspen	Fort Nelson, BC	22.7	21.0	0.032	0.054
Trembling aspen	Fort Nelson, BC	22.7	21.9	0.032	0.034
Trembling aspen	*G. trabeum*	27.4	27.3	0.078	0.076
Trembling aspen	*G. trabeum*	30.7	32.0	0.093	0.095
Trembling aspen	*G. trabeum*	40.3	39.2	0.139	0.137
Trembling aspen	*G. trabeum*	44.1	41.9	0.198	0.149
Trembling aspen	*G. trabeum*	52.8	38.3	0.169	0.153
Trembling aspen	*G. trabeum*	68.3	64.7	0.282	0.295
Trembling aspen	*P. bubakii*	23.3	21.5	0.028	0.046
Trembling aspen	*P. chrysosporium*	22.5	21.6	0.037	0.043
Trembling aspen	*P. igniarius*	20.5	24.3	0.053	0.061
Trembling aspen	*P. igniarius*	25.1	22.2	0.059	0.056
Trembling aspen	*P. placenta*	40.4	40.2	0.159	0.142
Trembling aspen	*P. placenta*	24.0	25.4	0.079	0.067
Western hemlock	*G. trabeum*	30.2	28.0	0.134	0.123
Western hemlock	*G. trabeum*	28.9	30.2	0.127	0.132
Western hemlock	*G. trabeum*	48.4	39.6	0.206	0.199
Western hemlock	*P. chrysosporium*	11.9	15.0	0.020	0.048
Western hemlock	*P. pini*	14.7	19.0	0.054	0.075

Species	Location/Fungus	Caustic Solubility Measured	Caustic Solubility Predicted	Buffering Capacity Measured	Buffering Capacity Predicted
Western hemlock	*P. pini*	16.6	16.6	0.055	0.065
Western hemlock	*P. pini*	16.8	29.9	0.100	0.141
Western hemlock	*P. placenta*	15.0	13.9	0.043	0.047
Western hemlock	*P. placenta*	22.3	21.8	0.102	0.084
Western hemlock	*P. placenta*	17.3	15.2	0.067	0.053
Western hemlock	Kispiox Valley, BC	16.1	12.0	0.068	0.050
White birch	Quebec	24.9	36.2	0.095	0.115
White spruce	*G. trabeum*	15.9	16.7	0.083	0.059
White spruce	*G. trabeum*	31.3	29.3	0.144	0.133
White spruce	*G. trabeum*	37.7	33.2	0.151	0.159
White spruce	*G. trabeum*	41.6	31.1	0.170	0.144
White spruce	*G. trabeum*	47.8	39.4	0.184	0.205
White spruce	*P. bubakii*	12.7	14.4	0.040	0.040
White spruce	*P. chrysosporium*	20.0	17.3	0.090	0.092
White spruce	*P. chrysosporium*	12.8	13.7	0.032	0.032
White spruce	*P. pini*	12.0	12.0	0.040	0.022
White spruce	*P. igniarius*	17.7	19.3	0.058	0.073
White spruce	*P. igniarius*	14.7	20.0	0.083	0.078
White spruce	*P. placenta*	38.8	37.0	0.195	0.170
White spruce	*P. placenta*	45.9	45.8	0.261	0.220
Balsam fir	Smooth Rock Falls, ON	14.6	12.4	0.042	0.030
Balsam poplar	Smooth Rock Falls, ON	21.5	15.7	0.000	0.026
White spruce	Smooth Rock Falls, ON	13.4	16.0	0.042	0.049
White spruce	Williams Lake, BC	14.0	14.2	0.064	0.045
Yellow cedar	BC	17.8	19.3	0.069	0.078

* Location/Fungus denotes the location field samples were obtained or the fungus used to prepare the sample in the lab

Caustic Solubility and Buffering Capacity Validation Dataset

		Caustic Solubility		Buffering Capacity	
Species	Location/Fungus	Measured	Predicted	Measured	Predicted
Alaskan spruce	BC	12.0	17.9	0.037	0.072
Black spruce	Donnacona, QC	17.8	16.1	0.043	0.046
Black spruce	Donnacona, QC	15.1	15.6	0.042	0.048
Douglas fir	Port Alberni, BC	16.0	13.1	0.080	0.053
Douglas fir	Cranbrook, BC	16.6	15.7	0.063	0.026
Douglas fir	Cranbrook, BC	26.2	26.5	0.112	0.085
Jack pine	Smooth Rock Falls, ON	13.3	20.2	0.057	0.069
Larch	Smooth Rock Falls, ON	16.2	13.0	0.037	0.025
Lodgepole pine	BC	12.7	11.4	0.051	0.024
Lodgepole pine	BC	14.0	13.4	0.053	0.041
Lodgepole pine	BC	12.7	10.5	0.047	0.015
Lodgepole pine	Enderby, BC	15.0	16.4	0.047	0.065
Lodgepole pine	BC	19.8	11.4	0.055	0.036
Lodgepole pine	BC	13.3	15.7	0.054	0.048
Mixed softwood	Taylor, BC	12.8	11.5	0.036	0.032
Mixed softwood	Quevillon, QC	13.7	12.7	0.034	0.028
Mixed softwood	Quevillon, QC	14.4	12.9	0.049	0.030
Mixed softwood	Quevillon, QC	14.1	14.9	0.062	0.052
Sub-alpine fir	BC	14.6	11.0	0.028	0.028
Trembling aspen	Fort Nelson, BC	21.9	19.1	0.028	0.028
Trembling aspen	Fort Nelson, BC	25.7	25.4	0.076	0.071
Trembling aspen	BC	22.8	26.1	0.062	0.077
Western hemlock	BC	14.7	15.8	0.062	0.051
White spruce	BC	15.8	13.6	0.047	0.036
Lodgepole pine	*G. trabeum*	23.6	22.6	0.116	0.114
Lodgepole pine	*G. trabeum*	35.7	30.9	0.173	0.149
Lodgepole pine	*P. bubakii*	23.5	21.9	0.103	0.095
Lodgepole pine	*P. pini*	16.7	19.5	0.071	0.078
Lodgepole pine	*P. pini*	16.1	19.8	0.075	0.074
Lodgepole pine	*P. pini*	20.1	17.6	0.120	0.069
Sub-alpine fir	*G. trabeum*	37.3	33.7	0.146	0.164
Sub-alpine fir	*G. trabeum*	42.1	35.2	0.175	0.173
Sub-alpine fir	*P. bubakii*	15.0	16.4	0.020	0.054
Sub-alpine fir	*P. chrysosporium*	13.2	14.8	0.027	0.048
Sub-alpine fir	*P. placenta*	17.6	17.7	0.105	0.072
Sugar maple	Wisconsin	20.6	25.4	0.056	0.068
Trembling aspen	Wisconsin	19.9	20.9	0.034	0.052
Trembling aspen	*G. trabeum*	41.8	38.2	0.152	0.139
Trembling aspen	*P. bubakii*	22.7	25.9	0.076	0.074
Trembling aspen	*P. chrysosporium*	24.6	24.0	0.052	0.062
Trembling aspen	*P. igniarius*	25.8	24.3	0.064	0.063
Trembling aspen	*P. igniarius*	24.9	29.3	0.071	0.090
Trembling aspen	*P. placenta*	25.0	22.1	0.135	0.052
White spruce	*G. trabeum*	38.2	37.0	0.159	0.171

Density Calibration Dataset

	Basic Wood Density		Caustic Solubility		Buffering Capacity	
Sample	Measured	Predicted	Measured	Predicted	Measured	Predicted
1	0.362	0.369	14.0	14.9	0.054	0.044
2	0.362	0.369	14.0	12.9	0.054	0.047
3	0.362	0.364	14.0	12.7	0.054	0.055
4	0.362	0.371	14.0	13.7	0.054	0.054
5	0.375	0.358	12.7	14.5	0.051	0.050
6	0.375	0.356	12.7	13.0	0.051	0.051
7	0.375	0.359	12.7	17.0	0.051	0.065
8	0.375	0.356	12.7	15.0	0.051	0.061
9	0.375	0.364	12.7	14.4	0.051	0.060
10	0.353	0.382	14.0	13.5	0.053	0.044
11	0.353	0.382	14.0	11.9	0.053	0.043
12	0.353	0.373	14.0	14.9	0.053	0.058
13	0.353	0.373	14.0	14.3	0.053	0.057
14	0.353	0.367	14.0	12.7	0.053	0.056
15	0.376	0.363	13.7	14.2	0.048	0.042
16	0.376	0.360	13.7	13.0	0.048	0.047
17	0.376	0.360	13.7	14.3	0.048	0.060
18	0.376	0.364	13.7	14.6	0.048	0.058
19	0.376	0.359	13.7	14.1	0.048	0.061
20	0.367	0.393	14.4	10.1	0.048	0.043
21	0.367	0.393	14.4	10.1	0.048	0.042
22	0.367	0.385	14.4	12.5	0.048	0.053
23	0.367	0.390	14.4	12.9	0.048	0.052
24	0.367	0.399	14.4	8.8	0.048	0.049
25	0.355	0.372	11.8	8.9	0.030	0.038
26	0.355	0.370	11.8	8.5	0.030	0.039
27	0.355	0.369	11.8	10.3	0.030	0.049
28	0.355	0.373	11.8	12.1	0.030	0.047
29	0.355	0.372	11.8	9.9	0.030	0.050
30	0.393	0.407	16.0	19.6	0.056	0.049
31	0.393	0.404	16.0	19.0	0.056	0.050
32	0.393	0.403	16.0	18.3	0.056	0.059
33	0.393	0.403	16.0	18.1	0.056	0.060
34	0.393	0.403	16.0	18.7	0.056	0.064
35	0.389	0.396	18.4	21.2	0.084	0.056
36	0.389	0.393	18.4	21.6	0.084	0.058
37	0.389	0.390	18.4	23.3	0.084	0.069

	Basic Wood Density		Caustic Solubility		Buffering Capacity	
Sample	Measured	Predicted	Measured	Sample	Measured	Predicted
38	0.389	0.396	18.4	21.0	0.084	0.066
39	0.389	0.402	18.4	22.3	0.084	0.066
40	0.407	0.377	15.3	15.8	0.057	0.056
41	0.407	0.383	15.3	14.6	0.057	0.056
42	0.407	0.379	15.3	14.8	0.057	0.056
43	0.407	0.380	15.3	14.4	0.057	0.055
44	0.407	0.376	15.3	13.7	0.057	0.053
45	0.387	0.367	26.3	24.0	0.087	0.078
46	0.387	0.364	26.3	23.1	0.087	0.075
47	0.387	0.361	26.3	24.3	0.087	0.076
48	0.387	0.363	26.3	22.9	0.087	0.076
49	0.387	0.362	26.3	23.3	0.087	0.078
50	0.400	0.396	15.9	13.0	0.050	0.058
51	0.400	0.383	15.9	14.1	0.050	0.059
52	0.400	0.391	15.9	14.0	0.050	0.064
53	0.400	0.395	15.9	13.4	0.050	0.066
54	0.400	0.385	15.9	15.0	0.050	0.066
55	0.394	0.386	18.6	19.0	0.064	0.063
56	0.394	0.369	18.6	19.0	0.064	0.068
57	0.394	0.374	18.6	23.2	0.064	0.071
58	0.394	0.379	18.6	23.3	0.064	0.071
59	0.394	0.380	18.6	22.6	0.064	0.071
60	0.343	0.362	34.6	34.1	0.091	0.101
61	0.343	0.352	34.6	31.3	0.091	0.098
62	0.343	0.362	34.6	31.9	0.091	0.107
63	0.343	0.361	34.6	33.4	0.091	0.106
64	0.343	0.364	34.6	33.7	0.091	0.104
65	0.343	0.343	42.2	43.0	0.104	0.126
66	0.343	0.328	42.2	39.4	0.104	0.115
67	0.343	0.339	42.2	40.7	0.104	0.117
68	0.343	0.352	42.2	41.0	0.104	0.117
69	0.343	0.340	42.2	41.5	0.104	0.117
70	0.325	0.336	45.6	41.7	0.105	0.125
71	0.325	0.324	45.6	39.6	0.105	0.126
72	0.325	0.334	45.6	39.3	0.105	0.132
73	0.325	0.341	45.6	38.5	0.105	0.131
74	0.325	0.337	45.6	38.9	0.105	0.128
75	0.396	0.390	15.5	15.6	0.060	0.062
76	0.396	0.378	15.5	15.7	0.060	0.063

	Basic Wood Density		Caustic Solubility		Buffering Capacity	
Sample	Measured	Predicted	Measured	Sample	Measured	Predicted
77	0.396	0.390	15.5	17.1	0.060	0.072
78	0.396	0.391	15.5	16.7	0.060	0.070
79	0.396	0.384	15.5	19.1	0.060	0.074
80	0.395	0.386	13.2	17.0	0.036	0.062
81	0.395	0.380	13.2	15.7	0.036	0.064
82	0.395	0.384	13.2	16.5	0.036	0.070
83	0.395	0.377	13.2	19.1	0.036	0.073
84	0.395	0.385	13.2	17.5	0.036	0.072
85	0.402	0.387	16.3	18.3	0.052	0.071
86	0.402	0.386	16.3	20.3	0.052	0.073
87	0.402	0.385	16.3	17.3	0.052	0.078
88	0.402	0.386	16.3	17.3	0.052	0.079
89	0.402	0.386	16.3	17.8	0.052	0.080
90	0.362	0.379	19.2	16.4	0.103	0.055
91	0.362	0.379	19.2	16.1	0.103	0.049
92	0.362	0.379	19.2	14.6	0.103	0.063
93	0.362	0.384	19.2	14.0	0.103	0.064
94	0.362	0.377	19.2	15.7	0.103	0.067
95	0.346	0.368	16.1	18.0	0.072	0.065
96	0.346	0.364	16.1	16.2	0.072	0.058
97	0.346	0.361	16.1	21.4	0.072	0.069
98	0.346	0.362	16.1	22.0	0.072	0.067
99	0.346	0.363	16.1	22.7	0.072	0.068
100	0.377	0.379	19.2	20.6	0.092	0.069
101	0.377	0.371	19.2	18.7	0.092	0.067
102	0.377	0.380	19.2	20.8	0.092	0.077
103	0.377	0.376	19.2	21.4	0.092	0.077
104	0.377	0.380	19.2	20.0	0.092	0.076
105	0.324	0.320	43.1	44.7	0.196	0.141
106	0.324	0.310	43.1	40.0	0.196	0.140
107	0.324	0.323	43.1	42.1	0.196	0.140
108	0.324	0.330	43.1	40.9	0.196	0.138
109	0.324	0.322	43.1	42.2	0.196	0.143
110	0.291	0.291	50.6	51.5	0.182	0.175
111	0.291	0.293	50.6	50.0	0.182	0.175
112	0.291	0.303	50.6	47.2	0.182	0.175
113	0.291	0.302	50.6	47.8	0.182	0.173
114	0.291	0.298	50.6	47.5	0.182	0.174
115	0.249	0.240	56.1	64.3	0.218	0.240

	Basic Wood Density		Caustic Solubility		Buffering Capacity	
Sample	Measured	Predicted	Measured	Sample	Measured	Predicted
116	0.249	0.225	56.1	61.1	0.218	0.234
117	0.249	0.263	56.1	57.3	0.218	0.222
118	0.249	0.254	56.1	58.8	0.218	0.222
119	0.249	0.257	56.1	58.3	0.218	0.228

Density Validation Dataset

	Basic Wood Density		Caustic Solubility		Buffering Capacity	
Sample	Measured	Predicted	Measured	Predicted	Measured	Predicted
1	0.414	0.367	13.1	10.1	0.033	0.037
2	0.414	0.369	13.1	9.4	0.033	0.037
3	0.414	0.366	13.1	10.8	0.033	0.051
4	0.414	0.368	13.1	9	0.033	0.047
5	0.414	0.371	13.1	10.1	0.033	0.048
6	0.424	0.396	18.8	18.1	0.056	0.053
7	0.424	0.395	18.8	18.4	0.056	0.054
8	0.424	0.395	18.8	16.5	0.056	0.067
9	0.424	0.394	18.8	16.1	0.056	0.066
10	0.424	0.389	18.8	17.4	0.056	0.066
11	0.39	0.368	14.5	16.8	0.054	0.069
12	0.39	0.366	14.5	15.6	0.054	0.064
13	0.39	0.369	14.5	15.6	0.054	0.065
14	0.39	0.37	14.5	14.7	0.054	0.062
15	0.39	0.371	14.5	15.8	0.054	0.066
16	0.373	0.373	28.2	25.1	0.093	0.073
17	0.373	0.372	28.2	25.5	0.093	0.077
18	0.373	0.368	28.2	26.6	0.093	0.082
19	0.373	0.371	28.2	26.4	0.093	0.08
20	0.373	0.377	28.2	25.4	0.093	0.077
21	0.404	0.388	17.6	18.3	0.066	0.065
22	0.404	0.379	17.6	16.9	0.066	0.063
23	0.404	0.369	17.6	20.8	0.066	0.066
24	0.404	0.369	17.6	21.7	0.066	0.068
25	0.404	0.37	17.6	20.4	0.066	0.069
26	0.390	0.398	17	13.3	0.083	0.047
27	0.390	0.386	17	17.1	0.083	0.063
28	0.390	0.394	17	14.9	0.083	0.065
29	0.390	0.391	17	16.2	0.083	0.069
30	0.390	0.397	17	14.9	0.083	0.065
31	0.320	0.344	38.7	41.2	0.132	0.117
32	0.320	0.331	38.7	39.1	0.132	0.118
33	0.320	0.34	38.7	34.1	0.132	0.103
34	0.320	0.34	38.7	32.9	0.132	0.103
35	0.320	0.339	38.7	34.9	0.132	0.105
36	0.330	0.363	16	15.6	0.05	0.064
37	0.330	0.358	16	16.5	0.05	0.066

	Basic Wood Density		Caustic Solubility		Buffering Capacity	
Sample	Measured	Predicted	Measured	Predicted	Measured	Predicted
38	0.330	0.36	16	17.6	0.05	0.077
39	0.362	0.362	12.7	14.7	0.047	0.054
40	0.362	0.358	12.7	14.5	0.047	0.057
41	0.362	0.361	12.7	16.8	0.047	0.067
42	0.362	0.36	12.7	17.1	0.047	0.068
43	0.362	0.358	12.7	16	0.047	0.07
44	0.395	0.397	17.6	18.5	0.056	0.048
45	0.395	0.393	17.6	19	0.056	0.049
46	0.395	0.391	17.6	18.3	0.056	0.059
47	0.395	0.395	17.6	17.8	0.056	0.058
48	0.395	0.39	17.6	19.1	0.056	0.061
49	0.376	0.336	36.4	34.4	0.118	0.127
50	0.376	0.337	36.4	33.7	0.118	0.122
51	0.376	0.332	36.4	34.4	0.118	0.124
52	0.376	0.332	36.4	34	0.118	0.124
53	0.376	0.327	36.4	33.5	0.118	0.125
54	0.340	0.343	38.3	38.3	0.135	0.115
55	0.340	0.334	38.3	36.9	0.135	0.109
56	0.340	0.351	38.3	38.6	0.135	0.116
57	0.340	0.343	38.3	38.2	0.135	0.114
58	0.340	0.342	38.3	38	0.135	0.116
59	0.401	0.393	17	14.4	0.033	0.061
60	0.401	0.388	17	13	0.033	0.057
61	0.401	0.396	17	13.3	0.033	0.064
62	0.401	0.394	17	14.2	0.033	0.066
63	0.401	0.394	17	14	0.033	0.065
64	0.404	0.383	13	16.9	0.055	0.068
65	0.404	0.37	13	16.2	0.055	0.07
66	0.404	0.379	13	15.5	0.055	0.071
67	0.404	0.379	13	17.4	0.055	0.074
68	0.404	0.377	13	17.4	0.055	0.075

Appendix II – Partial Least Squares Modeling

Partial Least Squares seeks to estimate the factors that capture the variance in both the concentration and spectral datasets at the same time. PLS uses the Nonlinear Iterative Partial Least Squares (NIPALS) algorithm to do this (Geladi and Kowalski,1986). PLS is based on the following equations:

$$\mathbf{R} = \mathbf{TP} + \mathbf{E}$$

$$\mathbf{C} = \mathbf{UQ} + \mathbf{F}$$

where **R** and **C** are the spectral and concentration matrices, respectively, the elements of matrices **T** and **U** are the score matrices, elements of **P** and **Q** are the factor loading matrices, and **E** and **F** are the associated error matrices (Beebe and Kowalski, 1987).

Models were developed using Grams/AI 7.01 Chemometrics software (ThermoGalactic Corp., Salem, NH). Spectra and concentration data were imported to create a training data file. A correlogram was then developed from this file and examined in order to select the regions to model. Spectral preprocessing was also selected at this time (ex: derivative spectra, MSC, etc.). Models were then determined by the software. The PRESS diagram was examined first to determine the optimum number of factors to use. Based on the number of factors selected, plots of predicted vs. measured data were developed and the r^2, and RMSECV were determined. Models were further examined to look for outliers and biases by plotting Studentized residuals as a function of sample leverage. To use the model to predict new spectra, a calibration file was created based on the best modeling parameters determined and the optimum number of factors.

Experimental Data
FTIR – Caustic Solubility and Buffering Capacity

**** DATAINFO ****

Description :
Tot. Spectra: 163
Tot. Constit: 2
Tot. Points : 1946
X Unit Type : 1
Y Unit Type : 2
First X : 4369.997
Last X : 479.9995

**** EXPINFO ****

Experiment : Calibration msc 1864-1684 20f cv pls-1
Num. Spectra: 117
Num. Constit: 2
Calibration : PLS1
Regions : 1
Factor Sets : 2

Cal Factors : 5 5
Preprocessing Used:
Mean Center
MSC

**** BANDS ****

Left	Right	Space	Points	Group
1863.998	1683.999	1	91	Avg

**** CNAME ****

	Mean Concentration
Caustic	20.8641
Buffer	.07711111

**** PLSCAL ****

	Low	High	Bias	Slope
Caustic	10.8	68.3	0	1
Buffer	0	.282	0	1

Slims	Fratio
.0008139562	.01447163
.00111937	.01821818

PLS Cross Products:
50.64503 47.27146 118.8362 78.5845 88.57378 .2974773 .215655 .8754187 .3456156 .6686719

FTIR - Density

**** DATAINFO ****

Description :
Tot. Spectra: 70
Tot. Constit: 1
Tot. Points : 1976
X Unit Type : 1
Y Unit Type : 2
First X : 4399.997
Last X : 449.9995

**** EXPINFO ****

Experiment : 1842-1486 23pt 1st deriv 25f pls-1 cv wo rand
Num. Spectra: 47
Num. Constit: 1
Calibration : PLS1

Regions : 1
Factor Sets : 1
Cal Factors : 5
Preprocessing Used:
Mean Center
Derivative - SG 1st

**** BANDS ****

Left	Right	Space	Points	Group
1841.998	1485.999	1	179	Avg

**** CNAME ****

	Mean Concentration
Density	.3691064

**** PLSCAL ****

	Low	High	Bias	Slope
Density	.249	.424	0	1

Slims	Fratio
.0005992955	.01180198

PLS Cross Products:
1.365652 1.551384 1.216619 1.60893 1.023563

NIR - Caustic Solubility and Buffering Capacity

**** DATAINFO ****

Description :
Tot. Spectra: 300
Tot. Constit: 2
Tot. Points : 2151
X Unit Type : 3
Y Unit Type : 129
First X : 350
Last X : 2500

**** EXPINFO ****

Experiment : Calibration 1000 to 2400 nm 1st SG 23pt 20f
Num. Spectra: 225
Num. Constit: 2
Calibration : PLS1
Regions : 1

Factor Sets : 2
Cal Factors : 10 10
Preprocessing Used:
Mean Center
Derivative - SG 1st

**** BANDS ****

Left	Right	Space	Points	Group
1000	2400	1	1401	Avg

**** CNAME ****

	Mean Concentration
Caustic	21.28578
Buffer	.07905778

**** PLSCAL ****

	Low	High	Bias	Slope
Caustic	10.8	68.3	0	1
Buffer	0	.327	0	1

Slims	Fratio
.00001127898	.0009116035
.00001093102	.0009052454

PLS Cross Products:
261.8274 1537.036 2362.879 1472.814 5236.932 1072.125 1879.451 2724.957 3385.829 3227.361 1.142844 18.76603 7.839204 13.55923 13.9496 9.244175 5.616222 22.92923 20.6917 16.45571

NIR - Density

**** DATAINFO ****

Description :
Tot. Spectra: 189
Tot. Constit: 1
Tot. Points : 2151
X Unit Type : 3
Y Unit Type : 129
First X : 350
Last X : 2500

**** EXPINFO ****

Experiment : LevRes Calibration 1458-1721, 2062-2336 nm 20f 23pt 1st deriv SG
Num. Spectra: 119

Num. Constit: 1
Calibration : PLS1
Regions : 2
Factor Sets : 1
Cal Factors : 3
Preprocessing Used:
Mean Center
Derivative - SG 1st

**** BANDS ****

Left	Right	Space	Points	Group
1458	1721	1	264	Avg
2062	2336	1	275	Avg

**** CNAME ****

	Mean Concentration
Density	.3629664

**** PLSCAL ****

	Low	High	Bias	Slope
Density	.249	.407	0	1

Slims	Fratio
.000003479781	.000114049

PLS Cross Products:
15.57925 9.266508 11.89317

Appendix III – Factor Loadings for PLS Models

FTIR - Caustic Solubility Model

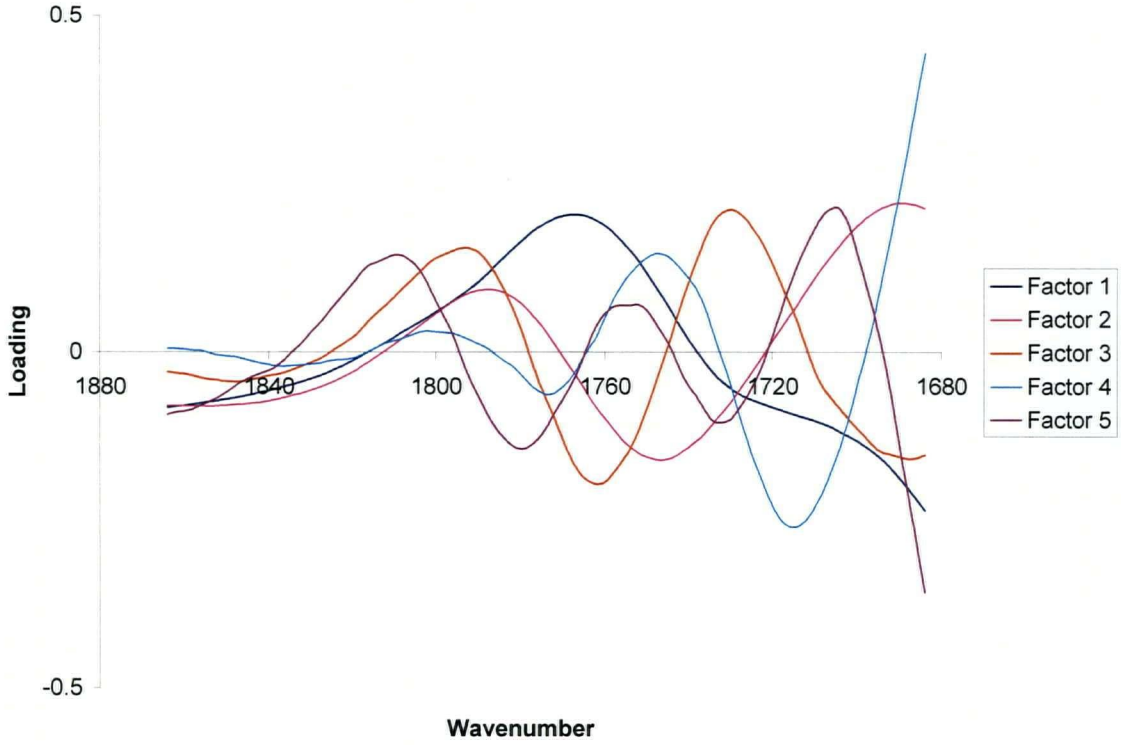

FTIR - Buffering Capacity Model

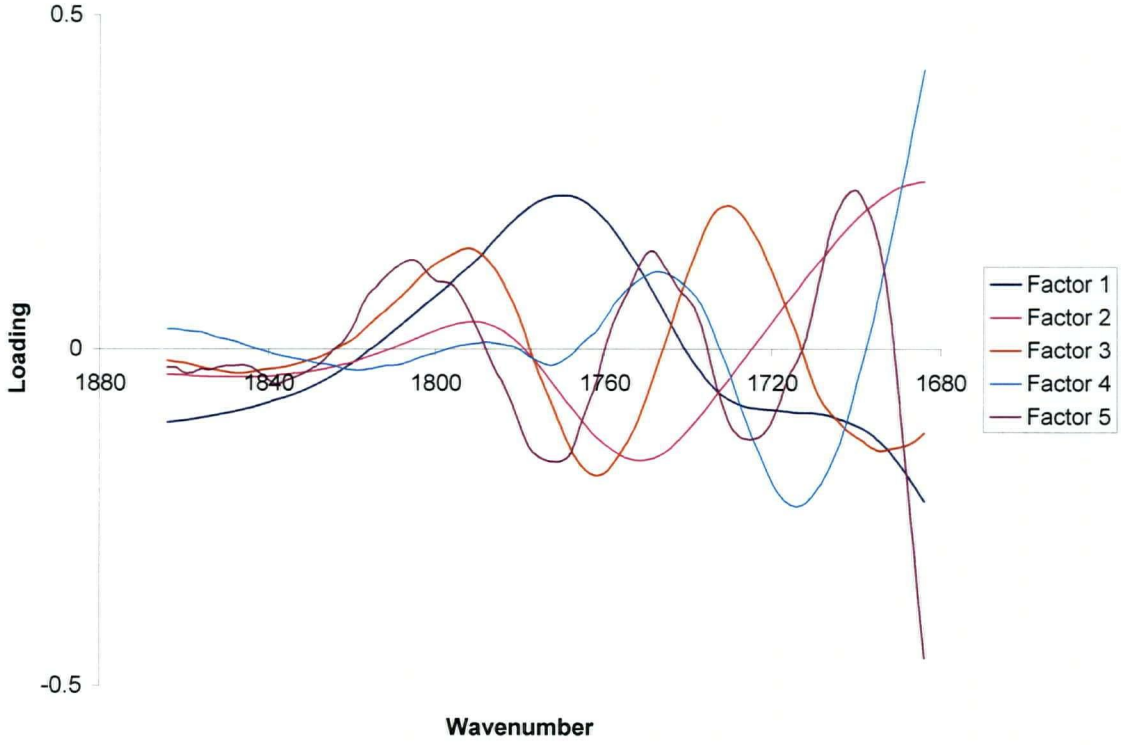

FTIR - Basic Wood Density Model

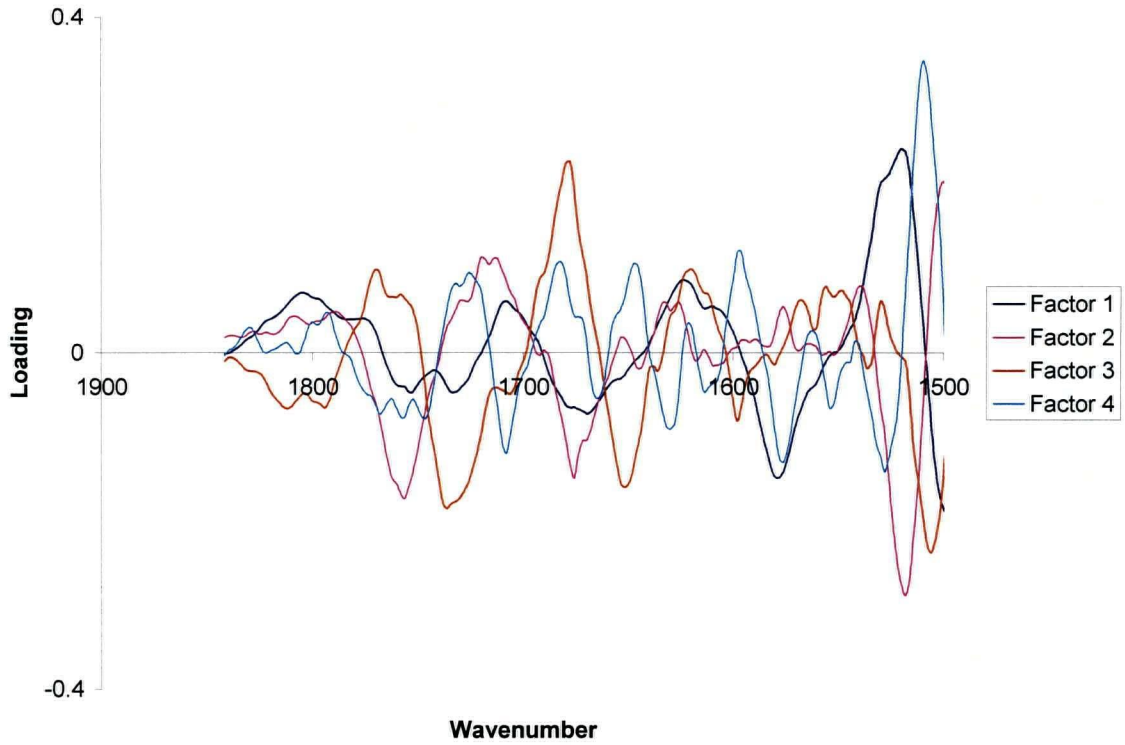

NIR - Caustic Solubility Model

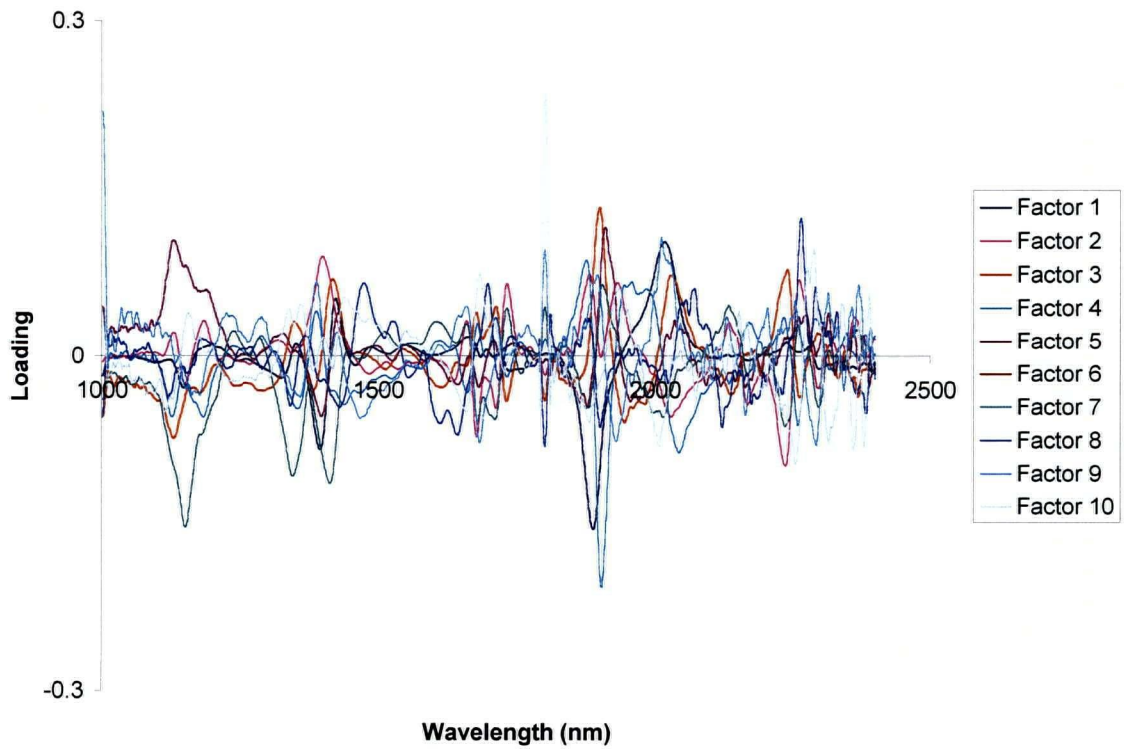

NIR – Buffering Capacity Model

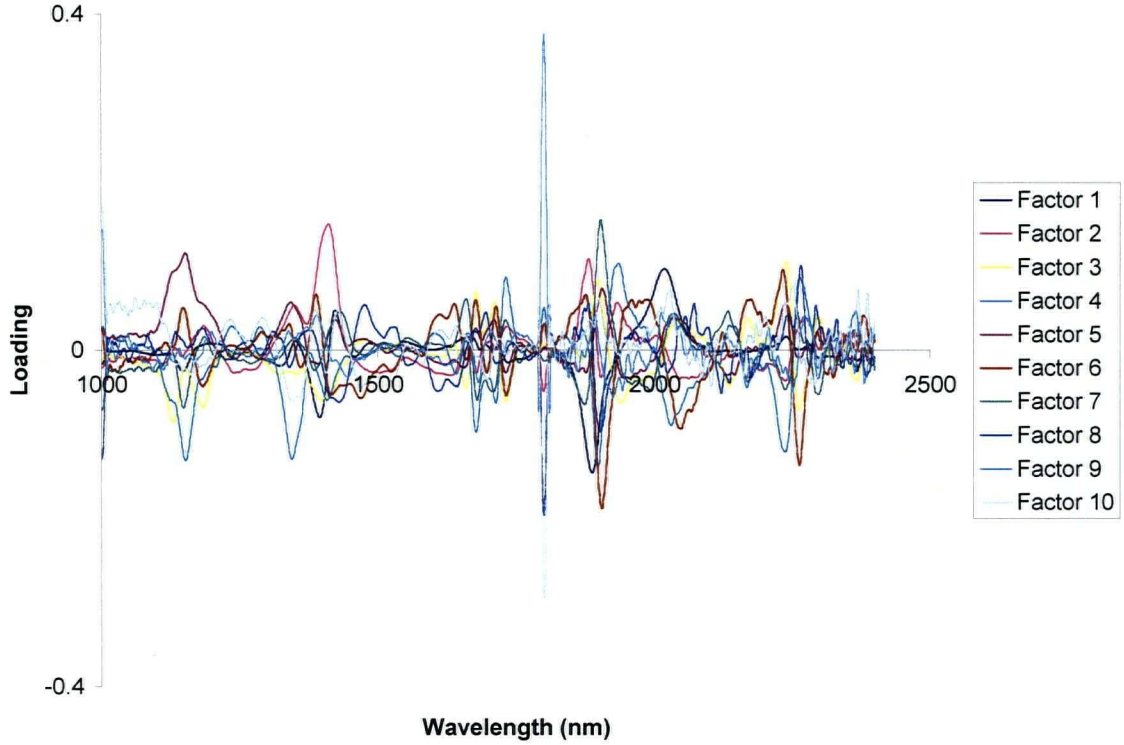

NIR – Basic Wood Density Model

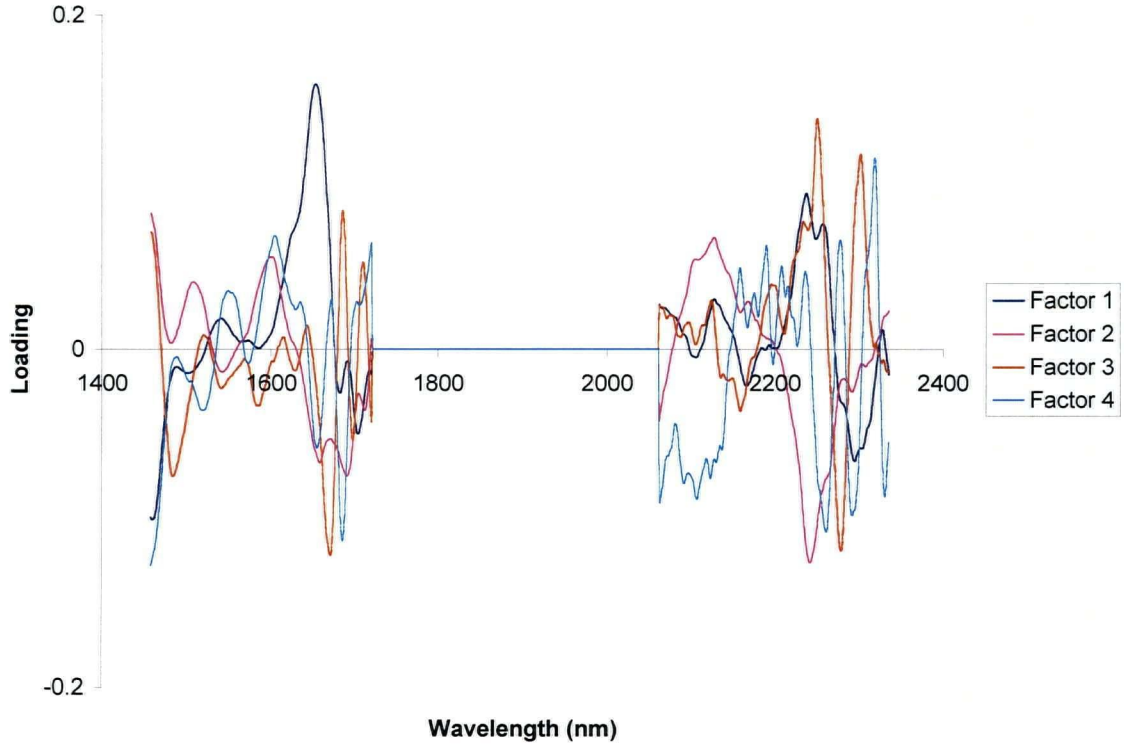

Appendix IV – Correlograms for PLS Models
FTIR-Based Decay Correlogram

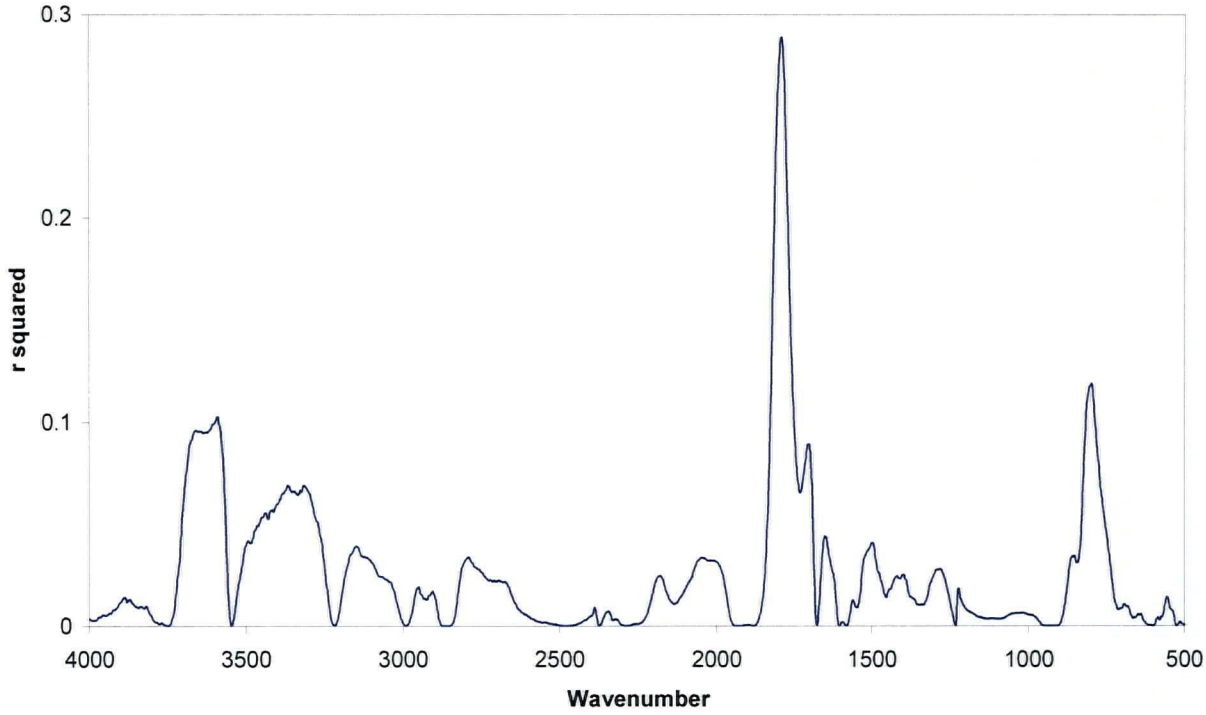

FTIR-based Density Correlogram

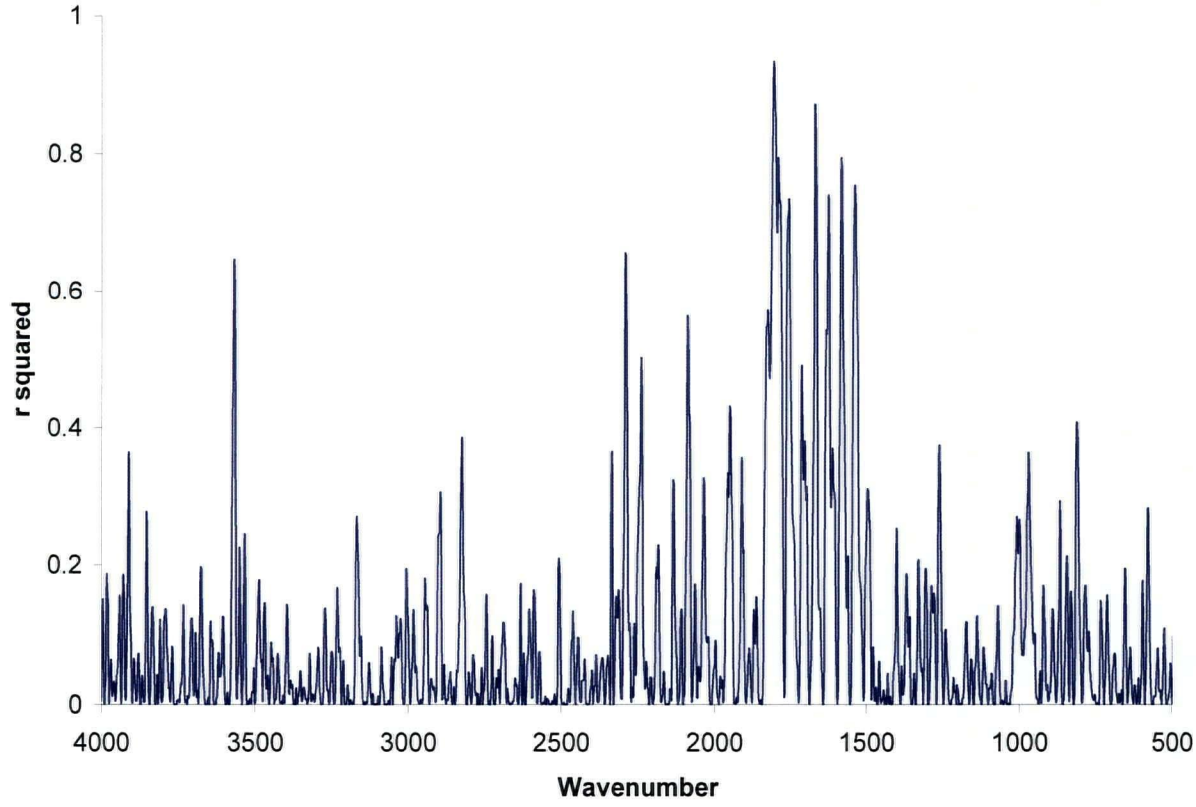

NIR-based Decay Correlogram

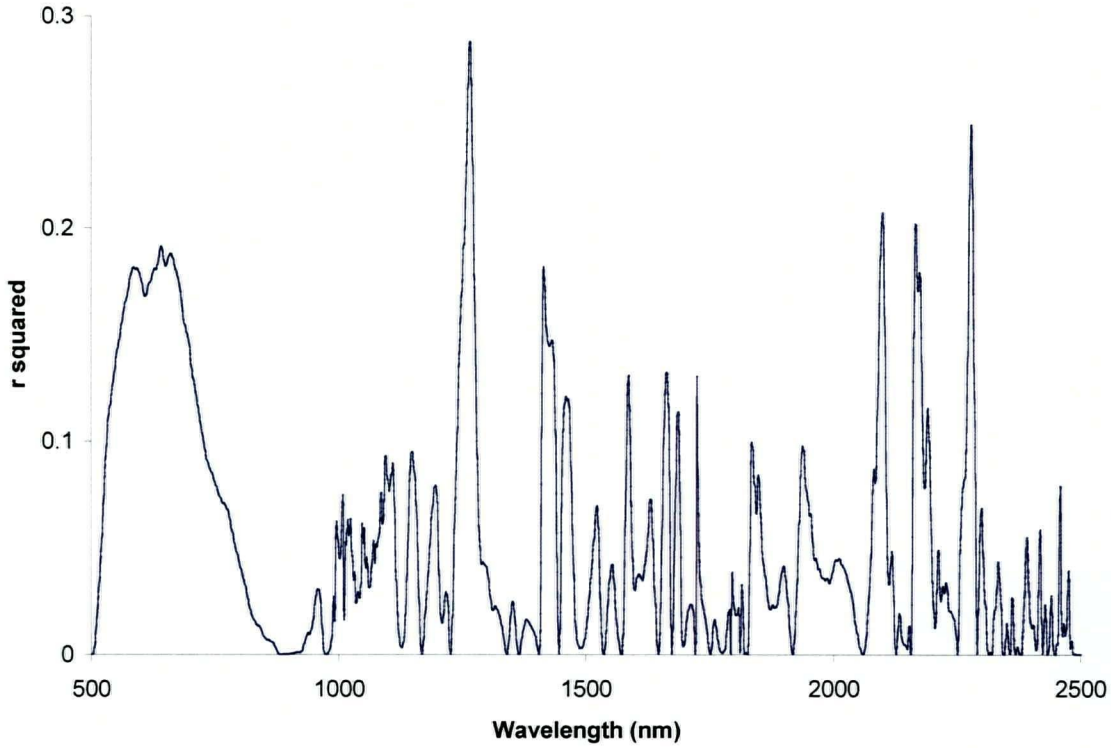

NIR-based Wood Density Correlogram

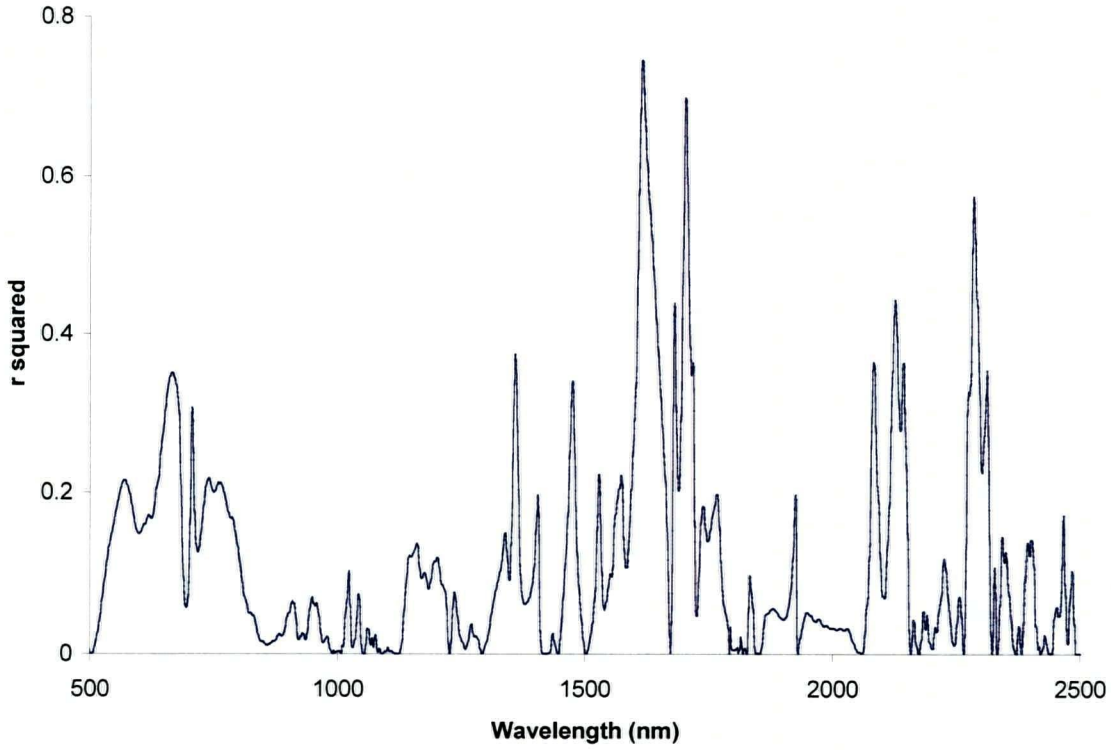

Appendix V - PRESS Diagrams for PLS Models

FTIR-Based PRESS Diagrams for Caustic Solubility and Buffering Capacity

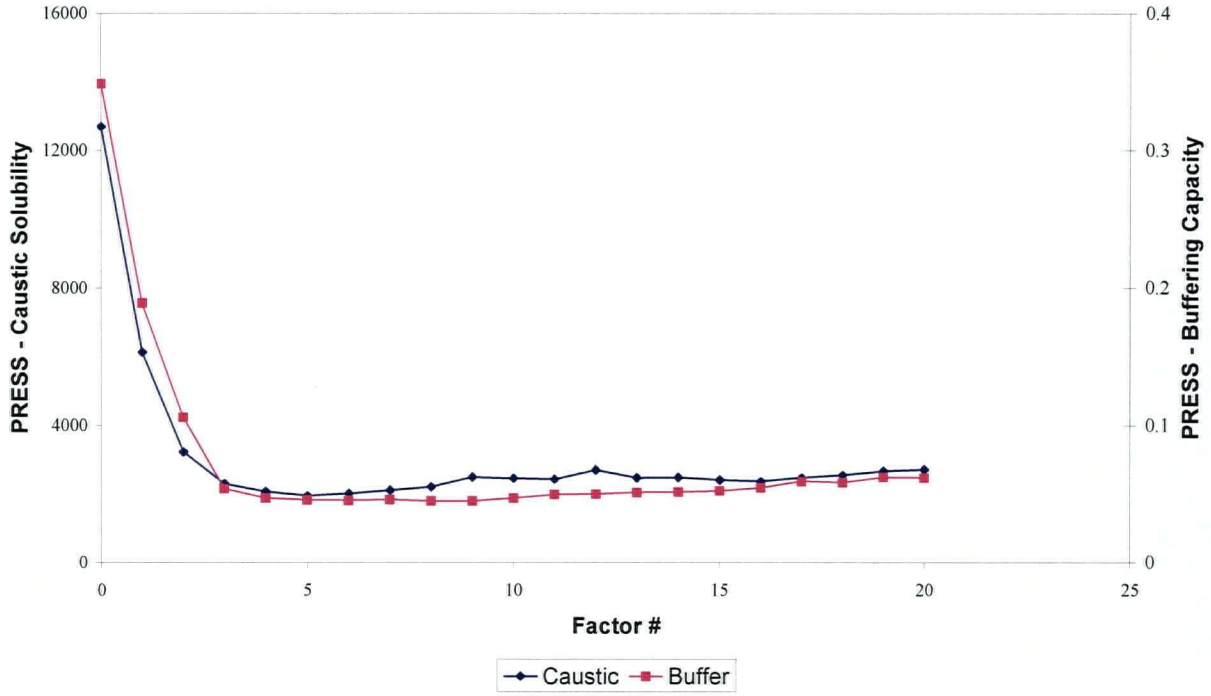

FTIR-Based PRESS Diagram for Basic Wood Density

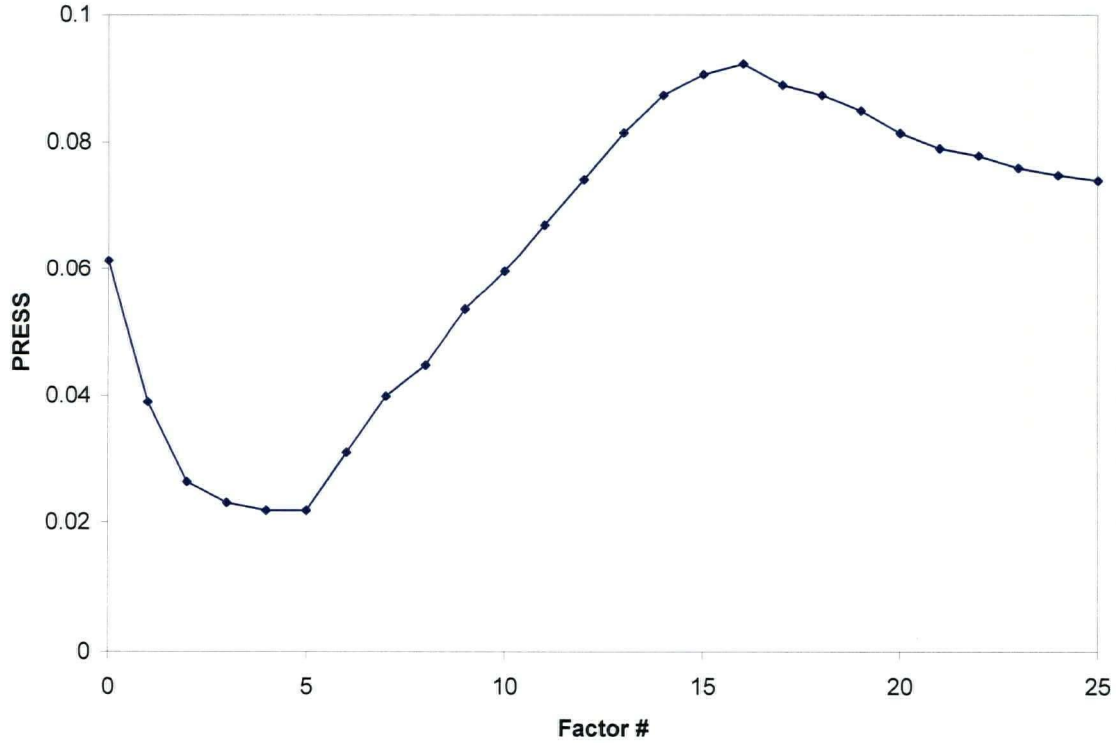

NIR-Based PRESS Diagrams for Caustic Solubility and Buffering Capacity

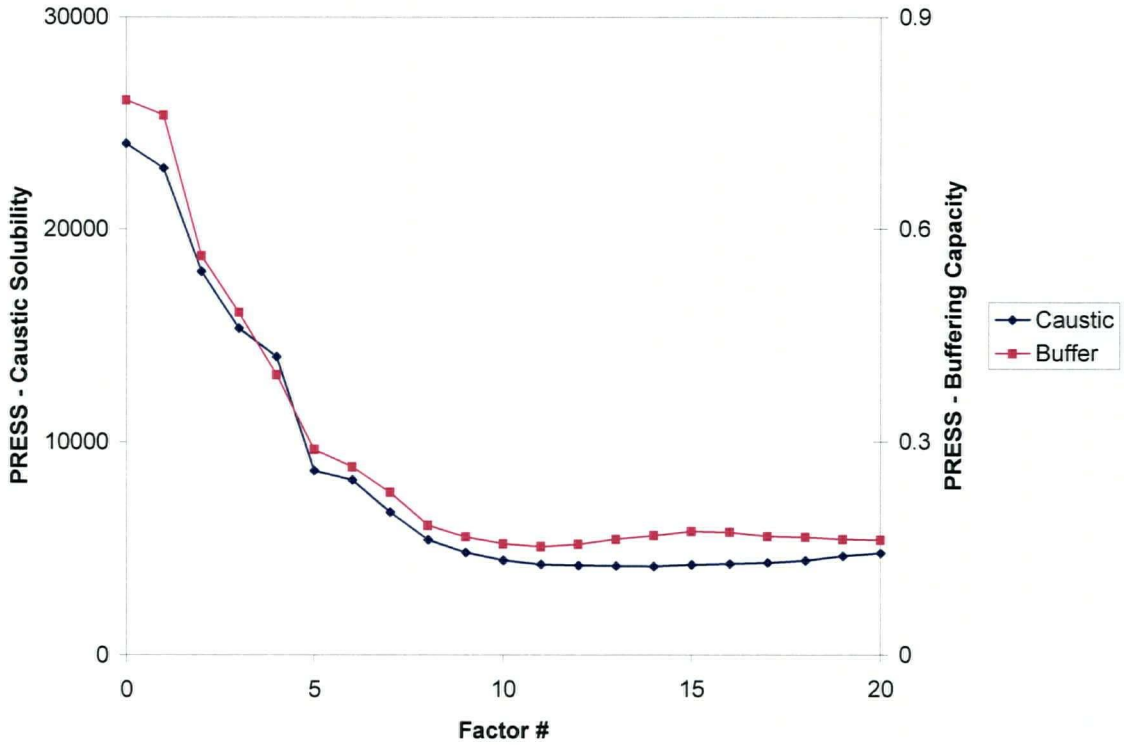

NIR-Based PRESS Diagram for Basic Wood Density

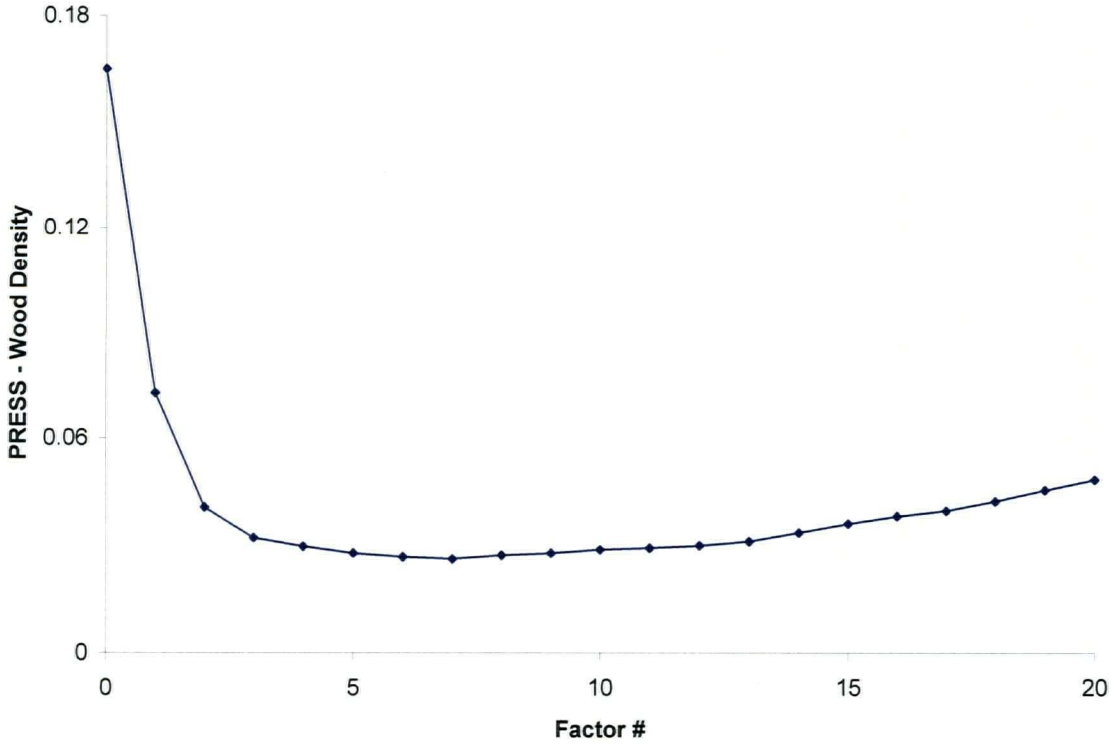

Appendix VI - Chromatograms of Alditol Acetates

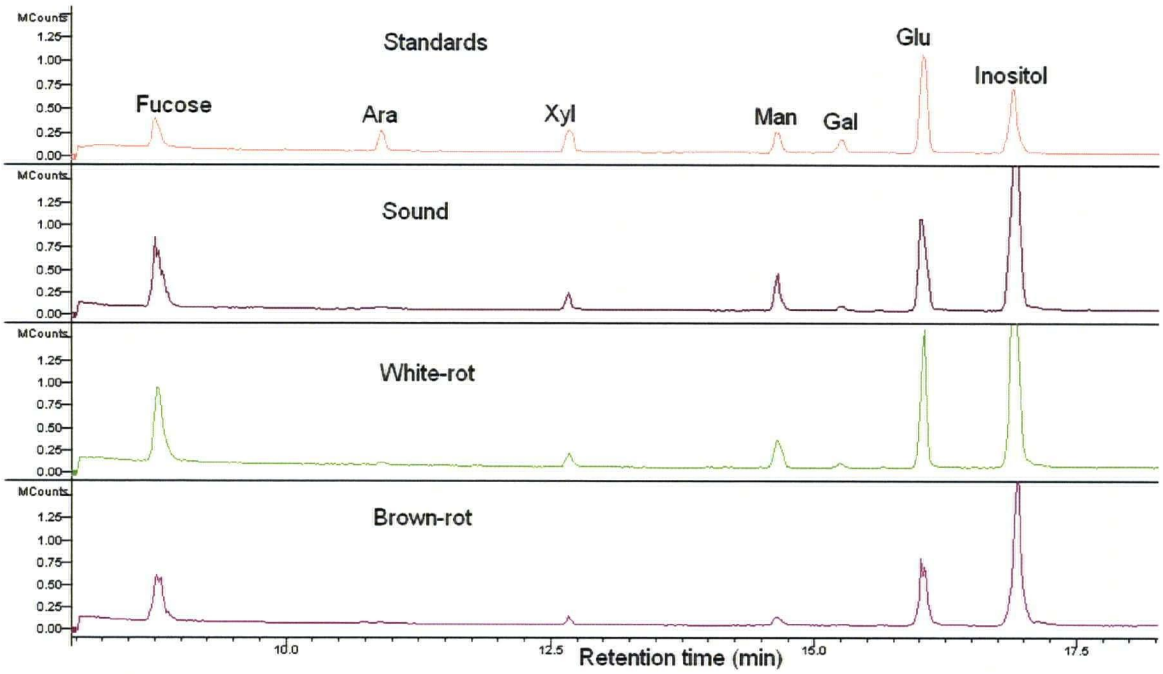

Sugars automatically quantified using Saturn GC/MS Workstation version 5.52. Concentration data are presented in Table 4.2.

Analyte	Retention time (min)	Sound Peak Area	White-rot Peak Area	Brown-rot Peak Area
Fucose (IS)	8.78	2319059	1608939	1855123
Arabinose	10.88	104258	320754	37107
Xylose	12.63	528923	565728	216316
Mannose	14.62	1191331	1705706	235408
Galactose	15.22	130183	155524	60072
Glucose	15.97	4426472	5714324	2629136
Inositol (IS)	16.87	11647736	10745621	7896555

Appendix VII - Mass Spectra and GC Data

Data from the Chromatogram Presented in Figure 4.5

Sample	Propanoic acid TMS	2-Butanoic acid TMS	4-Butanoic acid TMS	4-Pentanoic acid TMS	SUM
Peak Areas					
Sound	12022	8602	9843	9170	39637
P.igniarius	33592	16507	10081	17805	77985
G. trabeum	60571	18606	7371	56207	142755
Peak Areas Relative to Internal Standard					
Sound	0.2056	0.1471	0.1684	0.1569	0.6780
P.igniarius	0.4899	0.2407	0.1470	0.2597	1.1374
G. trabeum	2.4173	0.7425	0.2942	2.2432	5.6972
Concentration in Caustic Extract (mg/L)					
Sound	60	43	49	45	197
P.igniarius	142	70	43	75	330
G. trabeum	701	215	85	651	1652

Internal Standard – Xylitol, 290 mg/L

Sample	Area of Internal Standard
Sound	58460
P.igniarius	68567
G. trabeum	25057

Library search results: Acetic acid phenylmethyl ester
Purity: 697
Fit: 834
Reverse fit: 770

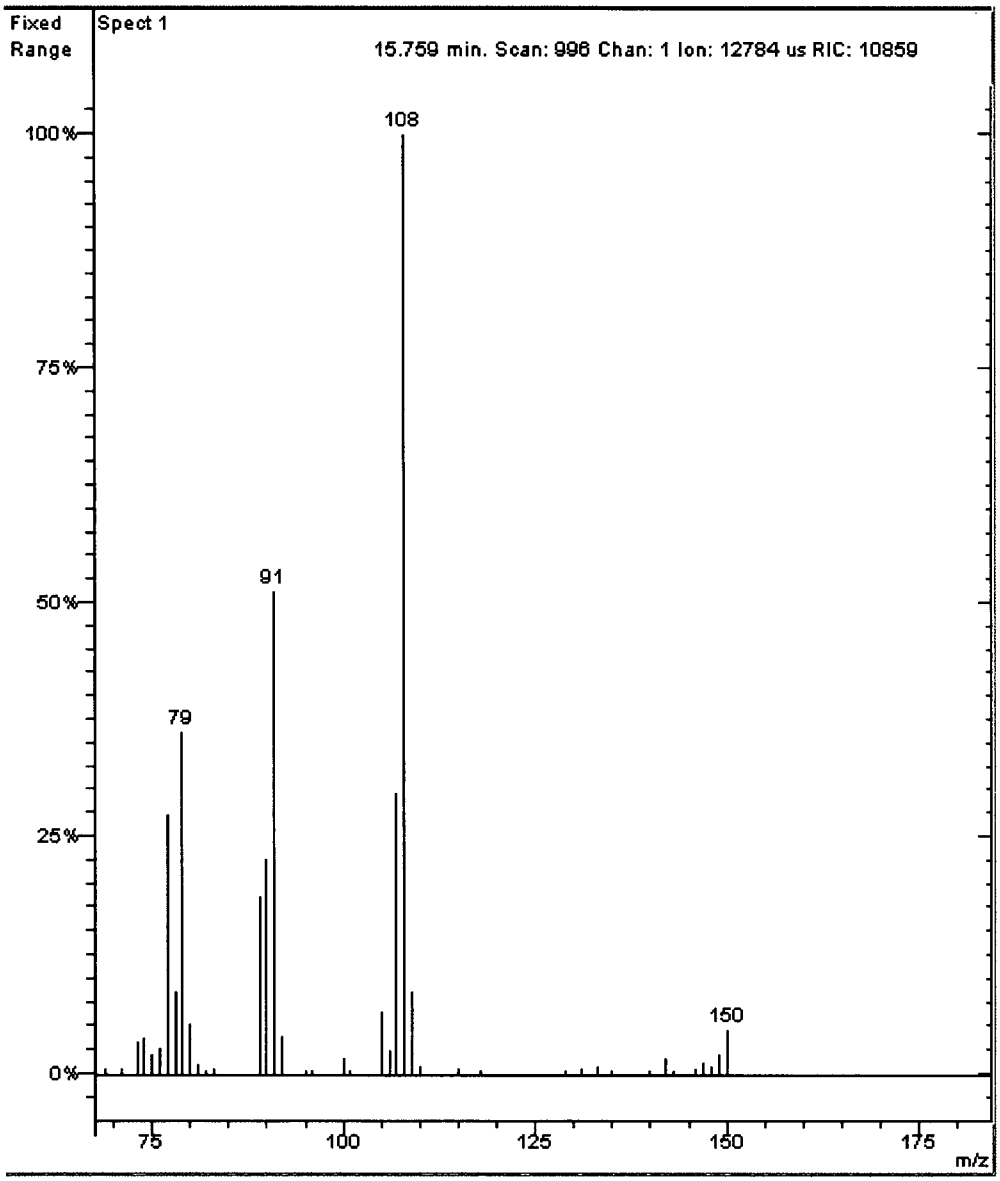

Library search results: Benzyl but-2-enoate (Internal Standard)
Purity: 523
Fit: 860
Reverse fit: 547

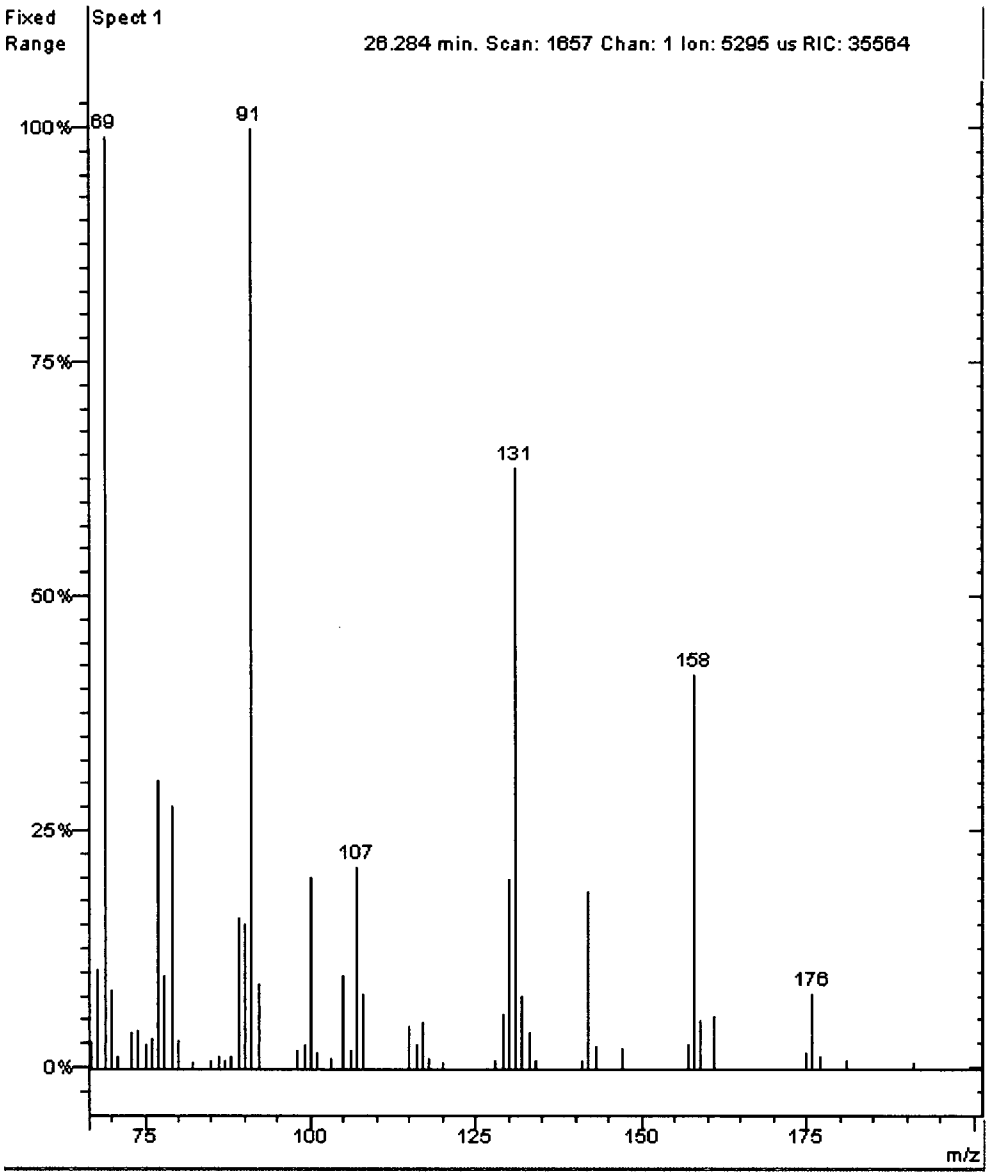

Library search results: Propanoic acid, 2-TMS ester
Purity: 656
Fit: 868
Reverse fit: 707

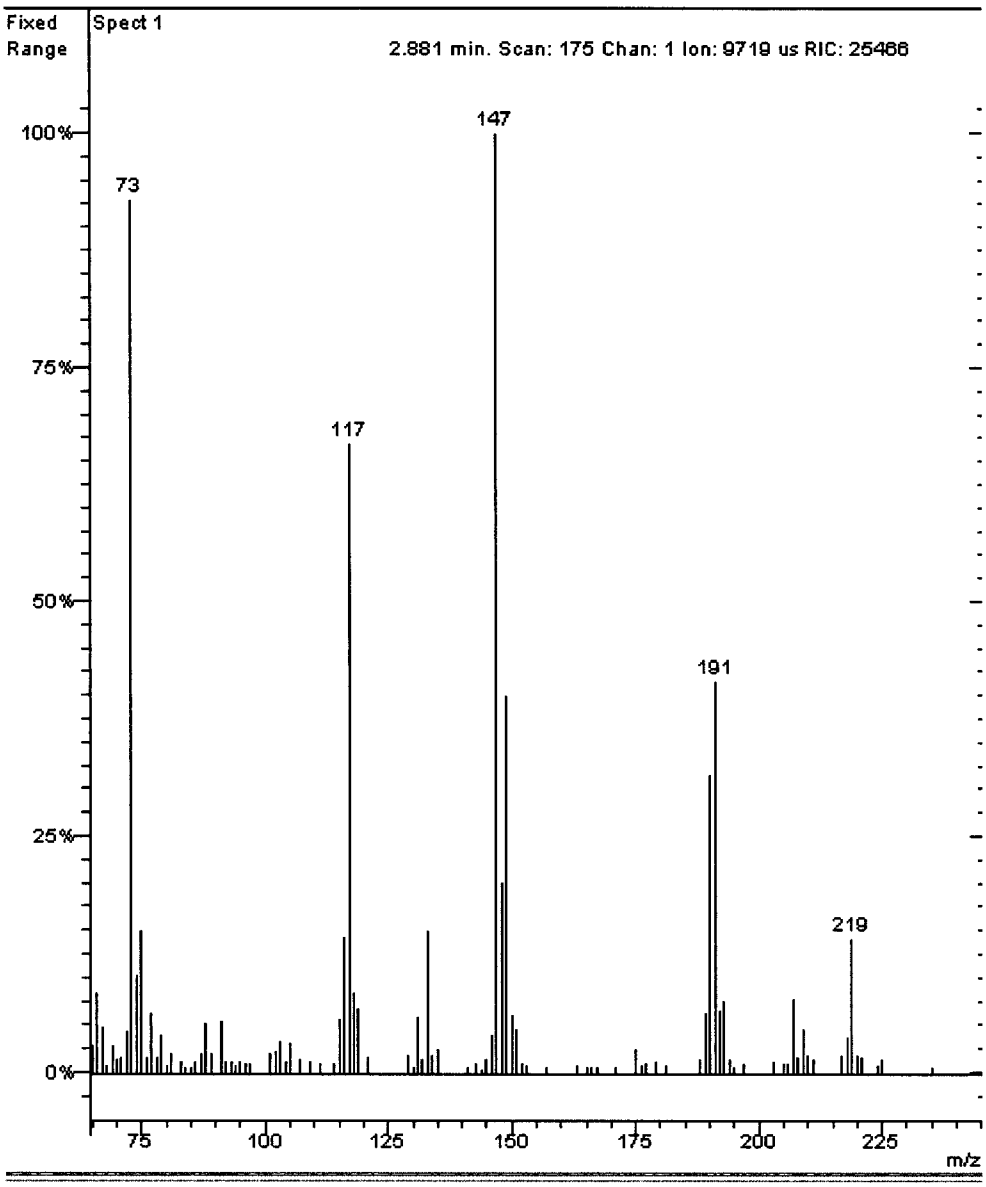

Library search results: Butanoic acid, 2-TMS ester
Purity: 683
Fit: 866
Reverse fit: 731

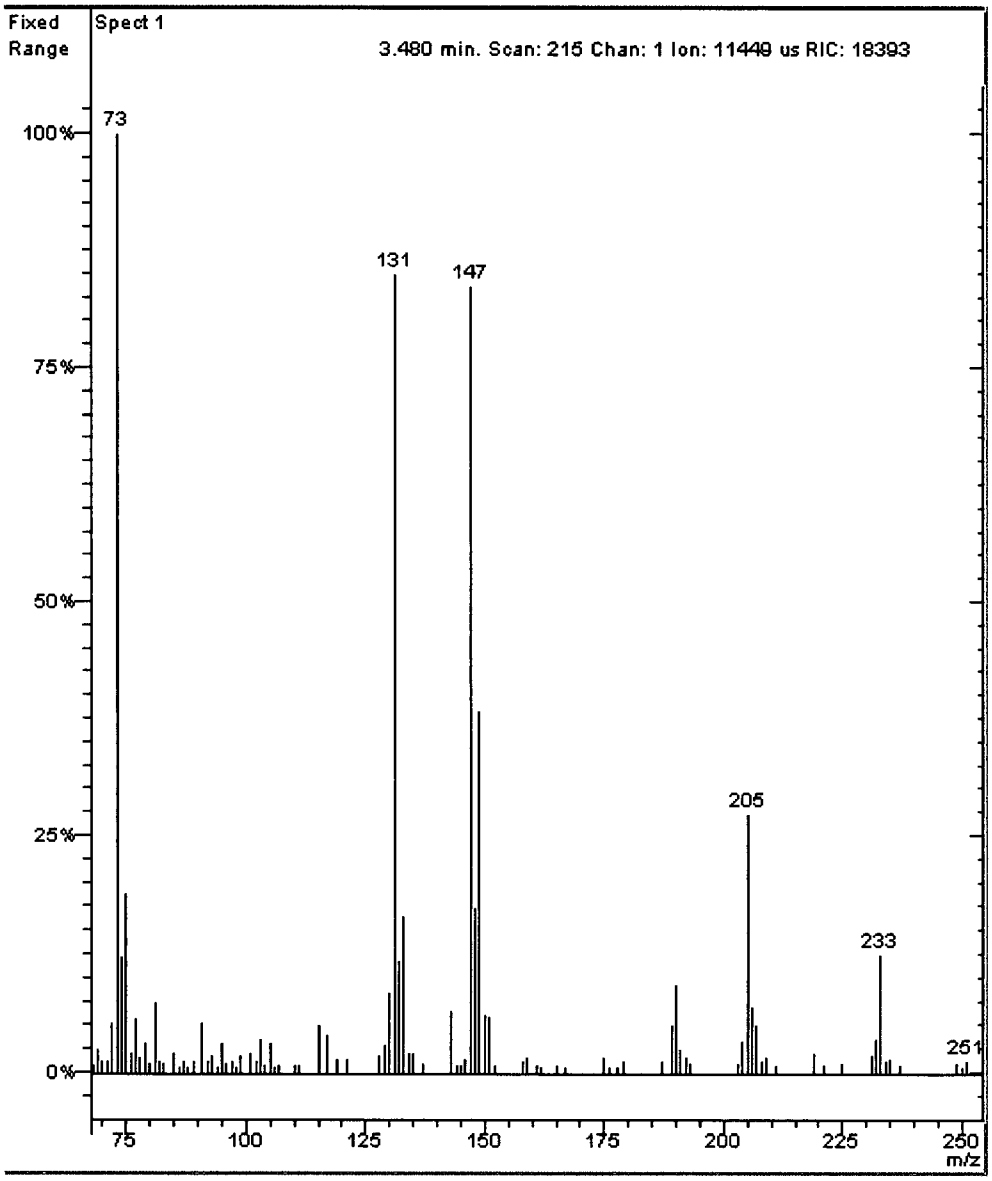

Library search results: Pentanoic acid, 4-TMS ester
Purity: 470
Fit: 706
Reverse fit: 518

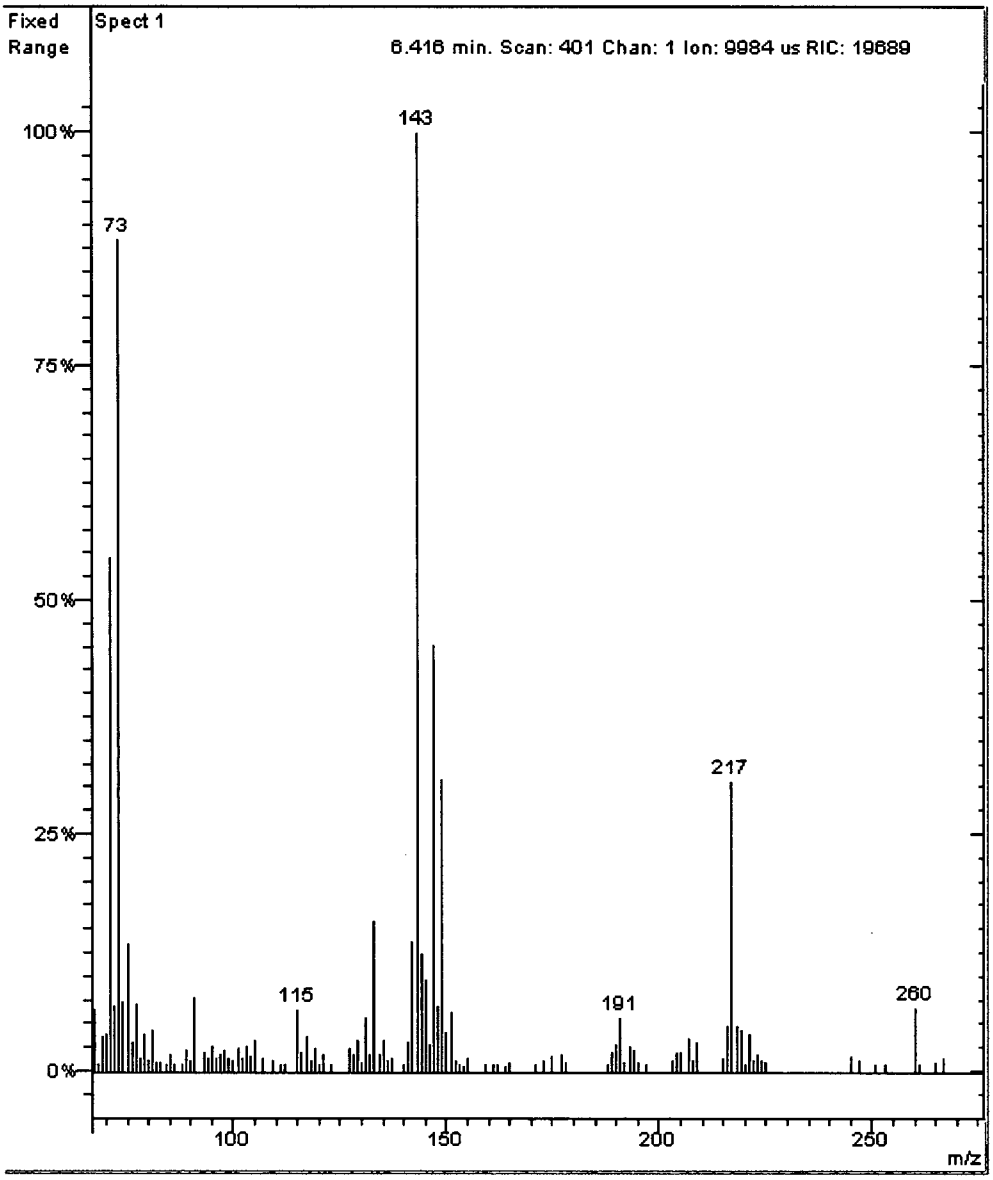

Library search results: Xylitol, 1,2,3,4,5-pentakis-O-TMS ether (Internal Standard)
Purity: 661
Fit: 914
Reverse fit: 667

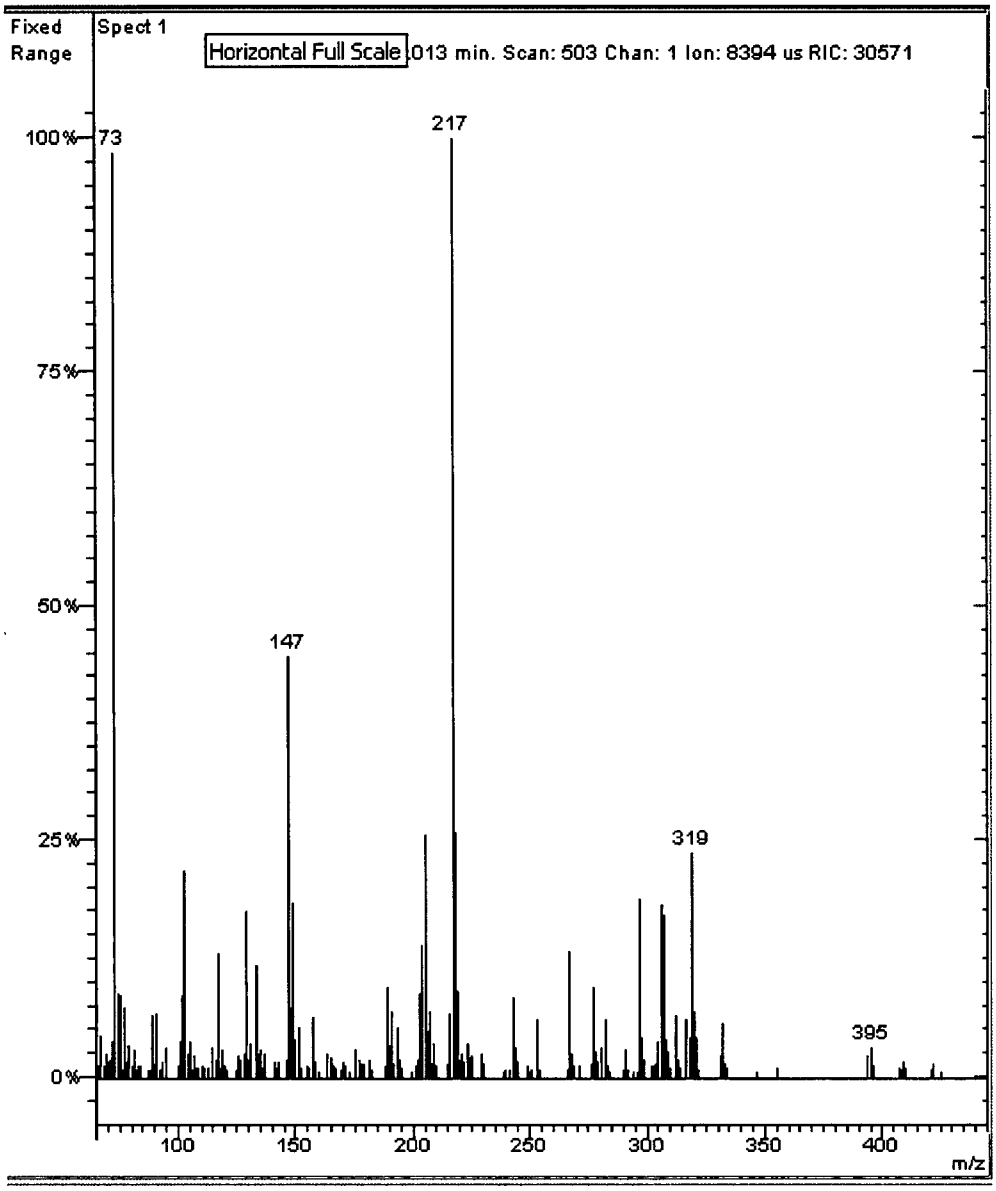

Appendix VIII – FTIR Spectra

Full FTIR Spectra from which Figure 4.6 was taken

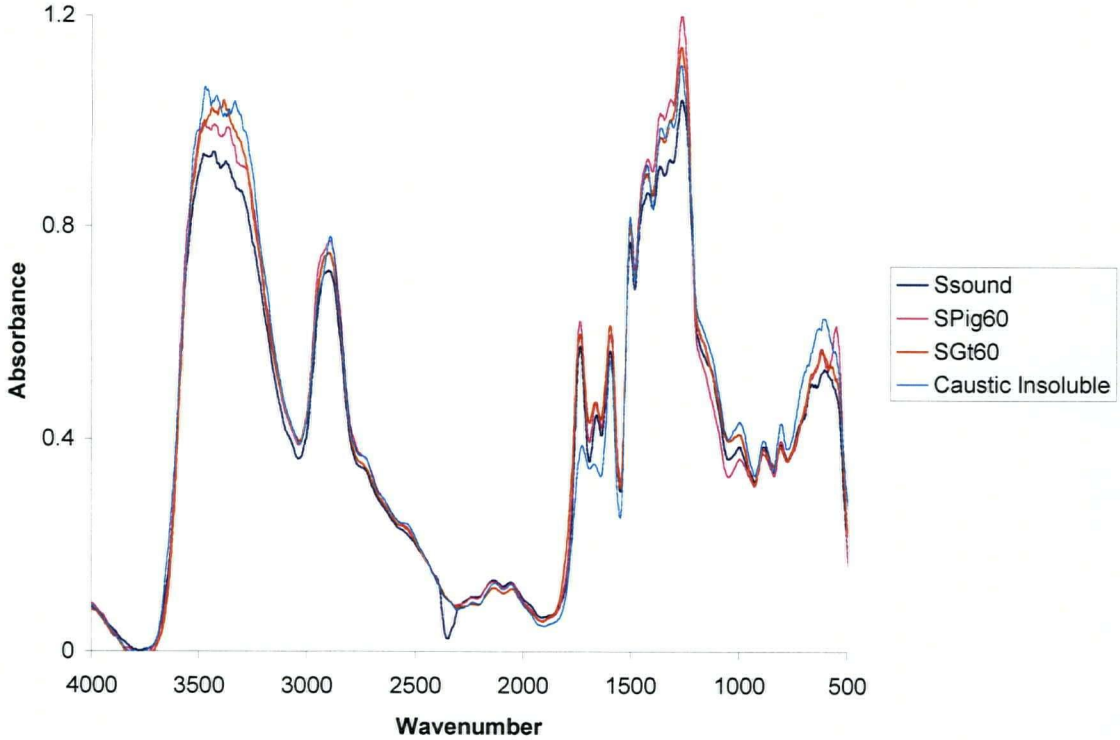

First Derivative (31-point Savitzky-Golay) FTIR Spectra of Sound, White-rot and Brown-rot Decayed Spruce

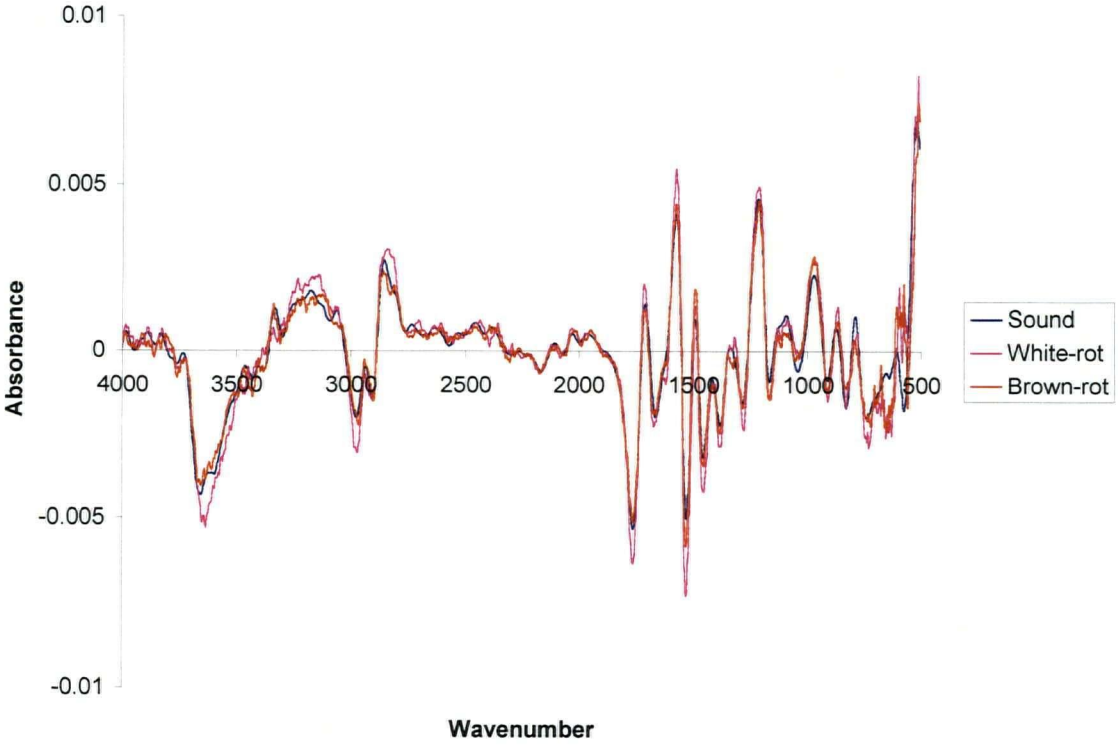

Full FTIR Spectra from which Figure 4.7 was taken

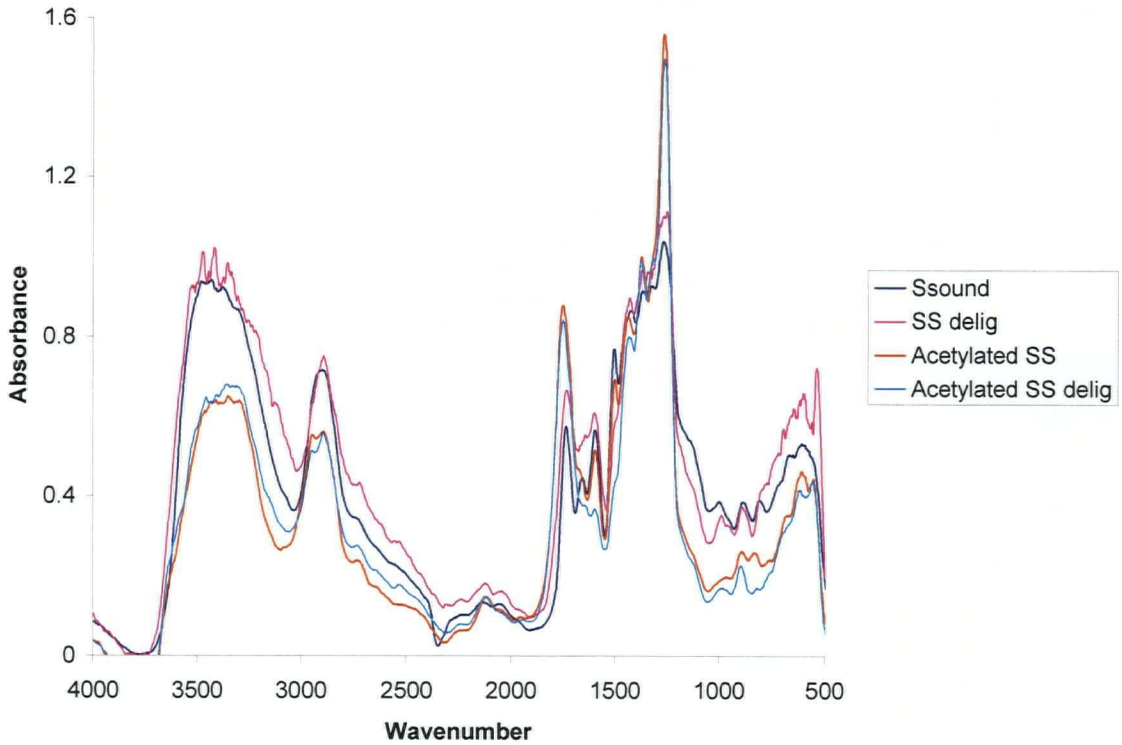

Appendix IX - Thermomechanical Pulping Data *

Property	Sound		
Unscreened CSF (mL)	86	141	196
Specific Energy (MJ/kg)	13.7	10.6	8.7
Canadian Standard Freeness (mL)	90	160	216
Reject (% od pulp)	0.0	0.0	0.0
Apparent Sheet Density (kg/m^3)	370	323	294
Burst Index (kPa•m^2/g)	2.2	1.8	1.6
Tensile Index (N•m/g)	36.8	27.9	26.0
Stretch (%)	1.37	1.11	1.15
Tear Index (mN•m^2/g) (4 Ply)	6.1	6.6	6.3
Brightness (%)	56	57	57
ISO Opacity (%)	96.2	94.7	93.4
Scattering Coeff. (cm^2/g)	598	560	532
Sheffield Roughness (SU)	167	252	297
Bauer McNett R-14 (%)	0.9	1.6	2.1
Bauer McNett 14/28 (%)	20.1	24.2	26.0
Bauer McNett 28/48 (%)	25.9	26.2	25.9
Bauer McNett 48/100 (%)	18.2	17.8	17.2
Bauer McNett 100/200 (%)	9.3	8.2	7.9
Bauer McNett (P-200) (%)	25.7	22.0	20.8
W. Weighted Average Fibre Length (mm)	1.61	1.66	1.72
L. Weighted Average Fibre Length (mm)	1.16	1.22	1.25

* To obtain an estimate of the error associated with the pulp physical tests, refer to the standard deviations provided for the refiner mechanical and kraft pulping data (Appendices X and XI)

Property	Stored-Sound			
Unscreened CSF (mL)	91	118	154	230
Specific Energy (MJ/kg)	12.8	11.4	9.8	6.0
Canadian Standard Freeness (mL)	102	120	173	243
Reject (% od pulp)	0.0	0.0	0.0	0.1
Apparent Sheet Density (kg/m^3)	348	338	310	278
Burst Index (kPa•m^2/g)	2.2	2.1	1.9	1.6
Tensile Index (N•m/g)	39.1	35.8	33.6	25.9
Stretch (%)	1.57	1.40	1.49	1.27
Tear Index (mN•m^2/g) (4 Ply)	6.6	6.6	6.9	6.7
Brightness (%)	49	49	49	48
ISO Opacity (%)	97.6	97.3	96.7	95.9
Scattering Coeff. (cm^2/g)	572	565	544	516
Sheffield Roughness (SU)	184	213	275	339
Bauer McNett R-14 (%)	1.9	2.0	2.5	3.3
Bauer McNett 14/28 (%)	24.5	25.6	26.2	27.8
Bauer McNett 28/48 (%)	23.1	23.6	23.9	22.9
Bauer McNett 48/100 (%)	17.4	18.1	17.4	16.9
Bauer McNett 100/200 (%)	8.0	7.7	7.2	7.4
Bauer McNett (P-200) (%)	25.2	23.0	22.9	21.7
W. Weighted Average Fibre Length (mm)	1.68	1.68	1.70	1.73
L. Weighted Average Fibre Length (mm)	1.21	1.20	1.21	1.24

Property	Low Inoculation			
Unscreened CSF (mL)	95	106	154	227
Specific Energy (MJ/kg)	13.9	12.7	10.8	8.9
Canadian Standard Freeness (mL)	95	108	147	218
Reject (% od pulp)	0.0	0.0	0.0	0.0
Apparent Sheet Density (kg/m^3)	349	331	301	282
Burst Index ($kPa \cdot m^2/g$)	2.4	2.2	1.9	1.7
Tensile Index ($N \cdot m/g$)	37.1	37.2	31.8	29.1
Stretch (%)	1.31	1.45	1.42	1.35
Tear Index ($mN \cdot m^2/g$) (4 Ply)	6.4	6.5	7.0	6.4
Brightness (%)	46	46	45	45
ISO Opacity (%)	98.1	97.7	97.4	96.4
Scattering Coeff. (cm^2/g)	574	549	534	497
Sheffield Roughness (SU)	198	225	276	332
Bauer McNett R-14 (%)	1.4	1.6	2.4	2.6
Bauer McNett 14/28 (%)	25.7	26.4	29.7	30.7
Bauer McNett 28/48 (%)	23.6	23.8	24.1	23.5
Bauer McNett 48/100 (%)	14.6	14.4	14.5	13.6
Bauer McNett 100/200 (%)	7.7	7.9	7.1	6.7
Bauer McNett (P-200) (%)	27.1	25.9	22.3	23.0
W. Weighted Average Fibre Length (mm)	1.73	1.72	1.79	1.80
L. Weighted Average Fibre Length (mm)	1.29	1.29	1.35	1.37

Property	Medium Inoculation			
Unscreened CSF (mL)	88	98	174	223
Specific Energy (MJ/kg)	12.7	11.5	9.3	7.7
Canadian Standard Freeness (mL)	85	101	168	253
Reject (% od pulp)	0.0	0.0	0.1	0.1
Apparent Sheet Density (kg/m^3)	355	333	296	269
Burst Index (kPa•m^2/g)	2.4	2.3	1.9	1.6
Tensile Index (N•m/g)	40.6	36.4	31.9	27.5
Stretch (%)	1.56	1.37	1.35	1.34
Tear Index (mN•m^2/g) (4 Ply)	6.1	6.4	6.8	6.7
Brightness (%)	46	46	45	45
ISO Opacity (%)	98.2	98.0	97.5	96.7
Scattering Coeff. (cm^2/g)	573	569	535	493
Sheffield Roughness (SU)	201	229	299	348
Bauer McNett R-14 (%)	1.6	1.9	2.8	3.9
Bauer McNett 14/28 (%)	25.5	26.9	29.5	31.0
Bauer McNett 28/48 (%)	23.5	23.6	23.1	22.8
Bauer McNett 48/100 (%)	14.3	14.6	13.5	13.4
Bauer McNett 100/200 (%)	6.4	7.2	6.7	6.1
Bauer McNett (P-200) (%)	28.7	25.8	24.4	22.8
W. Weighted Average Fibre Length (mm)	1.71	1.73	1.79	1.83
L. Weighted Average Fibre Length (mm)	1.26	1.27	1.34	1.36

Property	High Inoculation			
Unscreened CSF (mL)	78	107	151	210
Specific Energy (MJ/kg)	13.6	11.9	9.9	8.3
Canadian Standard Freeness (mL)	88	105	176	238
Reject (% od pulp)	0.0	0.0	0.0	0.0
Apparent Sheet Density (kg/m^3)	352	346	313	278
Burst Index ($kPa \cdot m^2/g$)	2.5	2.4	2.2	1.8
Tensile Index ($N \cdot m/g$)	43.0	41.2	35.6	30.3
Stretch (%)	1.69	1.69	1.55	1.47
Tear Index ($mN \cdot m^2/g$) (4 Ply)	6.4	6.6	7.5	7.2
Brightness (%)	43	44	43	42
ISO Opacity (%)	98.2	98.0	97.6	97.2
Scattering Coeff. (cm^2/g)	545	529	513	485
Sheffield Roughness (SU)	205	209	271	346
Bauer McNett R-14 (%)	2.4	2.9	4.2	4.6
Bauer McNett 14/28 (%)	26.0	29.0	32.6	33.9
Bauer McNett 28/48 (%)	22.6	21.9	21.6	21.4
Bauer McNett 48/100 (%)	13.2	13.1	12.4	11.9
Bauer McNett 100/200 (%)	6.6	5.7	5.3	5.6
Bauer McNett (P-200) (%)	29.3	27.5	24.0	22.6
W. Weighted Average Fibre Length (mm)	1.81	1.84	1.90	1.93
L. Weighted Average Fibre Length (mm)	1.37	1.41	1.44	1.46

Trembling aspen (*Populus tremuloides*) was obtained from the Peace District in British Columbia. In order to prepare wood chips for and chemithermomechanical pulping, two plastic bags were stored at 34°C for 90 days: one containing 11.2 kg of aspen chips inoculated with *G. trabeum*; and one containing 12 kg (OD equivalent) of un-inoculated aspen chips. These samples were stored at -6°C prior to CTMP. Before and after storage the caustic solubility and buffering capacity of the wood chips was measured.

Aspen Chips before and after Storage

Sample	% Inoculum	Storage time (days)	Initial Caustic Solubility (%)	Initial Buffering Capacity (mol/g)	Final Caustic Solubility (%)	Final Buffering Capacity (mol/g)
Aspen - Control	0	90	23.2 (0.2)	0.070	21.9	0.053
Aspen - Inoculated	8.2	90	24.5 (0.3)	0.077	27.9	0.071

CTMP pulp was prepared from aspen chips using the equipment described for TMP (Table 5.1). Aspen chips were steamed under atmospheric pressure in the chip hopper for seven minutes and then fed using a screw feeder with a compression ratio of 3:1 into a built-in PREX impregnator containing an aqueous solution of 2.5% Na_2SO_3 and 1.25% NaOH solution (pH 13.8). The chemical uptake was measured by taking the difference in height in the sodium hydroxide/sodium sulphite solution vessel before and after chip impregnation. The high freeness first-stage CTMP pulp was given one or more further passes in the 30.5 cm Sprout Waldron open-discharge laboratory refiner equipped with type D2A507 plates at 17-26% refining consistency. Each sample was refined at four energy levels to give CTMP pulps in the freeness range from 294 to 469 mL Canadian Standard Freeness (CSF).

CTMP Conditions

Plates	Rotor, No. 3809 modified Stator, No. 3804 modified
Preheater pressure	152 kPa
Refiner housing pressure	186-193 kPa
Chip presteaming time	7 min (atmospheric pressure)
Preheater residence time	7 min
Pulp consistency	22.6 to 23.5 % od pulp (cyclone exit)
Prex compression ratio	3:1

Less than 0.1% screen rejects were found for all CTMP pulp samples. CTMP pulp properties, interpolated to 300 mL CSF, showed few significant differences between the stored-sound and inoculated samples. Bulk and optical properties were relatively unaffected by the increase in decay. However, there was a 21% drop in the tear index of the decayed sample. This can be attributed to significant decreases in the long-fibre fractions.

Sodium Sulphite and Sodium Hydroxide Uptake for Aspen CTMP

Sample	Na_2SO_3 (% od wood)	NaOH (% od wood)
Stored-Sound	1.90	0.95
Decayed	1.35	0.68

Property	Aspen - Stored-Sound			
Canadian Standard Freeness (mL)	315	334	388	469
Specific Energy (MJ/kg)	9.1	7.1	6.0	4.9
Apparent Sheet Density (kg/m^3)	370	343	347	315
Burst Index (kPa•m^2/g)	1.3	1.1	1.0	0.8
Tensile Index (N•m/g)	23.0	21.9	19.1	15.1
Stretch (%)	0.86	0.81	0.72	0.64
Tear Index (mN•m^2/g) (4 Ply)	3.4	3.1	3.3	2.6
Brightness (%)	52	54	54	54
ISO Opacity (%)	95.8	94.8	94.7	94.8
Scattering Coeff. (cm^2/g)	520	509	496	480
Sheffield Roughness (SU)	278	308	317	356
Bauer McNett R-14 (%)	0.4	0.8	1.2	1.5
Bauer McNett 14/28 (%)	5.6	6.9	8.5	8.9
Bauer McNett 28/48 (%)	29.0	28.9	28.2	29.7
Bauer McNett 48/100 (%)	35.5	35.9	35.9	35.9
Bauer McNett 100/200 (%)	11.1	10.0	10.7	10.0
Bauer McNett (P-200) (%)	18.5	17.6	15.6	14.0
LWFL (mm)	0.76	0.77	0.78	0.80

Property	Aspen - Decayed			
Canadian Standard Freeness (mL)	294	322	367	432
Specific Energy (MJ/kg)	9.9	8.9	6.6	5.4
Apparent Sheet Density (kg/m^3)	368	365	342	312
Burst Index (kPa•m^2/g)	1.1	1.1	0.9	0.8
Tensile Index (N•m/g)	20.7	21.1	17.8	12.6
Stretch (%)	0.74	0.77	0.68	0.53
Tear Index (mN•m^2/g) (4 Ply)	2.8	2.7	2.7	2.4
Brightness (%)	53	54	56	56
ISO Opacity (%)	96.2	95.4	94.4	94.0
Scattering Coeff. (cm^2/g)	569	552	535	523
Sheffield Roughness (SU)	259	266	301	337
Bauer McNett R-14 (%)	0.3	0.4	0.8	1.6
Bauer McNett 14/28 (%)	4.1	4.9	6.4	7.6
Bauer McNett 28/48 (%)	29.1	29.2	29.7	29.2
Bauer McNett 48/100 (%)	33.4	34.0	33.1	34.5
Bauer McNett 100/200 (%)	12.4	12.2	11.8	10.3
Bauer McNett (P-200) (%)	20.7	19.3	18.3	16.9
LWFL (mm)	0.72	0.72	0.74	0.75

Appendix X - Refiner Mechanical Pulping Data [a]

Sample	Sound		
Specific Refining Energy (MJ/kg)	10.21	11.56	12.7
Screened CSF (mL) [b]	183	121	99
Apparent Density (kg/m^3)	270 (16)	285 (16)	297 (17)
Burst Index (kPa·m^2/g)	1.7 (0.1)	1.9 (0.1)	2.0 (0.1)
Breaking Length (km)	2.8 (0.2)	3.0 (0.2)	3.2 (0.2)
Tensile Index (N·m/g)	27.3 (2)	29.5 (2)	31.1 (2)
Stretch (%)	1.70 (0.2)	1.64 (0.2)	1.65 (0.1)
Tear Index (mN·m^2/g) (4 Ply)	6.0 (0.9)	6.5 (0.6)	6.3 (0.6)
Zero Span Breaking Length (km)	7.9 (1)	7.8 (2)	8.0 (0.7)
Air Resistance (Gurley) (sec/100 mL)	17.0 (0.9)	32.2 (2)	50.2 (3)
Sheffield Roughness (SU)	312 (5)	270 (10)	258 (21)
Brightness (%) [c]	55	57	56
Opacity (%) [d]	95.9	96.3	96.4
Scattering Coefficient (cm^2/g) [c]	524	548	560
LWFL	1.27 (0.02)	1.25 (0.01)	1.23 (0.01)
R14 (%) [e]	6	4	3
R14/28 (%) [e]	33	31	30
R28/48 (%) [e]	24	24	24
R48/100 (%) [e]	11	12	13
R100/200 (%) [e]	4	4	3
P200 (% fines) [e]	23	25	27

[a] n = 5, except for Apparent density (n = 15), LWFL (n = 4), Burst index (n = 10), and CSF (n = 2)
[b] CSF data were rejected if they varied by more than 10 mL
[c] Brightness data were rejected if they varied by more than 0.5 %
[d] Opacity and Scattering Coefficient data were averaged by the instrument
[e] Bauer McNett data (n = 1)

Property	Discoloured		
Specific Refining Energy (MJ/kg)	9.1	10.44	11.67
Screened CSF (mL)	195	136	99
Apparent Density (kg/m^3)	254 (16)	267 (16)	280 (17)
Burst Index (kPa·m^2/g)	1.4 (0.1)	1.6 (0.1)	1.8 (0.1)
Breaking Length (km)	2.0 (0.2)	2.6 (0.4)	2.8 (0.2)
Tensile Index (N·m/g)	19.4 (2)	26.0 (4)	27.4 (2)
Stretch (%)	1.65 (1)	1.53 (0.4)	1.45 (0.2)
Tear Index (mN·m^2/g) (4 Ply)	5.2 (0.5)	5.1 (0.5)	5.1 (0.5)
Zero Span Breaking Length (km)	6.9 (1)	7.2 (3)	7.5 (1)
Air Resistance (Gurley) (sec/100 mL)	11.5 (1)	21.2 (2)	41.0 (3)
Sheffield Roughness (SU)	345 (9)	310 (15)	278 (11)
Brightness (%)	47	49	49
Opacity (%)	97.3	97.6	97.6
Scattering Coefficient (cm^2/g)	504	529	550
LWFL	1.62 (0.02)	1.60 (0.03)	1.58 (0.02)
R14 (%)	4.7	3.2	1.9
R14/28 (%)	30.2	27.8	25.3
R28/48 (%)	26.0	26.1	25.7
R48/100 (%)	12.1	14.5	14.1
R100/200 (%)	5.0	4.2	4.3
P200 (% fines)	22.0	24.3	28.7

Property	Intermediate decay		
Specific Refining Energy (MJ/kg)	9.96	11.7	12.87
Screened CSF (mL)	176	115	86
Apparent Density (kg/m^3)	285 (24)	314 (26)	339 (28)
Burst Index (kPa·m^2/g)	1.8 (0.1)	2.1 (0.1)	2.2 (0.1)
Breaking Length (km)	2.7 (0.3)	2.8 (0.2)	3.5 (0.3)
Tensile Index (N·m/g)	26.2 (3)	27.8 (2)	34.4 (3)
Stretch (%)	1.33 (0.2)	1.27 (0.2)	1.52 (0.2)
Tear Index (mN·m^2/g) (4 Ply)	6.5 (0.5)	6.3 (0.7)	6.3 (0.6)
Zero Span Breaking Length (km)	7.9 (1)	8.3 (0.5)	8.3 (0.8)
Air Resistance (Gurley) (sec/100 mL)	17.9 (2)	55.8 (5)	102.1 (6)
Sheffield Roughness (SU)	299 (15)	232 (25)	219 (31)
Brightness (%)	43	45	45
Opacity (%)	97.8	97.9	98.2
Scattering Coefficient (cm^2/g)	493	523	542
LWFL	1.76 (0.02)	1.74 (0.02)	1.69 (0.01)
R14 (%)	4.1	2.8	2.2
R14/28 (%)	33.1	31.6	29.8
R28/48 (%)	24.3	25.1	24.6
R48/100 (%)	11.2	13.6	13.3
R100/200 (%)	4.3	4.0	4.0
P200 (% fines)	23.0	22.9	26.2

Property	Advanced decay	
Specific Refining Energy (MJ/kg)	4.98	5.78
Screened CSF (mL)	168	103
Apparent Density (kg/m^3)	302 (20)	311 (21)
Burst Index (kPa·m^2/g)	1.3 (0.1)	1.4 (0.1)
Breaking Length (km)	1.9 (0.09)	2.5 (0.3)
Tensile Index (N·m/g)	18.9 (0.9)	24.5 (3)
Stretch (%)	1.04 (0.1)	0.98 (0.1)
Tear Index (mN·m^2/g) (4 Ply)	4.7 (0.5)	4.5 (0.6)
Zero Span Breaking Length (km)	6.2 (2)	6.5 (1)
Air Resistance (Gurley) (sec/100 mL)	22.9 (1)	87.4 (8)
Sheffield Roughness (SU)	308 (11)	291 (23)
Brightness (%)	37	36
Opacity (%)	99.4	99.4
Scattering Coefficient (cm^2/g)	463	467
LWFL	1.75 (0.01)	1.68 (0.02)
R14 (%)	6.0	3.9
R14/28 (%)	27.8	24.1
R28/48 (%)	22.2	19.9
R48/100 (%)	12.9	11.6
R100/200 (%)	5.5	5.0
P200 (% fines)	25.7	35.5

Appendix XI - Kraft Pulping Data [a]

Property (Std. Dev.)	Sound			
PFI Rev.	0	3000	6000	12000
Screened CSF (mL) [b]	666	627	545	377
Apparent Density (kg/m^3)	575 (46)	657 (56)	678 (57)	697 (59)
Burst Index (kPa·m^2/g)	7.1 (0.3)	9.6 (0.3)	10.4 (0.6)	11.0 (0.5)
Breaking Length (km)	8.6 (0.4)	11.5 (0.3)	12.0 (0.6)	13.1 (0.3)
Tensile Index (N·m/g)	84.1 (4)	112.8 (3)	117.3 (6)	128.3 (3)
Stretch (%)	1.72 (0.2)	3.13 (0.2)	3.19 (0.3)	3.52 (0.3)
Tear Index (mN·m²/g) (1 Ply)	12.7 (0.9)	11.6 (0.8)	11.5 (1)	10.8 (0.7)
Tear Index (mN·m²/g) (4 Ply)	13.5 (0.6)	11.3 (0.5)	10.8 (0.7)	10.5 (0.3)
Zero Span Breaking Length (km)	17.2 (2)	15.2 (3)	15.6 (3)	16.0 (1)
Air Resistance (Gurley) (sec/100 mL)	5.5 (0.4)	12.1 (1)	20.0 (2)	55.8 (7)
Sheffield Roughness (SU)	213 (9)	191 (8)	177 (9)	102 (6)
Opacity (%) [c]	97.2	95.0	93.1	92.0
Scattering Coefficient (cm²/g) [c]	253	187	163	150

Property (Std. Dev.)	Discoloured			
PFI Rev.	0	3000	6000	12000
Screened CSF (mL) [b]	696	637	559	387
Apparent Density (kg/m^3)	563 (49)	646 (56)	676 (58)	695 (59)
Burst Index (kPa·m^2/g)	6.3 (0.3)	9.4 (0.4)	10.2 (0.4)	10.9 (0.5)
Breaking Length (km)	7.7 (0.5)	10.7 (0.6)	12.3 (0.7)	13.0 (0.3)
Tensile Index (N·m/g)	75.8 (5)	104.9 (6)	120.3 (7)	127.7 (3)
Stretch (%)	1.60 (0.2)	2.94 (0.3)	3.57 (0.4)	3.94 (0.1)
Tear Index (mN·m²/g) (1 Ply)	12.1 (0.7)	12.1 (1.3)	11.6 (1.4)	10.6 (0.8)
Tear Index (mN·m²/g) (4 Ply)	12.9 (0.8)	10.5 (0.2)	9.7 (0.5)	9.6 (0.2)
Zero Span Breaking Length (km)	15.9 (2)	14.3 (0.9)	15.4 (3)	15.2 (2)
Air Resistance (Gurley) (sec/100 mL)	0.0 (0)	6.9 (0.4)	15.3 (2)	51.1 (5)
Sheffield Roughness (SU)	221 (10)	198 (8)	165 (6)	110 (6)
Opacity (%) [c]	97.3	94.5	93.0	91.3
Scattering Coefficient (cm²/g) [c]	267	194	168	149

[a] n = 5, except for Burst index (n = 10), Apparent density (n = 15), and CSF (n = 2)
[b] CSF data were rejected if they varied by more than 10 mL CSF
[c] Opacity and Scattering Coefficient data were averaged by the instrument

Property (Std. Dev.)	Intermediate decay		
PFI Rev.	0	6000	12000
Screened CSF (mL)	668	489	304
Apparent Density (kg/m3)	573 (59)	673 (69)	707 (73)
Burst Index (kPa·m2/g)	7.6 (0.3)	10.5 (0.4)	11.3 (0.4)
Breaking Length (km)	8.0 (0.6)	11.3 (0.6)	12.6 (0.6)
Tensile Index (N·m/g)	78.8 (6)	110.5 (6)	123.2 (6)
Stretch (%)	1.58 (0.2)	2.99 (0.2)	3.47 (0.1)
Tear Index (mN·m²/g) (1 Ply)	12.0 (1)	10.6 (1)	9.7 (0.5)
Tear Index (mN·m²/g) (4 Ply)	12.5 (0.7)	9.9 (0.3)	9.4 (0.6)
Zero Span Breaking Length (km)	15.6 (2)	14.7 (2)	15.0 (2)
Air Resistance (Gurley) (sec/100 mL)	5.4 (0.2)	23.6 (1)	104.5 (7)
Sheffield Roughness (SU)	191 (6)	137 (2)	76 (25)
Opacity (%)	97.1	92.8	92.1
Scattering Coefficient (cm²/g)	274	174	161

Property (Std. Dev.)	Advanced decay		
PFI Rev.	0	6000	12000
Screened CSF (mL)	618	326	194
Apparent Density (kg/m^3)	545 (82)	691 (104)	713 (107)
Burst Index (kPa·m^2/g)	6.5 (0.3)	9.0 (0.6)	9.5 (0.6)
Breaking Length (km)	8.5 (0.6)	11.1 (0.2)	10.4 (0.7)
Tensile Index (N·m/g)	83.7 (6)	108.6 (2)	102.2 (7)
Stretch (%)	1.99 (0.3)	3.16 (0.2)	3.16 (0.3)
Tear Index (mN·m²/g) (1 Ply)	10.8 (0.6)	9.6 (0.7)	9.9 (0.6)
Tear Index (mN·m²/g) (4 Ply)	10.0 (0.5)	8.2 (0.4)	7.7 (0.2)
Zero Span Breaking Length (km)	14.4 (2)	14.1 (3)	14.4 (2)
Air Resistance (Gurley) (sec/100 mL)	10.0 (1)	63.0 (4)	278.6 (38)
Sheffield Roughness (SU)	202 (18)	81 (4)	48 (10)
Opacity (%)	98.5	96.6	96.7
Scattering Coefficient (cm²/g)	249	174	169